An Investigation into Textile Applications of Thermochromic Pigments

Waseem Ibrahim

Submitted for the degree of Doctor of Philosophy

Heriot-Watt University

School of Textiles and Design

August 2012

Abstract

Methods were developed for application of thermochromic pigments to textiles, based on printing and extrusion, for both leuco dye based and cholesteric liquid crystal thermochromics. The leuco dye based thermochromics were assessed in terms of heat stability, binder optimization and colour saturation using an instrumental colour measurement system. Enhancement of lightfastness of leuco dye based thermochromics was carried out using UV absorbers, HALS and antioxidants as additives. A comparative study was also carried out between printing and extrusion application methods. A colour measurement system with the facility for temperature variation was constructed using two traditional components – a reflectance spectrophotometer and a controllable hot stage. The dynamic colour change of leuco dye based thermochromics with temperature was assessed. The liquid crystals were assessed with temperature for their additive colour mixing properties by layering them over each other. They were also assessed in terms of aspects of applications, such as differences in the over-layering sequence and colour hysteresis on heating and cooling. The results were evaluated not only to provide a scientific understanding of the performance but also to provide useful information from a creative designer's point of view.

The research carried out as described in this thesis has established an improved understanding of the application methods for leuco dye based and liquid crystal thermochromic pigments for optimum performance. The availability and selection of colours achievable with liquid crystal thermochromics have been widened significantly by the improved understanding of the colours derived from over-layered liquid crystals. It is anticipated that this research will broaden the potential for use of leuco dye based and liquid crystal thermochromics in textiles, especially in the fields of functional textiles and creative design.

Dedication

In memory of my beloved Parents

Acknowledgements

Firstly, thanks to Heriot Watt University for giving me this opportunity to carry out my research.

I feel privileged to have been supervised by Professor Robert M. Christie, to whom I would like to give heartfelt thanks for his expertise, guidance, patience and support. I would also like to thank my second supervisor, Dr. Alex Fotheringham, for his advice and expertise in extrusion, Professor Roger Wardman for his advice and expertise in colour physics, and Dr. Sara Robertson for her cooperation and team work.

I would like to express my gratitude for the assistance and cooperation I have received from staff at the School of Textiles and Design at Heriot Watt University. In particular, I would like to thank Dr. Roger Spark, Ann Hardie, Jim McVee, Tony Peyton, and Margaret Robson.

LCR Hallcrest provided the thermochromic pigments used in this research and I would like to thank them for this contribution and for the technical information they have shared with me. Many thanks also to Yousaf Jamal, who helped create the software used for colour display.

I would like to thank the many friends I have made in Galashiels, and my friends abroad, for their kindness and motivation.

Thank you to my family for their unconditional love, for believing in me and supporting me throughout my life, and for helping me to achieve my ambitions. A special thank you to my late mother and father for teaching me the value of education and for inspiring me to follow my dreams.

Finally, I would like to thank my wife for her continuing encouragement, patience and support.

Table of Contents

Lists of Tables

Lists of Figures

Chapter 1. Introduction

Thermochromic pigments are materials which change colour as a function of temperature. Types of pigments are known that change colour either reversibly or irreversibly. The materials which change colour reversibly and may be used in textiles are leuco dye based and cholesteric liquid crystal thermochromic pigments. The leuco dye based thermochromic pigments generally change from coloured to colourless or to another colour with an increase in temperature. The cholesteric liquid crystals exhibit 'colour play' by passing through the whole spectrum with an increase in temperature.

The leuco dye based thermochromic pigments consist of a colour former, a developer and a solvent in a specific combination. The colour former is a pH sensitive dye, mostly belonging to the spirolactone or fluoran class. The developer is a proton donor and normally is a weak acid such as Bisphenol A. The solvent is a low melting hydrophobic, long aliphatic chain fatty acid, amide or alcohol and its melting point is used to associate the system with a specific temperature at which the colour former and developer interact. The liquid crystals with a chiral centre, known as cholesteric liquid crystals, change colour as a function of temperature. Initially, the products were derivatives of cholesterol as in their name. However, synthetic chiral molecules are now also used and are known as chiral nematic liquid crystals. The cholesteric liquid crystals against a black background manipulate the incident light and reflect back selected wavelengths of light which vary with change in temperature. The particular reflected wavelengths depend on the pitch length of the helix formed by the liquid crystals, a parameter which changes with temperature. For integration and application purposes, the leuco dye based and liquid crystal thermochromic pigments are normally microencapsulated.

Thermochromic pigments have been commercialized since the late 1960s and used, for example, in thermographic recording materials. The thermochromic pigments are also used as temperature indicators such as measuring the body temperature, in food containers to determine the temperature or history of the food storage, in medical thermography for diagnosis purposes, in thermal mapping of engineering materials to diagnose faults in product design and in mechanical performance, in the cosmetic industry for moisturizing and as a carrier for vitamins, etc. These materials also have been used in memory devices, in batteries for life indication and in the architecture field

for decoration or for its functionality. These materials have been reported as novelty materials in toys, ornaments, kettles, umbrellas, toilet seats etc. In textiles, these pigments have been applied by printing, coating, by a method involving cationization of cotton fabric and extrusion. They have been used in T shirts, children clothing, jeans, electronic heat profiling circuitry, incorporated in man-made cellulose fibres and acrylic fibres. Thermochromic materials have been used in textiles but not to a vast extent.

1.1 Aims of the Research

The overall aim of research in this study was to optimize application methods for thermochromic pigments on textiles, to assess the performance of these pigments instrumentally and to establish scientific explanations for the observations. The literature concerning thermochromic textiles mainly deals qualitatively with their functionality. An aim of the research described in this thesis was to assess the functionality of these pigments not only qualitatively but also quantitatively, by appropriate instrumental methods. This research is especially focused on developing application techniques which enhance the performance of thermochromic pigments on textiles and to provide a technical basis and inspiration for creative design applications.

1.2 Objectives of the Research

1.2.1 Optimizing Printing Application of Leuco Dye based Thermochromic Pigments

The leuco dye based thermochromic pigments are sensitive towards heat and also the available colour strength is less than traditional pigments. In the literature, there are no recommendations on the printing conditions for optimum performance of these pigments. Thus an investigation was carried out on the printing techniques to establish conditions for these pigments so they could be used in future to their full potential and level of performance. In this regard, colour stability towards heat, binder optimization, curing conditions, and colour saturation levels of these pigments were established.

1.2.2 Lightfastness Improvement

The leuco dye based thermochromic pigments show poor lightfastness. A number of additives are used by incorporation into the microcapsules to enhance their lightfastness during manufacturing. In this study, it was intended to aim to improve the lightfastness

of these pigments at their application or end user stage. For this purpose, UV absorbers, HALS and antioxidants were investigated as possible lightfastness enhancers.

1.2.3 Incorporation of Leuco Dye based Thermochromics into Polymers

Microencapsulated leuco dye based thermochromic pigments are normally applied on textiles by printing. To develop a new method for producing thermochromic textiles, an investigation was carried out of the extrusion of filaments with different polymers, incorporating these pigments and assessing the properties and performance of these filaments, compared to the thermochromic prints.

1.2.4 Colour Change with Varying Temperature of Leuco Dye based Thermochromic Pigments

The dynamic colour change of these pigments with varying temperature, made colour measurement challenging. A method was established to measure the colour of leuco dye based thermochromic pigments using a reflectance spectrophotometer in conjunction with a hot stage, with a view to providing explanations for the colour change phenomena with increase and decrease in temperature.

1.2.5 Over-layering Effect of Liquid Crystals

It had been observed during a complementary design study that liquid crystals with different colour-play start temperatures and bandwidths, layered over each other, give unusual bright colours. A study was therefore initiated to explore this phenomenon instrumentally to provide a scientific understanding to facilitate the use of over-layered liquid crystals in a way that is useful for creative design applications. A variety of ways of carrying out the overlaying was investigated. The results were displayed in different ways, in attempts to provide illustrations that would be useful for individuals from different backgrounds including scientists and designers.

1.2.6 Combination of Liquid Crystals and Leuco Dye base Thermochromic Pigments

In general, the cholesteric liquid crystals show colour play against a black background. It was anticipated that it would be of interest to assess their colour play with a black background produced using a leuco dye based thermochromic pigment and to

characterise the colour play of liquid crystals with the simultaneous colour change of leuco dye based thermochromic pigment.

1.3 Overview of Thesis

Chapter 2 provides a comprehensive literature review relevant to this research. It has been divided into several main and sub sections. The first section provides information about the phenomena encompassed by the term chromism, and different types of chromic materials and systems. The second section of the chapter discusses the background to thermochromism and thermochromic systems. This section also discusses reversible intrinsic and indirect thermochromic systems and their sub classes. The third section of the chapter deals specifically with colour former or leuco dye based thermochromic pigments, their versatility, composition and the mechanism of operation. The fourth section concerns the liquid crystals and their different classes. The fifth section specifically discusses the cholesteric liquid crystals which have been used in this study and the sixth concerns the microencapsulation of thermochromics and the different techniques used. In the seventh section, the application of thermochromic pigments have been discussed both from a general and also a specific textile point of view. The principles underlying lightfastness, photodegradation and the mechanism of additives used to improve lightfastness in this study are discussed in section eight of the chapter. Sections nine and ten of the chapter deal with the fibres and polymers used in this study, together with their synthesis and properties. The eleventh section discusses the extrusion and extrusion machines, i.e., ram and screw which were used in this study. In the twelfth section, drawing aspects of filament are discussed. The last section of this chapter provides an overview of the colour measurement systems. It also provides information about illuminants, viewing geometry and instrumental measurement of colour with special focus on temperature dependent measurement.

Chapter 3 of the thesis is the experimental section that details the materials, methods and techniques that have been employed in this research work. The first section describes the materials which have been used in this study. The second section details the preparation of printed samples of leuco dye based thermochromic pigments. Sections three to six discuss the procedures used to evaluate colour stability towards heat, binder optimization colour saturation and lightfastness enhancement. Section seven of the chapter describes the preparation of coated samples of liquid crystals. Sections eight and nine describe the procedures and machines used for extrusion and

drawing of filaments. The following seven sections discuss the procedures involved in the range of test methods to which the thermochromic samples were subjected. The final section of the chapter describes the colour measurement instruments and procedures, adapted to measure the thermochromic samples.

Chapter 4 presents the results and discussion of the research that has been carried out. The first section discusses the outcomes of an investigation into leuco dye based thermochromic pigments applied by screen printing, including the calibration conditions, colour stability, binder optimization, colour concentration and lightfastness enhancement. The second section discusses the extrusion of filaments with different polymers, incorporating thermochromic pigments. This section also discusses the properties of extruded filaments such as the thermochromism, SEM images, colour strength, wash and rub fastness, lightfastness, DSC traces of polymers and filaments, and the tensile properties of filaments. The next section discusses the measured colour change of leuco dye based thermochromic prints with varying temperature. In the final section of this chapter, an extensive investigation of the liquid crystals is discussed. This section discusses the colour change effects obtained from different combinations of over-layered liquid crystals on a black sheet in terms of a^*b^* diagrams, L^* values, RGB colour display and reflectance curves with varying temperature. The colour hysteresis observed involving heating and cooling cycles is also examined. Finally, the effect of individual liquid crystals coated on printed leuco dye based thermochromic pigments is discussed.

In Chapter 5, overall conclusions derived from the research carried out in this study, are presented, additional to the conclusions discussed individually in chapter 4. This chapter also suggests future research possibilities in this field. Finally, the references used in the thesis have been listed.

Chapter 2. Literature Review

Rays of light with wavelengths between the ultra-violet and infra-red regions stimulate the eye. This is known as the visible region. In the visible region, different wavelength ranges give rise to different colours. Also, they give a white effect collectively that can be considered as composed of seven basic colours – violet, indigo, blue, green, yellow, orange and red. In general, production of colour can be classified into five broad fundamental mechanisms i.e. [1]:

- Vibrations and excitations (external heat or energy transfer within molecules); this occurs in vapour lamps, incandescence and a few lasers;
- Ligand field effects (caused by single electrons in ions and complexes of transition metals); this can be seen in phosphorescence and lasers;
- Transitions between molecular orbitals; this occurs in dyes and pigments of both organic and inorganic origin, and in fluorescence;
- Transitions between energy bands; such as in metals and semi conductors;
- Geometrical and physical optics, such as the interference phenomenon, iridescence diffraction and liquid crystals.

2.1 Chromism

Chromism is the term used for a change in colour. Substances having the ability to exhibit the phenomenon of chromism are known as chromic materials. Normally, chromic phenomena involve processes causing reversible colour change, absorption and reflection of light, absorption of energy and emission of light, absorption of light and energy transfer or a conversion and manipulation of light [1]. Reversible change of colour can result from an alteration of the electronic state, especially involving π- or d-electrons, physical change of the material or rearrangement of molecules in a matrix. Normally, the change depends on the involvement of some stimuli. On the basis of the stimuli involved, chromism can be categorised in a variety of ways, including thermochromism – induced by heat, photochromism – induced by light irradiation, electrochromism – induced by addition and subtraction of electrons as a result of electric current flow, solvatochromism – induced by the polarity of solvent,

ionochromism – induced by ions, halochromism – induced by pH, tribochromism – induced by mechanical friction, vapochromism – induced by vapours, mechanochromism – induced by mechanical activity, chronochromism – induced by time, radiochromism – induced by ionizing radiation, magnetochromism – induced by magnetic field, biochromism – induced by biological sources and piezochromism – induced by mechanical pressure [1–3].

2.2 Thermochromism

The term thermochromism refers to a change in colour as a function of temperature [4,5]. J. H. Day defined thermochromism as 'an easily noticeable reversible colour change brought about by the boiling point of each liquid, the boiling point of the solvent in the case of a solution or the melting point for solids' [1,6]. This definition may be have been appropriate historically for a number of inorganic and organic materials, but the most important current materials exhibit thermochromism by means of other factors which are affected by heat, for example the environment [7]. Technically, it is possible to classify reversible thermochromism into 'intrinsic' systems, where colour change depends solely on heat and 'indirect' systems where the environment is changed by heat and this in turn causes the colour change [8]. Examples of mechanisms giving rise to intrinsic thermochromism are stereoisomerism, liquid crystals and molecular rearrangements. In contrast, indirect thermochromism is commonly due to pH sensitive dyes which themselves are not affected by heat but the complete system changes in pH values due to heating. In most cases, the materials themselves do not exhibit the chromism but need a combination of materials in specific ratios as well as microencapsulation for application. It is therefore referred to as a 'system' rather than a 'material'. Thermochromic systems may belong to both chemical groups – inorganic and organic.

2.2.1 Inorganic Thermochromic Systems

Many inorganic materials show thermochromic phenomena in solid or solution states. It is suggested that the thermochromic phenomenon in these cases depend on mechanisms such as phase transitions, changes in ligand geometry, equilibria between different molecular structures and changes in the number of solvent molecules in the coordination sphere, for example involving dehydration [9]. Inorganic thermochromic systems are normally based on transition metals and organo-metallics. Almost all

inorganic thermochromic systems are intrinsic systems, which means that the colour changes solely depend directly on heat. Some examples of inorganic thermochromic materials are the following [1,8–10]:

- Cu_2HgI_4 is red at 20°C but black at 70°C;
- ZnO is white at room temperature but yellow at higher temperatures;
- In_2O_3 is yellow at a lower temperature but yellow-brown at a high temperature;
- Cr_2O_3-Al_2O_3 is red at 20°C but grey at 400°C;
- $(Et_2NH_2)_2CuCl_4$ is bright green at 20°C but yellow at 43°C;
- $CoCl_2$ is pink at 25°C but blue at 75°C;
- VO_2 at about 68°C changes from transmissive semiconductor to an infrared-reflecting metallic conductor [11].

Inorganic thermochromic materials/systems have some limitations for textile applications. They often show their thermochromic behaviour at a high temperature or in solution form and colour change is also sometimes irreversible [12]. The thermochromic systems for textile applications require colour changes at close to ambient temperatures, for example around -10°C for ski wear and around body temperature at 35°C for apparel and smart textiles [9]. Thus, inorganic and organometallic materials/systems are mostly used in temperature indicating paints and crayons, to identify the temperature change and also to provide a permanent record of thermal data.

2.2.2 Organic Thermochromic Systems

Organic thermochromic systems provide both intrinsic systems and indirect systems and they act reversibly.

(a) Reversible Intrinsic Thermochromic Organic Systems

Reversible intrinsic thermochromic organic systems show colour change on application of heat without depending on anything else, such as the environment etc. and they revert to the more stable state as they cool down after removing the heat source. These

systems can be divided into the following types on the basis of their colour change mechanisms [1]:

- Molecular rearrangement;
- Stereoisomerism;
- Macromolecular systems;
- Supramolecular systems.

(i) Molecular Rearrangement

Molecular rearrangement may occur as the result of tautomerism, which may occur from acid-base, keto-enol or lactim-lactam equilibria, which lead to an increase or decrease in the electron conjugation in molecules, resulting in formation of different chromophores [9,13].

Schiff bases made by condensation reactions of salicylaldehydes and anilines, show enol-keto tautomeric structures due to hydrogen transfer [14,15]. The thermochromism occurs in Schiff bases which are planar molecules when the keto form is more favoured in the tautomeric equilibrium, and the colour changes from yellow to orange or red as shown, for example in Figure 2.1.

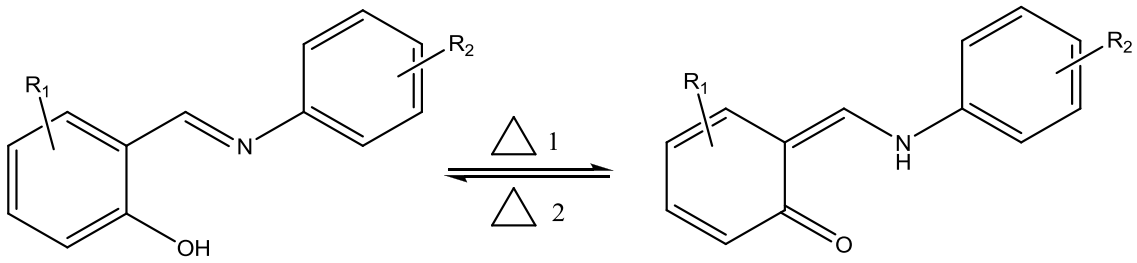

Figure 2.1 Tautomeric forms of a Schiff base

Spiropyrans and spirooxazines which are recognised more for their photochromism, may also show thermochromism. In solid or liquid form, the open-ring coloured merocyanine form can be obtained by heating. These compounds may also show solvatochromism, in that polar solvents may cause formation of the polar merocyanine structure[16].

Similarly, the bis-spiropyran shown in Figure 2.2 is a colourless compound. It shows a red colour in n-propanol at 60°C and at 70°C a blue colour. This is due to the structural formation of mono-merocyanine and bis-merocyanine respectively [1].

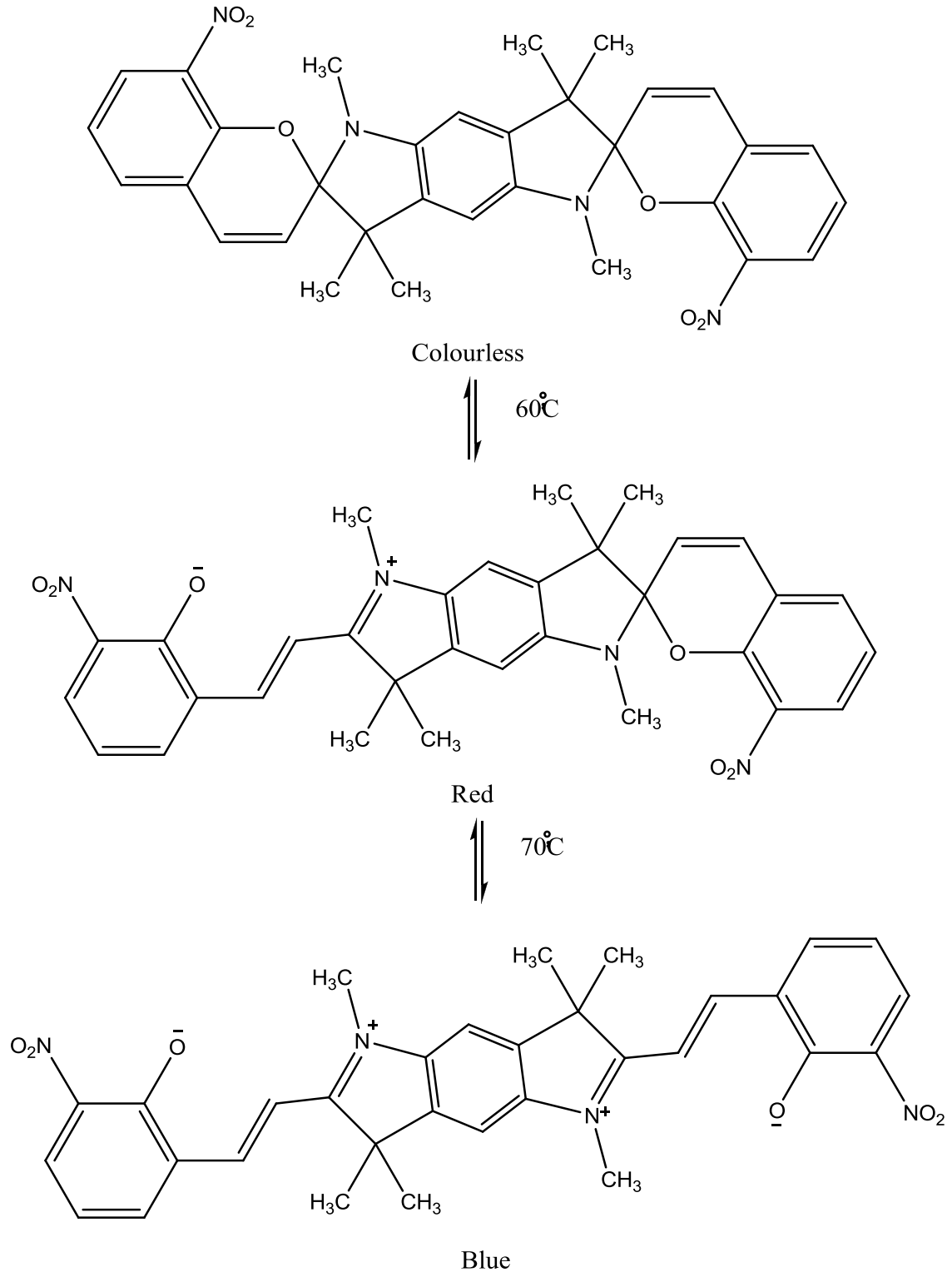

Figure 2.2 Sequential coloration of a bis-spiropyran with temperature

(ii) Stereoisomerism

Thermochromism may arise by stereoisomerism and normally occurs in compounds containing at least one ethylene group, a number of aromatic rings and one hetero-atom, such as nitrogen or oxygen. The ethylene group present in the structure restricts molecular orientations which in effect causes the difference in energy levels in different isomeric forms. When the system is subjected to heating, the molecule adopts different stereoisomeric forms and colour changes occur.

These materials are normally overcrowded ethylenes such as bianthrone, dixanthylene, and xanthylideneanthrone [9]. For example, bianthrones exhibit reversible colour change, from yellow, in A form, at room temperature and partially converted, when heated in solution, to B form which is green as shown in Figure 2.3 [1]. Stereoisomer systems such as this are not suitable for textiles because they show thermochromism in their molten state which commonly occurs at higher temperatures.

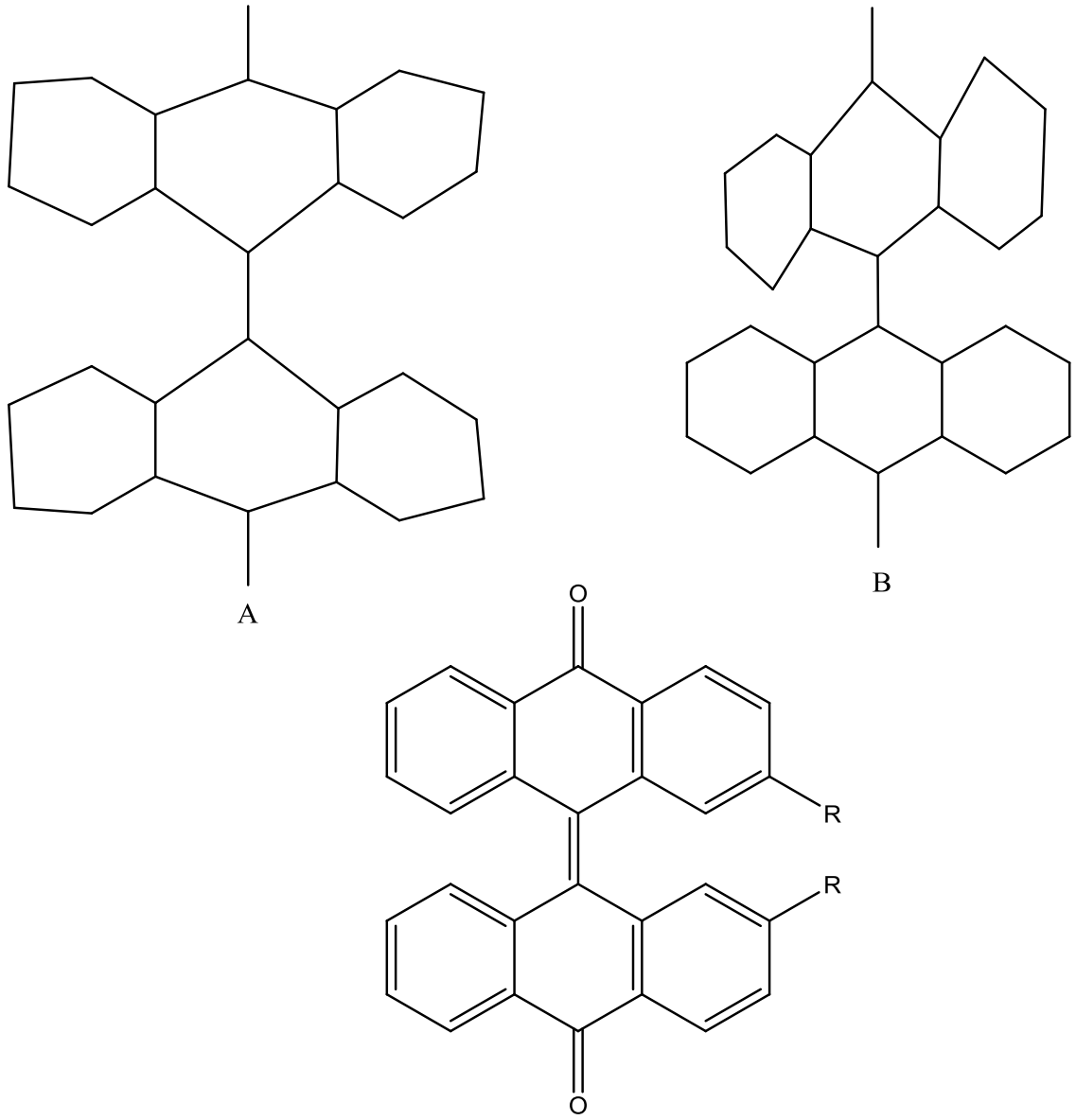

Figure 2.3 Thermochromic bianthrones: folded A and twisted B forms

(iii) Macromolecular systems

Polymers that show conjugation such as poly(3-alkylthiophenes) and poly(3-alkoxythiophenes) may show thermochromism along with other chromisms in solid and solution form. In macromolecular systems, a hypsochromic reversible colour change occurs, which is also known as negative thermochromism. For example, poly[3-oligo(oxyethylene)-4-methylthiophene] is violet at room temperature and yellow at 100°C. The effect occurs due to a planar molecular structure at room temperature which is effectively conjugated. On increasing temperature, the structure becomes disordered, twisted and non-planar and becomes less effectively conjugated as shown in Figure 2.4. If a solubilising group, such as the ethanesulphonate group in the case of water, is present or induced in the polymer chain then the colour change can occur in different

solvents. By controlling side chain length and flexibility, the temperature range in which colour change may take place can be varied.

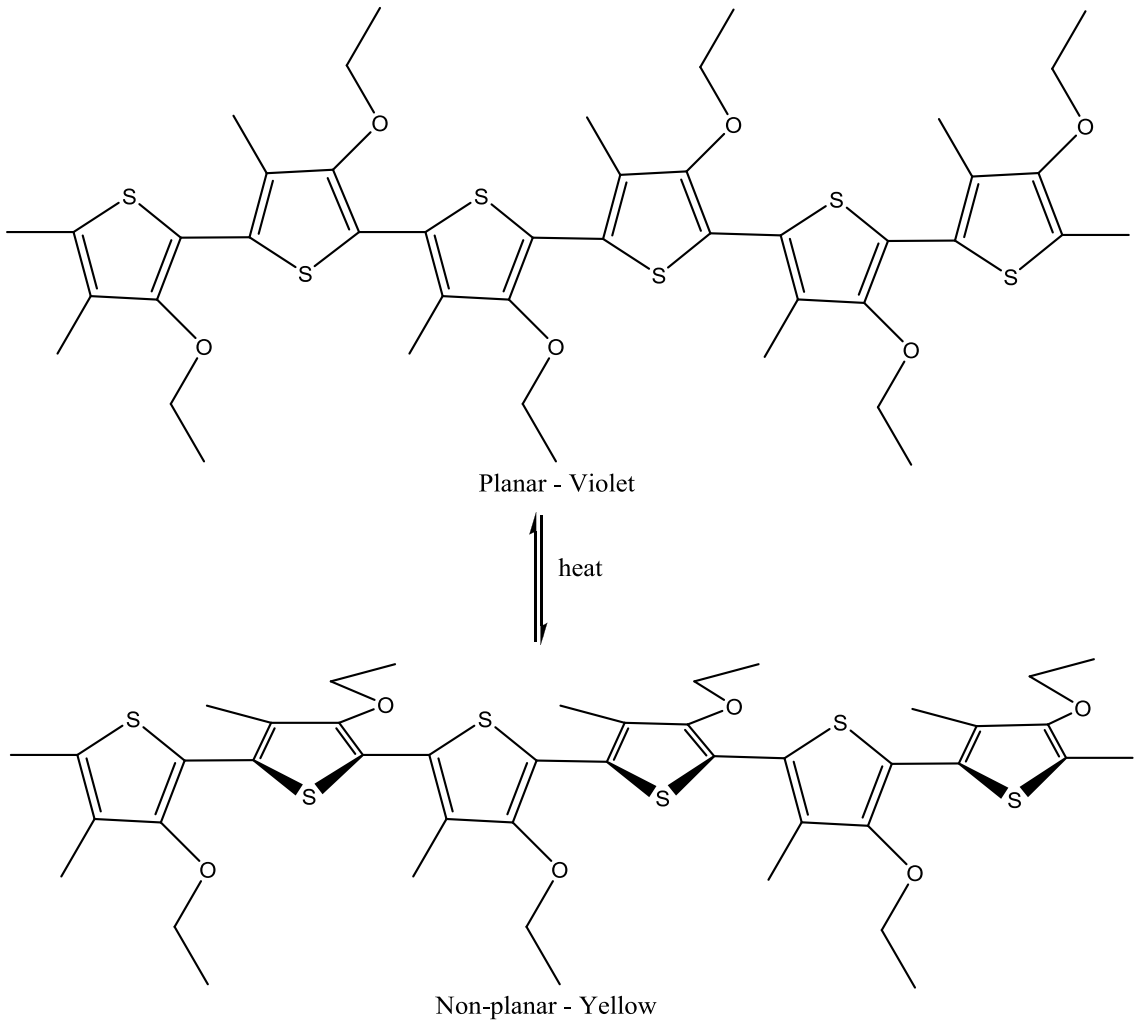

Figure 2.4 Macromolecular: different conformation and conjugation forms

(iv) Supramolecular systems

Some materials can exist in a state between solid and isotropic liquid, in which they exhibit the properties of a liquid, such as the ability to flow, but also have a crystalline-like molecular arrangement known as liquid crystals. Liquid crystals are anisotropic materials, also referred to as derived from calamitic molecules. They have a very large length to breadth ratio, that is the molecules are long and narrow [17,18]. On the basis of the molecular orientation arrangement, they are divided into three main types, i.e. smectic, nematic and cholesteric or chiral nematic as shown in Figure 2.5 which are also further divided into sub classes [17,19,20].

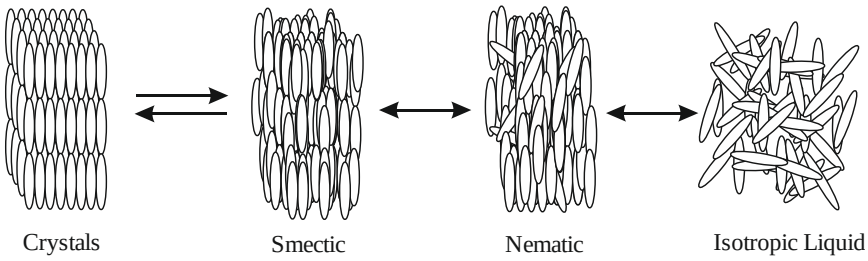

Figure 2.5 Liquid crystals phases

Liquid crystals are discussed in detail in section 2.4.

Most reversible intrinsic thermochromic systems operate at a high temperature which is not suitable for the textiles, except for liquid crystals etc. To cover all the colours in visible spectrum, many compounds need to be synthesised, which also creates significant technical problems.

(b) Reversible Indirect Thermochromic Organic Systems

In reversible indirect thermochromic organic systems, the chromophore responds to a change in its environment due to heating. The colours used in these systems are not thermochromic themselves but they show change in colour due to difference in the physical environment created by an increase or decrease in temperature. The chromophores in these systems are normally pH sensitive, the dyes belonging to the class of acidochromic or ionochromic.

Indirect systems normally operate within an ambient temperature range which mostly matches the temperature range faced by textile products during their life span. A large number of pH sensitive compounds have been synthesised and modifications are possible to provide a range of colours. By using these systems, precise and predetermined colour changes at specific temperatures are possible so that they have a wide potential usage in textiles in contrast to intrinsic systems.

Some thermochromic materials are suitable for use in textiles and have potential for their use at an industrial level. The organic thermochromic pigments containing colour formers and liquid crystal types are the most important, and these have been the material used in the study described in this thesis.

2.3 Organic Thermochromic Pigments containing Colour Formers

These products contain three components – colour formers, developers and co-solvents – in specific proportions. Normally these systems are coloured in their solid form and,

as the temperature rises, become colourless. They become coloured again on cooling. The colour former is a pH sensitive compound which accepts a proton to convert from colourless to coloured. These systems in the solid or molten state ascend or descend in pH respectively as a function of temperature change, and thus show indirect thermochromism. For the purpose of application, the whole system is microencapsulated to avoid any change or damage to the system or variation in the proportion of components.

2.3.1 Versatility

Organic thermochromic pigments containing colour formers, often referred to as leuco dye types, have interesting features such as:

- Sharp colour transition: over a few degrees temperature difference, a change from intense/deep colour to colourless is possible;

- Flexibility of temperature switching: colour changing effects can be obtained at different temperatures by choosing different co-solvents with appropriate melting points;

- Wide variety of colour changing effects: not only are the colour to colourless changes across whole visible spectrum available, but colour to colour changes are also possible by incorporating pH-insensitive dyes as a base colour or by using colour formers with a secondary chromophore.

2.3.2 Compositions

Normally, colour formers used in organic thermochromic pigments are N-acyl leuco-methylene blue derivatives, fluoran dyes, diarylphthalide compounds, diphenylmethane compounds or spiropyrans compounds. Crystal violet lactone analogues (diarylphthalide compounds) and fluoran dyes are mostly used [21]. These are colourless compounds in their ring-closed form and show colour in their ring-opened form.

The ring-opened form is obtained by protonation, using a weak acid developer such as phenolic compound. These compounds have also been referred to as catalysts or electron acceptors but are more appropriately considered as proton donors [9]. Many developers have been claimed - most are phenolic or nitrogen-containing heterocycles, including bisphenol B and bisphenol A. The latter gives deep and high contrast colours.

Bisphenol A and phenol have the same acidity level but have different effects which indicates the involvement of other factors in the efficiency of developers [8]. In some patents, 1,2,3-triazoles such as 1,2,3-benzotriazole, dibenzotriazole, thioureas, saccharin and its sderivatives, halohydrins, boric acid and its derivatives, guanidine derivatives for example, phenyl diguanide and 4-hydroxycoumarin derivatives have been used. The purpose of these compounds is claimed to be to improve lightfastness because phenol compounds give rise to quick fading when exposed to light [9].

Organic hydrophobic solvents are normally used as the co-solvents in thermochromic systems. Generally, the co-solvents used are alcohols, hydrocarbons, esters, ethers, ketones, fatty acids, amides, acid amides, thiols, sulphides and disulphides and alcohol-acrylonitrile mixtures. Mostly, aliphatic solvents have been used and are effective solvents for thermochromic systems as well as being good desensitisers at relatively low concentrations. A good desensitizing action of a solvent improves the rate of colour development and improves the likelihood of the complete colour change [9].

It is proposed that colour formers and developers interact in the solid form of the co-solvent and separate in the molten form as shown in Figure 2.6.

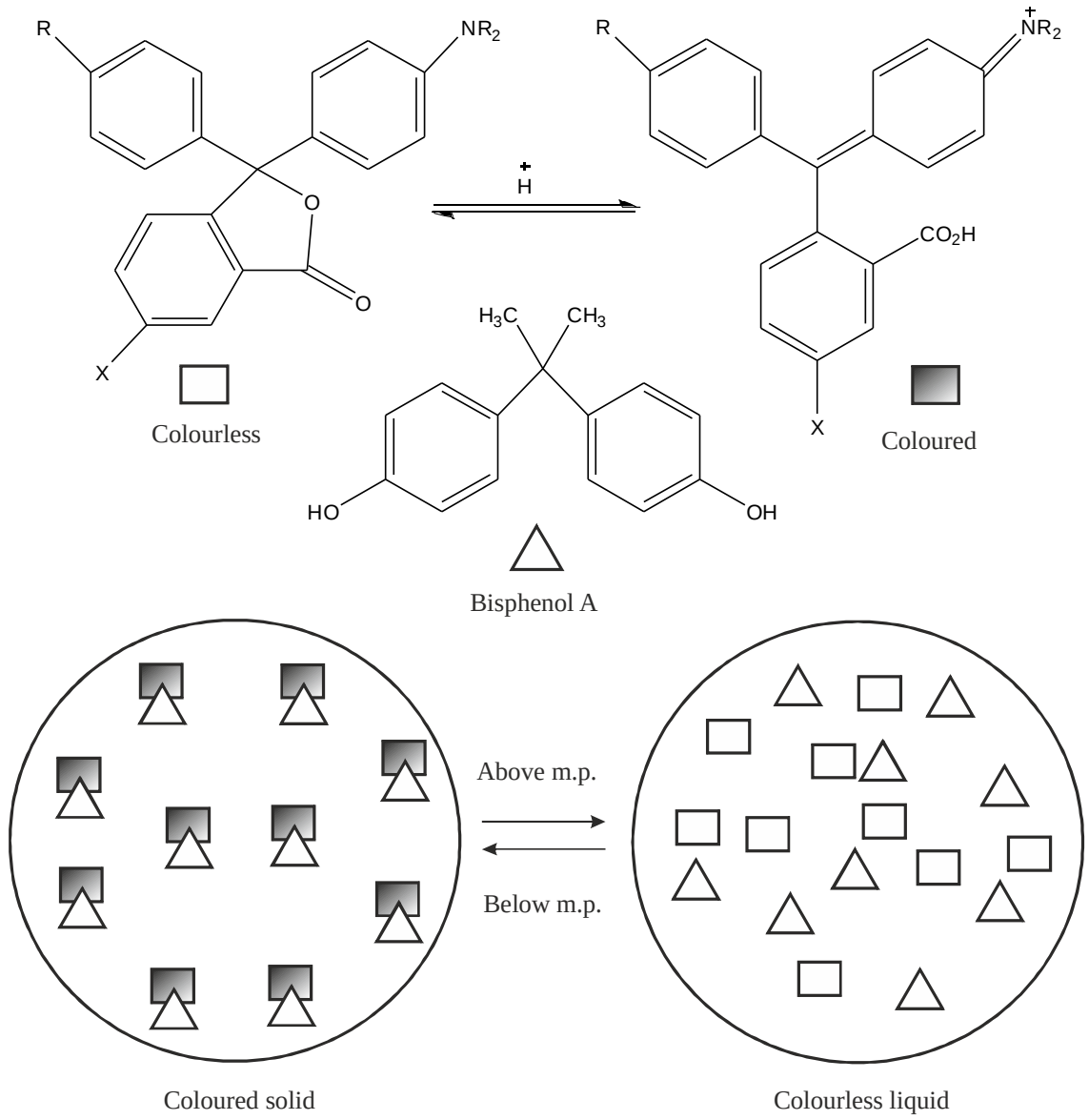

Figure 2.6 Coloured and colourless microcapsule

Normally, these type of materials show conversion from a coloured form to a colourless form, as the temperature is raised but between different colours using colour former with a secondary chromophore, for example as shown in Figure 2.7 [1,18].

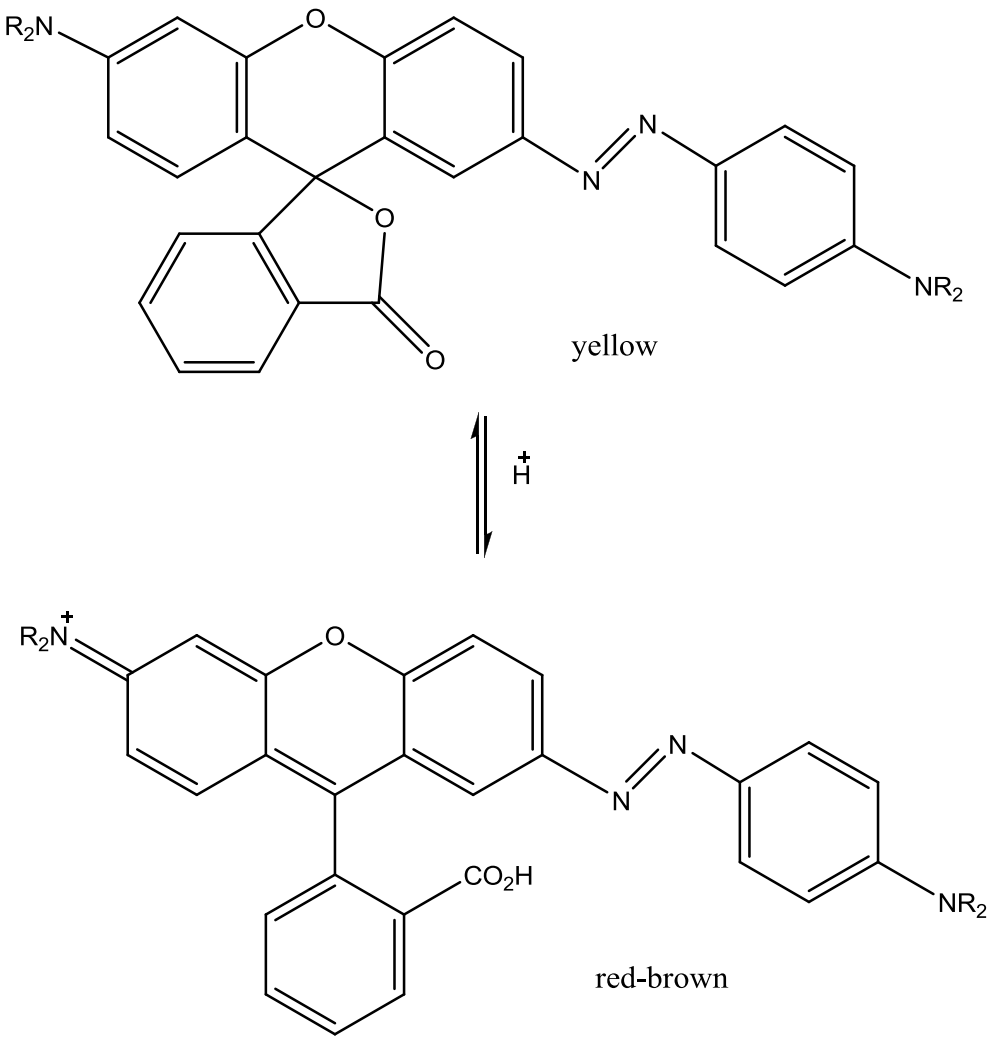

Figure 2.7 Colour change from yellow to red-brown

2.3.3 Mechanism

To explain the possible mechanisms of thermochromic pigments containing colour formers, steric and phase transition mechanisms have been studied.

(a) Steric Mechanism

According to the steric mechanism, it is suggested that in the ring-opened form, the colour former has a central sp^2 carbon with planar geometry, while in the colourless form, it contains a central sp^3 carbon with a tetrahedral geometry. Sp^2 hybridisation with planar geometry is favoured in the restricted environments of solids while a central sp^3 carbon is not. Thus, the existence of sp^2 hybridisation is favourable in solid solvents which place restrictions on movement while in the molten state it is less important and the ring-closed form can exist. However, X-ray structure determination [22] and computer modelling show the ring-opened form as not having completely planar

geometry and it may in fact appear little different from the ring-closed form [8,23]. Therefore, the steric factor is unable to explain the mechanism in a completely satisfactory way.

(b) Phase Transition Mechanism

According to the phase transition mechanism, the molten solvent is non-polar and does not support a charged complex between the soluble colour former and developer that causes the formation of lactonised (ring-closed) form which is colourless. When the solvent solidifies, colour formers and developers separate from the bulk phase, some together and some individually. In a relatively polar phase, colour formers and developers separate together and are in intimate contact, leading to ring-opened form, which is coloured. However, the acidity of the developer and basicity of the colour former, and their solubility in a solvent are important in their own right. This theory aiming to explain the mechanism of organic thermochromic pigments containing colour formers, is supported by experimental results [8,9,23,24].

2.4 Liquid crystals

Matter is normally capable of existing in three well known forms i.e. solid, liquid and gas. In solid form, the molecules are packed closely and cannot move freely and therefore retain a specific shape. The molecules may be present in either amorphous or crystalline states in the solid form and show specific properties due to these states. In a crystalline form, the molecules are arranged in regular three dimensional patterns. The regular three dimensional patterns play an important role in many physical properties, such as the diffraction of incident light. In liquid form, the molecules are not strongly bound to one another and as a result move reasonably freely, having no particular order between their molecules. The molecules are arranged randomly in liquids and they adopt the shape of the vessel in which they are contained but they do have a specific volume. Due to the randomness of the orientation of the molecules, the physical properties of liquids are independent of direction. These liquids are thus known as isotropic liquids. As a gas, molecules are in arbitrary form and can move anywhere with ease. Gases are independent of the shape of the vessel in which they are contained and its volume. Normally, their molecules can occupy any available space.

Certain materials, between their solid and isotropic liquid form, show another state in which they can flow but have specific arrangements between their molecules, that is, the

molecules are arranged in regular patterns. This state of material is known as the anisotropic form. These materials have the physical properties of liquids in combination with some characteristics of crystals so that they are also known as 'liquid crystals'. This term was first used by German physicist Otto Lehmann in 1889. The liquid crystalline state is also known as the fourth state of matter and is intermediate between solids and isotropic liquids, so it is also referred to as an intermediate or 'mesomorphic' form [25]. Normally, liquid crystals are lengthy and narrow, rod-like molecules, but some liquid crystals are disc shape. Liquid crystals are also formed by some polymers, in chain and side chain forms, such as Kevlar [1,8].

2.4.1 Classification of Liquid Crystals

Liquid crystals can be classified broadly as either thermotropic or lyotropic. This classification is based on the medium used to obtain the liquid crystal from the solid. In the thermotropic form, liquid crystals are obtained through the melting of solids that are capable of being liquid crystals. They may or may not be pure compounds. The lyotropic liquid crystals are obtained by dissolving materials in solvents, so they are always mixtures. Both classes can convert to an isotropic liquid form by further heating or by becoming degraded [25].

(a) Lyotropic Liquid Crystals

A material, such as common soap, has hydrophilic/lyophilic and hydrophobic/lyophobic ends in its molecular structure. When dissolved in a solvent such as water, its hydrophilic ends tend to attach to polar water molecules while the tails try to avoid them. This phenomenon results in specific alignment of soap molecules on the surface of water and as spheres inside the water, showing crystalline behaviour. This action of an appropriate solvent on amphiphilic molecules results in a shape which corresponds with the smectic phase. An increase in the amount of solvent results in an isotropic liquid. Thus, it can be said that the existence of lyotropic liquid crystals depends on the ratio of amphiphilic molecules to solvent molecules. Some lyotropic liquid crystal shapes are shown in Figure 2.8.

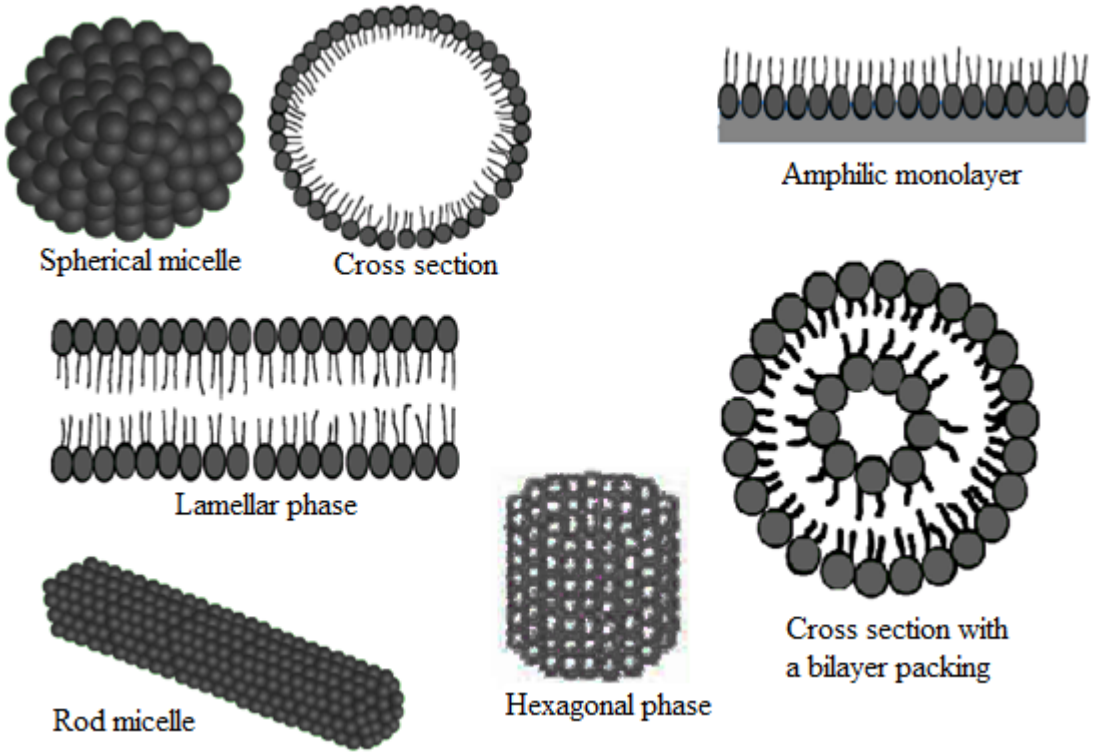

Figure 2.8 Some of lyotropic liquid crystals

(b) Thermotropic Liquid Crystals

Certain materials when subjected to heating, form the liquid crystals state between solids and isotropic liquids after melting. Thermotropic liquid crystals can interact with light in many ways which lead to a range of applications as shown in Table 2.1 [17].

Table 2.1 Liquid crystal interaction with light and consequent application

Interaction	Application
Twisted polarised light	Twisted nematic displays
Switchable birefringence film	Supertwisted nematic (STN), ferroelectric (FLC), electrically
Refraction of light	Polymer dispersed liquid crystals (PDLC), gel and polymer
Electrically switchable host for	guest-host and dyed phase change displays
Selective reflection of light	Thermochromic cholesteric devices, gel display

Thermotropic liquid crystals can exist in three main types of phases, the smectic phase, nematic phase, and the cholesteric or chiral nematic phase.

In the smectic phase the molecules are parallel to each other and arranged in raft-like layers [19]. The molecules in the smectic phase are found in both regular and random forms. They are parallel to each other and their molecular axes can be perpendicular to the surface of the layer or tilted as shown in Figure 2.9. The smectic phase is similar to the arrangement in soaps, as in lyotropic liquid crystals as discussed in section 2.4.1(a). Some materials exhibiting a smectic phase, show molecules that transfer between the layers along long axes of columns made by single or more layers of molecules. In the smectic phase, molecular movement is highly restricted and sometimes layers are strongly coupled with each other. Therefore, materials in the smectic phase are close in structure to solids or soft solids. They are further divided into sub-classes 'A' to 'J' which show subtle variations in structure.

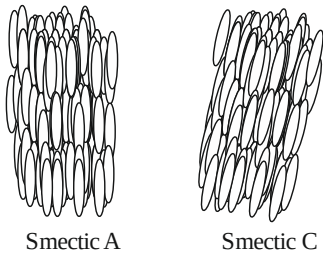

Figure 2.9 Smectic phase liquid crystals

In the nematic phase, the molecules are arranged in an alignment so that they are parallel to one another but they are not separated in layers as in the case of the smectic phase. Sometimes it behaves like smectic phase layers, but at short ranges. However, the molecules show more movement in comparison to the smectic phase. Molecules in the nematic phase when subject to heating, exhibit large changes in the direction of molecules which in turn cause variations in refractive index. Thus, the variations in refractive index due to heating increase the scattering of incident light and give a cloudy, dirty appearance. The molecules in the nematic phase give rise to dark discontinuous lines under crossed polarisers.

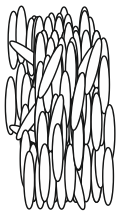

Figure 2.10 Nematic phase liquid crystals

2.5 Cholesteric Liquid Crystals

The cholesteric phase derives its name from cholesterol as the compounds exhibiting liquid crystal phenomena were originally cholesterol derivatives as shown in Figure 2.11. The cholesteric phase is similar to the nematic phase; the difference is that the molecules exhibiting the cholesteric phase show chirality, due to a chiral centre, while the molecules showing the nematic phase do not. Cholesteric liquid crystals are more important in textiles because they show thermochromic behaviour.

Synthetically developed chiral liquid crystals, as shown in Figure 2.12, can also provide the cholesteric phase or are used as dopants in nematic liquid crystals. Nowadays, the chiral nematic name is also used interchangeably with the term cholesteric [1]. It has also been proposed that the nematic phase is a special case of the chiral nematic phase with an infinite pitch length of the helix which characterises the chiral nematic phase. Bright, spectral colours and major optical activity is observed when the helix axis of chiral nematic liquid crystals is in alignment with the direction of incident light and the pitch length matches the wavelength of visible light.

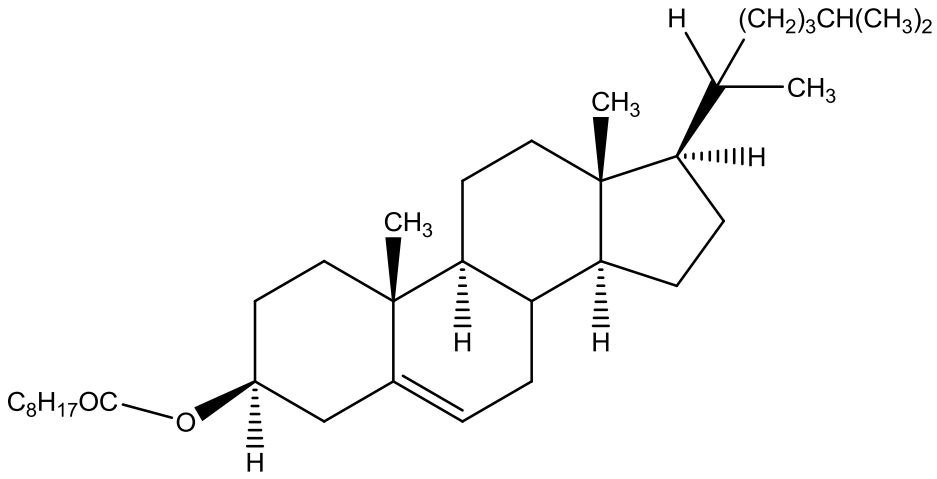

Figure 2.11 Cholesterol derivative

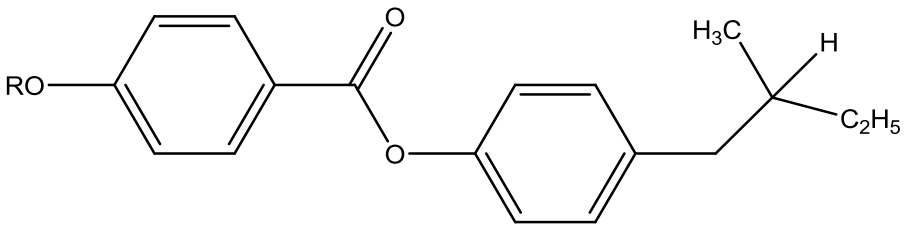

Figure 2.12 Synthetic chiral nematic

Chiral nematic liquid crystals have the ability to reflect the incident light. There is also a change in the reflected wavelength, i.e., reflected colour, by variation in temperature.

With temperature variation, the specific wavelength of the visible light is reflected back while the rest of the wavelengths are transmitted through. To observe the reflected colour, it is necessary to use a black or dark background to absorb the transmitted wavelengths as shown in the Figure 2.13 [17].

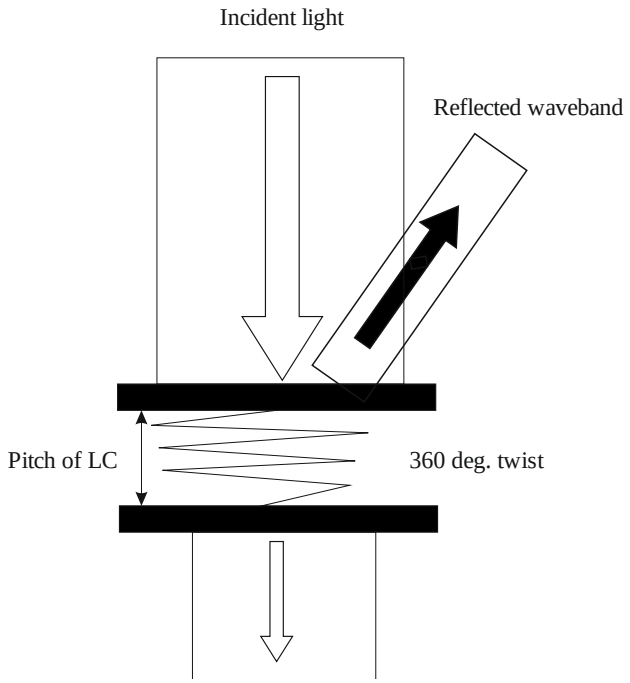

Figure 2.13 Chiral nematic interaction with light

The average direction of molecular axes in the nematic phase is known as the director. In chiral nematic liquid crystals, each layer of molecules experiences a gradual twist with respect to the director in adjacent layers. So the molecules twist gradually like a screw into a helical arrangement layer by layer until it reaches 360° against the original director. The thickness required for a turn of 360° is known as the pitch length of the helix as shown in Figure 2.14.

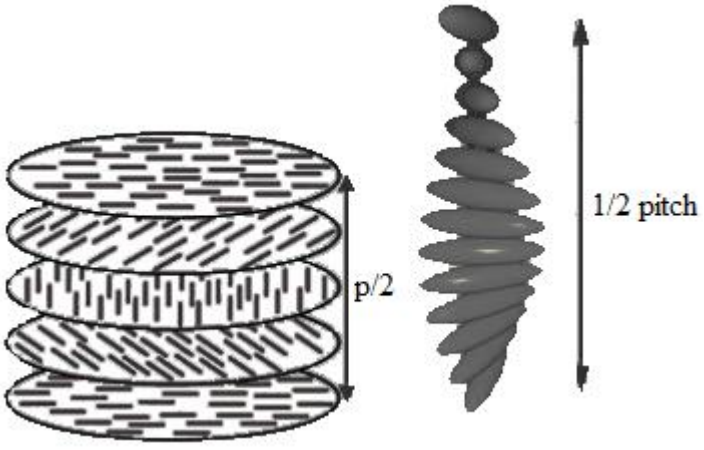

Figure 2.14 Helical arrangement of molecules in chiral nematic phase

The pitch length of the chiral nematic liquid crystals is normally in the range of 300-800 nm. It is possible to establish a relationship between the wavelength ($\lambda_\circ$) of the centre of the reflected band, pitch length (p) and average refractive index (n) of liquid crystals phase as given in Equation 2.1.

$$\lambda_\circ = np$$

Equation 2.1

and the bandwidth of the reflected light will be as follows:

$$\Delta\lambda = p\,(n_e - n_\circ) = p\Delta n$$

Equation 2.2

where n_e and $n_\circ$ are refractive indices of the liquid crystal phase parallel and normal to the director in the same plane respectively.

The pitch length of the helix varies with temperature. In chiral nematics that do not show changes of phases, the variation in pitch length of a helix is small, i.e., around 1nm/$^\circ$C, and therefore the effect is weak [20]. However, when molecules switch between two phases, for example from chiral nematic to smectic A, which does not support a twisted structure, an untwist takes place because of which a large variation in pitch length can be observed over a change in temperature of just a few degrees. This results in a dramatic change in colour, from red to blue.

2.6 Microencapsulation of thermochromic materials

Microencapsulation is a process in which materials, normally liquids are restricted in boundary walls, in the form of small, round capsules which are translucent, based on an impermeable polymer coating. The thermochromic materials used for textile purposes are based on leuco dyes or colour formers and on liquid crystals. In the case of colour formers, a specific proportion of the colour formers, developers and solvents are required and also, they require a matrix in which to exhibit colour change. Similarly, liquid crystals also need to be contained in a matrix to allow them to change molecular direction in order to exhibit the colour spectra. In textiles and other applications, these materials are applied as pigments with the assistance of binders or by some other means. It may be likened to keeping them in vessels, trapped in binders or some other systems to show thermochromic performance. For this purpose, the materials are microencapsulated, the capsules being very small and easy to apply as pigment

particles. Microcapsules not only protect materials from their environment but also are sometimes used for the slow release of materials such as medicines. Many techniques have been employed to microencapsulate thermochromic materials. Each technique plays an important role in determining microcapsule sizes, which range from a few microns to millimetres. Some of the general microencapsulation techniques used are air suspension coating, hardened emulsions, centrifugal extrusion, vacuum metalizing, liquid-wall microencapsulation, complex, thermal, non-solvent and interfacial coacervation, polymer to polymer compatibility, spray drying, liposomes and surfactant vesicles [25]. The main techniques used for thermochromic materials are discussed in the following section.

2.6.1 Coacervation

In coacervation processes, the molecules are aggregated by partially un-dissolving the complete dissolved macromolecules. Coacervation processes can be further divided into four sub techniques which are as follow:

- Complex coacervation process, which involves two oppositely charged colloids which neutralize each other and cause phase separation;
- Simple coacervation technique, which involves a non-electrolyte, such as an alcohol that causes a saturated polymer phase;
- Salt coacervation, in which a salt is added to the solution to create precipitation;
- Phase separation, which can be achieved by changing either the pH value of the solution or the temperature.

Complex and salt coacervation techniques are mainly used for thermochromic pigments.

(a) Complex Coacervation Process

In this process, two oppositely charged colloids are mixed together which ultimately cause a phase change. pH control is important in this technique. The material which is to be encapsulated is normally suspended in the water and, during phase separation, the colloids gather around the suspended particles and encapsulate them [26]. Normally, gum arabic and gelatine are used as microcapsule wall forming material[27].

The gelatine is water soluble and has an isoelelectric point between pH 4 and 9. If the pH of an aqueous solution of the gelatine and gum arabic is raised above 9, then both become anionic and there is very little interaction. But in the case of a pH lower than 4, cationic species are formed from gelatine which interact with gum arabic having anionic nature and form colloids. These colloids encapsulate the hydrophobic material present, suspended in the water. These microcapsules are then cured or cross-linked by reaction with an aldehyde [28].

(b) Salt Coacervation

In this process, to an aqueous solution of polymer, an electrolyte, an inorganic salt, is added. Phase separation occurs and thus the polymer may encapsulate any undissolved or hydrophobic material. Curing or cross linking can be achieved afterwards. This process also has some problems, such as stickiness causing clusters of microcapsules to form and salt adhering to microcapsules [29]. Polymers such as polyvinyl alcohol, carboxymethyl cellulose and gelatine can be used in this process [30].

2.6.2 Interfacial polymerisation

In this process, a polycondensation reaction takes place between two compounds. The compounds are mixed in separate miscible solvents and then mixed together by stirring at high speed. The compounds react with each other to form polycondensate droplets due to high speed stirring [31–34]. Hydrophilic and hydrophobic materials can be encapsulated in this technique. The materials used widely for microcapsulation in this technique are urea or melamine and formaldehyde [35–37]. Epoxy resin, acrylic resin, acid chloride/phenol and polyisocyanate have also been used [38]. In the case of phenol systems, an amine curing agent is also used [39–42].

2.7 Applications of Thermochromic Materials

Thermochromic pigments are mainly used for temperature indication purposes. For example, if a thermochromic pigment acquires a green colour at a specific temperature, then on achieving this green colour the eye can detect the change in colour and hence the temperature can be observed. The thermochromic pigments can be calibrated accurately to change colour at specific temperatures and grading of temperature can be achieved by a range of thermochromic pigments, painted or coated on a strip. A common example of this is strip type thermometers which are used to measure body

temperature. This can even be used to measure body temperature of sleeping children or patients under anaesthetic [43].

Thermochromic pigments are commonly used in food containers, such as bottles, cans, mugs, kettles etc. to detect the correct chilling or hot temperature of the food or drink [44]. The hysteresis in the change in colour of cholesteric liquid crystals, which happens due to texture, is used in frozen food to indicate if the frozen food has been thawed and refrozen. In the Grandjean texture of cholesteric liquid crystals, selective colours are shown with a change in temperature. Once it has become an isotropic liquid, cooling down results in formation of the focal conic texture, in which, the light is reflected diffusely and exhibits as opaque. So this property can be employed in thawed/frozen food exploitation and in clinical thermometers for hygiene purposes. For reuse, mechanically realigning of thermochromic material is possible.

Biomedical thermography is used to diagnose many medical conditions. The cholesteric liquid crystals are normally used as a coated layer on a black sheet. The sheet is either elastic, to conform to the body surface, or rigid to provide a flat surface to allow photographic recording, minimising angle related variations in reflected colours. This has been used in detection of breast cancer and in locating the placenta of an unborn child.

Thermal mapping of materials can provide useful information in testing and diagnosing faults in engineering design. The thermochromic materials used in testing of engineering materials depend on sensitivity towards small temperature variations. If a small component is heated then defects can be identified by variation in thermal conductivity. The method has been used in the air craft industry in identifying blockages in coolant channels and also in identifying defects in heat resists elements on windscreens. The defective areas become visible immediately by colour changing due to variation in temperature. They also have been used in paints and crayons for hot spot indication on equipment [6].

Stress/strain identification can be made by thermochromic materials. When strain takes place in some materials, heat is produced and may be used to visualize the effect of strain. This technique can also be applied to locate weld flaws. Electronic circuits generate a large quantity of heat during operation. The abnormalities or variation in temperatures indicate underlying problems in the form of short circuits over heating due

to design or construction flaws, poor electrical joints, or areas which are non-operative. Some thermochromic materials are very sensitive towards variation in heat so they can be used to rule out microelectronic flaws [45].

Thermochromic liquid crystals have been used in the cosmetic industry in oil and moisturizers which use properties other than its change in colour phenomena. It is also found that liquid crystals can be used as carrier phase for vitamins etc. for skin products which are not only used for slow release of these products but also for prolonging the effective period.

Some of the thermochromic materials have been used as memory devices. In these devices, the cholesteric liquid crystals with coloured Grandjean texture are used. In the active form of a helical structure, the cholesteric liquid crystal is quenched in a smectic phase and becomes a glossy state. The colour change takes place when the material is heated from the glossy state to the smectic phase due to relaxation of the helical structure.

Thermochromic materials are used to indicate a visual response of the temperature change. Some thermochromic materials show change in colour with a slight change in temperature. Due to this characteristic, they are also used in batteries for battery life indication. They show the change in colour with slight variation in heat, produced by a working battery. Nowadays, the thermochromic materials are also being used in architecture as well as coating on walls, or in tiles, inside or outside of houses. The purpose of this use can be decoration, colour change effect with variation in heat or using its functionality to determine temperature, and absorbing and reflecting the sun light and ultimately using the data to save energy [46].

Conjugated intrinsic systems are used in optical temperature indicators and thermal recording [47,48]. Thermochromic materials also have been reported in toys, ornaments, hairbrushes, kitchen utensils, toilet seats, golf balls, kettles, umbrellas, jewellery display etc. [49–53]

2.7.1 Thermochromic Materials in Textiles

In textiles, two types of thermochromic materials have been applied, that is, leuco dye based thermochromic pigments and liquid crystals. Both of these classes of thermochromic materials need microencapsulation prior to application. The application

of thermochromic materials as dyes onto textile fibres, whether these are natural or synthetic fibres, experiences difficulties due to lack of affinity and water insolubility. Due to these reasons these are normally applied as pigments with some binder systems on the surface of the fabrics. Coating of filaments and fabrics with some polymeric binder systems containing encapsulated thermochromic materials have also been reported [54,55]. The colour strength of these pigments is less as compared to other commercially available pigments. This is due to a low amount of dye being present in the final formulation which is about 2% in weight prior to microencapsulation and lesser in the final product. Therefore, to avoid pale shades, these pigments are used at 15-30% by weight in the coating [9]. Due to the large quantity of pigments, the feel and handle of the fabric is affected.

Printed and coated leuco dye based thermochromic pigments with permanent colour have been used in T shirts marketed by the Global Hypercolor brand in 1991. The permanent colour was used to provide a change of colour from one to another instead of colourless. However, fastness properties of these products were poor especially wash fastness. Some children's clothing with thermochromic effects have also been reported, to visualise the change in body temperature [56]. The thermochromic material is applied prior to, or after, the garment's manufacturing in the form of coating and printing with the help of a binder system [57]. Similarly, leuco dye based thermochromic pigments have been used in jeans which become colour to colourless with body temperature. The idea was to simulate the indigo-faded effect of jeans by means of thermochromic pigments [58].

Thermochromic pigments containing colour formers have been incorporated in man-made cellulose fibres during filament formation [59]. The wet spinning technique was used for this purpose. The leuco dye based thermochromic pigments were mixed with cellulose in a spinning bath and filaments obtained in this way showed the thermochromism. Thermochromic materials have also been incorporated with different polymers during melt spinning. Thermochromic acrylic fibres have been produced in this way [60]. Industrial fabric incorporating thermochromic materials have been produced for heat profiling of thermal processes [61]. Nonwoven fabrics having leuco dye based thermochromic pigments also have been developed by a melt spinning technique [62]. Waterproof apparels made by flexible PVC sheet or other polymers have been reported. These materials incorporate thermochromic materials which change colour with change in ambient temperature [63,64]. A multilayer polymer

composite has been developed with one or more thermochromic incorporated and with other polymer layers. In the development of this composite, a melt extrusion technique has been employed [65].

A thermochromic dry offset ink has been developed by dispersing microencapsulated thermochromic material in the dry offset ink medium. This ink has been used for printing articles. It has been found that thermochromic offset ink is pressure resistant and heat resistant. This technique can be used for uniform prints using high speed continuous printing on different materials [66].

The thermochromic materials have almost no affinity for textile filaments due to which dyeing with these materials is very difficult. A dyeing method has been developed by cationization of cotton fabric. In this method, the cotton is first treated with a cationic compound and then this fabric is treated by immersing in the dispersion of reversible thermochromic materials present in a high polymer compound [67].

To develop new methods for the implementation of thermochromic materials in textiles, some research has been carried out on evaluation and also improvement of performance. Subjective colour perception of colour change was originally used. Bryant developed a technique to measure thermochromic liquid crystals instrumentally [19,20,25]. An arrangement of a spectrophotometer together with a hot stage was set up to take the colour measurements at different temperature intervals. For measurements lower than room temperature, ice chilled water was circulated with the help of peristaltic pump. The cholesteric liquid crystals which normally require a black background for colour play, were also evaluated over backgrounds of other colours. The coated and printed samples were evaluated for film thickness, reversibility, hysteresis and various fastness properties.

An investigation of leuco dye based thermochromic pigments has also been carried out, in which the thermochromic pigments were screen printed and UV cured for evaluation purposes [68]. The colour measurements were taken at different temperature intervals with the help of a spectrophotometer. These samples were evaluated for durability, reversibility, combinations of different colours and the activation temperature of these pigments. Irreversible thermochromic pigments have been used in metallic/textile fibres for the visual detection of density atomic species present during the nitrogen plasma treatment [69]. The plasma treatment process depends upon the density of

active species present on the surface of the substrate and hence diagnostic processes are also available but at higher cost. The irreversible thermochromic materials used in this study can be at lower cost and detection can be carried out without any highly qualified personnel.

From a textile designer's perception, an investigation has also been carried out based on the potential of thermochromic materials in textiles used with electronic heat profiling circuitry [70,71]. The different potential applications of thermochromic materials, both leuco dye based and liquid crystals, from a designer's point of view, were discussed [72]. The main focus of this investigation was interior textile design in a study at the design and technology interface.

In normal dyeing and printing, a change in colour or fade in colour is undesirable and considered a flaw. Sometimes, the dyer needs to be cautious in colour matching when a sample is taken out from a dryer as colour may change due to heat. This effect has been observed in acid dyes, especially in the case of yellow and orange, applied on nylon. One such typical example is 'Tectilon Orange 3G' (CI Acid Orange 156) as shown in Figure 2.15 [43].

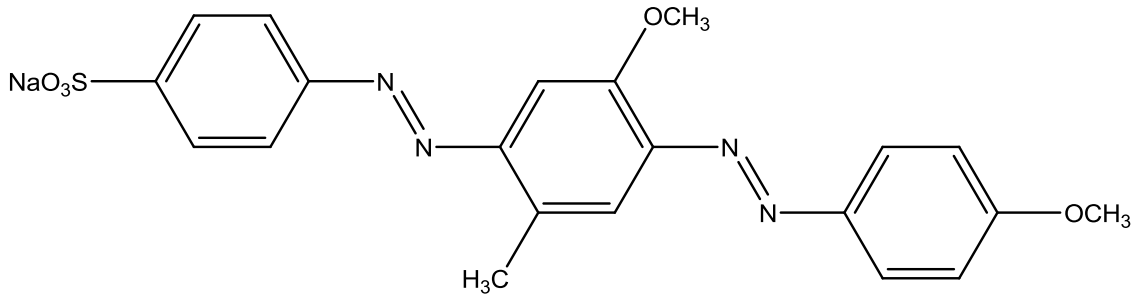

Figure 2.15 CI Acid Orange 156

Thermochromic leuco dye based and liquid crystals are thus being used in textiles but not to a vast extent. They have some issues such as inadequate wash and light fastnesses, their high cost and limited availability. However, these materials have good commercial potential especially in the case of smart textiles. As much research is in progress in this area, it is to be hoped that the deficiencies of these materials will be overcome and they will have a significant commercial application in future.

2.8 Light fastness

The fastness properties of a material refer to the resistance of the material so that it maintains its original state against foreign intervention. The lightfastness is the property of a material referring to its ability to withstand exposure to sunlight or artificial light so that it retains its original form and resists degradation due to light. This may be degradation of structure, colour or physical or chemical properties.

2.8.1 Photodegradation of colour

It is commonly observed that colours are faded or degraded with prolonged exposure to sunlight. The ultraviolet light present in sunlight raises the energy level of loosely-held electrons in chromophores so that they become more active. Thus, the ultraviolet component of sunlight initiates degradation reactions in chromophores, and these reactions are normally accelerated in moist conditions [73]. Normally, three types of mechanisms are involved in degradation of colours in textiles, i.e., photo-oxidation through singlet oxygen, photo-oxidation through superoxide and photo-reduction through radical species [74]. In the first two processes, the light raises the coloured molecule to an excited state, i.e., its triplet form as shown in Equation 2.3. In the first mechanism, the excited triplet form sensitises the oxygen which further react with the coloured molecule to degrade it as shown in Set of equations 2.4. In the second mechanism, an electron from the excited triplet form of the coloured molecule transfers to the oxygen to form superoxide which further reacts to decompose the molecule as shown in Set of equations 2.5. There is less chance of oxidation if the excited triplet form remains for only a short time.

$$Dye + h\upsilon \rightarrow {}^{3}Dye^{*}$$

Equation 2.3

$${}^{3}Dye^{*} + O_2 \rightarrow Dye + {}^{1}O_2$$

$${}^{1}O_2 + Dye \rightarrow Decomposition$$

Set of equations 2.4

$$Dye^{*} + O_2 \rightarrow Dye^{+\bullet} + O_2^{-\bullet}$$

$$O_2^{-\bullet} + Dye \rightarrow Decomposition$$

Set of equations 2.5

In the third mechanism, the excited triplet form of the colour reacts with a nearby substrate, impurity etc. to abstract a hydrogen atom which leads to the decomposition of the dye as shown in Set of equations 2.6. The presence of oxygen does not affect this process which normally happens in presence of impurities.

$$Dye^{*} + RH \rightarrow HDye^{\bullet} + R^{\bullet}$$

$$HDye^{\bullet} + R^{\bullet} \rightarrow Decomposition$$

$$R^{\bullet} + O_2 \rightarrow RO_2^{\bullet}$$

$$R^{\bullet}/RO_2^{\bullet} + HDye \rightarrow Decomposition$$

Set of equations 2.6

2.8.2 Photo-degradation of Thermochromic Pigments

In section 2.3.2, it has been described that crystal violet lactone analogues (diarylphthalide compounds) and fluoran dyes are the compounds mostly used as colour formers in the leuco dye type thermochromic pigments. These dyes have been observed to react adversely with the sunlight and fade very quickly. As the use of these thermochromic pigments is increasing day by day, attempts have been made to improve their lightfastness. In some research papers, ultra violet absorbers capable of acting as amphoteric counter ions have been mentioned to be good lightfastness improvers. In these research work, zinc and nickel (2,4-dihydroxybenzophenone-3-carboxylates), [5-(2-benzotriazolyl)-2,4-dihydroxybenzoates], [3-(2-benzotriazolyl)-2-hydroxy-1-naphthoate] and their derivatives have been proposed as good stabilizers against fading due to light [75–77].

2.8.3 Lightfastness Improvement Additives

The additives used in the study described in this thesis in attempt to achieve lightfastness improvement are ultra violet (UV) absorbers, hindered amine light stabilisers (HALS) and antioxidants.

(a) UV absorbers

As discussed in section 2.8.1, the UV portion of light causes photo-degradation of colours. Thus, one way of controlling photo-degradation is to reduce the UV content in the incident light. UV absorbers absorb certain wavelengths in UV light and dissipate it in the form of heat. As this happens in tautomeric forms of UV absorbers, these additives function for a long time [78,79]. Normally, UV absorbers are designed to absorb radiation in the 290-350 nm region but the range may extend up to 400nm to protect binders used in the application of pigments [80]. UV absorbers can be classified into two main groups on the basis of chemical classes, i.e., phenolic and non-phenolic.

In phenolic UV absorbers, an O—H---O bridge is present in the molecules. Some examples are given in Figure 2.16.

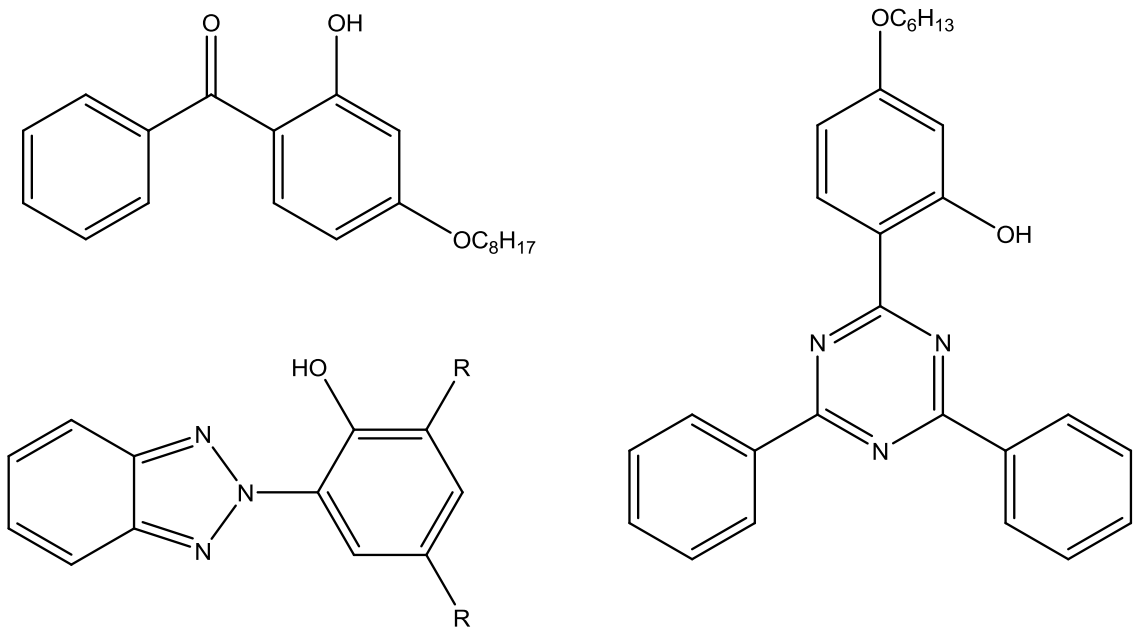

Figure 2.16 Phenolic UV absorbers

These phenolic UV absorbers absorb the harmful UV light of the sun by converting it into vibrational energy as shown in Figure 2.17.

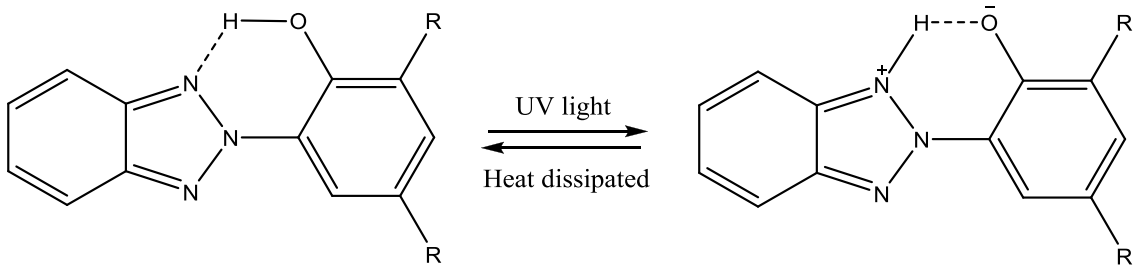

Figure 2.17 Mechanism of phenolic UV absorber

In non-phenolic UV absorbers, the detail of the mechanism is not very clear but it is assumed that an excited state is achieved, as in phenolic UV absorbers, by transfer of proton and UV energy is converted to vibrational energy. Some non-phenolic UV absorbers are given in Figure 2.18.

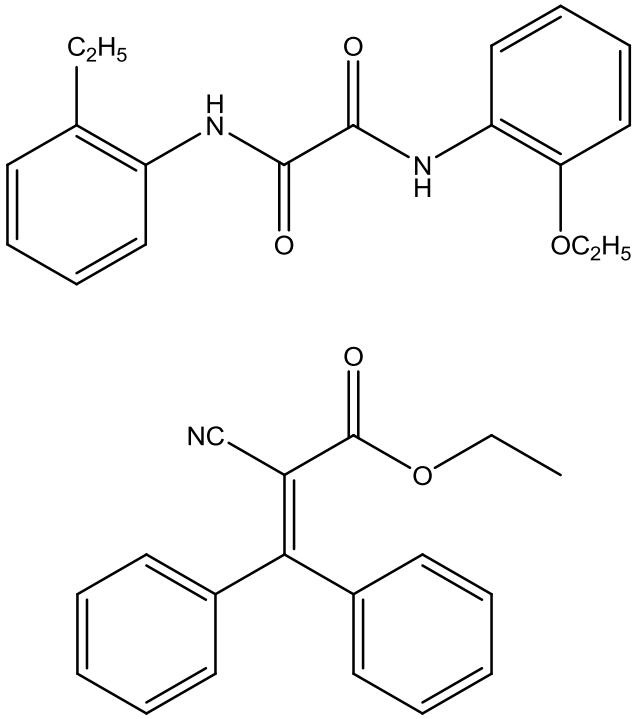

Figure 2.18 Non-phenolic UV absorbers

UV absorbers are normally used in polymers to protect them against photo-degradation but they also have been used in coatings and fabrics [80]. In textiles, they have been used to enhance the lightfastness of disperse, natural and reactive dyes [81–85].

(b) HALS

Hindered amine light stabilisers or HALS are normally used for improving resistance against photo-degradation of polymers. They are free radical scavengers that act as

'cleansing agents' by reacting with intermediate photo-degradation products. Some examples of HALS are given in Figure 2.19 [86–89].

The cyclic action of HALS is given in the following steps:

- Oxidation of HALS occurs to form radicals i.e., >NO•;
- Non-radical amino ethers >NOR are formed by the reaction of >NO• and free radicals R•;
- Reaction of >NOR with peroxy radicals to form >NO• radicals again.

A description of the HALS reaction mechanism is given in Figure 2.20.

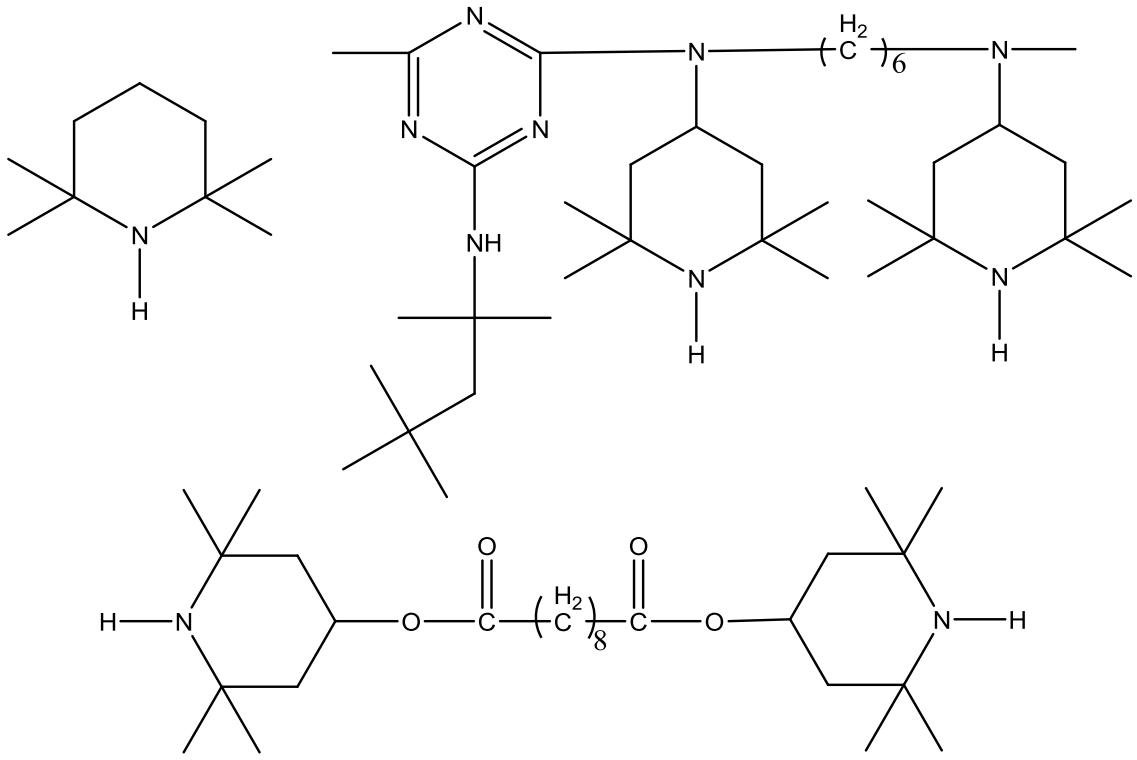

Figure 2.19 Some examples of HALS

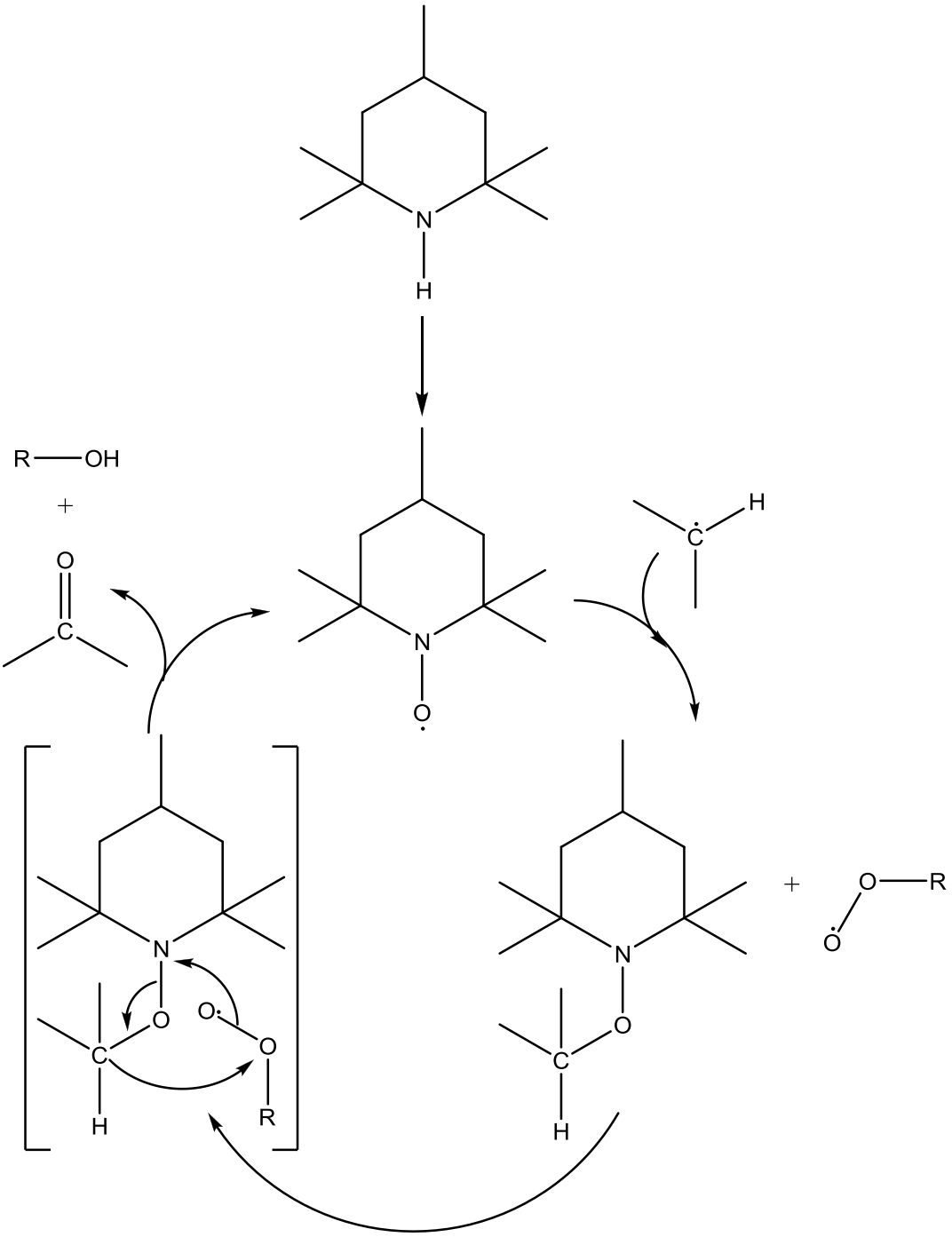

Figure 2.20 Mechanism of HALS

(c) Antioxidants

Antioxidants prevent degradation of colour by the process of oxidation, caused by exposure to light or heat, in three ways [90–92]:

- They trap carbon radicals, produced by degradation;
- They trap peroxy radicals produced by carbon radicals and oxygen reactions;

- They decompose hydroperoxide, produced by peroxy radicals.

Some antioxidants are shown in Figure 2.21 and their mechanism in Figure 2.22.

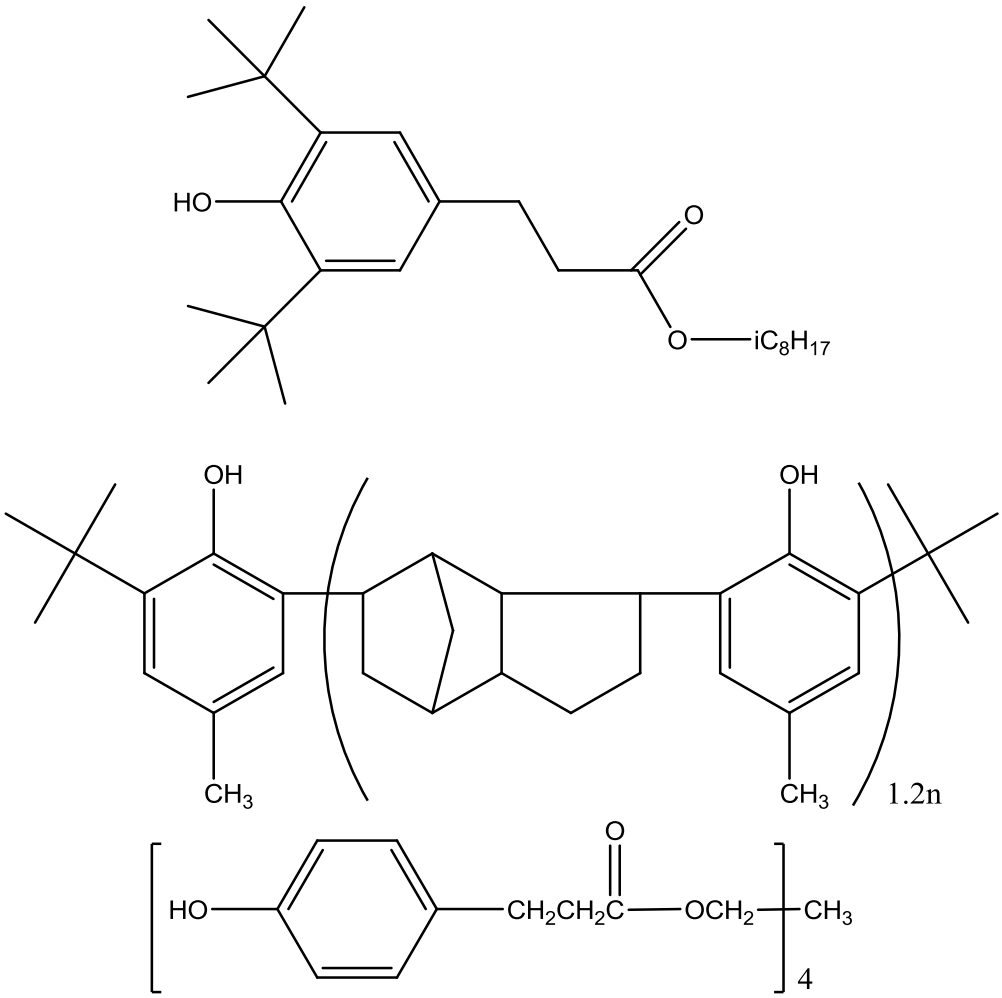

Figure 2.21 Antioxidants light stabilisers

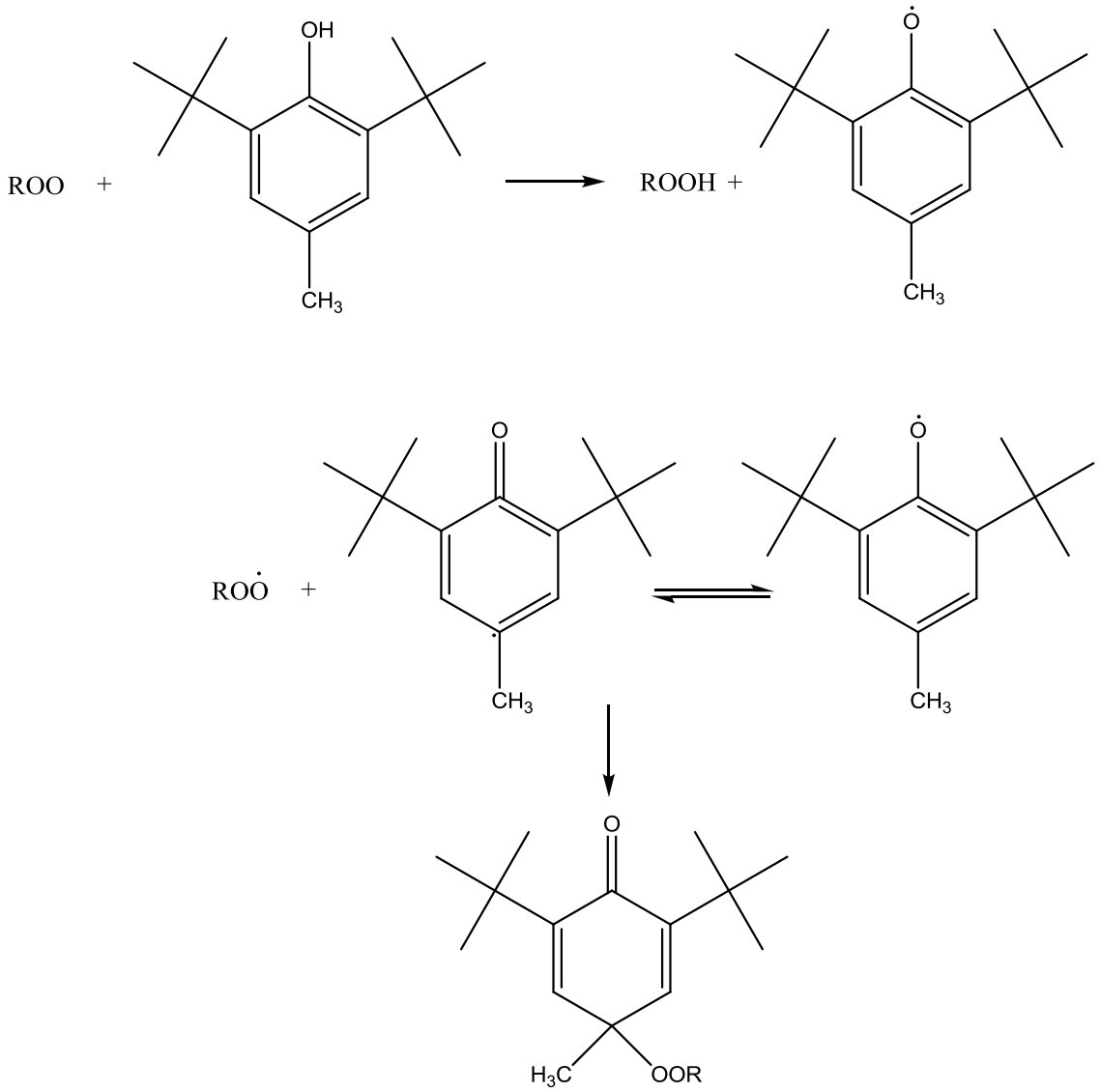

Figure 2.22 The mechanism of antioxidant light stabiliser

2.9 Fibre

The history of clothing goes as far back as the history of mankind. Among the earliest items to be used for the purpose of clothing were leaves from trees, animal skins, etc. These materials were stubborn, uncomfortable, redolent and difficult to process. With the development of human civilization, natural fibres such as cotton, jute, silk, wool etc. were spun and interlaced to make clothes which were flexible, comfortable and easy to process [93,94]. With increases in population, the demand for clothing also increased. Similarly, as civilization developed, fibres with versatile properties were needed for usage in other areas of life. The increasing demands of clothing and the need for fibres with enhanced properties opened the door for man-made fibres. Today, a number of man-made fibres are known, including fibres derived from natural origin and also purely synthetic fibres. The name of fibres in use are summarised in Figure 2.23.

2.9.1 Fibre Forming Polymers

A fibre is normally defined as polymer in a form that is at least 100 times longer than it is thick. However, most fibres are thousands of times longer than their thicknesses [73]. A filament is a very long fibre, sometimes a few hundred meters long as in the case of silk and sometimes in kilometres for example in the case of certain man-made fibres. The general properties that are desirable in a textile filament are as follows, although it is not necessary to have every one of these or even some of them:

- Hydrophilic;
- Chemically resistant;
- Linear;
- Long;
- Capable of being oriented;
- Polymer system with a high melting point.

The man-made fibres can be engineered according to required needs and uses envisaged, and depending also on the available material.

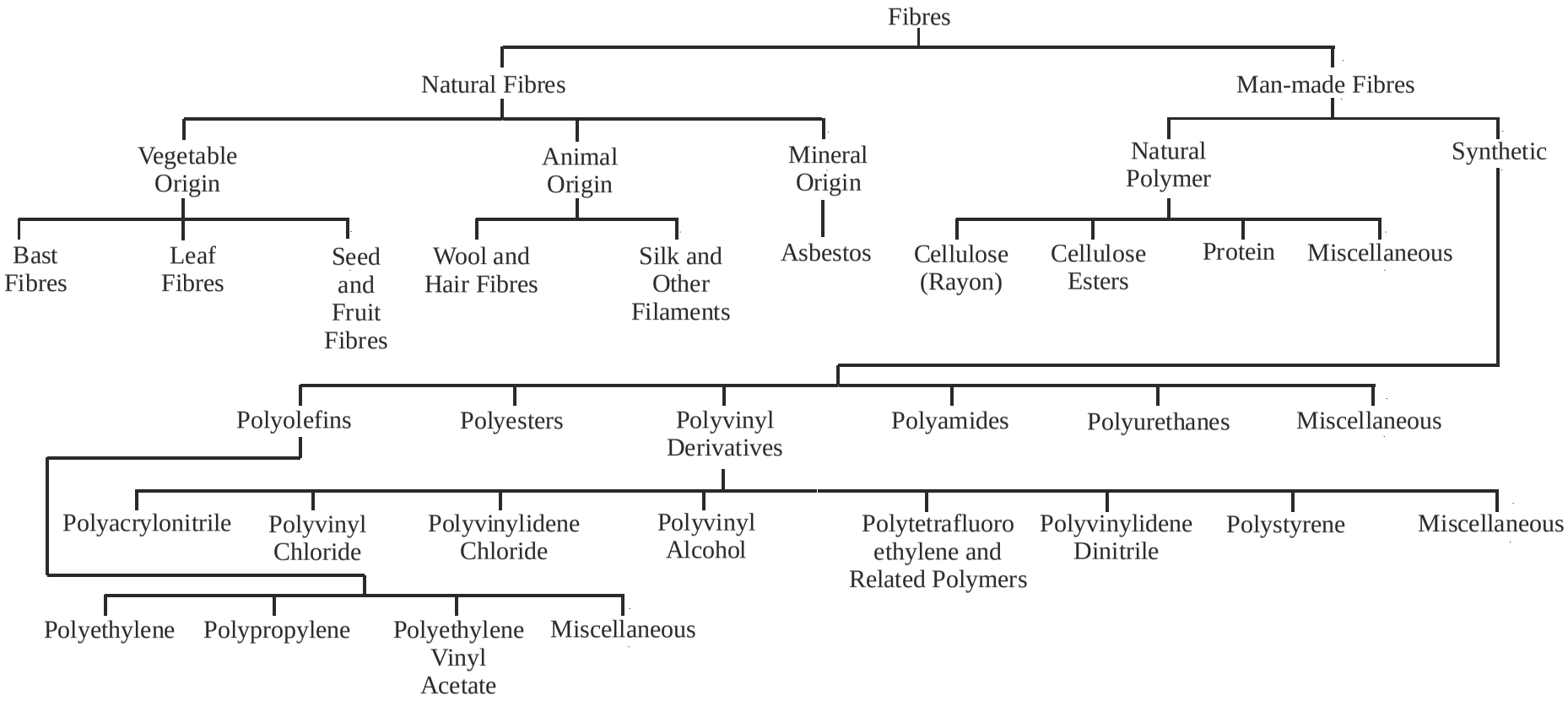

Figure 2.23 Fibre Chart [94]

2.10 Specific Polymers

This section contains a review of those polymers used in the work described in this thesis. The leuco dye based thermochromic pigments are known to be sensitive to heat during extrusion. To evaluate their behaviour towards heat and the possibility of successful extrusion, a range of polymers with different, although relatively low, extrusion processing temperatures, specifically polypropylene, linear low density polyethylene and ethylene vinyl acetate were used.

2.10.1 Polypropylene

The polyolefin class of polymer, also known as polyalkenes, such as polyethylene, polyisobutylene and isobutylene-isoprene copolymers were known up to middle of the 1950s. Other classes of polyolefins were known but polymerized only to low molecular weights. In 1954, Natta produced high molecular weight polymers from propylene and other olefins using specific Ziegler-type catalysts. Using modified Ziegler-type catalysts, he obtained higher molecular weight polypropylene with different grades [95].

Polypropylene can be obtained polymerized in three different types of stereoisomeric forms; atactic, syndiotactic and isotactic as shown in Figure 2.24. In the atactic form, the methyl groups are arranged randomly around the main chain. In the syndiotactic form, methyl groups alternate regularly between both sides of the chain and in the isotactic form, methyl groups are arranged all on one side of the main chain.

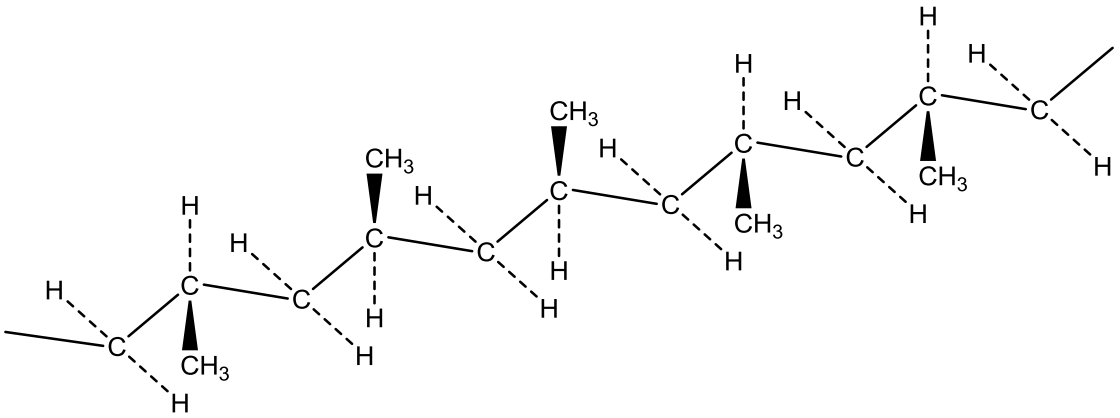

Atactic: methyl groups arranged randomly

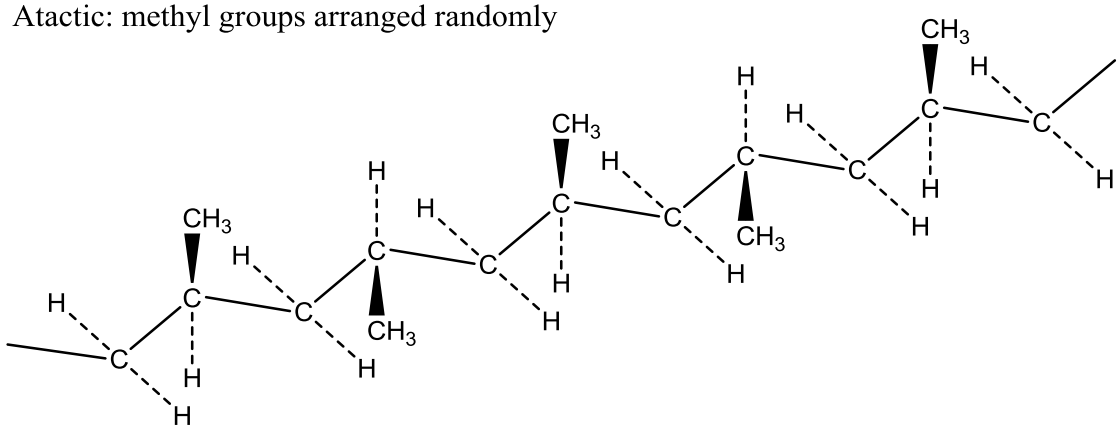

Syndiotactic: methyl groups arranged alternately

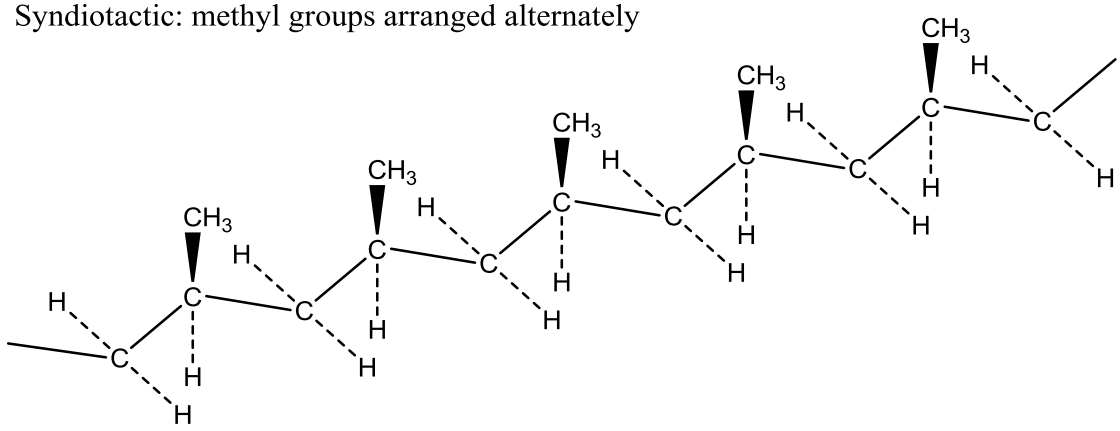

Isotactic: methyl groups arranged on same side

Figure 2.24 Stereoisomeric forms of polypropylene

The syndiotactic and isotactic forms have a regular pattern and are crystalline while the atactic form has an irregular pattern and is amorphous. In actual conditions, perfect syndiotactic or isotactic forms are not available. There may be partly atactic arrangements found along with syndiotactic or isotactic forms and in mass quantity all three forms can also be present. The isotactic polypropylene in its crystalline state shows a helical formation with either a clockwise or anticlockwise twist. This formation provides the optimum balance between inter atomic repulsive forces and van

der Waals attractive forces present between methyl groups. Thus, this stereoisomeric form is most favourable as shown in Figure 2.25 [93,95].

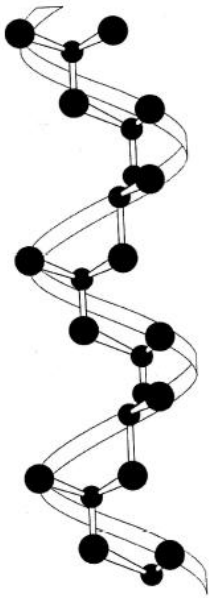

Figure 2.25 Helical arrangement of isotactic polypropylene

(a) Monomer

The propylene monomer is obtained by the cracking of petroleum products such as natural gas or light oils. It is a basic ingredient in the C3 fraction (propylene and propane) and can be separated easily from other gases by fractional distillation. It is more difficult to separate propane and propylene and this depends on the design of the distillation plant. Before polymerization, it is necessary to remove impurities such as water, methylacetylene etc.

(b) Polymerization of Propylene

Polymer properties rely on the composition of the catalyst as well as its particle shape and size. One of the catalyst systems used is prepared by the reaction of titanium trichloride with aluminium triethyl, butyl or diethyl monochloride in naphtha under nitrogen in the form of a slurry which contains 10% catalyst and 90% naphtha.

The first commercially developed method for polymerization of propylene was the suspension process. In this method, propylene is taken up in a vessel under pressure and catalyst solution and a diluent, usually naphtha, is added separately. The temperature of reactions is kept at 60°C for 1-4 hours in the case of a batch process. The yield of polymer obtained in this way is about 80-85%. This process is completed

at a temperature lower than the melting point of the polymer, and a suspension is formed. The molecular weight of polypropylene can be kept specific by a chain transfer reaction with hydrogen, brought about by changes in the catalyst composition and quantity, temperature of the reaction and the pressure within the reactor.

After polymerization in this process, isotactic and atactic polypropylene, solvent, monomer and catalyst are present in the reactor. The monomer is separated by transferring material into a flash drum. By centrifugation, the solvent along with atactic polymer which is soluble in the solvent are removed. A solvent such as methanol with traces of hydrochloric acid is used to treat the rest of the material to decompose the catalyst and to dissolve the residue. This solution is then centrifuged and the polymer that is deposited is washed and dried at 80°C. Sometimes, extra processes are used to reduce the quantity of the atactic form in the polymer [93–95].

Catalyst systems with magnesium compounds have also been developed to improve the production of isotactic polypropylene. Liquid and gas phase methods have also been developed, which offer the advantages of avoiding separate washing processes and also processes for separation of residual material such as catalyst, solvent, atactic polymer etc. The molecular weight distribution is also controlled by thermal and chemical treatments. In one of these types of systems, developed by Himont, three ingredients were used; a titanium composition with a magnesium halide, an organo-aluminium composition and a Lewis base.

Polypropylene may also be produced using metallocene catalysts. In this process, a reaction is created in the gas phase with a co-catalyst of methylaluminoxane (MAO). By appropriate catalyst selection, the required stereoisomeric form of polypropylene can be obtained. In this process, a polymer with isotactic units configured alternately has been developed and is known as hemi-isotactic polypropylene. Using a metallocene catalyst, copolymerization of propylene with long chain olefins, cyclic olefins and styrene is also possible [95].

(c) Properties of Polypropylene

The degree of crystallinity of polypropylene varies at both extreme ends. In the case of the atactic form it is totally amorphous while in the case of pure isotactic form it is 100% crystalline. Normally commercially available, polypropylene has content of 60-70% crystalline regions. The polypropylene filaments are smooth on the surface and are

waxy in appearance. Normally, these filaments are round in shape but they can be also produced in different shapes, according to the shape of the die.

The tenacity and tensile strength of polypropylene varies according to requirements and use. Normally, filaments have a tenacity of 3-5 g den^{-1} with a tensile strength in the 35,000-60,000 lb in^{-2}. For yarn, the tenacity is around 9 g den^{-1} although for special purposes, it can be around 13 g den^{-1}. The elongation at break is 15-25%, 20-30% and 20-35% for monofilaments, multifilament yarns and staple fibre respectively. The elastic property of polypropylene varies with the type of polymer and the processing conditions. The high tenacity fibres have 90% immediate recovery after 10% elongation. For medium tenacity fibres, with 5% elongation, it is 90-98% and 90-95% for multifilament and staple respectively. Low tenacity fibres show 95% immediate recovery and 100% recovery after 5 minutes with an extension of 50%. The creep resistance of polypropylene is satisfactory but not as good as polyamide fibres. On applying a load of 1.5 g den^{-1} for 16 hours, its cold flow is up to 0.5%.

Specific gravity of polypropylene is relatively low. For amorphous polymer, it is 0.85, for commercial fibres it is 0.90-0.91 and for highly crystalline fibres it is 0.92-0.94. Polypropylene is paraffin (alkane) in nature and thus does not absorb water. Water or steam does not degrade polypropylene and has no effect on the tensile properties of the polymer. The softening temperature is around 150°C for polypropylene fibres while the melting temperature is 160-170°C. Increasing temperature, below the softening point, affects the mechanical properties of fibres. The flexibility of polypropylene fibres remains the same up to -70°C. Shrinkage depends on the finishing of the fibres but if kept in boiling water for 20 minutes, they shrink by 15-20% in the case of monofilaments and 0-10% in case of multi-filaments and staple yarn.

Oxygen in air attacks polypropylene and can cause degradation by oxidation in the presence of sunlight. Stabilizers may be used to prevent this degradation. Polypropylene is a highly chemically resistant material. Acids and alkalis have no effect on the polymer. No common organic solvent dissolves the polymer at room temperature. Insects and pests cannot digest polypropylene. Micro-organisms such as bacteria or fungi have no effect on polypropylene. Polypropylene has high electrical insulation properties. As it shows no absorption of water, so in high humidity levels, its electrical insulation remains the same [94].

2.10.2 Linear Low Density Polyethylene

Polyethylene is a polymer of ethylene and produced by addition polymerization. On a commercial scale, the polyethylene was first developed by a high pressure method. The polymer produced in this method normally has more branches and is known as low density polyethylene (LDPE). Afterwards, catalysts methods were developed to produce a polymer with less branches, with high density which is named as high density polyethylene (HDPE).

Linear low density polyethylene (LLDPE) was produced to fill the gap in properties between low density polyethylene and high density polyethylene. LLDPE is replacing LDPE and HDPE blends and it is tougher than LDPE. It has a lower brittle temperature than LDPE. LLDPE has more resistance to puncture by hard particles than LDPE and is replacing it in film blowing and casting applications. A comparison of properties of LDPE, LLDPE and HDPE is given in Table 2.2 [96]:

Table 2.2 Properties comparison of different polyethylene [96]

Property	**LDPE**	**LLDPE**	**HDPE**
Melting point (K)	383	393-403	>403
Density (g cm^{-3})	0.92	0.92-0.94	0.94-0.97
Film tensile strength (MPa)	24	37	43

The structural difference between LDPE, LLDPE and HDPE is illustrated in Figure 2.26. The low density polyethylene (LDPE) has more branches due to which chances of amorphous regions are greater and the density of the polymer is relevantly low. In the case of high density polyethylene (HDPE), the branches are much less in comparison to LDPE and have a relevantly high density. Linear low density polyethylene is intermediate between LDPE and HDPE. It has more branches than HDPE but less than LDPE and has intermediate properties as well.

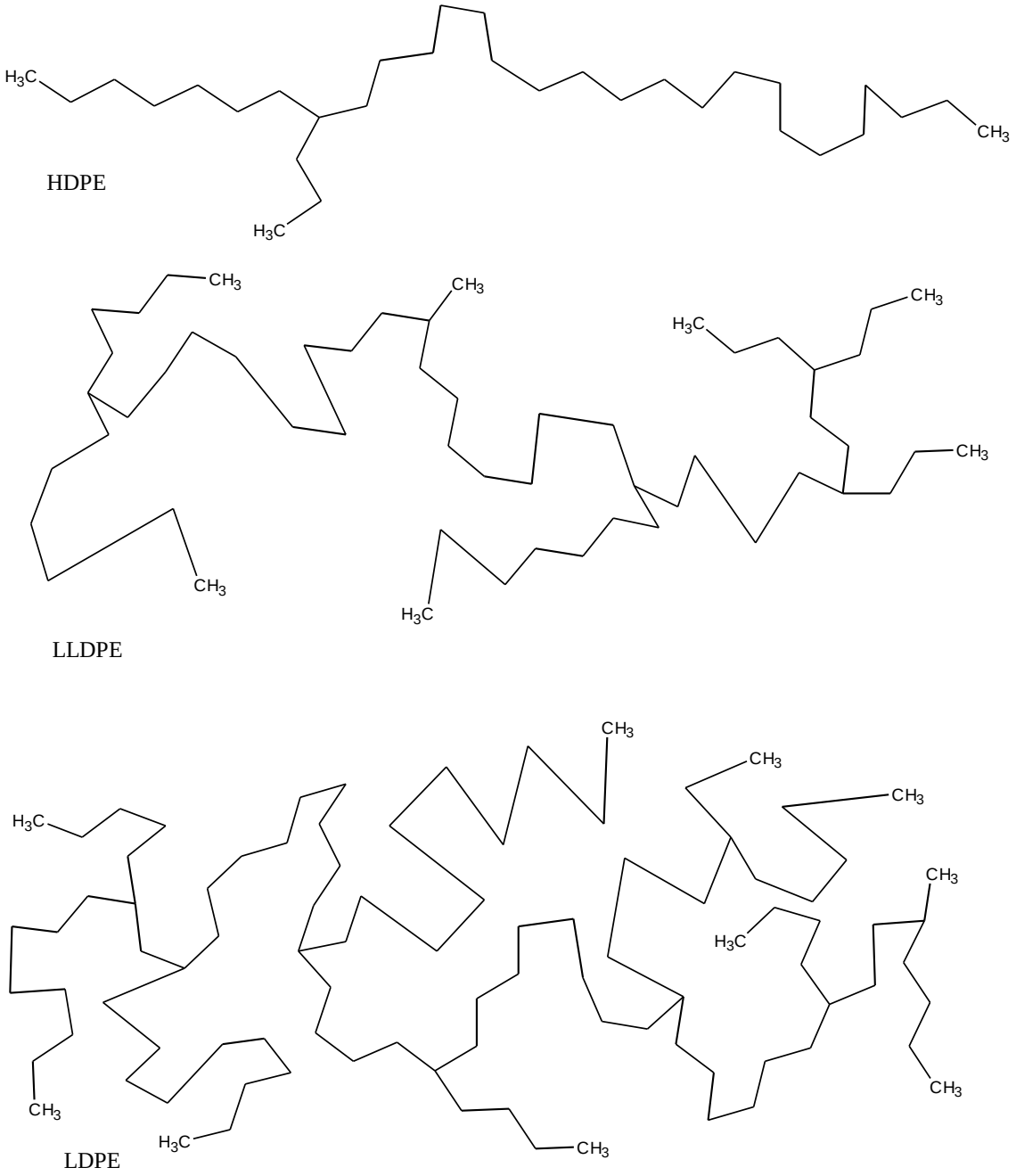

Figure 2.26 Essential structure difference of HDPE, LLDPE and LDPE

(a) Monomer

In former times, ethyl alcohol (ethanol), obtained from molasses as a by-product from sugar production, was used to manufacture ethylene. Ethylene was obtained by dehydration of ethyl alcohol. Nowadays, it is obtained from petroleum sources. From natural or petroleum gas, it is obtained on a large scale by high temperature cracking of ethane and propane. Ethylene can be obtained by fractional distillation and selective absorption of other gaseous products obtained from gasoline cracking.

(b) Manufacture of Linear Low Density Polyethylene

In the late 1980s, the metallocene single-site catalyst technology was developed. The metallocene catalysts are based on transition metals such as zirconium or titanium, incorporated with a cyclopentadiene type group. The olefin reacts only at a single side of the catalyst molecule which ensures better control over the polymerization process. Union Carbide developed a gas phase process. Gaseous monomers and a catalyst are fed to a fluid bed reactor with a pressure of 100-300 lb f in^{-2} and temperatures of 100°C and below. It is polymerized to provide a copolymer of ethylene with 8-10% of an α-olefin such as propene, but-1-ene, pent-1-ene, hex-1-ene or oct-1-ene. A liquid phase process was invented by Dow, and is considered to be based on a Ziegler-type catalyst, referred as constrained geometry homogeneous catalyst. Group IV transition metals such as titanium, bonded with mono-cyclopentadiene group and having a hetero-atom such as nitrogen as a bridge, make the catalyst.

In 1998, BP Chemicals jointly with Imperial College of London, and working independently, DuPont with the University of North Carolina made catalyst systems based on iron and cobalt. These systems are basically tridentate pyridine bis-imine ligands coordinated to iron and cobalt. By means of these systems, polymerization can be carried out at low pressures such as 200-600 psi and products can be obtained with melting points up to 139°C and with a low number of branches, for example 0.4 branches per 1000 carbon atoms. According to the claim of these inventors, many advantages of the metallocenes can be realised at a lower cost by using their systems [97]. The uses of higher alkenes normally introduce small branches. By appropriate selection of co-monomer type, different grades of linear low density polyethylene can be produced. For example, LLDPE produced using oct-1-ene result in keep in apart other chains due to longer branching as compared to LLDPE produced by but-1-ene. This results in a lower density [97,98].

(c) Properties of Polyethylene

Polyethylene is a wax-like thermoplastic material. In mass quantity, it appears translucent or opaque but may be transparent in thin films. Its softening point is about 80-130°C and the specific gravity is 0.92-0.97 which is less than water. Its tensile strength is moderate but it is a tough material. Its tenacity varies from 1-8 g den^{-1} depending upon the grade of the polymer. The tensile strength varies from 15,000 to

90,000 psi. The elongation at break is 10-50% depending on the type of polyethylene. The mechanical properties of polyethylene depend upon on a number of factors such as molecular weight, degree of branching of the polymer, temperature of the test, the sample preparation method, size, shape and the conditioning of the sample in some cases. The molecular weight and number of branches according to the type of polyethylene also play an important role in determining the mechanical properties.

Polyethylene is chemically resistant as it is a paraffin (alkane). It is inert to alkalis, non-oxidizing acids and aqueous solutions. Nitric acid oxidizes polyethylene and destroys its mechanical properties. Oxidation of polyethylene takes place at low temperatures, for example 50°C. Oxidation causes structural changes in polyethylene and ultimately deteriorates its properties. It is insoluble in common solvents at room temperature but at 70-80°C, the fibres swell and may dissolve in benzene, toluene and xylene, etc.

Polyethylene is a dielectric and non-polar material and has very good electrical insulating properties. Its dielectric constant and power factor are nearly independent of temperature and frequency. Polyethylene fibres show a creep effect when subjected to a load for a long time. The effect depends on the number of branches present in the polymer. Thus, polymers with a low number of branches show more creep as compared to polymers with a high number of branches. The glass transition temperature (Tg) of polyethylene is quoted differently in different literature sources ranging from -120°C to -20°C. Its flow properties when heated such as viscosity and melt flow index depend on average molecular weight. Polyethylene remains flexible when subjected to very low temperatures. At high temperatures, it does not degrade readily. In the presence of a stabilizer, it can be stable to 315°C for a short time interval.

Polyethylene undergoes oxidation by oxygen in air in the presence of ultra violet light. There is a more pronounced effect on low density grades as compared to high density grades. In the case of filaments, where the exposed area ratio is higher, the effect is more pronounced. By using a stabilizer, there has been a significant improvement. The absorption of water by polyethylene is zero and thus moisture does not have any effect on the polymer. The dry and wet strengths of polyethylene are the same. Insects and other living creatures cannot digest polyethylene. It is entirely resistant to bacteria, mildew and other micro-organisms [94,97–99]. In general, the properties depend on molecular weight and the density of material, those of LLDPE lying between LDPE and HDPE.

2.10.3 Copolymer of Ethylene Vinyl Acetate (EVA)

Ethylene vinyl acetate is a copolymer of ethylene and vinyl acetate, commonly referred to as EVA. The amount of vinyl acetate varies from 10-40% in the copolymer, so that ethylene contributes a larger part. The polymer behaves as an elastomeric material when considering softness and flexibility. It has the ability to be processed in the same way as other thermoplastic materials.

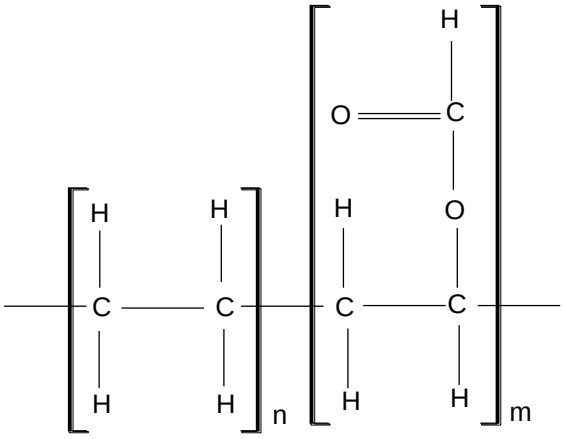

Figure 2.27 Polymer of ethylene vinyl acetate

(a) Monomers

The monomers of ethylene vinyl acetate are ethylene and vinyl acetate. The production of ethylene monomer has been discussed in section 2.7.2 (a). On an industrial scale, vinyl acetate is produced by reaction of acetylene and acetic acid or by oxidation of ethylene. In a liquid phase process, acetylene is reacted with a solution of glacial acetic acid, acetic anhydride and mercuric sulphate in agitation to obtain vinyl acetate. Vinyl acetate is removed from the reactor quickly to prevent the formation of ethylidene diacetate at higher temperatures. In the vapour phase process, the acetylene and acetic acids are passed through a tube at 210-215°C in the presence of cadmium acetate, zinc acetate and zinc silicate as catalysts. The monomer is obtained from these two reactions by distillation.

The Celanese Corporation of America prepared vinyl acetate using light petroleum gases. The oxidation of butane produces acetic acid and acetone. From these products, acetic anhydride and acetaldehyde are obtained. These products react with each other to produce ethylidene diacetate. By mixing ethylidene diacetate with an aromatic sulphonic acid in the presence of acetic anhydride as a diluent at 136°C, vinyl acetate is obtained with other products, which can be separated and recycled.

Nowadays, vinyl acetate is obtained by oxidation of ethylene. The ethylene is carried through a palladium chloride solution in acetic acid containing sodium acetate. The vinyl acetate is produced in good yield as a result. This reaction is possible in liquid and vapour phases, but the vapour phase is preferred due to corrosion problems in the liquid phase. Vinyl acetate can also be produced in one step. In this process to obtain vinyl acetate, ethylene is carried through a solution of acetic acid containing cupric chloride and copper or sodium acetate with a palladium catalyst [100].

(b) Manufacture of Copolymer of Ethylene Vinyl Acetate

The copolymer of ethylene vinyl acetate is obtained by the combined polymerization of ethylene and vinyl acetate monomers at a high pressure. The pressure of the vessel is kept at between 25-125 MPa and the temperature is between 250-375°C [101]. The development of Pd/phosphine-sulfonate catalysts made it possible to copolymerize vinyl acetate with linear polyethylene. By a coordination copolymerization mechanism, the copolymer of ethylene vinyl acetate is obtained. The ethylene and vinyl acetate are mixed with Pd/alkylphosphine-sulfonate type complex at 80°C [102].

In another method, a tridentate Fe(II) dichloride complex, toluene and methylaluminoxane are added to an autoclave at 50°C. Then vinyl acetate and ethylene are added into the autoclave to provide the copolymer of ethylene vinyl acetate [103]. Improved control of the copolymerization process of ethylene vinyl acetate and production of different grades of the product were achieved by the use of dynamic neural networks and dynamic simulation and the operation of a high pressure autoclave reactor [104,105].

(c) Properties of Copolymer of Ethylene Vinyl Acetate

The specific gravity of ethylene vinyl acetate is 0.93-0.95. Its yield strength is 1.3×10^{3} lb f in^{-2} and the tension modulus is 11×10^{3} lb f in^{-2}. Ethylene vinyl acetate is a tough material. Its softening point is 83°C. It becomes brittle at -70°C. Ethylene vinyl acetate is a good insulating material. Its dielectric constant is 2.8. It is used for cable insulating materials due to its good resistance to cracking caused by stress.

The amount of crystallinity can be controlled by the amount of vinyl acetate. Polymers with vinyl acetate (45%) are rubbery and peroxide can be used to vulcanize them. The commercial name of this type of polymer is Levapren. The polymer with 30% vinyl

acetate content is known as Elvax. This polymer is flexible and at room temperature, it is soluble in toluene and benzene. The tensile strength of this polymer is 1000 lb f in^{-2} and density is 0.95 g cm^{-3}. The polymers with 10-15% vinyl acetate content are flexible just like plasticised PVC. They can also be used as waxes in adhesives and melt coatings. The polymer with 3% vinyl acetate content is effectively a modification of polyethylene. It imparts more flexibility, softness, surface gloss than low density polyethylene [95].

2.11 Extrusion

Basically, extrusion is a process in which some suitable raw material is passed through an orifice or die under controlled conditions to provide the material with a specific shape and cross section. A simple everyday example of extrusion is toothpaste. In this case, the plastic tube is the equipment which is operated by the pressure of fingers, the toothpaste is the material which is conditioned by softening agents and the tube end is the orifice or die through which material passes and retains its shape [106,107].

Commercially, three general types of extrusion mechanism are in common use, i.e.:

- Ram and cylinder;
- Pumps of various types;
- Barrel and rotating screws.

and three types of general extrusion techniques are in use for plastic materials [106], i.e.:

- wet extrusion;
- spinning or spinneret extrusion;
- dry or melt extrusion.

The technique used in filament extrusion in the study described in this thesis is dry or melt extrusion. The mechanisms used in this study are ram and barrel and rotating screw.

2.11.1 Ram Extrusion

Ram extrusion is a semi-continuous extrusion method in which material is fed into the machine and pushed through a small orifice (die) under the influence of pressure and heat as shown in Figure 2.28. Icing on a cake is simple example of a ram extrusion. A hand operated plunger or ram forces icing out of the cylinder through a small hole. When the cylinder becomes empty it can be refilled [107].

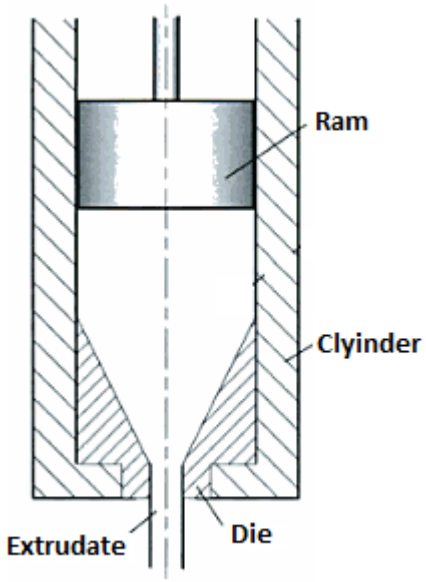

Figure 2.28 Ram Extrusion

The earliest extrusion machines used rams or pistons operating in cylinders to process the prepared (ready for extrusion) raw materials. Nowadays, these machines are equipped with heaters and temperature controllers to melt the material. The material is fed into the machine which is preset for the appropriate temperature and pressure. With the correct adjustment of ram speed, the material melts in the cylinder with heat and is pushed out through the die with a specific cross section. The extrudate is cooled down immediately to achieve the required form of the material. These machines are still in use for many purposes having many advantages, as follows [106]:

- The pressure within the machine can be kept high and uniform as required and is controllable to a certain extent;
- Some materials are sensitive to shear forces during agitation or do not need mixing, and these are suitable to process with ram extrusion.

Materials which are prepared in a plastic state and need no further conditioning during extrusion are easy to extrude using a ram extrusion machine.

The drawback of ram extrusion is that it is limited to a discontinuous process. When the ram approaches the end of its power stroke, the process stops and the ram has to withdraw to insert more material into cylinder for further extrusion. Thus, it becomes a discontinuous or semi-continuous process which is not suitable in the case where a continuous length of extrudate is required. The limitation of not being capable of mixing the material is another drawback for cases where consistency and thorough mixing is required.

The production of rod, strip, sheet and tube shapes with a suitable material is still carried out on ram extruder due to its low machine and operating cost, and mostly multi-aperture dies are used to compensate for the low production rates of small portions [106].

Some manufacturers have made efforts towards continuous flow ram extruders. The most outstanding inventions have been made by Westover, and Yi and Fenner [108]. In the case of Westover, two hoppers are connected to the plasticating ram cylinders which melt the material and push it through valves to the die head. Here, two additional rams push the material through the die as shown in Figure 2.29. In the Yi-Fenner machine, two rams feed the material to the barrel with a rotating shaft, where the material is melted and pushed through the die head as shown in Figure 2.30.

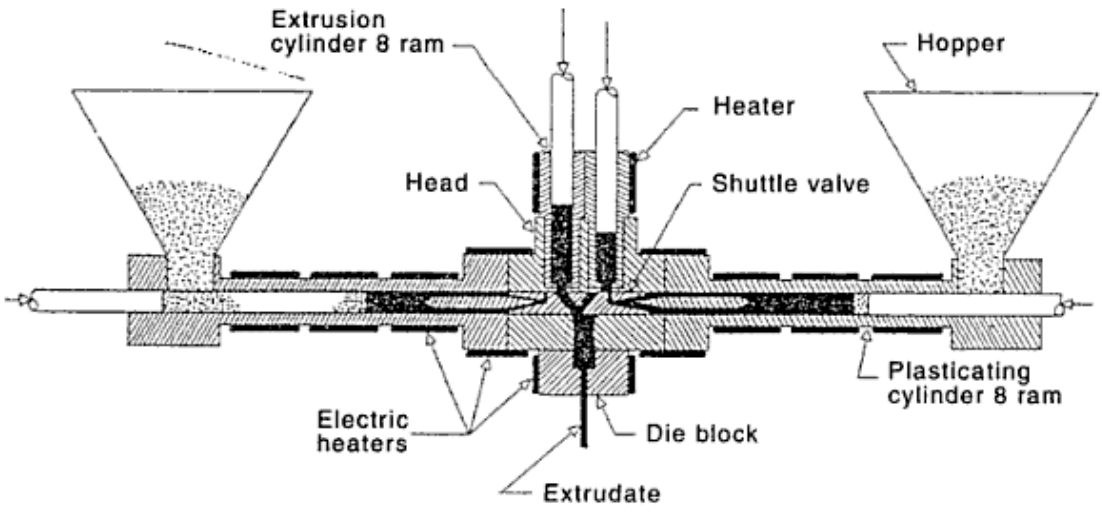

Figure 2.29 Westover continuous flow ram extruder [108]

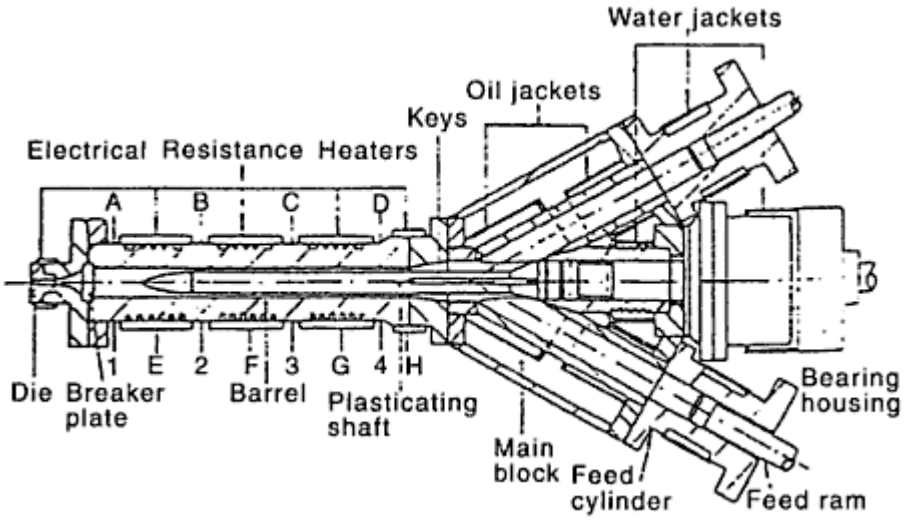

Figure 2.30 Yi-Fenner continuous flow ram extruder [108]

2.11.2 Screw Extrusion

For extrusion of polymers, it is generally desirable to extrude the material continuously. This can be carried out by using roller pumps, gear pumps or screw pumps, the last being the most commonly used [107]. A simple screw extruder consists of a hopper and a screw pump with a barrel and a die. To extrude thermoplastic materials, it is necessary to apply heat to soften and melt the materials; making them capable of flowing. The barrel covering the screw pump is normally surrounded by a heater. The heat required to melt the polymer is obtained not only from heaters but also from the frictional heat during processing.

(a) Feed Hoppers

To feed the polymer into the extruder, different types of hoppers are in use. Ideally hoppers should be round and tapered throughout for gradual compression with a circular cross section, but many manufacturers provide them shaped in a square which is easy to produce. Square hoppers work well with material in the form of granules of similar sizes but for materials with variation in shape and size, circular hoppers are needed. Normally, all of the hoppers feed the material using gravitational pull and no extra mechanism is provided. However, some bulk materials with poor flowing properties need some extra accessory to feed the material into the extruder. In some cases, a vibrating pad is used while, in other cases, a stirrer is used which also assists in mixing the material and/or preventing/wiping the material from the hopper wall if the bulk material has a tendency to stick [109]. In situations where there are air entrapment

problems, vacuum hoppers with some additional hoppers are used. Some of the hoppers are shown in Figure 2.31.

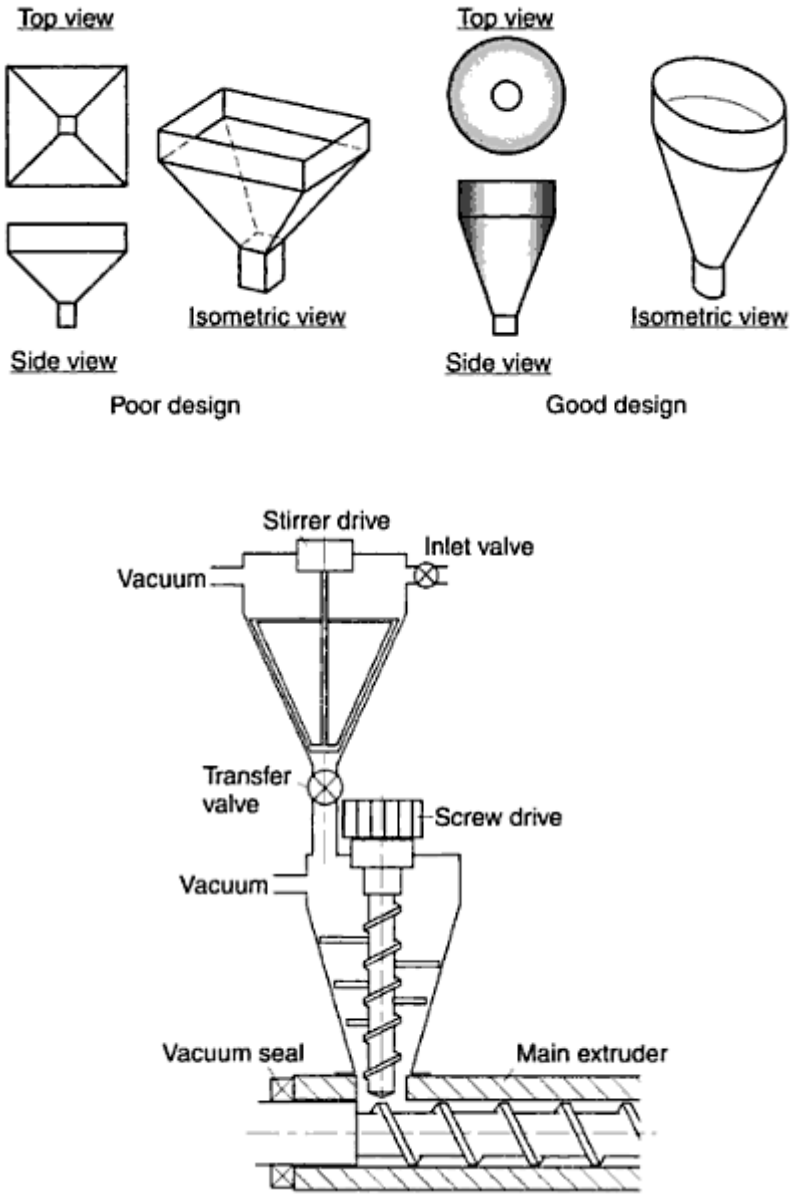

Figure 2.31 Different Hoppers [109]

(b) Extruder Screw

The extruder screw is the heart of the screw extrusion machine. Simply defined, a screw is a cylindrical rod of varying diameter with helical flights wrapped around it. A general illustration of the terminology used in the screw is shown in Figure 2.32. The clearance between screw and barrel is small; generally, the ratio of radial clearance to screw diameter is 0.001, within a range of 0.0005 to 0.0020mm [109].

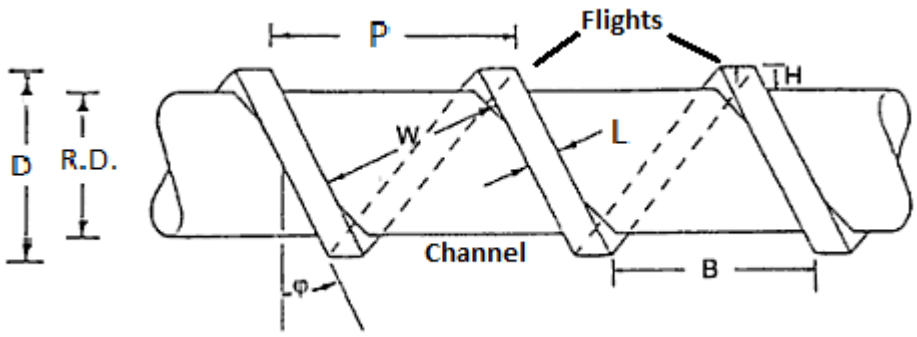

Figure 2.32 Typical screw nomenclature

where

P	is the pitch
R.D	root diameter
D	is the screw diameter
W	is the channel width
H	is the channel depth
L	is the land width
φ	is the helix angle
B	is the axial distance between flights

The principal functions of a screw involve pumping, heating, mixing and pressurising the material. On the basis of these functions, the screw can be divided into three zones; a feed zone starting at the hopper, followed by a compression zone and afterwards a melt zone as shown in Figure 2.33.

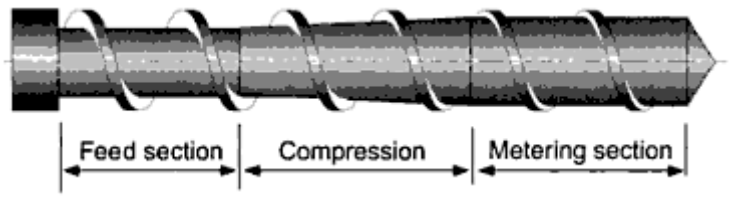

Figure 2.33 Screw zones [109]

A standard or conventional screw extruder generally, operates on the basis of the following approximate parameters [109]:

- Total length 20-30 D;

- Length of feed section 4-8 D;
- Length of metering section 6-10 D;
- Number of parallel flights 1;
- Flight pitch 1 D (helix angle 17.66°);
- Flight width 0.1 D;
- Channel depth in feed sections 0.15-0.20 D;
- Channel depth ratio 2-4.

A standard screw is shown in Figure 2.34 with some of its dimensions.

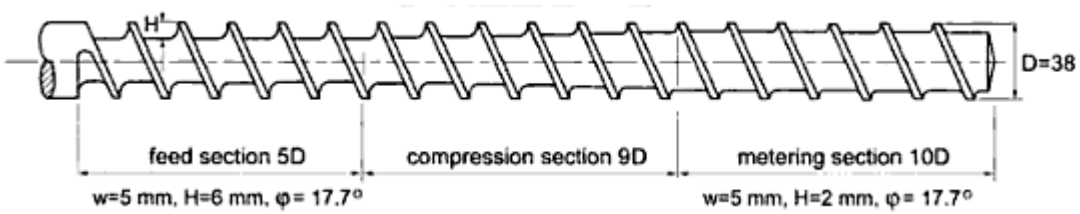

Figure 2.34 A standard screw [109]

The function of the feed section zone of the screw is to pick up the cold material from the hopper and feed it to the compression section of the screw. However, feed materials can adopt a variety of forms such as free-running fine powders, regular cubes, random cut chips with a certain amount percentage fines, small cylinders, spheres etc. As the feed zone thus has to deal with materials with a variety of physical shapes and properties, a helix angle of screw flight suitable for one material may not be appropriate for another. Thus, the most common helix angle of flight at the feed zone is 17.7° but it may be vary from 10° to 25° [106]. The feed zone should also provide the material to the metering or melting zone in such a way that it should not run out of the supply, neither should it overrun the material otherwise it will cause surging or pulsation in either of these situations. The friction on the material within the screw and barrel should also be optimum so that the material can be pushed further. Normally, the friction on material within the screw is kept lower and it is greater within the barrel.

The compression zone of the screw starts just after the feeding zone with a gradual increase in root diameter of the screw until the root diameter of the melt or metering

zone is achieved as shown in Figure 2.35. This could involve increase in root diameter within less than half a turn of the flight [Figure 2.35(a)], or more turns [Figure 2.35(b)] depending on the materials melt behaviour and whether the screw was made for a specific use. The compression zone not only compresses the material but also ensures that the rate of melting and volume change as the material changes from solid to a viscous liquid state are accommodated. It pushes back any entrapped air to the feeding zone and compresses the material to improve thermal conductivity so the material reaches the metering zone having homogenously melted so that the next zone just has to deal with the viscous fluid [106,107]. Most commonly, the compression zone is achieved by a gradual increase in root diameter of the screw, i.e., the depth of flight decreases gradually. However, it can also be achieved by decreasing the pitch of the screw and keeping the depth of the flight the same.

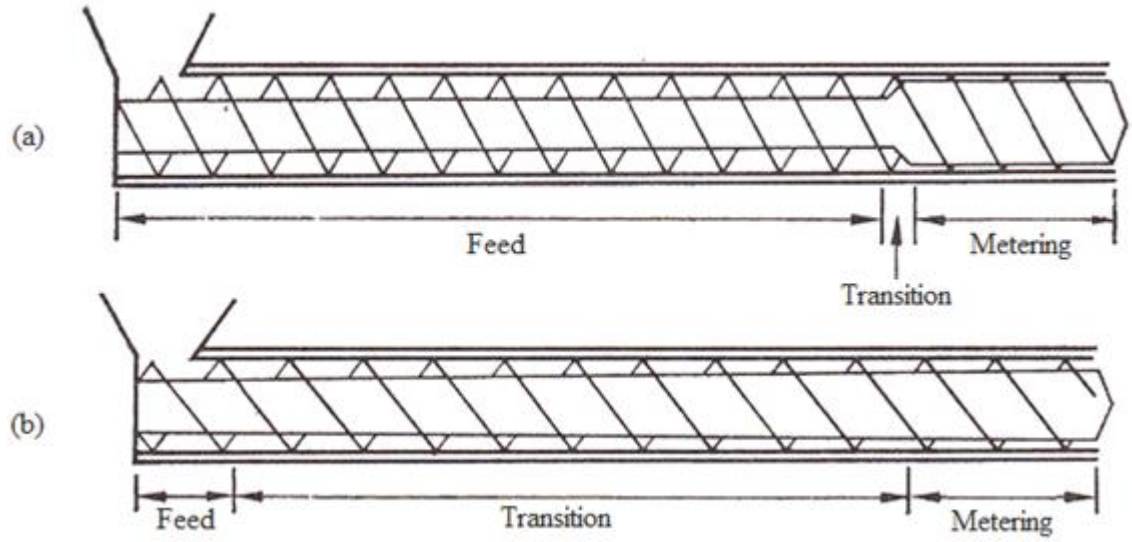

Figure 2.35 Two different types of compression or transition zones [107]

The melt or metering zone of the screw is the final zone of the screw. The ratio of the volume of one flight of the feeding zone to the volume of the melt zone flight is known as the compression ratio of the screw [106]. The melt zone of the screw deals with viscous fluid, so that the behaviour of materials is more defined at this stage rather than at the previous stages. A high shear force ensures thermal homogeneity and also homogenous mixing of the material. The pressure at the melt zone can be increased more than die head pressure with certain screw designs [106].

Some screws also use torpedoes and mixing heads which are normally located just after the melt zone of the screw [108,109]. This section of the screw ensures homogeneous

mixing of the polymer, and sometimes of polymers with other additives. Some types of mixing heads or sections with their geometries are shown in Figure 2.36.

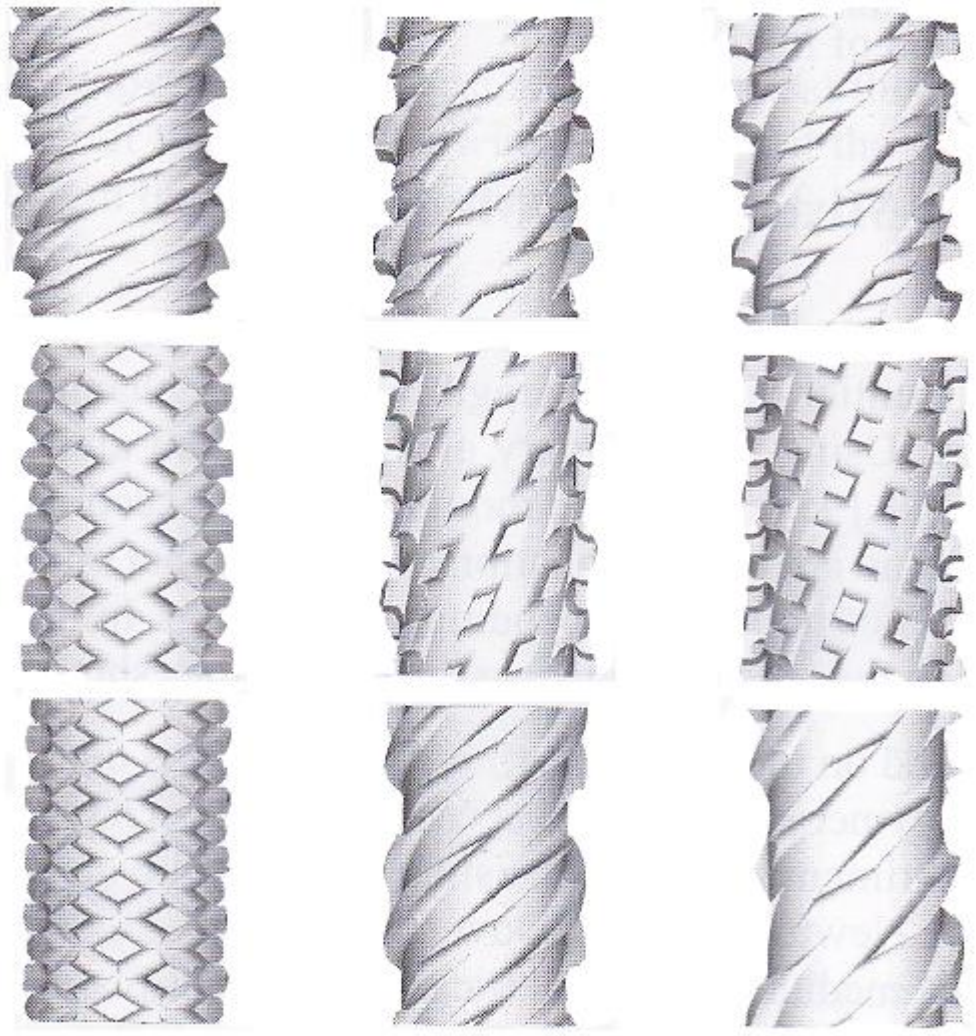

Figure 2.36 Mixing heads [109]

(c) Die Assembly

In almost every screw extrusion machine, it is common to use a breaker plate between the barrel and the die assembly. A breaker plate is a thick metallic disc with narrowly spaced holes parallel to the screw axis. The main functions of the breaker plate are to break the rotational moment of the polymer melt into a straight line flow and build a die head pressure to mix the polymer more consistently, and also for more consistent flow of the polymer melt. Generally, a screen filter is also used with the breaker plate which ensures the purity of extrudate by filtering any contamination and unplasticised polymer from the polymer melt. The breaker plate also supports the screen filter to sustain the heavy extrudate pressure. Another function of the breaker plate is to improve heat transfer to the polymer melt by reducing the heat transfer distance. Thermal

homogeneity of the polymer melts increases with reducing heat transfer distance [107,109].

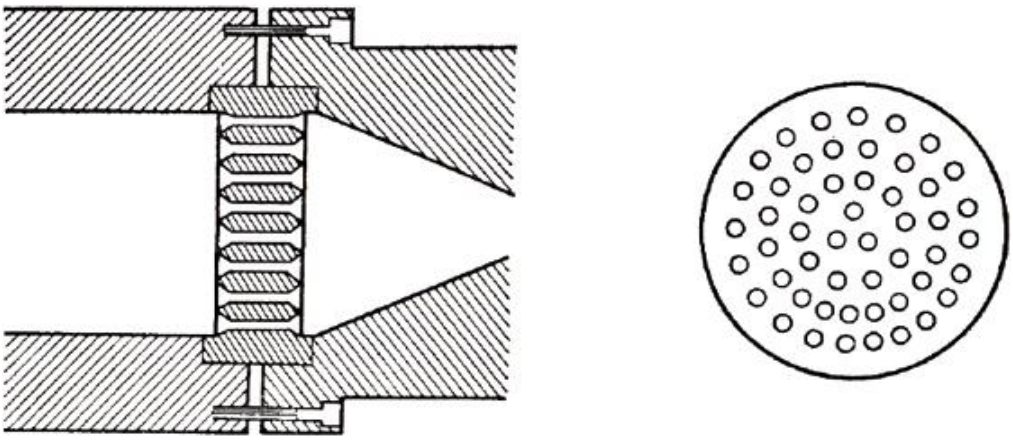

Figure 2.37 Breaker plate

Normally, an adaptor is used between the die assembly and screw barrel due to a mismatch between the exit and entry openings of the barrel and the die assembly, respectively. In the case of a machine specially designed for a specific polymer, there will not be a need for an adaptor and mostly standard equipment is used. A die is arguably the most important part of the extrusion machine as polymer shape development takes place at this point. Basically, the purpose of rest of the machine is to transport the polymer up to the die with the required pressure and consistency. Most commonly, the dies used are circular in form but they can adopt other shapes according to the cross section of the material required. A die can have one or a number of holes as required. For tapes, a die with a slit opening is used. For filaments shapes other than circular, a number of different types of dies are used as shown in Figure 2.38.

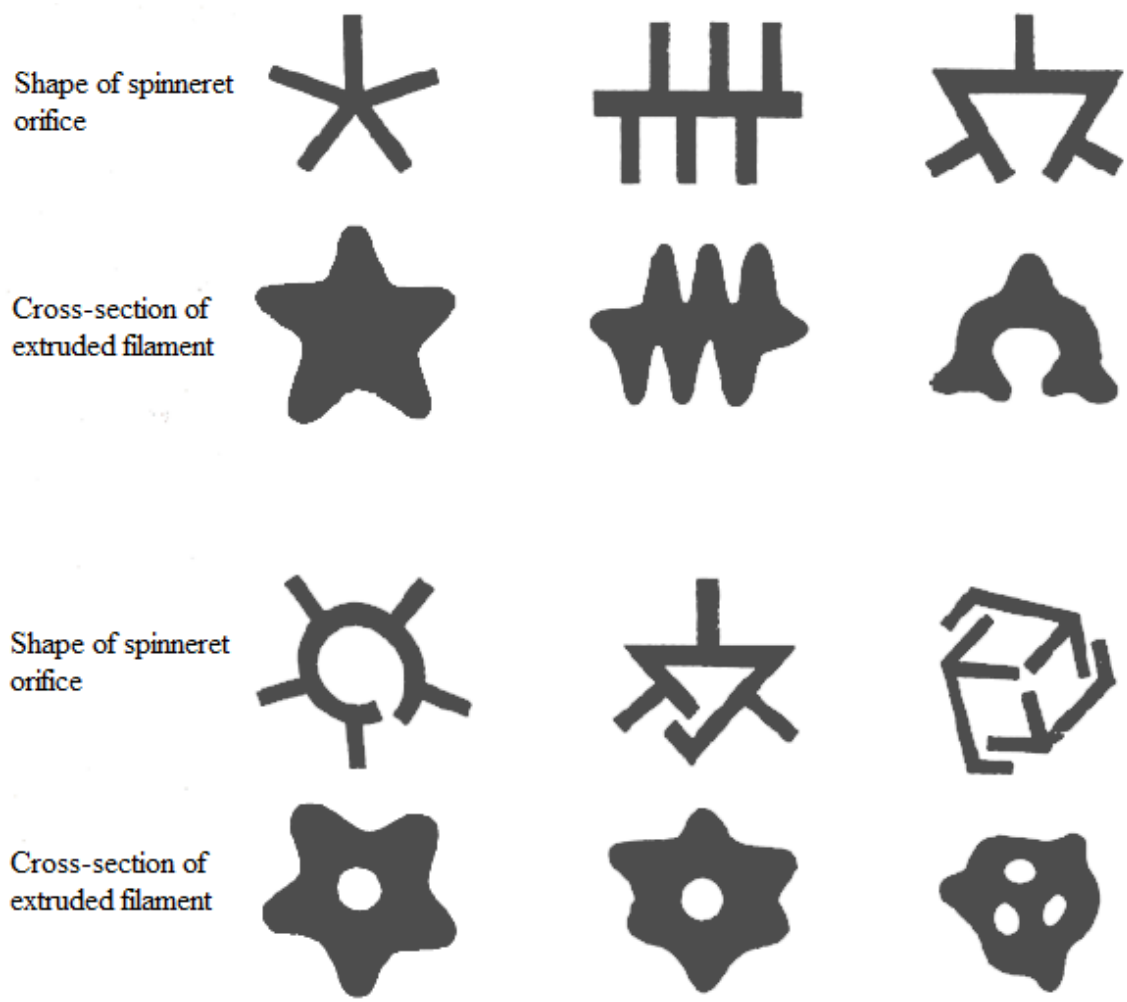

Figure 2.38 Different shapes of dies and filaments extruded [73]

2.11.3 Parameters in a Screw Extrusion Machine

Polymers, for extrusion purposes, are normally available in different forms such as granules, flakes, powders etc. These forms of the polymers are subjected to heat, pressure etc. to convert them from solid to viscous fluid and ultimately into filaments. The temperature, pressure and speed are controlled at various parts in the screw extrusion machine. The general controllable parameters of a screw extrusion machine at various parts are as follows:

- Screw speed;
- Metering pump speed;
- Temperatures at feeding, compression and melt zones of the screw;
- Temperature at the metering pump;

- Temperature zones at the die head.

The optimum temperature at certain parts of the screw machine ensures melting of a polymer and its flow throughout the screw extruder. The lower temperature at the feeding zone causes the polymer to push forward as, otherwise, in viscous form, it can simply stay at the same place turning around the screw. It also helps to build up a forward pressure which causes the fluid polymer to push towards the low volume regions at the compression and melt zone of the screw. The high temperature in the compression zone makes the polymer melt completely through this zone so that when the polymer reaches the melt zone it is fully in molten form. The temperature at the metering zone and at the die head helps the polymer material in achieving thermal homogeneity and consistent viscosity. The speed of the screw not only delivers the optimum polymer to the metering zone and die head but also makes sure that the polymer has enough time in the compression and melt zone for thorough melting and achieving homogenous viscosity. The speed of the metering pump builds an optimum pressure at the die head which is suitable for proper extrusion of filament and it also prevents gathering of the polymer delivered by the screw into the metering section. Each polymer has a specific softening and melting temperature and flow properties and thus these parameters are also polymer dependent.

2.12 Drawing

Drawing is a process in which the filament is stretched under tension and deformed permanently. The filament becomes finer while mechanical strength and tensile modulus are improved. In this process, the chains of polymers slip over each other and become more parallel to each other as shown in Figure 2.39. This process is used in the production of fibres, tapes and films and is an important stiffening and strengthening technique.

During the extrusion process, some orientation of the polymer molecules also results. This is more noticeable at the outer surface of the filament than inside the filament. Outer surface orientation is influenced by the edges of spinneret hole and this phenomenon is known as a skin effect [94]. The skin effect plays an important role in fibre properties. However, further orientation of the long polymer molecules is achieved by stretching along the longitudinal axis of the filament. In this way, molecules are caused to align with each other and this increases the strength of cohesive

forces between them. These cohesive forces have an important effect on the physical behaviour of the fibre.

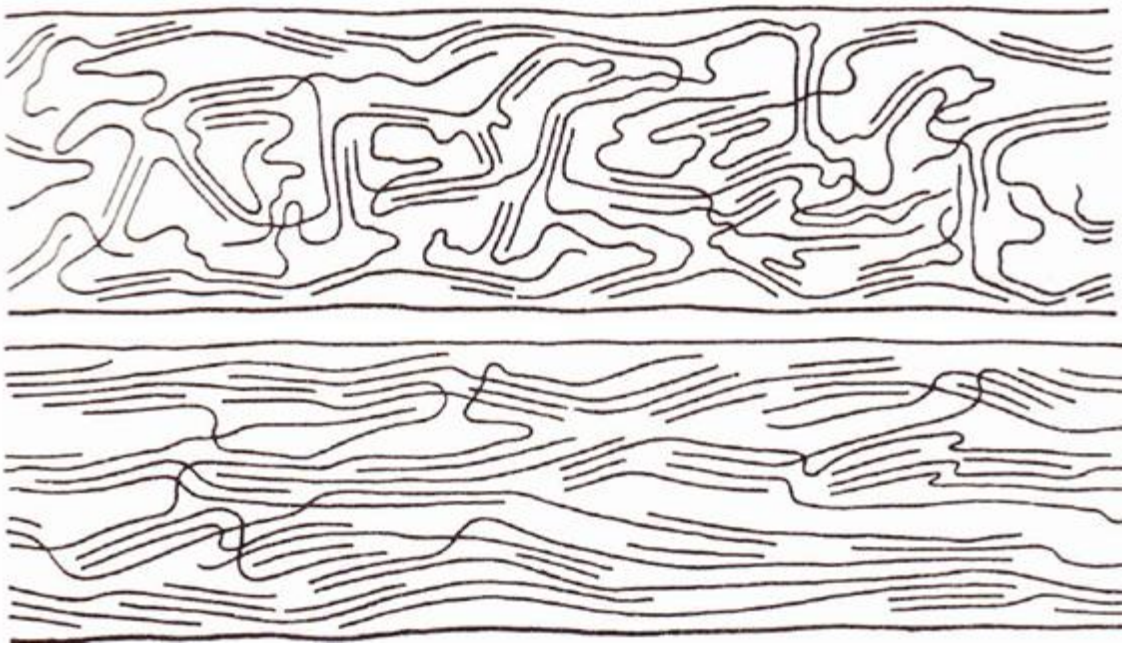

Figure 2.39 Molecular chains in an undrawn and drawn filament [94]

The orientation of molecular chains always occurs during drawing but crystallinity may either increase or decrease as a result. The following types of trend can occur depending on the drawing conditions and the polymers involved [98,110,111]:

- Drawing does not affect crystalline or amorphous region and no change occurs in their proportionality;
- Partial deformation occurs in structure and there is a decrease in crystallinity;
- Increase in orientation of molecular chains in drawing accompanying an increase in crystallinity.

The first of these effects occurs in amorphous materials such as atactic polystyrene, where chains move to become oriented in the amorphous region but without formation of any crystallites. It can also be observed in partially crystalline materials such as polyethylene when molecular chains move in the amorphous region without distortion of crystalline region [111]. It is also observed in highly swollen cellulose fibres where no changes occur in the crystalline region and in some partially crystalline wet spun filaments [111,112].

In the second case, destruction takes place with building a substandard structure oriented in the direction of the applied tension. However, at low temperatures, instead of any destruction, drawing results in a highly substandard crystalline material. The degree of crystallisation decreases during cold drawing of polyethylene and sometimes it also results in a change in the dimensions of crystallites and their degree of perfection [113,114]. It has also been observed that plastic distortion takes place in this type of mechanism, rather than melting and recrystallisation of an amorphous material [110,113,115].

In the third case, the heat applied in hot drawing and the heat produced during moving of polymer chains increases the temperature in the material and this assists in modifying the crystalline structure resulting in an increased degree of crystallisation. In the case of polyethylene, it has been observed that crystallisation increases during cold or hot drawing. In this case the effect is often influenced by an increase in draw ratio or in drawing temperature [112,116].

2.13 Colour Measurement

Colour is essentially a sensation in the mind of the observer and present difficulties in measurement. Colour is not simple to describe to a person who has never experienced it before. However, some parameters associated with colour can be measured. The sensation of colour depends on the object, the incident light and the observer [117]. The reflected light from an object is perceived by an observer's eye as shown in Figure 2.40.

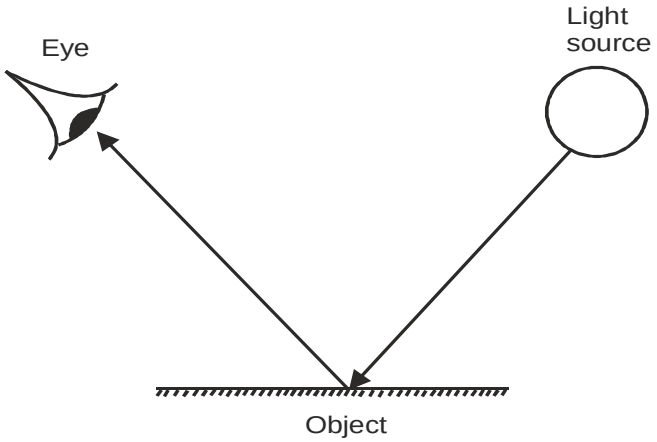

Figure 2.40 Viewing of colour

The back of the eye contains rods and cones which are photosensitive cells. The rods are responsible for responding to the low intensity of light that is characteristic of night vision. The cones operate in normal light and are more sensitive to colours, and

towards three regions of visible light which are roughly between 400nm and 700nm. The observer perceives colour by a ratio of the intensity of the responses of the R, G and B cones which convert the perceived light into electrical signals and send these to the brain. Thus, the colour observed depends on the spectral power distribution of the light source, the reflectance of object and the spectral response of the eye [118].

Coloured lights are easy to define and can be used as primaries for a colour specification system. A wide range of colours can be matched using red, green and blue primaries. If red, green and blue primary light sources are represented by [R], [G] and [B], and [C] has to match with them, then C units of [C] can be matched with R, G and B units of [R], [G] and [B] respectively as shown in Equation 2.7.

$$C[C] = R[R] + G[G] + B[B]$$

Equation 2.7

Similarly, if

$$C_1[C] = R_1[R] + G_1[G] + B_1[B]$$

Equation 2.8

and

$$C_2[C] = R_2[R] + G_2[G] + B_2[B]$$

Equation 2.9

then the additive mixture can be given as in Equation 2.10.

$$C_1[C] + C_2[C] = (R_1 + R_2)[R] + (G_1 + G_2)[G] + (B_1 + B_2)[B]$$

Equation 2.10

The amounts R, G and B of the three primaries used to match C units of the colour [C] are known as tristimulus values of the colour [C] [118]. Some saturated colours such as pure cyan are hard to match with blue and green. Thus, some red colour can be added into cyan to provide an unsaturated colour which can be matched by red and green as shown in Equation 2.11.

$$C[C] + R[R] = G[G] + B[B]$$

Equation 2.11

Re-arranging the equation, provides Equation 2.12.

$$C[C] = -R[R] + G[G] + B[B]$$

Equation 2.12

Hence, a negative R value is required to match cyan which is undesirable. Although a wide range of colours are matched by real primaries, still there are real colours which cannot be matched using only these primaries. To avoid negative values, and cover all the real colours, imaginary primaries [X], [Y] and [Z] have been defined. So C units of colour [C] can be matched by X, Y and Z units of [X], [Y] and [Z] imaginary primaries respectively and now these X, Y and Z are known as the tristimulus values.

Colour measurement can be defined according to two broad ways [117]:

- Visual comparison with some physical standard reference material;
- Instrumental measurement of relative amounts of each wavelength present with specified illuminants and viewing conditions.

Thus, considering these parameters, the Commission Internationale de I'Eclairage (CIE) derived a method to explain colour mathematically using XYZ tristimulus values[118]. The XYZ tristimulus values are defined as:

$$X = \sum_{\lambda=400}^{700} \overline{x}_\lambda R_\lambda S_\lambda \ , \qquad Y = \sum_{\lambda=400}^{700} \overline{y}_\lambda R_\lambda S_\lambda \ , \qquad Z = \sum_{\lambda=400}^{700} \overline{z}_\lambda R_\lambda S_\lambda$$

Equation 2.13

where x, y and z are colour matching functions, R is the reflectance of the object and S is the spectral power distribution of the light source [118].

2.13.1 Light Sources and Illuminants

A light source is an actual physical emitter of light energy while an illuminant is a standardized table of values which described the spectral power distribution of a particular light source. Illuminants are based on the colour temperature of a light source. A black-body radiator or Planckian radiator is a theoretical light source that is considered to emit energy by thermal excitation and is known as a perfect energy emitter. The spectral power distribution of a black-body radiator is specified as absolute

temperature (K) and is known as colour temperature. As black-body radiators are not commonly available, another quantity is used which is the correlated colour temperature (CCT). The correlated colour temperature of a light source is determined by the colour temperature of the black-body radiator when it has the same colour as the light source. The CIE has specified some illuminants for colorimetry as follows [119]:

- CIE illuminant A is a Planckian radiator with 2,856 K as colour temperature. For consideration of incandescent illumination, it is used for colour measurement;

- CIE illuminant C is a spectral power distribution form of illuminant A, modified by specific liquid filters. It is considered as a daylight simulator with 6,774 K correlated colour temperature;

- CIE illuminant D50 is based on average daylight with a correlated temperature of 5,003 K and is used in graphic arts applications;

- CIE illuminant D65 represents average daylight with a 6,504 K correlated temperature and is commonly used in colour measurement;

- There are total of 12 CIE F illuminants which represent distinctive spectral power distributions for fluorescent sources. For example, F2 shows cool white fluorescence with a 4,230 K correlated colour temperature. Illuminant F8 represents fluorescent D50 simulator and has a correlated temperature of 5,000 K. Similarly F11 shows a triband fluorescent source with 4,000 K correlated colour temperature. These illuminants are notable for their efficiency, efficacy and good colour-rendering properties;

- CIE illuminant E or equal-energy illuminant is defined as providing relative spectral power of 100.0 at all wavelengths.

2.13.2 Illumination and Viewing Geometry

The methods and angles of illuminating and viewing can affect colour measurement. Thus, the CIE defines four types of illuminating and viewing geometries which are described in two pairs as follows:

- Diffuse/normal (d/0) and normal/diffuse (0/d);

- 45/normal (45/0) and normal/45 (0/45).

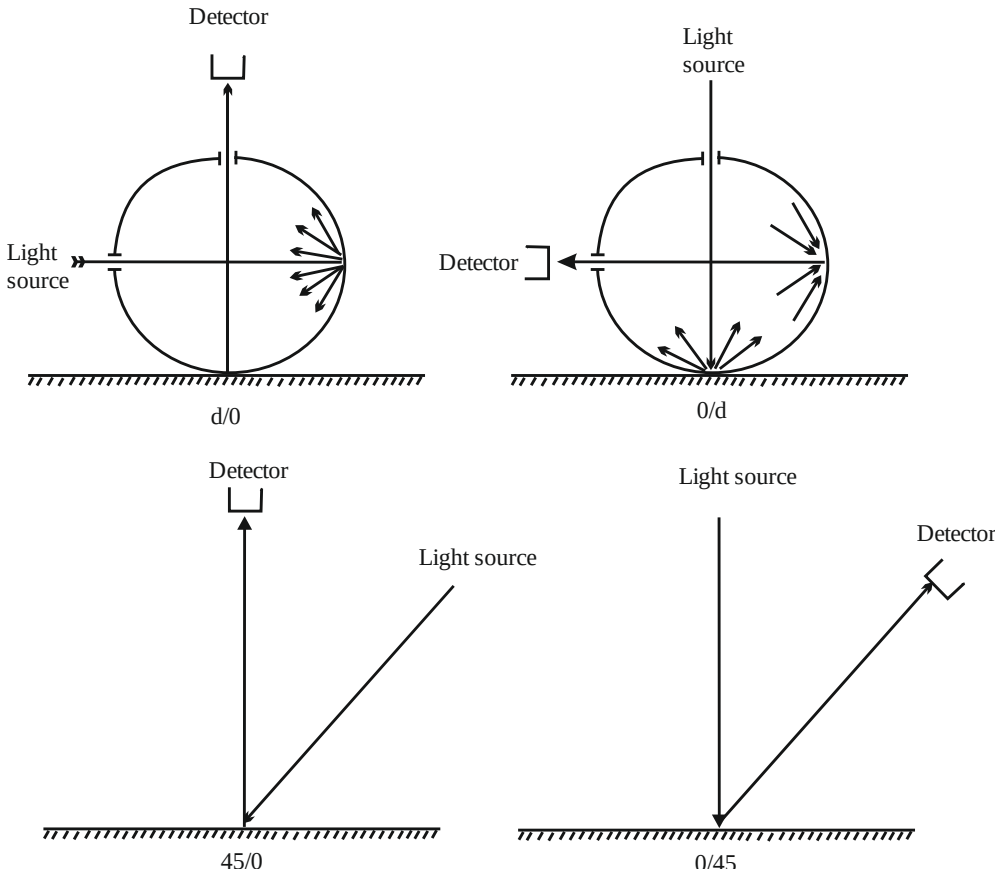

Figure 2.41 CIE illuminating and viewing geometries

In diffuse/normal geometry the sample is illuminated from all sides using an integrated sphere and viewed normal to the sample while in normal/diffuse geometry the sample is illuminated normal and reflected light is assessed collectively from all sides using an integrated sphere.

In 45/normal, illumination is at an angle of 45° and reflection is measured normal to the sample while in the other case it is the sample that is illuminated normal and the reflection measured at an angle of 45°.

In diffuse/normal and normal/diffuse, the measurements are identical and are the same in the case of 45/normal and normal/45. In the second pair of geometries, the gloss component is totally excluded from measurements. These are useful for measurement in graphic arts, photography etc. with various levels of gloss.

Reflectance is normally taken as the ratio of reflected light to the incident light. It is satisfactory in the case of diffuse/normal or normal/diffuse geometries but in the case of 45/normal and normal/45, this ratio is very small due to a small viewing angle. Thus,

for the measurement of reflectance for any type of geometry, the reflectance factor is measured. This factor is defined as the ratio of the energy reflected by the sample to the energy reflected by the perfect reflecting diffuser (PRD) with the same illuminating and viewing geometry. A perfect reflecting diffuser (PRD) is a theoretical material which reflects perfectly and is perfectly Lambertian, i.e. radiance is equal in all directions. Therefore, the reflectance factor is identical to reflectance in the case of diffuse/normal and normal/diffuse geometries and has a scale of zero-to-one in the case of 45/normal and normal/45 geometries [119].

The more commonly used geometries from those discussed above are d/0 and 45/0. The diffuse geometry minimizes the effect of surface texture and appearance of the sample which is due to uniform illumination. The CIE has allowed the viewing beam to be 10° away from the normal by providing a gloss port which enables the opportunity for specular reflectance to be either included or excluded. Normally in measuring instruments, the viewing beam is assessed with d/8 which is 8° from the normal less than 10°, allowed by the CIE. In quality control instruments, normally 45/0 is used because it is closer to the situation involved with colour matching in the colourists light booth. In 45/0, the specular reflectance is always excluded [118].

2.13.3 Instrumental Measurement

To measure colour numerically, two types of instruments are used, the tristimulus colorimeter and the spectrophotometer.

(a) The Tristimulus Colorimeter

Tristimulus colorimeters are the simplest colour measurement instruments. In these devices, the light source projects light on the sample or object at a 45° angle and light reflected normal is filtered by three filters with light sensitive diodes according to the red, green and blue colours. The responses of the diodes are combined to measure the colour. The tristimulus colorimeter is a cost effective instrument and is appropriate for measuring colour differences in quality control.

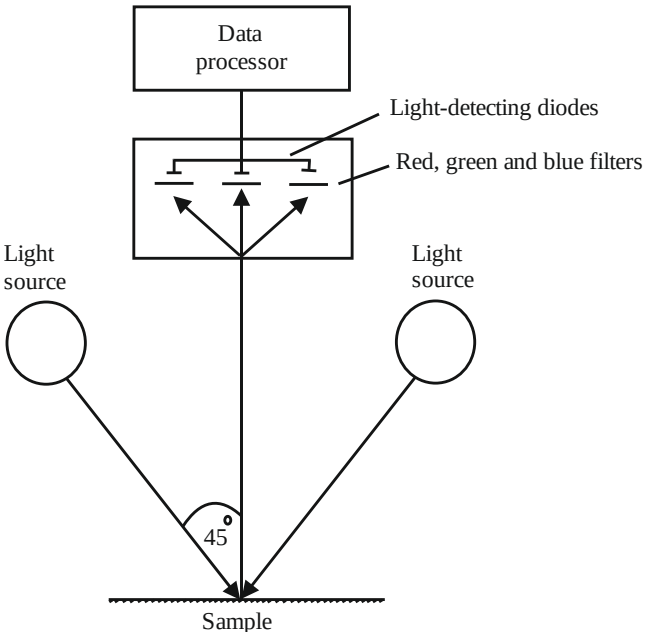

Figure 2.42 Simple characteristics of colorimeter

The tristimulus colorimeters have a limitation in terms of absolute accuracy due to the light source and filter/diode response. Due to light source limitation, colorimeters are not capable of indicating any metamerism present [118].

(b) The Spectrophotometer

A spectrophotometer uses spectral analysis to measure the reflectance at various wavelengths in the visible region. The reflectance is the ratio of reflected light to incident light as shown in Equation 2.14 and is generally expressed as a percentage.

$$Reflectance = \frac{Reflected\ light}{Incident\ light}$$

Equation 2.14

A perfect reflecting diffuser has a reflectance of 100% but in the case of colorimetric calculations, as in Equation 2.13, a perfect reflecting diffuser has a reflectance of unity and reflectance values are decimal fractions [118].

The spectrophotometer uses a simple mechanism. A specific light source illuminates the sample with specific illumination and viewing geometry. The reflected or transmitted light is passed through a spectral analyser where it is split into spectral components. In this way, light detectors and control electronics take measurements at many regular wavelengths in visible region. The spectrophotometer has the advantage over a simple colorimeter of incorporating the spectral analyser [118].

The spectral analyser is a device which splits the spectral components of light in such a way that they can be individually assessed. A spectral analyser is a very important component in a spectrophotometer on which its performance depends.

In early spectrophotometers, a prism would be used to separate the light into spectral components. A filter wheel with narrow bandwidth interference filters was also used but such mechanical methods had the disadvantage of taking a long time in taking measurements. Modern spectrophotometers use an array of silicon diodes which split the light into spectral components in seconds. The dispersing element used is normally a grating. A diffraction grating has a large number of grooves produced with a diamond point into a glass surface. The light that passes through this grating is diffracted at an angle θ, the value of which depends on wavelength. A line diagram of a dual beam spectrophotometer is shown in Figure 2.43.

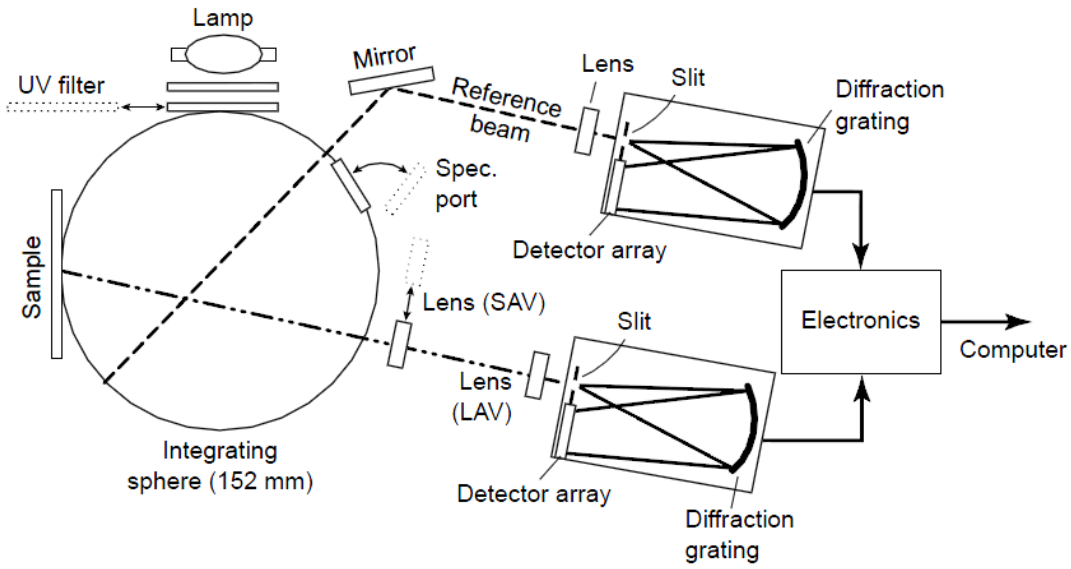

Figure 2.43 Basic characteristics of dual beam spectrophotometer [118]

2.13.4 Temperature Dependent Colour Measurements

The thermochromic pigments based on leuco dyes and on liquid crystals which are the subject of the research in this thesis have been traditionally assessed visually and also without a controlled heat mechanism. Previously, a method has been reported by Bryant to assess the colour of thermochromic liquid crystals instrumentally [25]. A hot stage with precisely controlled temperature was used in contact behind the liquid crystal printed sample during measurement using the spectrophotometer. The printed thermochromic sample was gradually heated to a specific temperature, which was then maintained for a couple of minutes at the required level before taking measurements.

A self constructed arrangement was used for this purpose using a standard Linkam hot stage with a temperature control unit. The colour measurements were taken using a spectrophotometer. A heat sink compound was applied between the sample and the hot stage was used for efficient heat transfer and insulation was used around the hot stage to minimise heat loss during measurements. To take measurements at low temperatures, cooling water was circulated through the device using a peristaltic pump as shown in Figure 2.44.

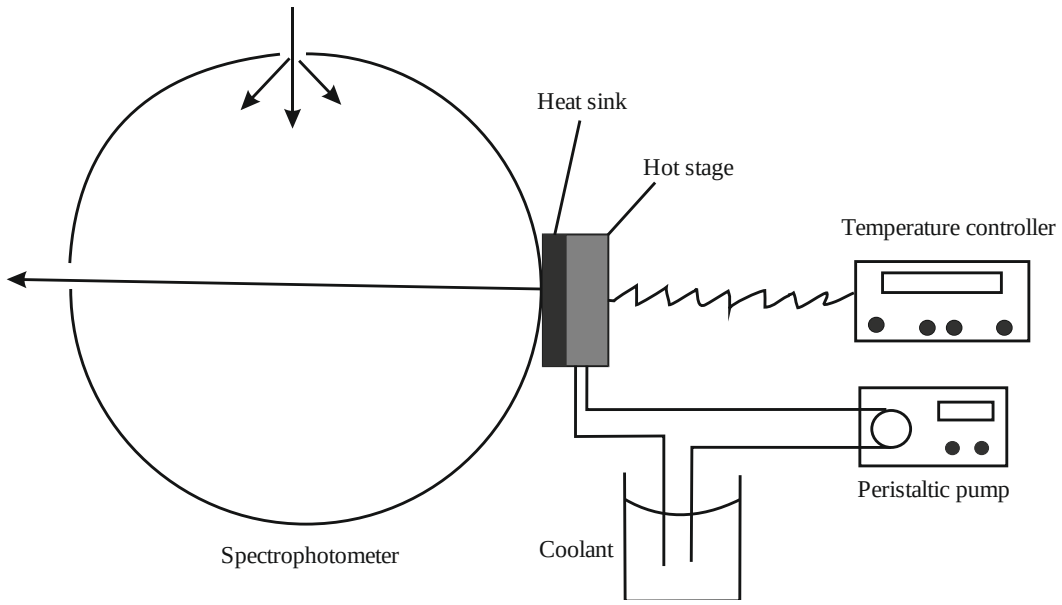

Figure 2.44 Temperature dependent colour measurements

2.13.5 Colour Mixing

In reality, we can observe a very large number of colours. Some of these may be considered as primary colours but most are mixtures of two or more primary colours. The mixing of colours can be divided into two types.

(a) Additive Colour Mixing

When two coloured light beams are mixed, rather than cancelling each other's effect, they mix with each other and give a combined additive effect of colours. For example, if blue and yellow coloured lights are mixed, white light is obtained and by mixing red and green light, yellow coloured light is obtained [117,118]. In the latter case, if red and green lights are projected together on a white screen, the entire combined incident light on the white screen is reflected. The red and green coloured lights are mixed and reach the observer's eye. The observer experiences a yellow colour which is due to additive colour mixing. The additive primaries are red, green and blue colours whose

spectra overlap each other very little [120]. Additive colour mixing has particular importance as the CIE system is based on a mixture of lights.

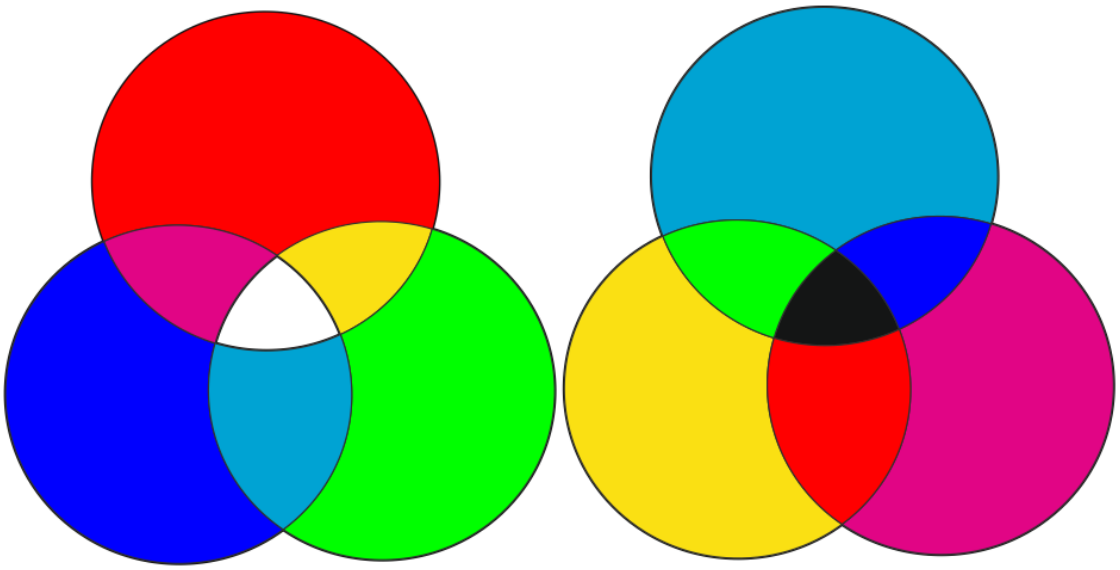

Figure 2.45 Additive and subtractive colour mixing

(b) Subtractive colour mixing

Natural white light is commonly considered as a mixture of seven basic colours such as those observed in a rainbow. White light can also be achieved by additively mixing specific proportions of red, green and blue lights. When white light falls on a coloured object, it absorbs all of the wavelengths of the visible light except for the wavelengths of its colour which is reflected back and reaches the observer's eye [121]. In this way, the wavelengths absorbed are subtracted from the white, and light with specific wavelengths is reflected. For example, consider the case of two filters placed in the way of the beam of white light. If the first filter is red, it absorbs light in the wavelength range from 400-650nm and transmits the wavelengths above 650nm. If the second filter is green, it transmits only in the range 500-550nm. The first filter absorbs all low wavelengths and transmits the light only in the range 650-700nm. The second filter which is green can transmit light with wavelengths from 500-550nm. Thus, all the light will be absorbed and there will be no reflected light and it will appear black. In this case, the first filter subtracts the light up to a 650nm wavelength and rest of the wavelengths are subtracted by the second filter [118]. Magenta, yellow and cyan are known as subtractive primaries because they cover two-thirds of the visible spectrum [120]. Coloration using mixtures of dyes and pigments is based on subtractive primaries.

2.13.6 Colour Display Systems

(a) Chromaticity diagram

It is difficult to display a colour as a three dimensional presentation. Thus, to avoid this complexity and for convenience a method for two dimensional colour presentation was developed which is known as a chromaticity diagram. To present the colour in two dimensions, the chromaticity coordinates x, y and z are calculated from tristimulus values and then y is plotted against x. The chromaticity coordinates are calculated as shown in Set of equations 2.15 [118,119,121]:

$$x = \frac{X}{X+Y+Z}$$

$$y = \frac{Y}{X+Y+Z}$$

$$z = \frac{Z}{X+Y+Z}$$

Set of equations 2.15

As the chromaticity diagram is drawn using x and y coordinates, the third coordinate can easily be calculated, as the sum of the three coordinates for every colour is always equal to 1 as shown in Equation 2.16.

$$z = 1.0 - x - y$$

Equation 2.16

For the complete specification of an object colour, usually the Y tristimulus value is given in addition to two or three chromaticity coordinates. X or Z can be used instead of Y, but Y is preferred because it represents the lightness. The two tristimulus values X and Z can be calculated from chromaticity coordinates and the Y tristimulus value by Set of equations 2.16 [119]:

$$X = \frac{xY}{y}$$

$$Z = \frac{(1.0 - x - y)Y}{y}$$

Set of equations 2.17

A chromaticity diagram with the visible range of wavelengths is shown in Figure 2.46.

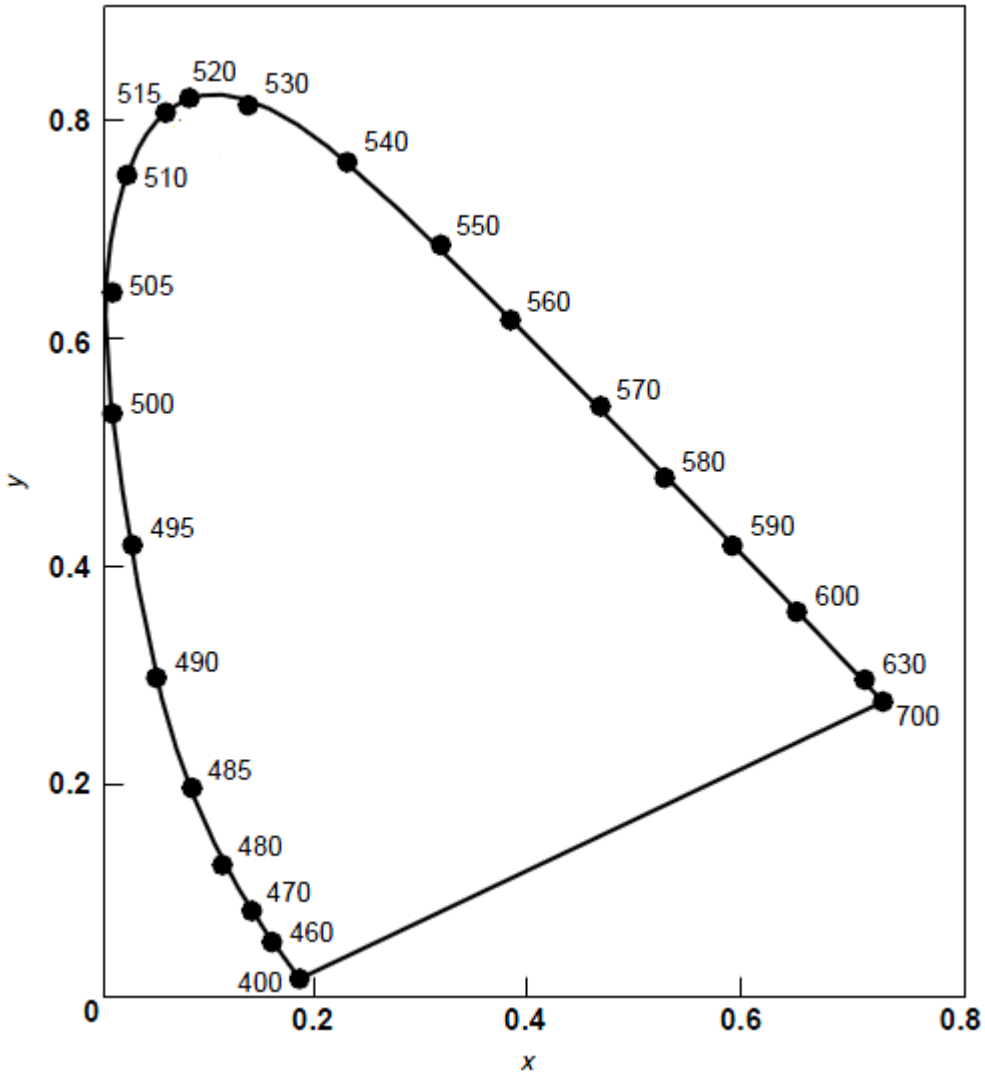

Figure 2.46 Chromaticity Diagram [118]

All available colours lie within the locus area. Another characteristic of a chromaticity diagram is that if two coloured lights are represented by two points on the chromaticity diagram, then additive mixture of the lights will be located on the straight line joining the two points [118].

(b) CIELab

The CIELab colour space extends the use of tristimulus values from two dimensions to three dimensions and overcomes the use of the chromaticity diagram. This concept was developed on the basis of the colour difference between a white reference and a stimulus. In 1976, CIE recommended two colour space systems CIELAB and CIELUV, in which the Euclidean distances between two points in these spaces are considered as

the colour differences ΔE^*_{ab} or ΔE^*_{uv} respectively. In 1994, CIE recommended a single and better colour difference formula for CIELab colour space which is known as ΔE_{94}. The CIELab coordinates are calculated using the tristimulus values of stimulus XYZ and tristimulus values of a reference white or perfect reflecting diffuser $X_nY_nZ_n$. The CIELab coordinates are calculated as shown in Set of equations 2.18 [119]:

$$L^* = 116(Y/Y_n)^{1/3} - 16$$

$$a^* = 500\left[(X/X_n)^{1/3} - (Y/Y_n)^{1/3}\right]$$

$$b^* = 200\left[(Y/Y_n)^{1/3} - (Z/Z_n)^{1/3}\right]$$

Set of equations 2.18

The $L^*a^*b^*$ values are used for Cartesian coordinates while for cylindrical coordinates L^*C^* and h° are used. The L^* value represents the lightness, while a^* and b^* show the approximate redness-greenness and yellowness-blueness respectively. C^* and h° represent chroma and hue and are calculated as given in Set of equations 2.19:

$$C^*_{ab} = \sqrt{(a^{*2} + b^{*2})}$$

$$h^\circ_{ab} = \tan^{-1}(b^*/a^*)$$

Set of equations 2.19

The C^* has the same coordinate unit as a^* and b^*. If a stimulus has a C^* value of 0.0, there is no chroma. The hue angle h°_{ab} is presented in degrees and starts from positive a^* and proceeds in an anticlockwise direction. The Cartesian and cylindrical presentations of CIELab are shown in Figure 2.47 and Figure 2.48, respectively.

The use of the above equations to calculate $L^*a^*b^*$ values are only valid for X/X_n, Y/Y_n and Z/Z_n values greater than 0.01. In the case of low values, the above equations are used with a factor f as given in Set of equations [119].

$$L^* = 116f(Y/Y_n) - 16$$

$$a^* = 500[f(X/X_n) - f(Y/Y_n)]$$

$$b^* = 200[f(Y/Y_n) - f(Z/Z_n)]$$

Set of equations 2.20

$$f(\omega) = \begin{cases} (\omega)^{1/3} & \omega > 0.008856 \\ 7.787\ (\omega) + \ 16/116 & \omega \ \leq 0.008856 \end{cases}$$

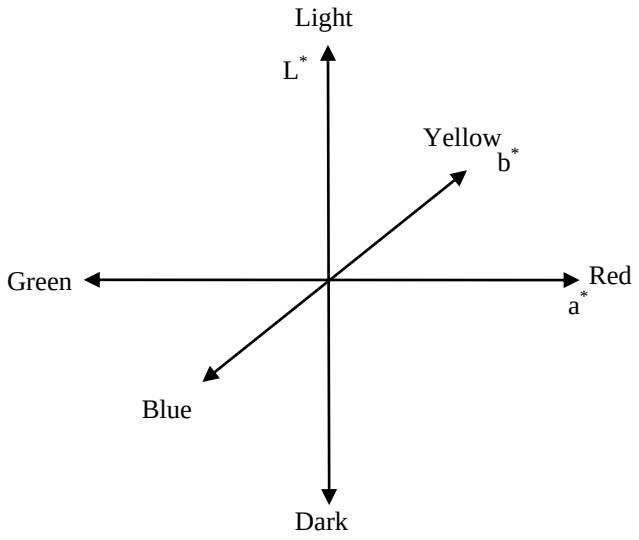

Figure 2.47 Cartesian representation of CIELab

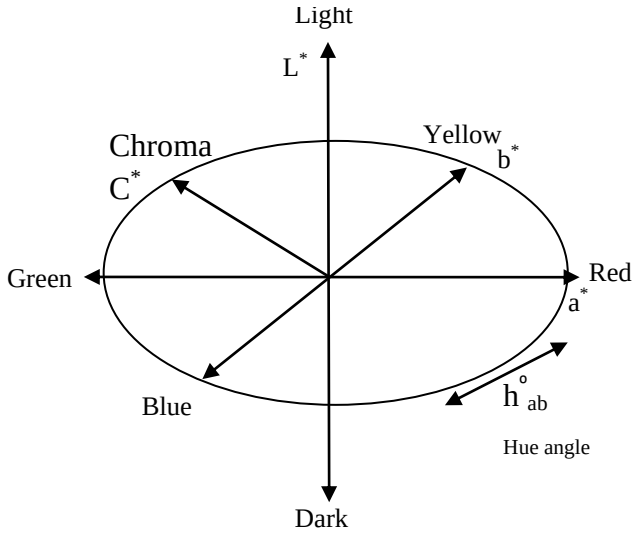

Figure 2.48 Cylindrical representation of CIELab

(c) Integ Value

The integ value for a colour can be defined as being derived from an integration of the weighted function of reflectance values covering all wavelengths in the visible region. It may also be defined as a surface in colour space showing the same depth of colour at all points [122]. In common practice, colour of a substrate, in particular its strength, is assessed visually. By means of the integ value, it is possible to represent colour and strength of the colour in a quantitative way. Normally, it is assumed that the depth of

colour is proportional to the Kubelka-Munk function $(K/S)_\lambda$, also referred to as F_λ by Derbyshire [118,122], which can be calculated as given in Equation 2.21.

$$(K/S)_\lambda = \frac{(1-R_\lambda)^2}{2R_\lambda}$$

Equation 2.21

In the case of high colour concentrations, it will be expressed as shown in Equation 2.22 or Equation 2.23 [118,122,123].

$$(K/S)_\lambda = \frac{(1-R_\lambda)^2}{2R_\lambda} - \frac{(1-R_s)^2}{2R_s}$$

Equation 2.22

or

$$F_\lambda = (K/S)_\lambda = \frac{[1-(R_\lambda - R_o)]^2}{2(R_\lambda - R_o)} - \frac{[1-(R_s - R_o)]^2}{2(R_s - R_o)}$$

Equation 2.23

where R_λ is the fractional reflectance of the coloured substrate at wavelength λ

R_s is the fractional reflectance of the uncoloured substrate

R_o is a constant with a small value which is defined as given below

Theoretically, R_o represents the surface reflectance at infinitely high concentration. Practically, it is a disposable constant which gives the best linearity between colour strength and F_λ or $(K/S)_\lambda$for a particular system and coloration process. Thus, the integ value was calculated according to Garland's suggestion of complementary tristimulus values using Kubelka-Munk function as a summation of the product of $(K/S)_\lambda$, illuminant energy and the sum of CIE colour matching functions, where k is a proportionality constant [118] as shown in Equation 2.24 or Equation 2.25.

$$Integ = k \sum_{\lambda=400}^{\lambda=700} (K/S)_\lambda E_\lambda \, (X_\lambda + Y_\lambda + Z_\lambda)$$

Equation 2.24

or

$$Integ = \sum_{\lambda=400}^{\lambda=700} I_\lambda F_\lambda \, (X_\lambda + Y_\lambda + Z_\lambda)$$

Equation 2.25

F_λ has been defined in Equation 2.23. I_λ is the spectral distribution of illuminant C, and X_λ, Y_λ and Z_λ are colour matching functions calculated at the 2° standard observer [122]. Integ values for particular colours are normally given associated with their location in the Colour Map, which is the CIELab a^*b^* diagram, to show the hue together with the depth [118].

(d) RGB Display

The term RGB stands for red, green and blue. Any colour in computer software is normally processed as RGB values before being displayed on a monitor screen. It is also possible to convert tristimulus values measured by a spectrophotometer into RGB values. These RGB values are presented in some application software, such as Microsoft Excel, and can be directly read and displayed as actual colours on the monitor screen by using specific software, for example as programmed in visual basic, plugged into Excel.

Normally, RGB colours are used for sensing, representing and displaying images in electronic systems such as television and computers etc. The devices using the ability to produce different colours include cathode ray tubes, liquid crystal and plasma displays or light emitting diodes. RGB colours also depend on the device and its colour management systems. Thus, different devices can detect or produce colour with some variation. This may be due to differences in the colour producing materials (such as dyes or phosphors) or manufacturers' RGB specifications.

The colours used by printers are normally CMYK i.e., cyan, magenta, yellow and black. For printing colour images, the computerised RGB colours are converted into CMYK which are processed according to the printer's specifications. Thus, the CMYK reproduction depends on the colours used by printers, which may be liquid colours in the case of ink jet printing or solid particles in the case of charged toners. It also depends on the colour management systems used by printers which are in place to ensure the correct mixing of CMYK colours to print a specific colour. Another factor which affects printed colours is the paper type and quality such as gloss, matte, etc. A

standard system used to convert RGB into CMYK is given in Set of equations 2.26. RGB values in this case have been normalized from 0-1.0 [124].

$$\text{Black} = \text{minimum}(1-\text{Red}, 1-\text{Green}, 1-\text{Blue})$$

$$\text{Cyan} = (1-\text{Red}-\text{Black}) / (1-\text{Black})$$

$$\text{Magenta} = (1-\text{Green}-\text{Black}) / (1-\text{Black})$$

$$\text{Yellow} = (1-\text{Blue}-\text{Black}) / (1-\text{Black})$$

Set of equations 2.26

Chapter 3. Experimental

3.1 Materials

3.1.1 Thermochromic Slurry

Dispersions of thermochromic pigments based on colour formers (leuco dye type), with the brand name Chromazone, also referred to as thermochromic slurries, provided by LCR Hallcrest, Connah's Quay, Wales, were used in this study. The colour change temperatures of the thermochromic slurries were quoted as 31°C and 40°C. For the 31°C products, magenta, green, blue and orange colours were used, while a black was used for the 40°C product; this last product was suitable for the study of combinations of liquid crystals with leuco dye based thermochromic pigments to provide a black background.

LCR Hallcrest provided the following information about the composition of the thermochromic slurries; they contain 52% water and 48% solids of which 40% is the internal phase. This phase consists of the colour developer, colour former and a solvent which controls the colour change temperature. The other 8% is the wall of the capsules which consists mainly of cross-linked melamine formaldehyde construction. Further details of the composition were not available due to industrial confidentiality.

3.1.2 Thermochromic Powder

Chromazone free flowing powders, provided by LCR Hallcrest, were incorporated into polymers by extrusion. Blue and red colours were used with a reported 31°C colour change temperature. These Chromazone microencapsulated thermochromic pigments are coloured below a certain temperature and become colourless as they are heated above this temperature. These pigments are also available in various colours and activation temperatures.

3.1.3 Liquid Crystal Themrochromics

The liquid crystals used in this study were Chiral Nematic TLC Sprayable Coatings provided by LCR Hallcrest. The liquid crystals provided were specially made for research purposes. They have various specific starting colour play temperatures and temperature bandwidths, which refers to the transition from red through to blue. The

liquid crystals used in this study were R25C20W, R30C20W, R35C1W, R35C5W and R40C5W. In this nomenclature, the numeral following R indicates the starting temperature of colour play in °C and the numeral following C shows the temperature bandwidth in °C over which the products change from red to blue. The liquid crystal samples provided contained polyvinyl alcohol as a binder so there was no need for an additional binder. The PVA cures at room temperature so there was no need to use elevated temperature curing.

For the assessment of the solid content of liquid crystals, a 0.979g sample was taken of product no. Bm/R35C1W/C17-10, batch no. 030203-2. It was placed in a vacuum oven at room temperature for a day, at a pressure of 635mmHg. The weight after one day was 0.371g. It was kept under vacuum for another three days with no further weight loss. The final weight loss was 0.608g, assumed to be water. The solid content was thus 37.90%.

3.1.4 Binders

Binders used for printing were Bricoprint Binder SF20E, Perapret PU New, Thermostar (textile bath dyeing binder) and LA-B 1096 BASF. Bricoprint Binder SF20E was provided by Selectasine Serigraphics Ltd, Chislehurst, Kent, England. It is a white paste containing a cross-linking polyacrylate, with mineral oil in water. It is a ready-for-use pigment print paste and contains thickener and other auxiliaries. This binder was selected as it was easily accessible and has proved useful and versatile for printing textiles in the School of Textiles and Design at Heriot Watt University. It has been used previously for printing with thermochromic pigments [70]. Perapret PU New was provided by BASF, Ludwigshafen, Germany. It is a white aqueous polyurethane dispersion. It is normally used for finishing, with pigments or without (BASF Colour Fast Finish), of woven or knitted cellulosic/blends fabrics, and is especially suitable for embossed, schreiner and chintz finishes. Thermostar textile bath dyeing binder was provided by LCR Hallcrest, Connah's Quay, Wales. It is an aqueous white dispersion of carboxylated acrylic esters and butadiene polymer. LA-B 1096 was provided by Tego Chemie GmbH, Goldschmidstrasse, Germany. It is a silicone modified polyurethane dispersion which is a hazy liquid. As the thermochromic slurries are temperature sensitive and have the potential to lose colour depth at higher temperatures, the binders ideally need to be fixed at relatively low temperatures and at the same time

be able to give good fastness properties. On this basis, the above binders were recommended by the manufacturers.

3.1.5 Thickener

Magnaprint Clear M04, provided by Magna Colours Ltd., Dodworth, Barnsley, England, was used in the formulation of pastes for printing Chromazone slurries. It has a smooth, creamy consistency and is an inverse copolymer emulsion of ethylenically unsaturated monomers in hydrocarbons. This thickener was used with all the binders except SF20E which already contained all the necessary ingredients.

3.1.6 Light fastness Enhancers

The following different types of light fastness enhancers were used. Tinuvin 144 is a Hindered Amine Light Stabiliser (HALS) and is available in white to light yellow powder form provided by Ciba Speciality Chemicals, Germany. Chemically it is bis(1,2,2,6,6-pentamethyl-4-piperidinyl)-2-butyl-2-(4-hydroxy-3,5-di-tert-butylbenzyl) propanedioate. Stabilon AO is a water soluble phenolic antioxidant provided by Huntsman Textile Effects, Langweid a. Lech, Germany. It is anionic and is provided as a yellowish brown, low viscosity liquid. Tinuvin P is an UV light absorber (UVA) of the hydroxyphenyl benzotriazole class provided by Ciba Speciality Chemicals. Chemically, it is 2-(2H-benzotriazole-2-yl)-p-cresol and provided in a pale yellow powder form. It has strong absorption in the 300-400 nm region. Tinuvin 1577 is a low volatility hydroxyphenyl-triazine UV absorber provided by Ciba Speciality Chemicals. Its chemical name is 2-(4,6-diphenyl-1,3,5-triazin-2-yl)-5-hexyloxyphenol and is available as yellowish, free flowing granules. Uvinul 3049 is an UV absorber provided by BASF, Ludwigshafen, Germany. It is a pale yellow powder and chemically is 2,2-dihydroxy-4,4-dimethoxybenzophenone. UV Titan L181 was provided by Kemira Chemicals (UK) Ltd., Harrogate, United Kingdom. It is an ultrafine titanium dioxide which scatters UV light and transmits visible light. Its absorption is mainly in the range 350-370 nm.

3.1.7 Polymers

Polymers were used to extrude filaments incorporating leuco dye based thermochromic pigments. The pigments are reported to be sensitive towards heat, so it was assumed that maximum colour strength would be achieved at lower processing temperatures. To

investigate the possibility of colour loss at high temperatures and other aspects of thermochromic pigments, polypropylene, linear low density polyethylene, ethylene vinyl acetate and polycaprolactone were selected. These polymers have different extrusion processing temperatures which cover the temperature range from 130°C to 260°C.

Polypropylene was provided by Basell Polyolefins (UK) Ltd. The melt flow index (MFI) was 13g/10min, measured with 2.16kg weight at 230°C. Linear low density polyethylene was provided by Basell Polyolefins (UK) Ltd. The MFI of the linear low density polyethylene was 18g/10min, measured with 2.16kg weight at 160°C. Ethylene vinyl acetate (EVA) was provided by Dupont Engineering Polymers and DuPont Packaging & Industrial Polymers, Stevenage, United Kingdom, branded as Elvax 450 with MFI (190°C, 2.16kg) of 8g/10min. and Elvax 3175LGA with MFI (190°C, 2.16kg) of 6g/10min. Polycaprolactone provided by Perstorp, Sweden, was branded as Capa 6500. Its MFI was 7g/10min, measured with 2.16kg weight at 160°C. Melt flow indices were reported by the providers of the polymers.

3.1.8 Fabric

The fabric used for printing was 100% Cotton Duck PK44 White, provided by Whaleys (Bradford) Ltd. Cotton was selected for experimental purposes due to its common usage in textiles and its natural origin. As the thermochromic pigments were to be printed as pigments incorporated in a binder, it was anticipated that using different substrates was unlikely to show significant variations.

3.1.9 Polyester Sheets

Polyester sheets were provided by PSG Group Ltd., London, United Kingdom. Black polyester sheets named as Polymex Black Untreated Polyester Film with product code P1900-36-SH were 36 µm in thickness. Transparent polyester sheets named as Polymex Clear Untreated Polyester Film with product code PC100-75-SH were 75 µm in thickness.

3.2 Preparation of Printed Samples

3.2.1 Pigment Paste

The pigment paste was formulated with 10% binder as discussed in section 3.1.4, 4% thickener (Magnaprint Clear M04) and the rest water. The water used for this purpose was deionised and distilled. After mixing in a beaker manually, it was then subjected to a high speed stirrer (Silverson L4R) for 5 minutes to ensure a homogenous paste. The viscosity of the paste for each batch was around 2400 cP at 22 ± 1°C, measured using a Brookfield DV-11+ Pro viscometer. This paste was used subsequently, mixed with thermochromic pigments according to the required colour depths.

3.2.2 Screen Printing

Printing was carried out using the following design, screens and machine settings.

(a) Screen Engraving

The selected design was a stripe, with a width of 4cm, produced in Adobe Photoshop. This design was selected as it provided the required width of samples for the many fastness tests, such as washing, etc. The artwork was printed on a transparent sheet using an Encad Novajet Pro 50 printer.

The screen used to print the samples was of 77 mesh. This screen was coated with Pure Coat 14, a light sensitive material provided by Thanet Coatings Ltd. The prepared screen was then dried in a dark room and kept there until exposure to avoid pre-exposure curing. The screen was exposed on a RA Smart exposure unit. The machine was powered on, followed by turning on the tube lights. The glass base of the machine was checked to ensure it was clean, and the artwork was fixed on the glass with adhesive tape. The screen was taken from the dark room and placed on the artwork. The lid was pulled down and catches fastened. The vacuum was applied and after 60 seconds, a timing channel was chosen which is set to use 35 light units and by this timing channel, the machine automatically calculates the required time of exposure to light. This channel was the maximum and is normally that selected for solid figures, as in this case a design of stripes. The timing sequence was then started. After exposure, the vacuum, tubes and power switch were turned off in turn, the rubber lid lifted slowly and the screen washed thoroughly. The screen was then inspected carefully for any uncured areas.

(b) Settings of the Printing Machine:

The printing machine, Midi MDF31, used was manufactured by Johannes Zimmer Klagenfurt, Austria. This machine has a range of settings, including magnetic rod pressure and the speed at which the rod moves on the blanket. For the printing of leuco dye based thermochromic pigments on fabric, the magnetic rod pressure chosen was option 1 from the 2 available on the main magnetic rod pressure dial. This was further divided into 6 divisions from which option 3 was selected. The speed of the rod was selected as 6m/min, from a maximum speed of 12m/min. A rough fabric was placed on the blanket to prevent contamination due to excess printing paste. The cotton fabric, used for printing, was ironed well to avoid crease effects and then fixed on the rough fabric with tape. The screen was then placed on the fabric and the rod was placed at the printing position by applying the magnetic field. The paste was poured in front of the rod and the rod was moved by the magnetic pull at the fixed speed. After printing, the pressure was removed and the printed fabric was set aside for air drying. The rod with the 12.14mm diameter was used for printing the leuco dye based thermochromic pigments.

3.2.3 Curing

The printed fabric was cured in the Roaches Oven and Steamer. The dry heat facility was used, rather than steam, as is normal with pigment binders. The temperature and time was varied as per the requirements of the experiments as detailed in Tables 3.1 and 4.3.

3.3 Colour Stability towards Heat

Thermochromic colours are reported as being heat sensitive and therefore it was anticipated that they may lose colour strength or be destroyed at high temperatures. To check the stability of leuco dye base thermochromic pigments against temperature, four colours, magenta, blue, orange and green were printed and cured at different temperatures and time periods. The curing conditions and the results are discussed in section 4.1.2.

3.4 Binder Optimization

The colour chosen for binder optimization was magenta as it was available in greatest quantity. The samples were printed at 5% and 20% shade depths with all four binders

described in section 3.1.4 and were cured at the temperatures and time periods as shown in Table 4.3.

After evaluation of all binders, the Thermostar textile bath dyeing binder was judged to be the best as discussed in section 4.1.3. An optimization of the curing temperature and time period was carried out for this binder, using the magenta colour with a shade depth of 5% and 20%. The samples were cured according to the conditions listed in Table 3.1.

Table 3.1 Curing optimization conditions for thermostar binder

Sample	Pigment Conc. (%)	Temp (°C)	Time (min)	Sample	Pigment Conc. (%)	Temp (°C)	Time (min)
1	5	90	5	13	20	90	5
2	5	90	8	14	20	90	8
3	5	90	10	15	20	90	10
4	5	100	5	16	20	100	5
5	5	100	8	17	20	100	8
6	5	100	10	18	20	100	10
7	5	110	5	19	20	110	5
8	5	110	8	20	20	110	8
9	5	110	10	21	20	110	10

3.5 Colour Concentration/Saturation Point

The colour saturation point is the concentration of pigment beyond which increasing the quantity of pigment does not increase the colour strength observed visually or instrumentally. To investigate the effect of leuco dye base thermochromic pigment concentration and estimate the colour saturation point, the samples were printed at 2%, 5%, 10%, 20%, 30%, 40% and 50% shade depths for all available four colours; blue, magenta, orange and green. Initially, all samples were printed using the Bricoprint Binder SF20E. After finding that Thermostar binder was better suited for the thermochromic slurries as discussed in section 3.4 and section 4.1.3, all of these samples were reprinted using printing pastes with the Thermostar binder and colour measurements were taken. The samples were measured without curing to avoid colour loss due to thermal degradation.

3.6 Light Fastness Enhancement

With the aim to improve the light fastness of leuco dye based thermochromic pigments, three different types of light fastness enhancers, Tinuvin P (a UV absorber), Tinuvin 144 (a HALS) and Stabilon AO (an antioxidant) were used at a 5% concentration of blue and magenta colours. Light fastness enhancers were used in two ways; by mixing directly into the pigment print pastes and printing on white fabric, and by incorporating into separately print paste and then coating them over the printed fabrics, covering the thermochromic pigments with light fastness enhancers as protective layers. The quantity of light fastness enhancers used was 3% by weight of both coloured and colourless printing pastes. The covered layer of light fastness enhancer produced a slight creaminess over the colours.

The results obtained from this investigation showed that the UV absorbers gave the best light fastness enhancement as discussed in section 4.1.5. To investigate further, four different UV absorbers (Tinuvin P, Tinuvin 1577, Uvinul 3049 and UV Titan L181) were used with four leuco dye base thermochromic colours; blue, magenta, orange and green. Two concentrations of UV absorbers were used; 3% and 5% by weight. All of these samples were prepared both by mixing the UV absorbers directly in the pigment paste and printing on white fabric and also by the over-layering method. The pigment concentration used in this case was also 5%.

3.7 Preparation of Samples Coated with Liquid Crystal Thermochromics

3.7.1 Printing Machine

To coat liquid crystals on polyester sheets, the printing machine (as discussed in section 3.2.2(b)) was used for trials. All possible combinations of machine settings and available rods were used for trial purposes in attempts to coat the thermochromic pigments on polyester sheets. The polyester sheets were fixed on the printing blanket with tape and liquid crystals were poured in front of the rods. The polyester sheets have a highly smooth surface, without porosity and the rods were also highly polished. Thus, almost all of the liquid crystals was carried in front of rods and failed to coat the sheets. It was envisaged that the lightest weight rod, at the lowest magnetic pressure and highest speed settings, might leave a reasonable amount of liquid crystals. In the event, a very thin layer of liquid crystals was formed, which was not thick enough to exhibit colour play with varying temperature.

3.7.2 Wire Wound Bars

Liquid crystals were also coated using wire wound bars. The wire wound bars were provided by R K Print Coat Instruments Ltd., Litlington, Royston, Hertfordshire. These rods are manufactured to give film thicknesses as detailed in Table 3.2. However film thickness also depends on other variables such as the solid content and viscosity of the material to be coated and the pressure and speed of the wire wound bar [125]. Polyester sheets of A4 size were mounted on a sample holder and wire wound bars were placed on top. Small amounts of liquid crystals were poured in front of the wire wound bars which were then drawn across the polyester sheets by hand. Care was taken so that the speed and pressure applied were kept consistent. As this procedure required human involvement to keep speed and pressure constant, there was a high likelihood of variation in reproducibility of layer thicknesses. Thus, this method was not used further.

Table 3.2 Wire wound bars and expected wet film thickness

Bar No.	Wet film thickness (µm)	Bar No.	Wet film thickness (µm)
0	4	7	80
1	6	8	100
2	12	9	120
3	24	150	150
4	40	200	200
5	50	300	300
6	60	400	400

3.7.3 Coating Machine

A Coatema coating machine, provided by Coating Machinery GmbH, Germany was used to coat the liquid crystals onto polyester sheets. The liquid crystals were poured in the trough and the polyester sheet was passed at a constant speed with a minimum space between the squeegee and sheet. However, due to the flat surface and non absorbency of polyester sheets, the coating proved to be inconsistent and not suitable for experimental purposes.

3.7.4 Wire Wound Bars and Printing Machine

As the rod on the printing machine was providing only a very thin liquid crystal layer, and due to the inconsistency inherent in manual use of the wire wound bars, a method was developed combining wire wound bars and the printing machine. Layered cloth was laid on the printing machine, thick enough to avoid contact of the wire wound bar handle with the blanket. The polyester sheet was placed on the cloth and fixed with tape. The wire wound bar was placed on the polyester sheet and kept in place by switching on the magnet pressure of the machine. A small amount of liquid crystal was poured in front of the wire wound bar. The wire wound bar was drawn across the polyester sheet by magnetic pressure and at a constant speed. A number of trials were carried out to find the most suitable wire wound bar and machine settings for coating. The most acceptable results were achieved by using a No. 8 wire wound bar at highest magnetic pressure settings which was option 2 of 2 and 6 of 6 in sub divisions, and at a maximum speed setting of 12m/min of the printing machine.

In the study of combinations of liquid crystals, they were over layered on each other, in combinations of two, referred to as double combinations. In the case of transparent sheets, the individual liquid crystal coated sheets were overlaid on each other with a black sheet behind them at the time of colour measurement. For single coated black sheets, every over layered combination was prepared by coating the first liquid crystal and drying with a hair dryer. The second liquid crystal was then coated on the dried coating of the first liquid crystal.

3.8 Extrusion

Two types of extrusion machines were used in this study for extruding thermochromic pigments incorporated into filaments of different polymers.

3.8.1 Ram Extrusion Machine

The Ram extrusion machine was provided by Extrusion Systems Ltd., Bradford, England and is available in the extrusion lab at Heriot Watt University. In a Ram extrusion machine, a ram moves in a cylinder under hydraulic pressure. The diameter of the cylinder is related to the diameter of the ram in such a way that the ram can move easily but without gaps through which the extruding material can come out of the cylinder, except for the die hole. The Ram extrusion machine used in this study,

operates at up to 800psi pressure to move hydraulically in the cylinder, against the extruding polymer; beyond that the machine automatically cuts out to prevent damage caused by excess pressure. The temperature of the machine can be adjusted manually and maintained automatically, according to required level of the molten state of a polymer. A single hole die was used with this machine. The ESL ram extrusion machine available at Heriot Watt University is shown in Figure 3.1.

Figure 3.1 ESL Ram Extrusion Machine

All four polymers were extruded on this machine. The optimum pressure and temperature settings of the machine to provide prototype filaments were found by trial and error for every polymer as discussed in section 4.2.1. For these trial experiments, polymers were used alone without pigments. After establishing conditions for prototype filaments, filaments were extruded incorporating leuco dye based thermochromic pigments. However, poor mixing of thermochromic pigments and polymer were observed in extruded filaments due to the mixing limitations of this machine. Although homogeneously incorporated thermochromic pigmented filaments were not possible using this machine, the machine has the advantage of a small sample size (10-15g) depending on the density of the material. Therefore, all of the polymers were extruded first on this machine to provide a guide to the processing parameters and extrusion behaviour before processing them on a bench-top screw extrusion machine.

3.8.2 Screw Extrusion Machine

The bench top screw extrusion machine was used, provided by Extrusion Systems Ltd., Bradford, England, installed in the extrusion lab of Heriot Watt University. In screw extrusion machines, a screw is used inside a barrel. At one end of the screw, there is an opening to feed the material while at the other end, normally a metering pump and a die in a die head is situated. The function of the screw is to push the material from the feed section to the die head together with other functions, such as condensing, mixing etc. The function of the metering pump is to regulate the amount of molten polymer reaching the die head. The die head consists of filters, breaker plate, die etc. Mainly, the die head is responsible for producing the required shape continuity of the filament.

The screw machine used in this study has a screw with a mixing head. Although good mixing of polymer and incorporated materials is normally obtained in screw extrusion machines due to the shear forces, the presence of mixing head on a screw ensures even better mixing. Homogeneous incorporation of thermochromic pigments into filaments was obtained by this screw extruder. Temperature adjustments were available throughout the screw, metering pump and die head. Three temperature controlling zones at the screw were available, normally referred to as the feed, compression and mixing zones. One temperature controller was available at the metering pump and two at the die head. The temperature settings were individually operated and maintained independently. The temperature at the first screw zone was kept low so that the solid polymer would push material forward towards the die head. The temperatures at the compression and mixing zone of the screw were adjusted for each polymer in such a way that the polymer became totally molten up to the mixing head of the screw. The temperatures at the metering pump and die head were kept high enough that the polymers remained molten through these regions. The filaments obtained from die were quenched in cold water to provide solidification. The extruded filaments were then taken up by a winder provided by Leesona Corporation, Burlington, NC, USA. The distance between the die head and water, quenching length of filaments in the water and winding speed of the winder used for the different polymers were different as discussed in section 4.2.2.

The die head and screw was cleaned after every use to prevent cross contamination of colours and of polymers. The screw was taken out and cleaned with a brush and a blow torch. The die pack or head was cleaned by placing in an oven at 450°C overnight.

Cleaning was achieved by decomposing and burning the polymer into ash. The oven was provided by Kilns & Furnaces Ltd., Stoke-on-Trent, England. The bench top screw machine available at Heriot Watt University is shown in Figure 3.2.

Figure 3.2 ESL Bench top Screw Extrusion Machine

3.9 Drawing

The prototype extruded filaments were drawn to provide molecular orientation, mechanical strength and fineness. Two types of machine were used for drawing.

3.9.1 Cold Drawing

The cold drawing machine was provided by Extrusion Systems Limited (ESL), available in the extrusion lab of the School of Textiles and Design, Heriot Watt University as shown in Figure 3.3. The drawing machine has three pairs of rollers with adjustable speed controllers. The speeds of rollers were increased gradually roller by roller. The amount of stretching of filaments from their original length to a final length is known as the draw ratio. The draw ratio was adjusted to a maximum stretchable length without breakage of filaments for every polymer. This machine had no heating mechanism and operated at room temperature. It is used for small scale drawing such as that used in line with a Ram extrusion machine or when used alone. Therefore, the speed of drawing was low as compared to a hot drawing machine, which was an advantage for the drawing of thermochromic pigment incorporated filaments due to attempting to minimize sample size. However, the filaments obtained were very stiff

indicating that the molecular chains did not have much mobility at room temperature. This resulted in a rough surface and breakage of filaments during drawing, especially in the case of polyethylene and polypropylene. Therefore, it was decided that this machine was not suitable for drawing purposes in this study.

Figure 3.3 ESL Cold Drawing Machine

3.9.2 Hot Drawing

Hot drawing of filaments was carried out on a commercial scale drawing machine also provided by Extrusion System Limited (ESL) and installed in the extrusion lab of School of Textiles and Design. It has hot drawing rollers and plates. The temperatures of the drawing rollers and plates were adjustable. The temperatures of the rollers were kept high enough so that the polymer filaments would soften, and the polymer chains had sufficient mobility to allow stretching. The draw rollers had adjustable speed controllers. Their lowest speed was higher than that of the cold drawing machine and therefore, relatively large samples of filaments were used. A Leesona winder was used to take up the drawn filaments. The drawn filaments obtained from this machine were smooth and with less breakage. Hence the drawing of filaments on this machine was carried out effectively, although the speed of the draw frame was rather fast for the sample sizes of the filaments. The optimum drawing conditions are detailed in section 4.2.3. The hot drawing machine available at Heriot Watt University is shown in Figure 3.4.

Figure 3.4 ESL Hot Drawing Machine

3.10 Wash Fastness

The wash fastness of printed and extruded samples was evaluated using the 'ISO 105, part C10: colour fastness to washing with soap or soap and soda' test method. The test method sub section, A(1) was used. The test specimens were prepared by attaching a printed fabric strip of 100mm × 40mm to the SDC multifibre fabric with the same dimensions by a staple. In the case of extruded filaments, lees were made of the same dimensions as the printed sample and attached to multifibre fabric. The SDC multifibre fabric comprises six different fibre components; secondary cellulose acetate, cotton, acrylic, polyamide, polyester and wool [126]. The standard ISO soap solution of 5g/L was prepared in distilled water. The liquor ratio was kept at 50:1 ml/g. A Washtec P machine provided by Roaches was used for this test. The test was conducted for 30 minutes at 40°C. The samples were assessed by colour measurement using the DataColor Spectraflash SF600 spectrophotometer.

3.11 Rub Fastness

A standard manual crock meter was used for measurement of rub fastness. The specimen was clamped in the sample holder and a Standard AATCC white crock cloth was clamped in the upper holder. The upper part of the crock meter had a standard weight which applied specific pressure during rubbing. The number of rubbing cycles or the number of times the white crock cloth rubbed against the printed and extruded

filament samples was 10. The stain on the white crock cloth was measured by a DataColor Spectraflash SF600 spectrophotometer. The same procedure was followed for wet rubbing, in which case, the standard crock cloth was soaked in distilled water and squeezed to remove excess, leaving the cloth damp.

3.12 Light Fastness

The lightfastness of leuco dye based thermochromic pigments was examined. The printed samples, those treated with lightfastness enhancers and extruded thermochromic filaments were tested for light fastness. The samples were exposed to light on the Heraeus Xenotest 150S fadeometer. This test was performed for 1, 2, 3, 4, 6, 8, 12 and 24 hours. Normally, a blue wool scale is exposed in Xenotest together with the samples, and the samples compared after exposure visually with the blue wool scale to provide a grading of the light fastness of the samples. However, the leuco dye based thermochromic pigments were found to have poor light fastness and faded so quickly that, instead of using the blue wool scale, colour measurements were taken on the spectrophotometer and evaluated.

3.13 Differential Scanning Colorimetry

Differential scanning colorimetery (DSC) was carried out for all polymers, filaments and leuco dye based thermochromic powders used in extrusion to determine their behaviour with increasing temperature. For DSC measurements, a Mettler DSC 12 E instrument was used. The weight of the sample was measured using a Mettler TG50 Thermobalance which can measure with an accuracy of $\pm$0.0001mg.

Samples were placed in the pans and lids and their weights were measured, and kept in range 5-10mg. To ensure optimum contact with the pans, the polymers and filaments were cut into fine pieces and evenly distributed in the pans. The pans with the samples were placed on a crimping press to seal the lids. An empty pan and lid was used as a reference. The DSC investigation was carried out both in nitrogen and air environments.

3.14 Hot stage microscopy

The hot stage microscopy was used to investigate the thermal behaviour of polymers visually before extrusion. The hot stage used was a TH600 instrument with a temperature control unit PR600 provided by Linkam Scientific Instruments. Different

phases of polymers were observed visually with increases in temperature to provide information on the melting and flow properties of the polymers.

3.15 Tensile Strength

The tensile strength of filaments was measured on an Instron 3345K7484. The test method BS EN ISO 2062:1995 (textiles-yarn from packages-determination of single-end breaking force and elongation at break) was used. The test was performed for coloured and colourless filaments.

3.16 Scanning Electron Microscopy

Scanning electron microscopy was carried out on the thermochromic powder samples and on extruded filaments of the polymers to study the filaments and to observe the distribution of thermochromic pigment microcapsules in the filaments.

3.16.1 Preparation of Samples

The thermochromic powder was transferred to a stub by a spraying technique. Pigment (0.02g) and ethanol (10ml) in a beaker were placed in an ultrasonic bath, provided by Decon Ultrasonic Ltd., for 5 minutes. The dispersion obtained was sprayed on the stubs, and dried with a table lamp bulb. The sample prepared with this method showed re-aggregation of microcapsules in the SEM and did not give satisfactory results.

In the second technique, the thermochromic pigment powder container was shaken gently to produce a fine dust of pigment and the stub was passed through it. The dust on the stub was not visible to the naked eye but it gave good results using SEM.

The filaments were cooled using dry ice and an attempt was made to snap them. However, the filaments were not hard enough to snap. Therefore, a sharp razor blade was used to provide cross sections of the filaments. The cross sections obtained using this technique showed a small shear effect at one end which was visible only in SEM, but it did not have a serious effect on assessing the distribution of the microcapsules within the filaments.

3.16.2 Sputter Coating

The stubs were sputter coated with gold before SEM examination using a Polaron SC7620 Sputter Coater. Sputter coating of samples gave good results using SEM by providing a protective layer against the high voltage of the SEM.

3.16.3 SEM

Scanning electron microscopy was carried out using the Hitachi S-4300 Field Emission Scanning Electron Microscope available at School of Textiles and Design, Heriot Watt University, shown in Figure 3.5. This instrument was computer controlled and a scan of the sample was visible on the computer monitor. The source of electron in this machine was a field emission tungsten tip, fixed in the gun assembly. Two condenser lenses were used to de-magnify the electron beam. An objective aperture was used to pass only those electrons into the electron column, which was directed towards the sample. An objective lens was used to focus the beam on the sample. The distance between the objective lens and the sample is known as working distance. The working distance is shorter or longer according to the required image with higher or lower resolution or for a smaller or wider sample area, respectively.

The electron column was kept under vacuum at all times. A small chamber was used to exchange the samples. Before exchanging the samples, this chamber was disconnected from the SEM by closing the electron column and then allowing air into the chamber. The sample was screwed to an exchanging rod and the chamber was again connected to the electron column by creating a vacuum. Before placing the sample into the electron chamber, it was ensured that the sample holder's positional coordinates and angles were at rest or sample exchange position, i.e., X=40mm, Y=25mm, T=0°, R=0° and Z=15mm. The stub was placed in the sample holder in the electron column and the exchange rod was unscrewed and taken out. Before starting the electron emission gun, the electron column was again closed. The required power of the electron beam was selected and focused on the sample by adjusting the working distance and other positional coordinates of the sample. After selecting the required area of the sample or resolution of electron beam, SEM images were captured.

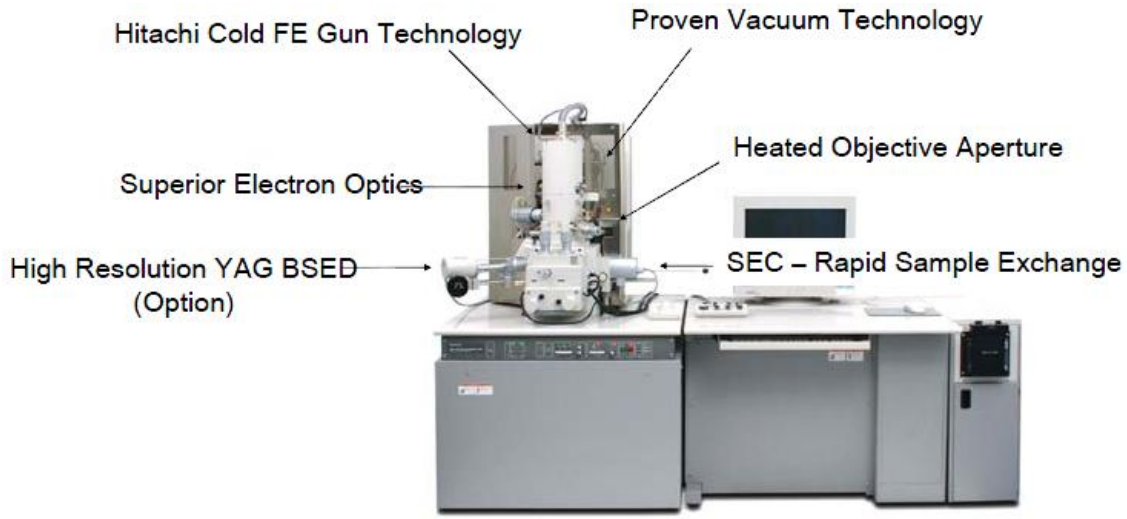

Figure 3.5 Hitachi SE-4300 FE SEM [127]

3.17 Colour Measurement

Colour measurements were carried out for the leuco dye based thermochromic pigments and for the liquid crystals and extruded filaments on a DataColor Spectraflash SF600 spectrophotometer. The colour measurements at room temperature were taken using only the spectrophotometer, while thermally dependent colour measurements were taken with a combination of the spectrophotometer and a hot stage.

3.17.1 Colour Measurement Conditions

For calibration process, to find optimum conditions for measuring prints from thermochromic slurries, the magenta pigment was selected because it had previously been used for the optimization of binders due to its availability. The sample was at a 5% concentration of pigment and was cured at 110°C for 3 minutes. This thermochromic slurry has a reported colour change temperature of 31°C. However, according to LCR Hallcrest (providers of the slurries) the colour can start to change at temperatures up to 4°C below this. Thus to avoid possible changes in colour due to variation in ambient temperature, all measurements were carried out at 22°C. A range of measurement variables was available in the spectrophotometer. Therefore, a number of combinations of variables were used as listed in Table 4.1.

For each set of conditions, the colour was measured 10 times and averaged. For assessment purposes, L^*, a^*, b^*, C^* and h^0 values were selected. The D65 illuminant, which is similar to daylight, was used in this study. Values for other illuminants were ignored. The optimum conditions selected for colour measurements of leuco dye based

thermochromic pigments were those which gave the more consistent and repeatable results. The set of parameters with the lowest standard deviation and error in colour coordinates over ten measurements was chosen as discussed in section 4.1.1. The selected conditions for subsequent colour measurements were a small aperture, 100% UV off, specular included, 3 flashes and accepting measurement after 3 readings.

3.17.2 Spectrophotometer used in Conjunction with Hot Stage

The leuco dye based and liquid crystal thermochromic pigments change colour with increase and decrease in temperature. Previously, a method to measure liquid crystal colours at different temperatures had been developed in our laboratories by using a combination of a hot stage and spectrophotometer [25]. This combination was re-built to study thermochromic pigments as a function of temperature, although using a different spectrophotometer to that which had been used previously. The hot stage was calibrated according to manufacturer's instructions. The hot stage was removed from its assembly as it was not possible when contained in the assembly to keep the hot stage in contact with the printed or coated samples against the spectrophotometer. For safe use of the hot stage a new assembly was built, which was level with the front side of the hot stage and which covered it completely from the sides and behind to avoid damage during handling. The hot stage in the new assembly was well insulated from the sides and from behind using glass wool to minimise thermal losses to the environment. Used with the PR600 control unit, the hot stage is capable of increasing and holding temperature to within $\pm 0.1^{\circ}C$. In the new assembly, it was not possible to install a peristaltic pump for cold water circulation to provide a lower temperature, as had been used previously [25], so an ice jacket and fan was used behind the hot stage assembly to provide a lower temperature when needed. A line diagram of the spectrophotometer assembled in conjunction with hot stage is shown in Figure 3.6.

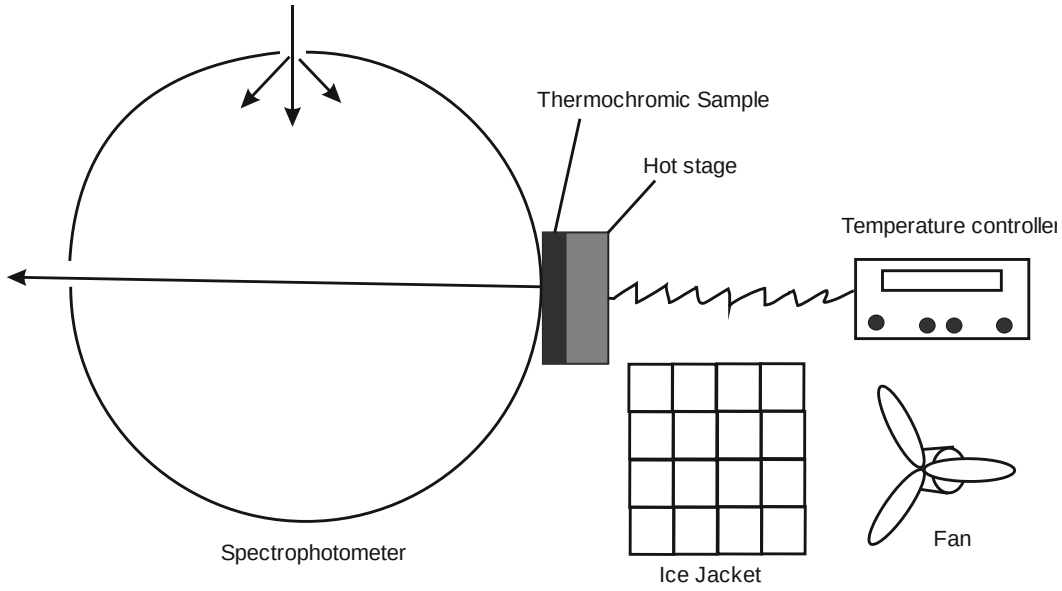

Figure 3.6 Spectrophotometer in conjunction with hot stage

The spectrophotometer calibration conditions used were those optimised for the leuco dye based thermochromic pigments and the liquid crystals, as discussed in section 4.1.1. It was envisaged that there was a possibility of variation in measuring the smooth surface of liquid crystal coated on polyester sheets, due to specular included, but as there was an ultimate intention to print on fabric, for consistency, the same conditions were used.

The colour measurements were taken at different temperatures. The rate of increase in temperature was set according to the thermochromic pigment in investigation. After achieving the temperature at which the colour was to be measured, it was maintained by the hot stage control unit for approximately 2 minutes to ensure the sample had reached the temperature of the hot stage. A heat sink compound, provided by RS Components, was applied between the hot stage and the fabrics and colour measurements were carried out both with and without it. There was no significant difference in the measured colour, in both cases, and the heat sink compound was also contaminating the sample, especially printed fabric, and so it was not further used in this study.

The colour measurements for leuco dye based thermochromic pigments were taken at 0.5°C intervals. The colour measurements for liquid crystals were carried out at 0.2°C intervals for a temperature bandwidth of 5°C or less until a clear blue colour was achieved. The colour measurements after achieving the blue colour and for liquid crystals with a temperature bandwidth of 20°C, were taken with 0.5°C increments. The

samples were also measured during cooling with the same intervals (0.2°C or 0.5°C) as for heating.

3.17.3 Assessment of Single and Double Combinations of Liquid Crystals

The five liquid crystals, as identified in section 3.1.3, were coated on transparent polyester sheets as described in section 3.7.4. The colour measurements at different temperatures were carried out by placing a black sheet behind these samples. The measurements were taken for single and double combinations of liquid crystals by overlaying the transparent sheets on one another and over a black sheet to absorb transmitted light waves. It was anticipated that this method of making combinations would be easier and anticipating that transparent sheets would not make a difference if the liquid crystal combinations were coated directly on a black sheet. However, major differences were found in brightness and intensity of colours when compared with a combination of liquid crystals on a black sheet. Therefore, liquid crystals were directly coated on black sheets individually and in double combination by over coating on each other as discussed in section 3.7.4.

3.17.4 Assessment of differences between Liquid Crystals coated directly on Single Black Sheet and on Transparent Sheets

The colour measurements of liquid crystals coated on black and transparent polyester sheets were taken as discussed in section 3.17.3. A comparative study was carried out between overlaid transparent sheets and black sheets.

3.17.5 Assessment of Change in Overlaying Sequence of Liquid Crystals

To investigate the effect of changes in the overlaying sequence of liquid crystals, the liquid crystals were coated in a different sequence on each other and colour measurements were taken for both samples.

3.17.6 Assessment of Specular Included and Excluded for Polyester Sheets

To investigate the effect of specular reflection for the polyester sheets coated with liquid crystals, the measurements were also taken both including and excluding specular.

3.17.7 Assessment of Combinations of Liquid Crystals and Leuco Dye based Thermochromic Pigments

Printed and cured fabric samples were prepared with black leuco dye based thermochromic pigment, having a colour change temperature of 40°C. Liquid crystals, R25C20W, R30C20W, R35C1W, and R35C5W were coated on these black samples. R40C5W was not coated as its colour play starts from 40°C which is the colour change temperature of the black pigment used in this study. The fabric was printed and cured with black leuco dye based thermochromic pigment as mentioned in sections 3.2.2, 3.2.3 and 4.1.3. The liquid crystals were coated on this black printed fabric as described in section 3.7.4. The colour measurements with temperature were carried out for the black alone and all four liquid crystal samples coated on the black thermochromic pigment.

Chapter 4. Results and Discussion

The microencapsulated leuco dye and liquid crystal thermochromic pigments used in this study were provided by LCR Hallcrest. Studies were carried out using these pigments individually and in combination. Thermochromic pigments containing colour formers, also referred to as leuco dye based, were investigated in terms of aspects of their performance in screen printing onto textiles, attempts were made at lightfastness improvement and incorporation within selected polymers during their extrusion to form fibres. Liquid crystal types were investigated in a study based on observations from a separate design-based project, aiming to broaden the scope of the colour play possibilities, when used in combinations of two or more liquid crystal types and also in combination with leuco dye based types [70].

4.1 Leuco Dye based Thermochromic Pigments applied by Screen Printing

Leuco dye thermochromic pigments were provided in two forms; as slurry and as powder. The slurry was described as containing 52% of water and 48% solids. The solid contents were reported to contain 40% internal phase which consists of colour developer, colour former and a solvent to control the colour change temperature as described in section 3.1.1. The rest of the internal phase is the wall of the microcapsule which mainly consists of cross-linked melamine formaldehyde polymer construction. As these pigments contained many components, the colour strength available is much less than traditional pigments. For example, if a traditional pigment gives a saturated colour strength in the 3-4% concentration range by the weight of pigment paste, then these pigments may give this colour strength at around 15-30% [9].

Five colours, magenta, blue, orange, green and black, were provided in water-based slurry form, which was used in the formulation of screen printing pastes. The colour change temperature for magenta, blue, orange and green was reported as 31°C while for black, it was 40°C. The powder forms of these pigments were free of water and hence they are composed of only colour former, colour developer, and solvent contained in microcapsules. In powder form, two colours, blue and red, were provided, with a colour change temperature reported as 31°C. The powders were used in the investigation of extrusion into filaments.

4.1.1 Calibration of the Colour Measurement System

The variables involved in measuring colour using a reflectance spectrophotometer include UV light included or excluded, specular component included or excluded, aperture size, the number of light flashes to measure average reflectance of the sample in one reading and the number of readings from which an average measurement is taken. The set of variables chosen to establish the appropriate colour measurement conditions is given in Table 4.1.

Table 4.1 Calibration conditions

	Aperture	**Specular**	**UV**	**Flashes**	**Measurements before acceptance**
A	Small	Included	On	3	3
B	Small	Included	Off	3	3
C	Small	Excluded	On	3	3
D	Small	Excluded	Off	3	3
E	Ultra Small	Included	On	3	3
F	Ultra Small	Included	Off	3	3
G	Ultra Small	Excluded	On	3	3
H	Ultra Small	Excluded	Off	3	3
I	Small	Included	On	1	1
J	Small	Included	Off	1	1
K	Small	Excluded	On	1	1
L	Small	Excluded	Off	1	1
M	Ultra Small	Included	On	1	1
N	Ultra Small	Included	Off	1	1
O	Ultra Small	Excluded	On	1	1
P	Ultra Small	Excluded	Off	1	1

A large aperture size was also available but was not used as it was not appropriate for the small sizes of fabric samples, for example as used to assess fastness to washing, rubbing and light. In the set, a greater number of light flashes were combined with a greater number of readings, and vice versa. These combinations were studied to determine whether any colour reduction occurred due to heat produced by the

spectrophotometer during colour measurement. Colour measurement used the D65 illuminant since it closely simulates daylight.

The selected pigments used were reported to change colour at either 31°C or 40°C, although LCR Hallcrest, provided the information that the fading could start as early as 4°C before the reported temperature. Therefore, it was decided to take all colour measurements at 22 ± 1°C, except for those colour measurements where temperature was varied, to avoid any colour change at ambient temperature.

A print from the magenta pigment was selected for calibration purposes, as it was available in large quantity. The colour concentration used was 5% on the weight of the printing pastes. The printed samples were cured at 110°C for 10 minutes, for reasons given later in section 4.1.3.

The most suitable conditions for colour measurement are those which are reliable, consistent and repeatable. For evaluation of results, L^*, a^*, b^*, C^* and h° values were chosen from colour measurement, which represent different attributes of their colours as discussed in section 2.13.6(b). For each set of variables, the colour measurements were taken ten times, to provide information on consistency and repeatability. In Table 4.2 and the graphs in Figures 4.1-4.5, the mean values, standard deviations and 95% confidence intervals of these ten measurements are displayed. The mean values are presented in both tables and graphs, while standard deviations and 95% confidence intervals are presented in tables and as error bars in graphs respectively. Standard deviation is a measure of variance and the 95% confidence interval represents the upper and lower range of a mean value between which the chance of the occurrence of a reading is 95%. The standard deviation was calculated using Equation 4.1 and 95% confidence interval using Equation 4.2.

$$Standard\ Deviation\ (\sigma) = \sqrt{\frac{\sum(x - \bar{x})^2}{n}}$$

Equation 4.1

$$95\%\ Confidence\ Interval = \bar{x} \pm 1.96\left[\frac{\sigma}{\sqrt{n}}\right]$$

Equation 4.2

where, x = reading of the sample

$\bar{x}$ = mean value

σ = standard deviation

n = number of readings

In Table 4.2 and Figures 4.1-4.5 which show the data obtained for magenta prints, the standard deviation and 95% confidence interval for L^*, a^* and C^* values are lower for conditions B, J, L and P, for b^* values, they are lower for conditions B, J, L, P and especially for F and for h° values, the values are lower for conditions B, H, N which, except for B, differ from the results for the other parameters. In the colour measurements, except for h° values, the standard deviation and 95% confidence interval are lower mostly in the case of B, J, L and P conditions. The h° values (hue angle) which, in the case of leuco dye based thermochromics, is concerned with the change from a single colour to colourless due to heat, is not likely to be significant. The L^* value, the lightness, is likely to be an important factor since leuco dye based thermochromic pigments become colourless or lighter from coloured with temperature rise if there is any heating effect during measurement.

In conditions B, J, L and P, UV light is excluded, which suggests that UV light included may affect the colour measurement system and its capability to measure the colour with accuracy. The specular component is both included and excluded in this set of conditions, so it is assumed that it has no significant effect on the colour measurement. In conditions B, J and L, the small aperture was used while in the case of P, the ultra small aperture was used. The small aperture covers a larger area of the sample to be measured than the ultra small aperture, it is expected that its use would introduce fewer errors. Practically, this effect is consistent with conditions B, J and L, which contain the small aperture in combinations. In conditions B, the flash was used 3 times, and the measurement was accepted as an average of 3 readings, while in the case of J, L and P, the flash was used one time and a single reading was accepted. Thus, more readings and averaging of results shows higher repeatability and consistency, as expected.

Hence, it was concluded that the calibration conditions within option B which are small aperture, specular included, UV light off, with 3 flashes and 3 readings before acceptance, was most reliable and consistent. Therefore, these conditions were used to take all further colour measurements for this study.

Table 4.2 Mean and standard deviation for magenta over 10 measurements for each set of conditions:

Calibration Conditions	L^*		a^*		b^*		C^*		h°	
	Mean	St. Dev.	Mean	St. Dev.	Mean	St. Dev.	Mean	St. Dev.	Mean	St. Dev.
A	65.69	0.11	43.61	0.11	-19.62	0.04	47.82	0.11	335.78	0.02
B	65.64	0.05	43.43	0.04	-19.45	0.01	47.58	0.04	335.88	0.01
C	65.25	0.08	44.02	0.08	-19.79	0.02	48.26	0.09	335.79	0.01
D	65.39	0.08	44.20	0.07	-19.85	0.02	48.45	0.07	335.81	0.01
E	64.34	0.25	45.59	0.21	-20.21	0.07	49.87	0.20	336.09	0.11
F	61.03	0.10	48.05	0.05	-20.38	0.00	52.20	0.05	337.02	0.02
G	64.79	0.24	44.27	0.20	-19.92	0.05	48.55	0.21	335.77	0.04
H	65.88	0.08	42.62	0.07	-19.17	0.02	46.73	0.07	335.79	0.01
I	65.91	0.05	43.31	0.05	-19.62	0.01	47.55	0.05	335.63	0.02
J	65.41	0.04	44.00	0.04	-19.79	0.01	48.25	0.04	335.78	0.01
K	65.11	0.12	43.69	0.11	-19.50	0.04	47.85	0.12	335.94	0.02
L	64.69	0.05	44.54	0.04	-19.90	0.01	48.79	0.04	335.93	0.01
M	65.69	0.15	44.00	0.15	-19.69	0.05	48.20	0.16	335.89	0.02
N	65.91	0.06	42.97	0.05	-19.48	0.02	47.18	0.06	335.62	0.01
O	66.58	0.07	41.54	0.06	-18.60	0.02	45.52	0.06	335.88	0.02
P	66.17	0.03	42.42	0.03	-18.79	0.01	46.39	0.03	336.11	0.01

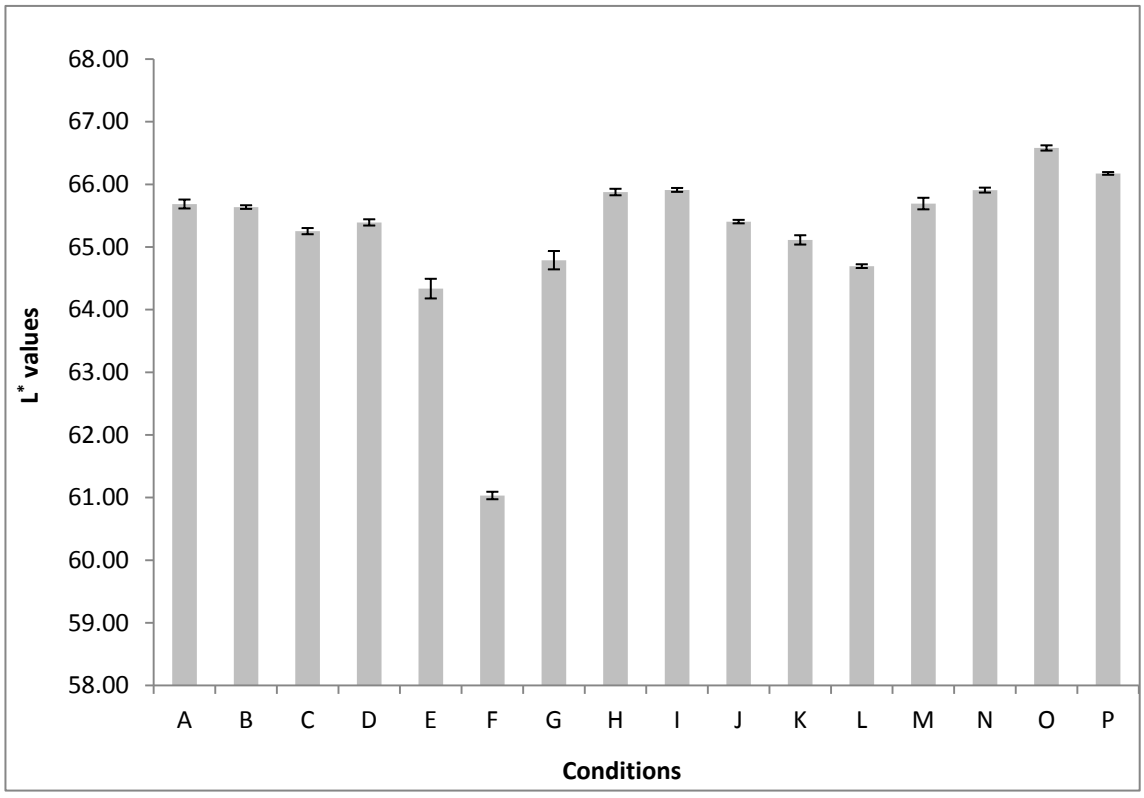

Figure 4.1 Mean and confidence interval for L^* of magenta prints over 10 measurements

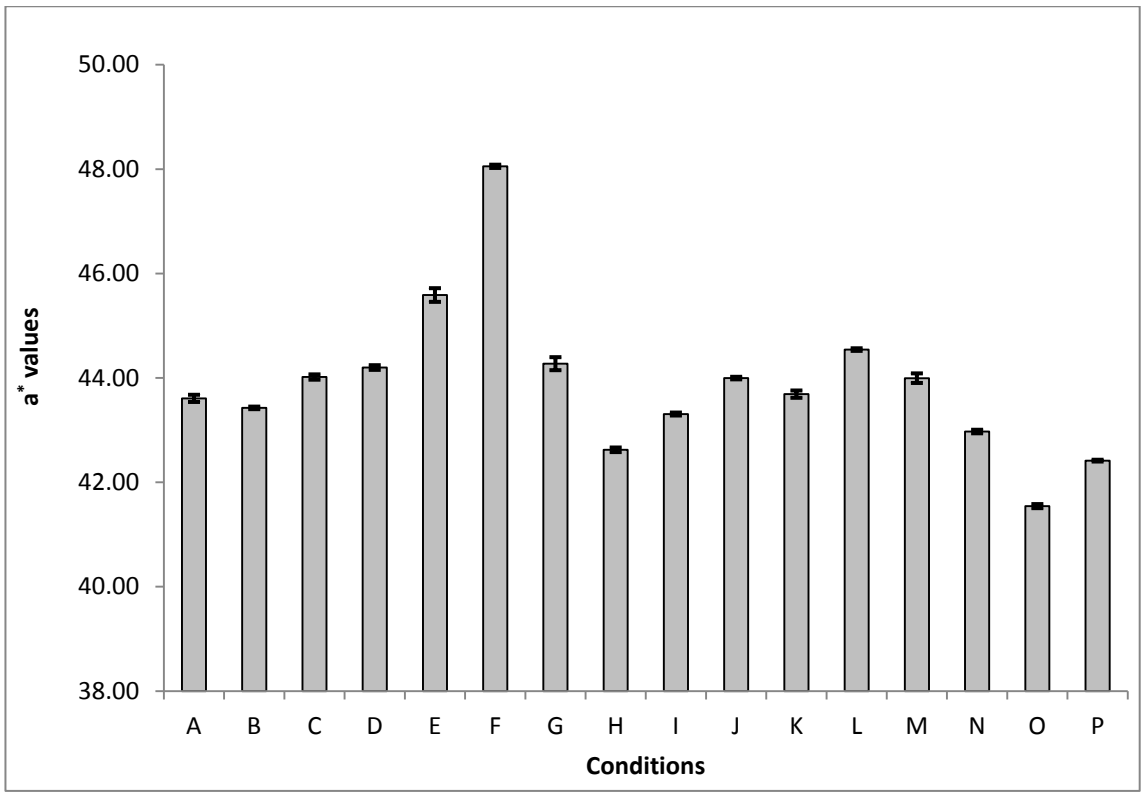

Figure 4.2 Mean and confidence interval for a^* of magenta prints over 10 measurements

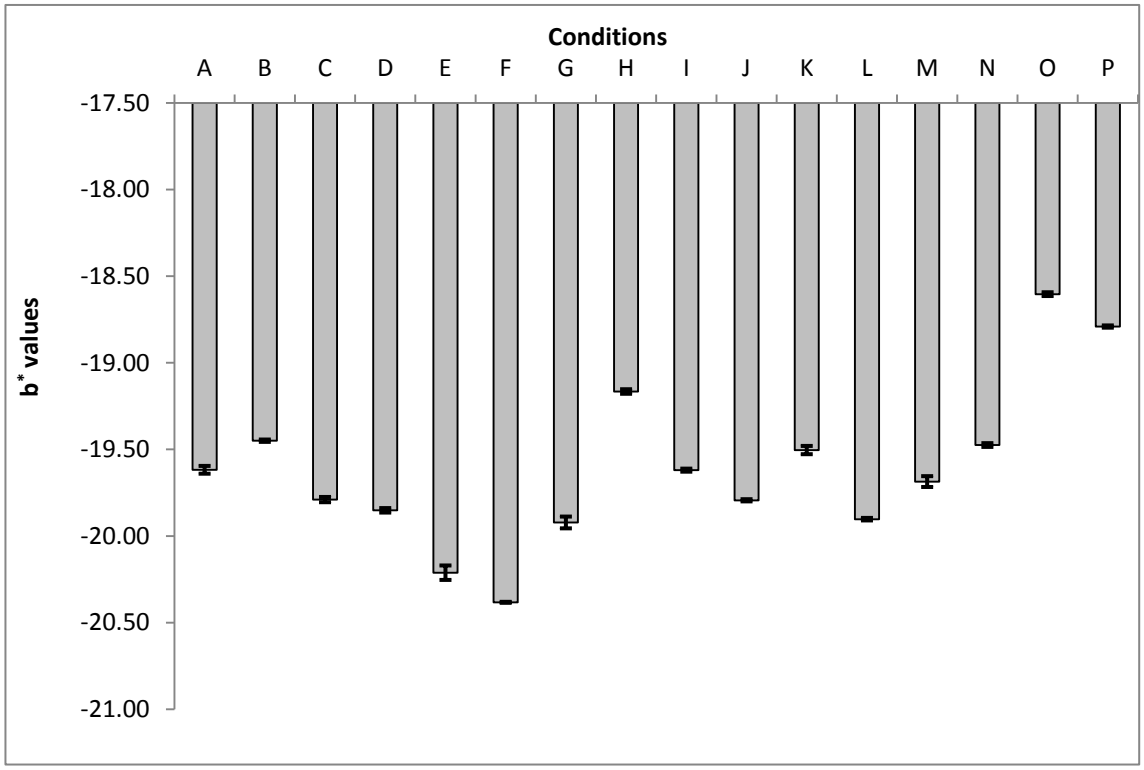

Figure 4.3 Mean and confidence interval for b^* of magenta prints over 10 measurements

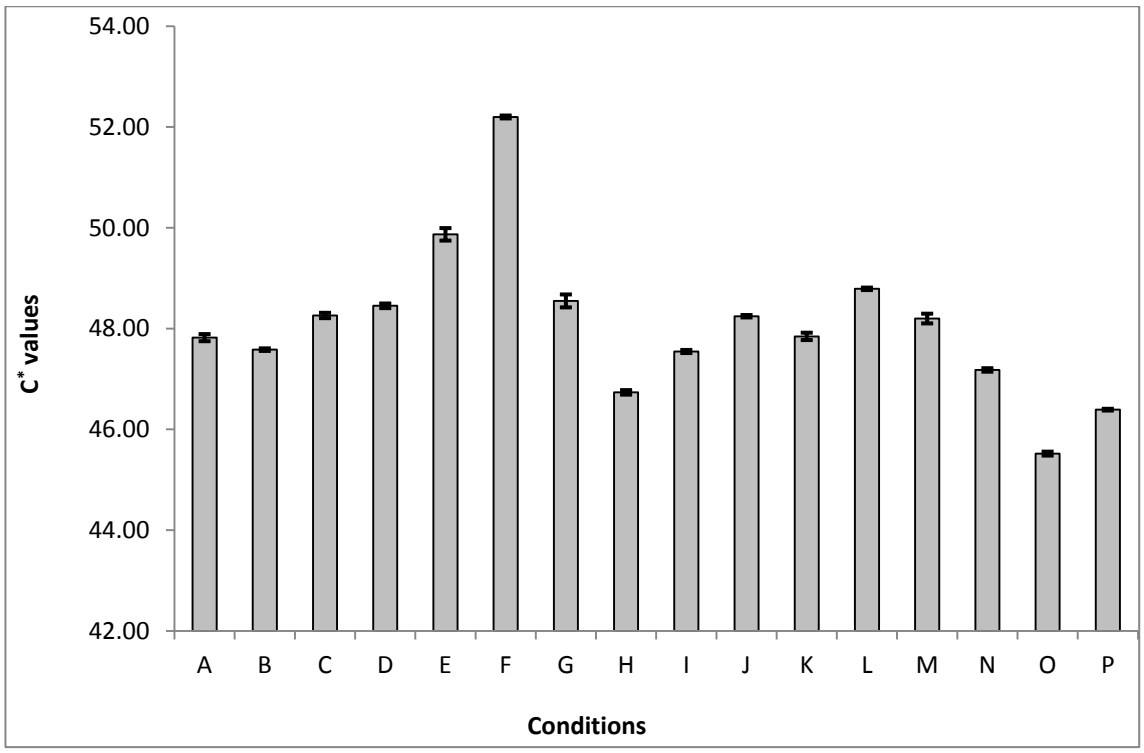

Figure 4.4 Mean and confidence interval for C^* of magenta prints over 10 measurements

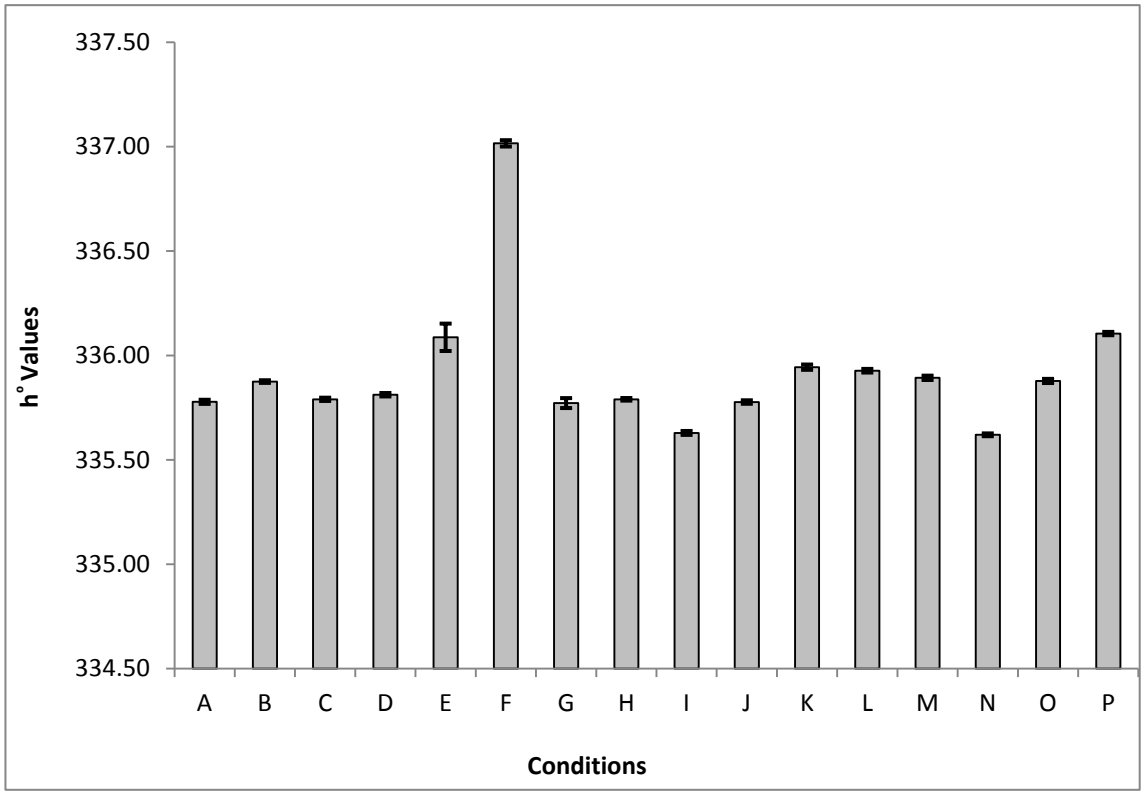

Figure 4.5 Mean and confidence interval for h° of magenta prints over 10 measurements

4.1.2 Colour Stability towards Heat

Thermochromic colours are reported as being heat sensitive. Therefore, it was anticipated that they may lose colour strength, or even be destroyed at high temperatures, to an extent dependent on exposure temperature and time of heating. To establish the thermal stability of leuco dye based thermochromic pigments, four colours, magenta, blue, orange and green were printed and cured at different temperatures and for different time periods. Each colour was printed at two concentrations, 5% and 20%, using Bricoprint binder SF20E and subjected to different curing conditions. The curing conditions used are shown in Table 4.3.

All printed samples, both uncured and cured, were measured by the spectrophotometer according to the optimised calibration conditions as discussed in section 4.1.1. Since possible colour loss was anticipated at high temperatures, integ values which are directly related to the visually assessed strength of the colour, rather than the hue, as discussed in section 2.13.6(c), were chosen for evaluation. Integ values calculated from these measurements are illustrated graphically in Figures 4.6-4.9 for magenta, orange, blue and green prints respectively.

Table 4.3 Curing conditions

Sample No.	Conc. (%)	Temp. (°C)	Time (min)	Sample No.	Conc. (%)	Temp. (°C)	Time (min)
1	5	110	3	13	20	110	3
2	5	110	5	14	20	110	5
3	5	110	8	15	20	110	8
4	5	130	3	16	20	130	3
5	5	130	5	17	20	130	5
6	5	130	8	18	20	130	8
7	5	150	3	19	20	150	3
8	5	150	5	20	20	150	5
9	5	150	8	21	20	150	8
10	5	170	3	22	20	170	3
11	5	170	5	23	20	170	5
12	5	170	8	24	20	170	8

From Figures 4.6-4.9, the uncured samples show higher colour strength than the cured samples, which demonstrates that colour loss occurs in most thermally treated samples. In the case of magenta, orange and blue prints, a gradual colour loss is generally observed with a progressive increase in both curing temperature and time of exposure. In the case of magenta and orange prints at 5% concentration, and blue prints at both 5% and 20% concentrations, a slight increase in colour strength was observed at a

curing temperature of 110°C with an increase in time. This was the lowest selected temperature and might be expected to have the least effect on the colour strength. A possible explanation is that the binder paste was not completely cured at that temperature for the limited curing time and the incomplete curing, may have given a more transparent film. In all other cases, a gradual and regular decrease in colour strength is seen with time. At the highest temperature, 170°C, almost total colour loss occurs, especially in the case of orange prints. In the case of green prints, as shown in Figure 4.9, rather different results were observed. The integ values at both concentrations showed irregular and unpredictable behaviour. The results indicate that the green pigment is more stable thermally as compared to the magenta, orange and blue pigments and the fluctuations may be within the limits of experimental error.

Thus, generally, the thermochromic prints are sensitive towards high temperatures and exposure time. Hence, it is suggested that the curing temperature and time should be kept as low as possible. However, at a low temperature, as shown in Figures 4.6-4.8, in this case 110°C, the time of exposure has less impact on colour loss compared with other curing temperatures.

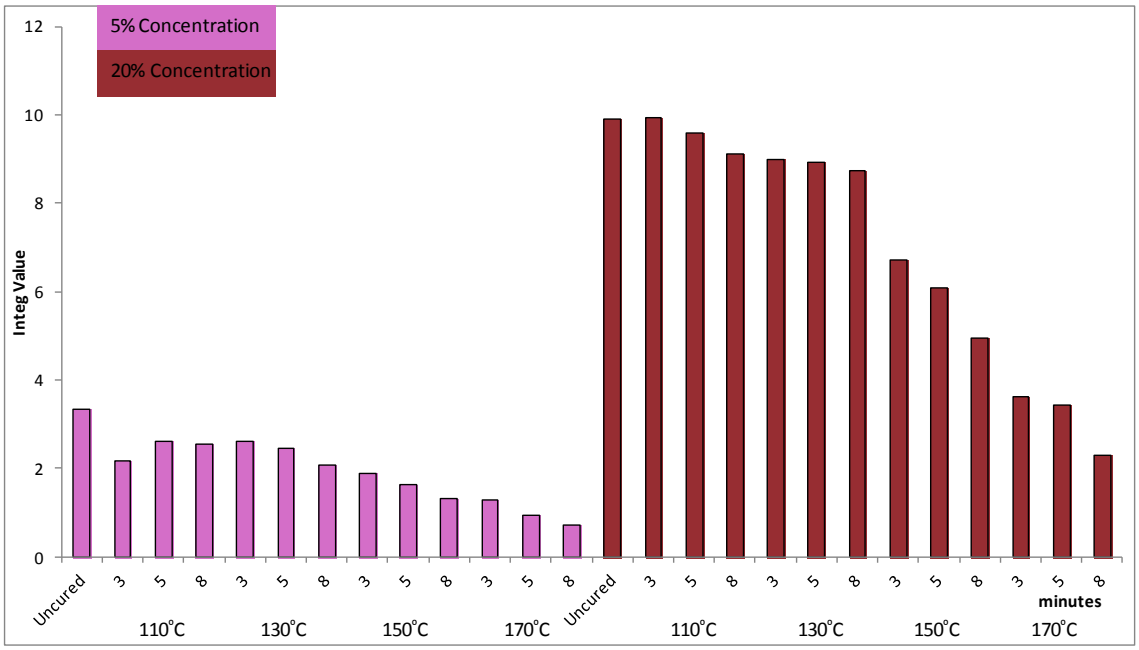

Figure 4.6 Integ values illustrating thermal colour stability for magenta prints, at various exposure temperatures and times (min.)

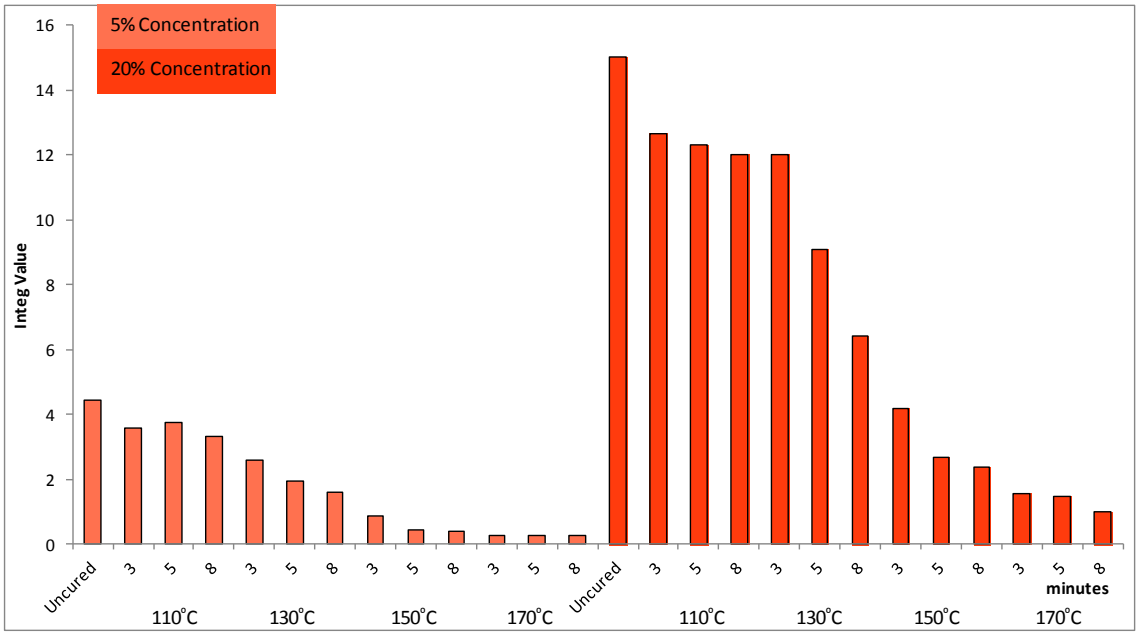

Figure 4.7 Integ values illustrating thermal colour stability for orange prints, at various exposure temperatures and times (min.)

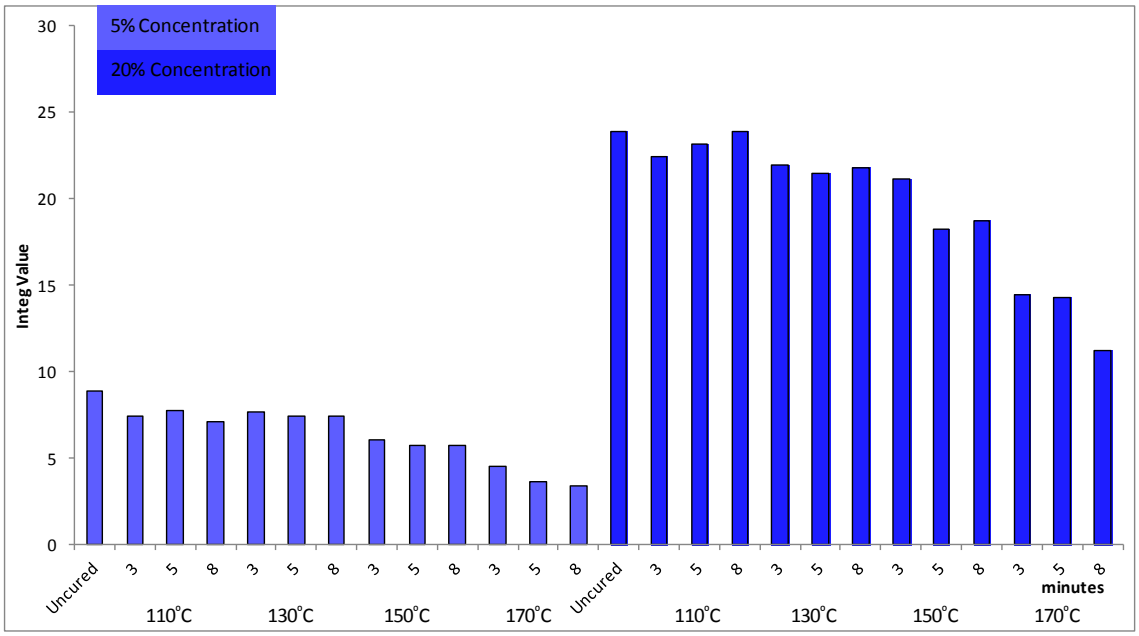

Figure 4.8 Integ values illustrating thermal colour stability for blue prints, at various exposure temperatures and times (min.)

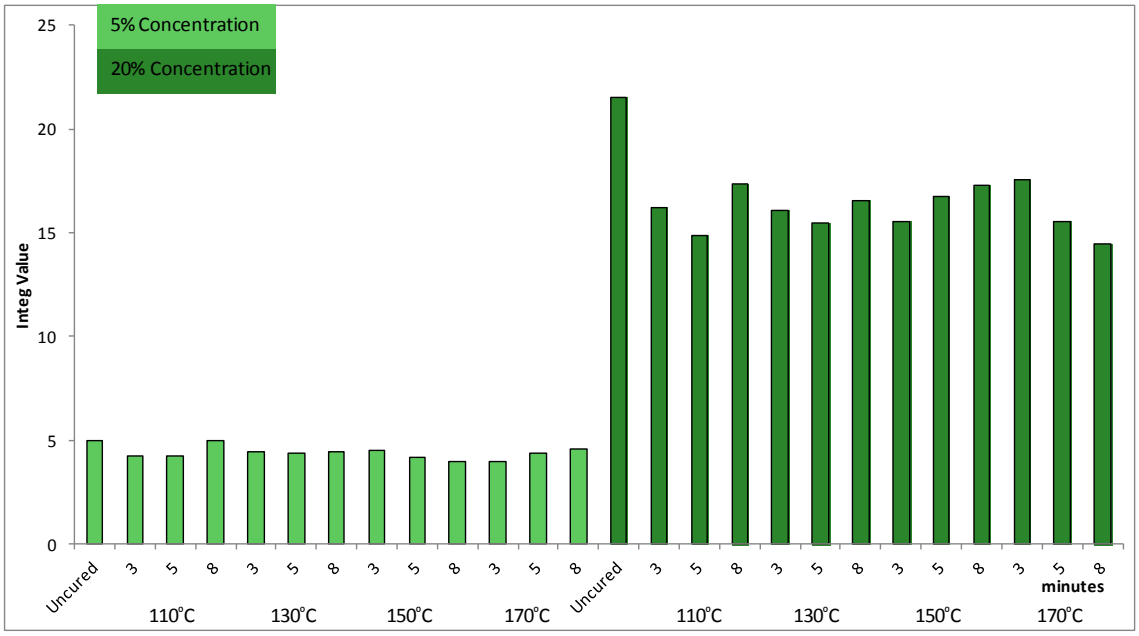

Figure 4.9 Integ values illustrating thermal colour stability for green prints, at various exposure temperatures and times (min.)

4.1.3 Binder Optimization

Printing with leuco based thermochromic pigments has been reported previously but optimisation of binder and curing conditions were not evaluated [70]. These pigments are designed to change colour with temperature, normally becoming colourless from coloured but, together with this special characteristic, they also degrade when subjected to high temperatures and curing times, as discussed in section 4.1.2. For this reason, the normal range of screen printing binders which are fixed at high temperature may not be suitable. For this investigation, four binders were selected, to a certain extent based on recommendation by the suppliers as discussed in section 3.1.4, on the basis that they could be cured at relatively low temperatures while providing a good set of fastness properties. Bricoprint binder SF20E (Selectrasine Serigraphics Ltd.) is a polyacrylate based binder also containing mineral oil in water. Binder LA-B 1096 (Tego Chemie GmbH) is a silicone modified polyurethane dispersion. Perapret PU New (BASF) is a polyurethane dispersion. Thermostar binder (LCR Hallcrest) is a butadiene-based dispersion.

Binder SF20E is a ready-for-use pigment print paste which also contains thickener and other auxiliaries. This paste was selected as it was easily accessible and has proved useful and versatile for printing textiles in the School of Textiles and Design at Heriot Watt University. It has also been used previously for printing thermochromic pigments [70]. The other binders were water-like dispersions and for printing purposes it was judged that they needed an increase in viscosity. Therefore, for every binder, a print

paste was formulated with 10% binder, 4% thickener (Magnaprint clear M04) and the rest was water, this formulation being based on the author's previous experience in industry. After mixing manually, a high speed Silverson L4R stirrer was used for 5 minutes to prepare a homogenous paste. These pastes containing the different binders were used with the magenta thermochromic pigment as it was available in the greatest quantity. For consistency, two colour concentrations were used, 5% and 20% by weight of the paste. The printed samples were produced using a screen with a design consisting of stripes. The samples were cured according to the conditions listed in Table 4.3.

The cured samples were subjected to washing according to 'ISO 105, part C10: colour fastness to washing with soap or soap and soda, method A(1)'. The test specimens were prepared by attaching a printed fabric strip of 100mm × 40mm to the SDC multifibre fabric with the same dimensions by means of staple pins. The standard ISO soap solution (5g/l) was prepared using distilled water. The liquor ratio was 50:1 ml/g. The test was conducted for 30 minutes at 40°C in a Washtec P machine. Dry and wet rubbing tests were also performed. The AATCC crocking cloth, in both dry and wet conditions, was used in a manual crock meter for 10 cycles for dry and wet rubbing. Generally, a grey scale is used to assess the wash and rub fastness samples. For the purpose of accuracy and avoiding human visual assessment, the samples were measured by the spectrophotometer using the calibration conditions established in section 4.1.1. Integ values have been plotted as in graphs against time for different temperatures.

The integ values given by printed samples using different binders, cured at different temperatures and time intervals, are shown in Figures 4.10 (a)-(d), with the two concentrations (5% and 20%) shown side by side. At both concentration levels, and for all binders, it is clear that the temperature plays a significant role in reducing the colour depth with an increase in the temperature from 110°C to 170°C. Increasing the time of curing also reduces the colour depth, but less significantly. In Figures 4.10 (a)-(d), the colour depths obtained in prints using the Thermostar binder are higher compared with other binders at the 5% pigment concentrations, while at the 20% concentrations, Thermostar and Perapret PU New provided similar colour depths. The differences in colour depth show that the nature of the binders has an impact on colour strength, possibly due to development of opacity or slight colour tones in the cured binder.

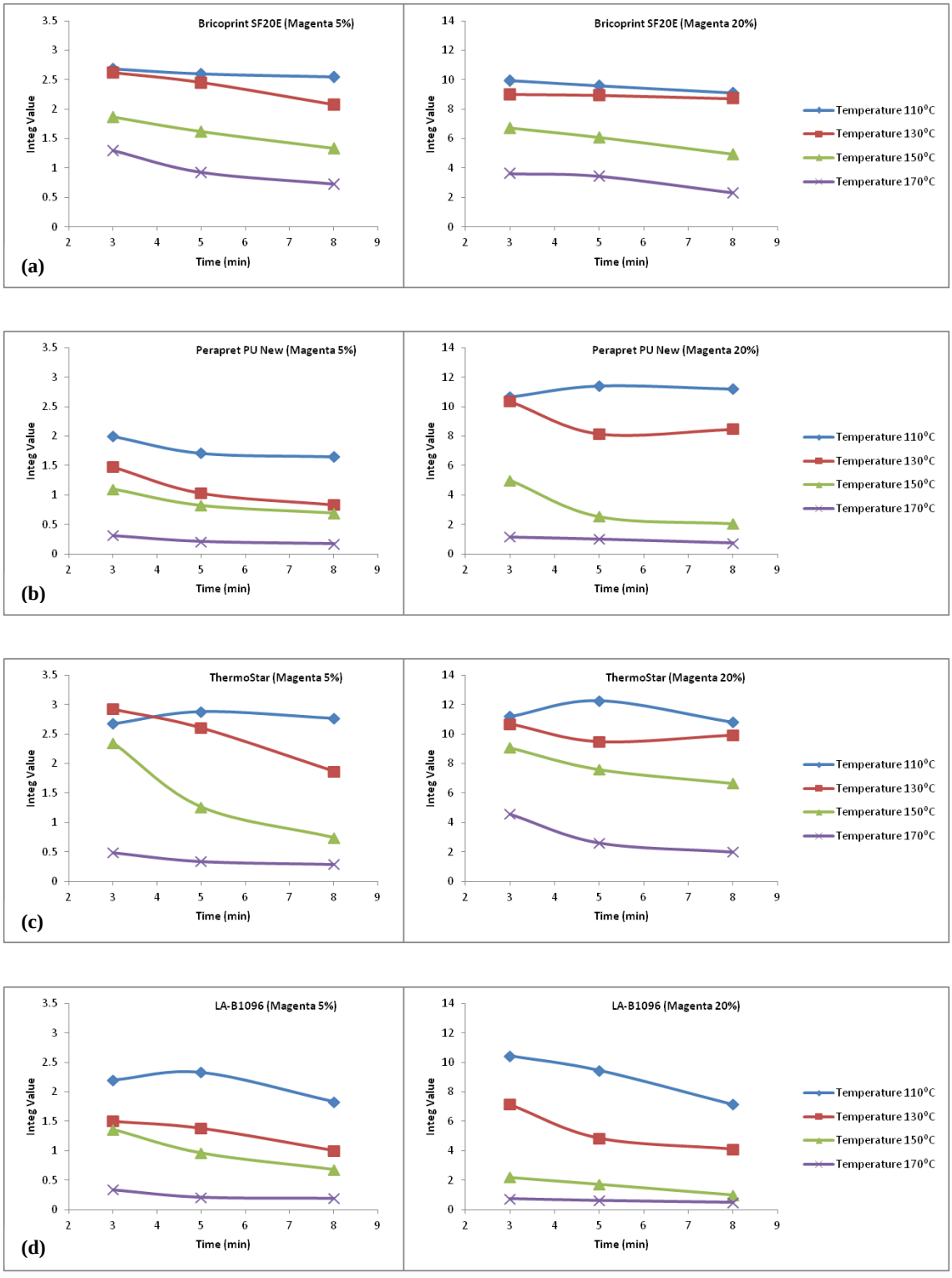

Figure 4.10 Printed and cured samples with different binders

Figures 4.11(a)-(d) show the integ values of washed samples, printed and cured at different temperatures. The prints show poor washfastness properties, losing colour depth significantly after washing, illustrated by comparing the data before and after washing (i.e., Figure 4.10 compared with Figure 4.11). The Thermostar binder shows better washfastness properties than the other binders at both concentrations. Bricoprint

SF20E binder shows better washfastness at the lower concentration. The differences may be due to different chemical natures of binders. The Thermostar binder, a dispersion of carboxylated acrylic esters and butadiene polymer, gives better washfastness than Bricoprint SF20E, Perapret PU New and LA-B1096 which are cross-linking polyacrylate, polyurethane and silicone modified polyurethane based binders, respectively. Figure 4.11(c) for the Thermostar binder, also shows that the washed samples at both concentrations, cured for 8 minutes, have better fastness properties which indicates more efficient curing at this time interval.

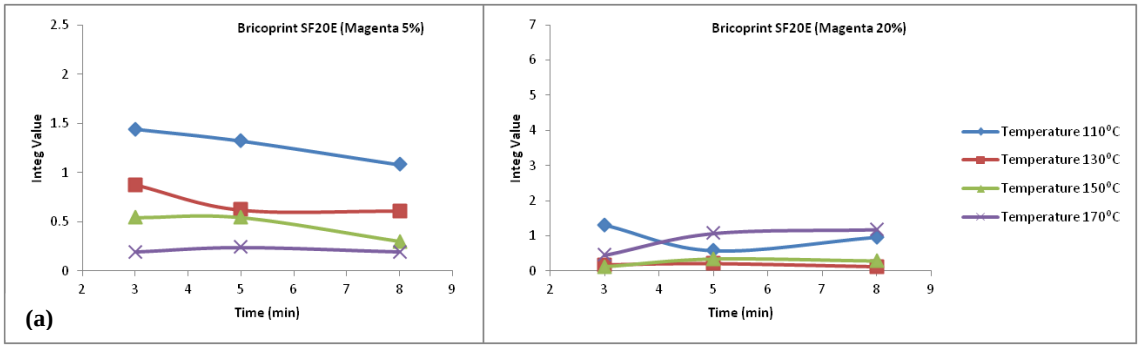

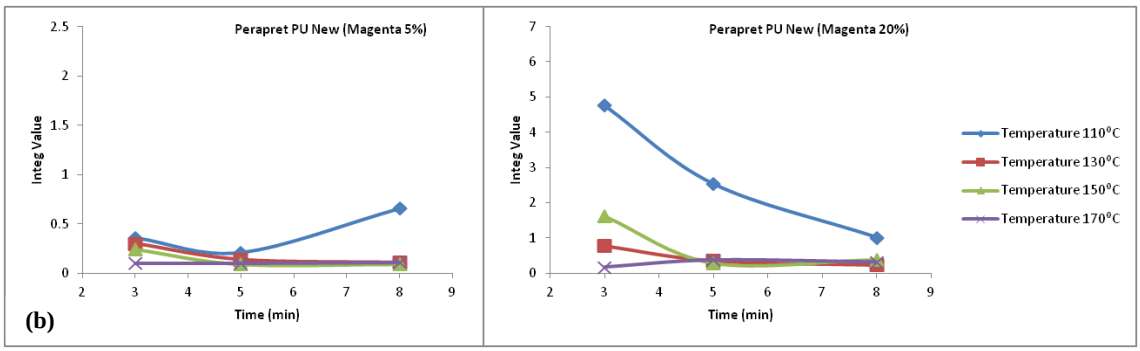

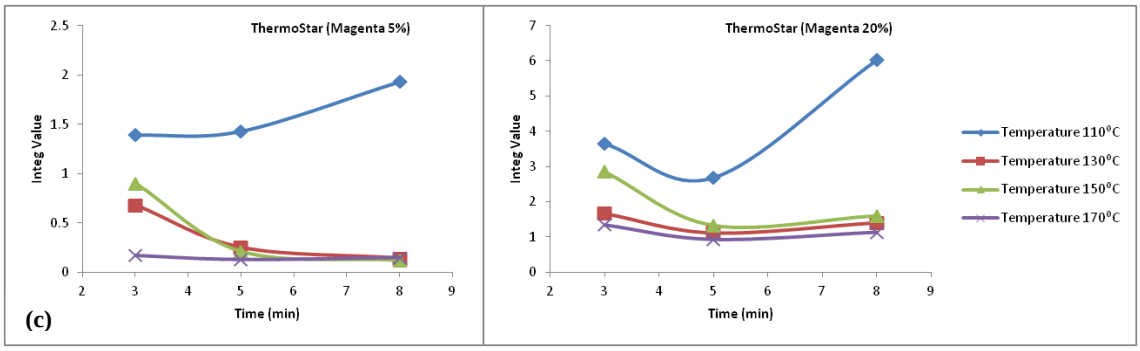

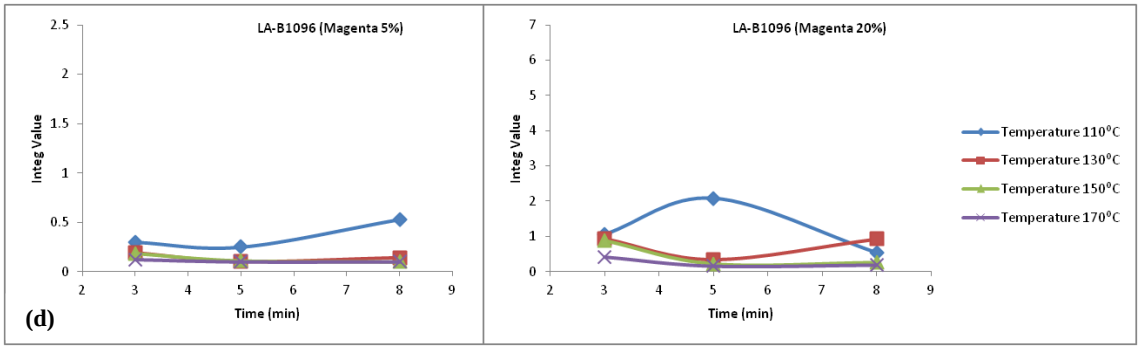

Figure 4.11 Printed, cured and washed samples with different binders

The loss of colour by washing of the printed samples is illustrated in Figures 4.11(a)-(d). Figures 4.12(a)-(d) show the most colour stained part of the multifibres. This property mainly depends on the affinity of the pigment for each of the fibres. These microencapsulated pigments have little affinity for any fibre as they neither fix on the fibres chemically, nor become physically trapped in a fibre. For this reason, they are normally applied with a binder. The integ values shown in Figures 4.12(a)-(d) are very small and almost the same for all binders with a few exceptions. For example, in the case of Perapret PU New and LA-B 1096 binders there are minor differences and slightly higher values are given for some curing temperatures and times. For both these binders, the colour loss after washing was also higher, as is evident from Figures 4.11(a)-(d), which may explain a higher value for staining in the exceptional cases. However, these abnormalities are probably within the limits of experimental error.

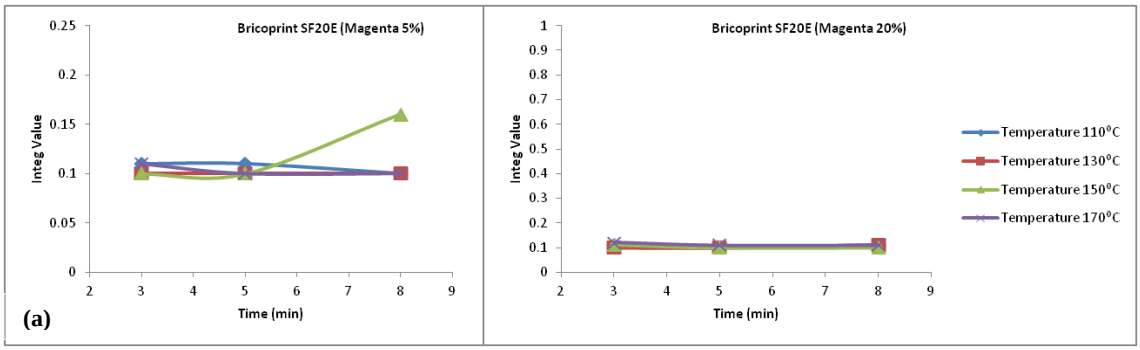

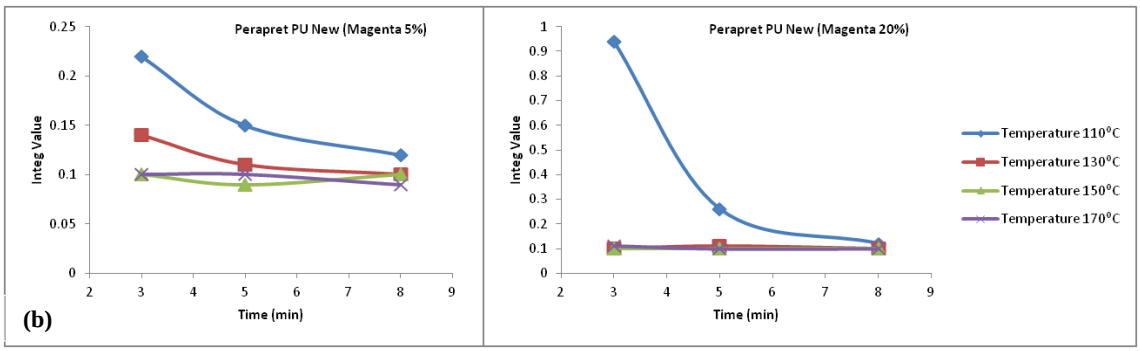

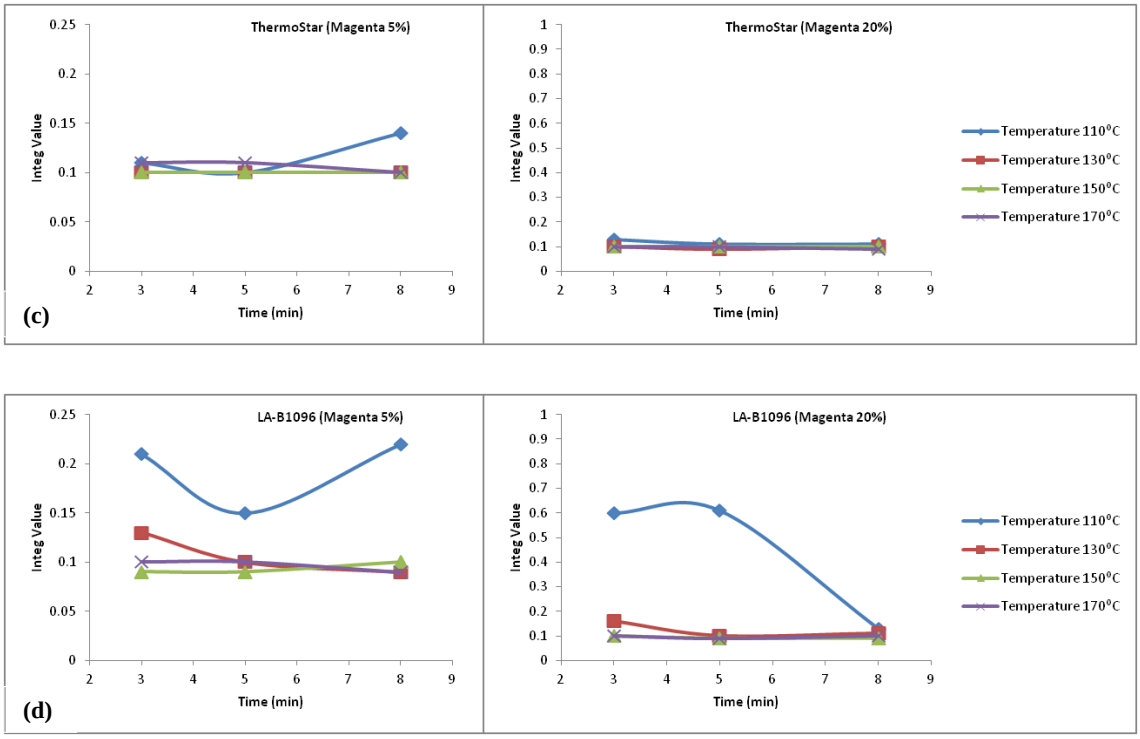

Figure 4.12 Staining of adjacent fabrics in wash test

Figures 4.13(a)-(d) show integ values for the staining on the dry rubbed white cloth after 10 cycles on the crock meter. These values indicate that for 5% colour concentration, all of the prints show good rubbing fastness giving very low integ values just above the integ value of white cloth used for rubbing. However, for 20% pigment concentrations, some binders show occasional abnormalities but the integ values are small with very little differences between the white cloth and stained white cloth which may be within the limits of experimental error. Figures 4.14(a)-(d) show the integ values of the staining of colour on wet rubbed cloth after 10 cycles on the crock meter. At 5% concentrations, all the binders show good wet rub fastness, with some minor abnormalities, and all integ values are just above the integ value of white rub cloth. At 20% concentrations, again all binders show good wet rub fastness with some abnormalities such as Perapret PU New at 110°C for 3 minutes and Thermostar binder at 110°C for 3 and 8 minutes but differences between the stained white cloth and the white cloth are very small. Therefore, it can be concluded that all the binders show good dry and wet rub fastness at all temperatures and times.

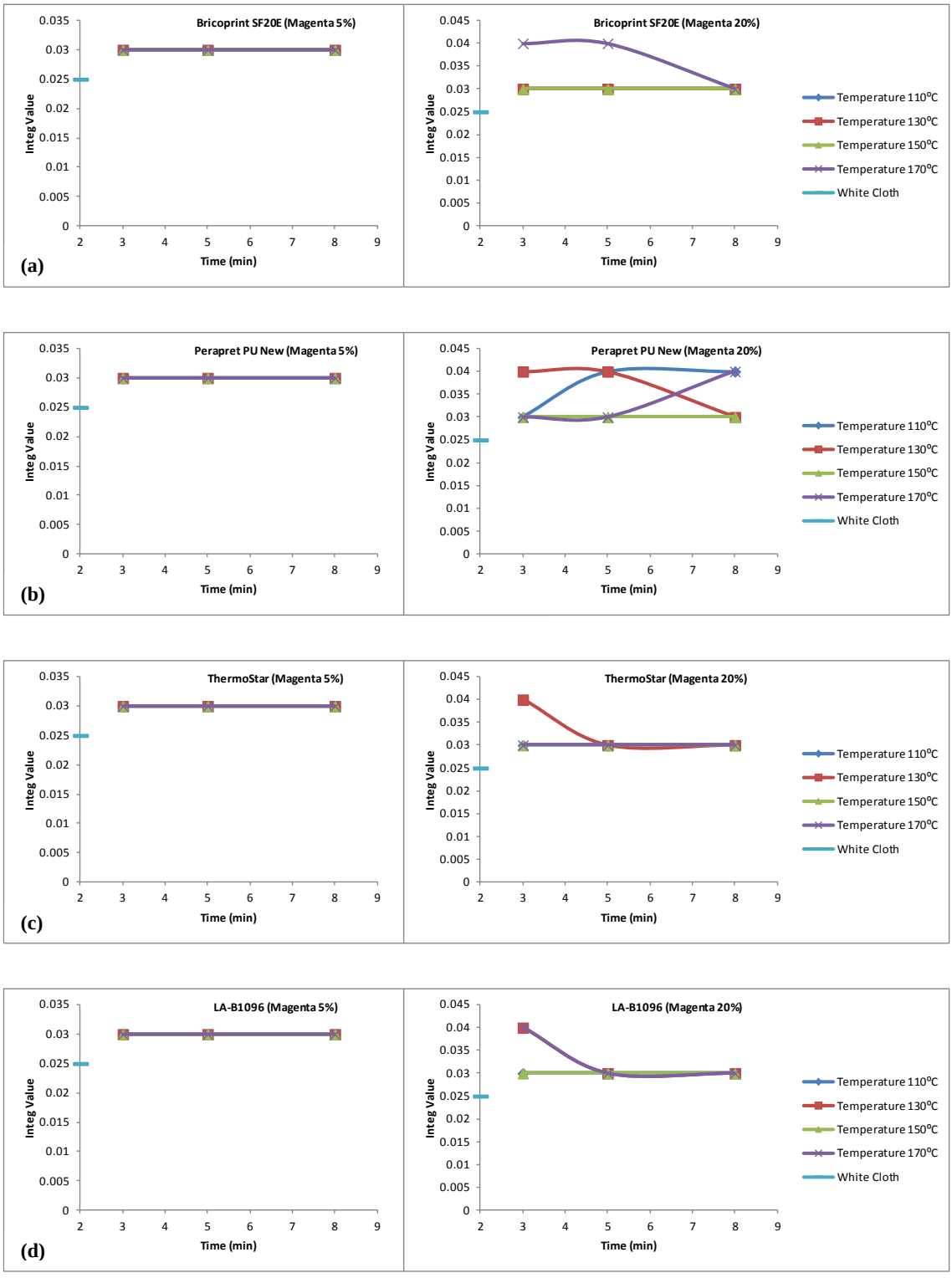

Figure 4.13 Stained dry rubbing samples

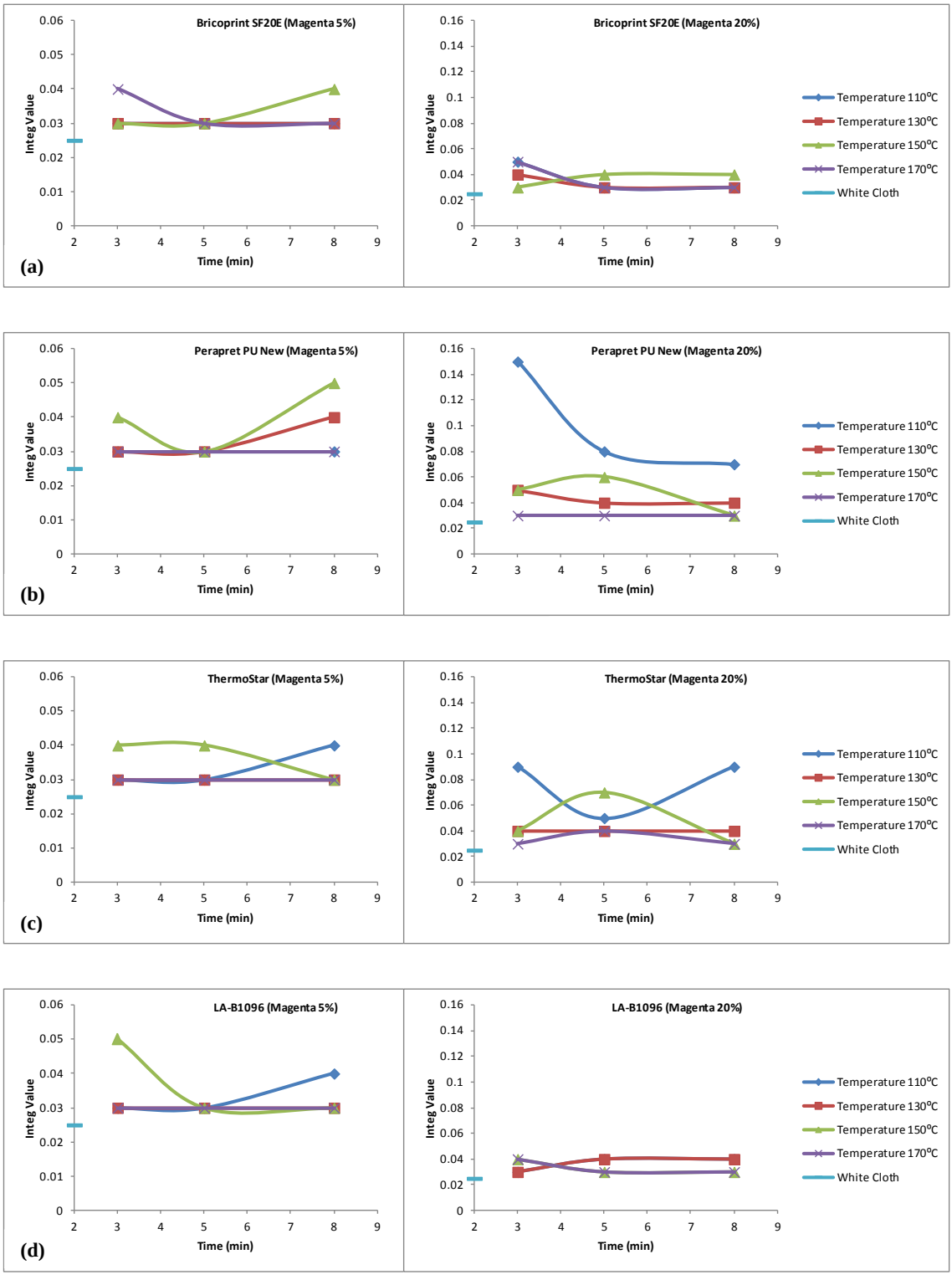

Figure 4.14 Stained wet rubbing samples

It is clear that the highest colour depth is given by the Thermostar binder as shown in Figures 4.10(a)-(d). The highest colour depth of samples subjected to washing is given by Thermostar binder as shown in Figures 4.11(a)-(d) which suggests enhanced curing of this binder. In Figures 4.12(a)-(d), the washed samples assessed for staining show similar very good results for all binders. From Figures 4.13(a)-(d) and Figures 4.14(a)-

(d), the printed samples show good dry and wet rub fastness with all the binders. Overall, the Thermostar binder, on the basis that it gives better colour depth in printing and better washfastness, was selected as the best binder to print the leuco dye based thermochromic pigments.

From the results given in section 4.1.2, it was concluded that the leuco dye based thermochromic pigments are more stable at 110°C than at higher temperatures. Thermostar binder also gives higher colour strength and good washfastness when cured at this temperature for 8 minutes. Although 8 minutes curing time at 110°C, gives slightly reduced colour strength as compared to 3 and 5 minutes, washfastness is significantly higher after 8 minutes as shown in Figure 4.11(c). To investigate further the curing conditions for the Thermostar binder, printed samples were cured at 90°C, 100°C and 110°C for 5, 8 and 10 minutes, as shown in Table 3.1. The reason for investigating an increased time interval was that shorter times gave inferior performance. These printed and cured samples, were subjected to washing and rubbing tests. The results as integ values are shown in Figures 4.15(a)-(e).

In Figure 4.15 (a), it is observed that the integ values are higher using the lower curing temperature (90°C) and they reduce as temperature is increased to 110°C, especially for the 5% concentration. The samples for the 20% concentration show almost the same trend at all curing temperatures and times, with the exception of the higher integ value for curing at 90°C for 8 minutes. In Figure 4.15 (b), the integ values for washed samples show higher colour loss for samples cured at the shorter time (5 minutes) than for a period of 10 minutes. The colour loss for samples cured at 90°C is considerably more compared with other temperatures, which indicates reduced cross-linking and fixation of binder on the fabric. For samples cured at 100°C, the trends are not consistent for 5% and 20% concentrations, showing a rise in colour depth with time at 5% and a reduction for 20% concentrations. The colour depth of washed samples cured at 110°C shows a consistent trend for both concentrations and higher for 10 minutes curing. In the case of the washed samples assessed for the most stained parts of the multifibre strips, as shown in Figure 4.15(c), less staining is observed for a curing temperature of 110°C for both concentrations, while for 90°C and 100°C, there is higher colour staining and also they show different trends of staining with different curing times at both concentrations. The dry rubbing, Figure 4.15(d), shows a similar level of staining for all curing temperatures and times and just above the integ value of white

cloth. The wet rubbing, Figure 4.15(e), shows slight variations of integ values at different curing temperatures and time intervals. However, those variations are very small and not significant. From the above analysis, curing at 110°C gives good colour depth before and after washing and there is a consistency in the trends of integ values with increasing time intervals for both concentrations and the colour depth is good for 10 minutes curing. At 100°C, there are slightly higher integ values than 110°C but there is inconsistency in trends with increasing time for the 5% and 20% concentrations, especially for washed samples. At 5%, the integ values increase with time while for 20%, they decrease. The washed samples show less staining for 110°C curing and are good at a time of 10 minutes. Dry and wet rub fastness is similar for all curing conditions. Thus, it was concluded that the optimum curing for the Thermostar binder is at 110°C for 10 minutes although this involves a small element of compromise.

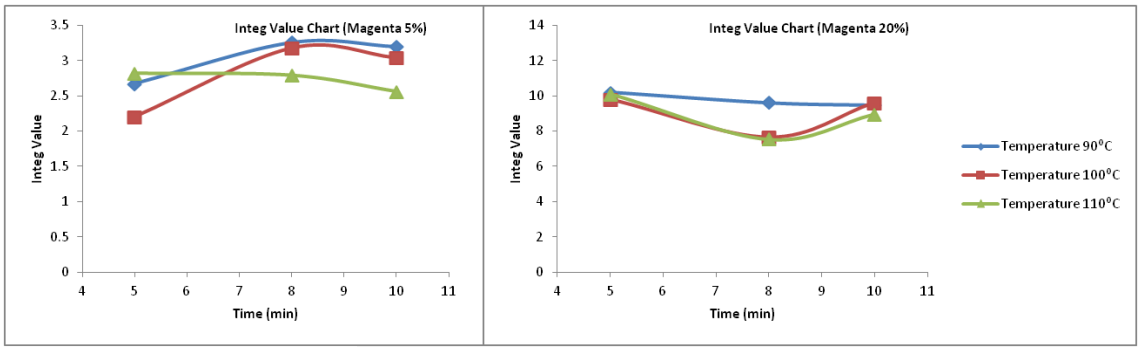

(a) Printed and cured samples

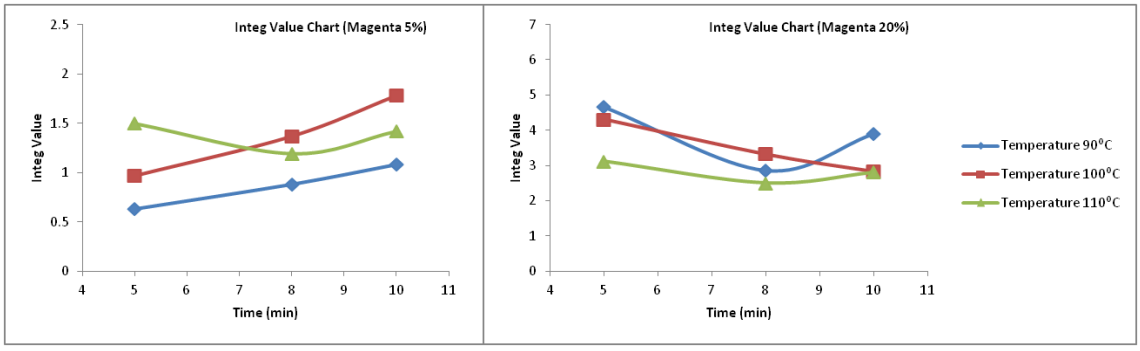

(b) Washed samples

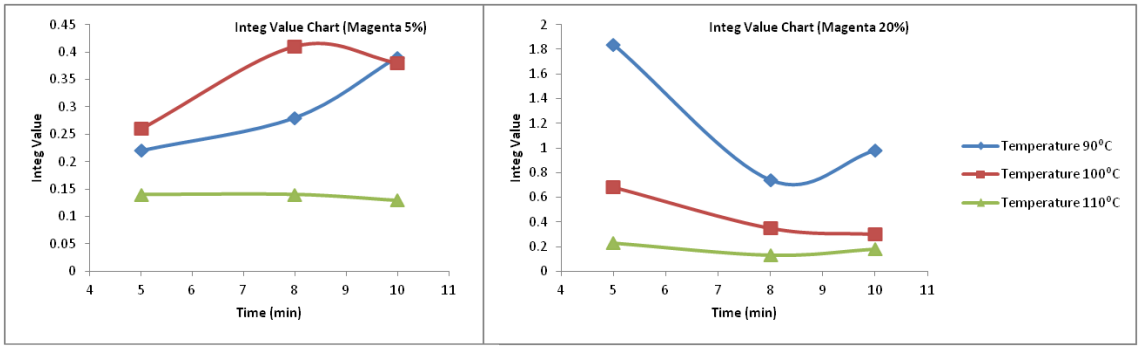

(c) Staining of adjacent fabrics in wash test

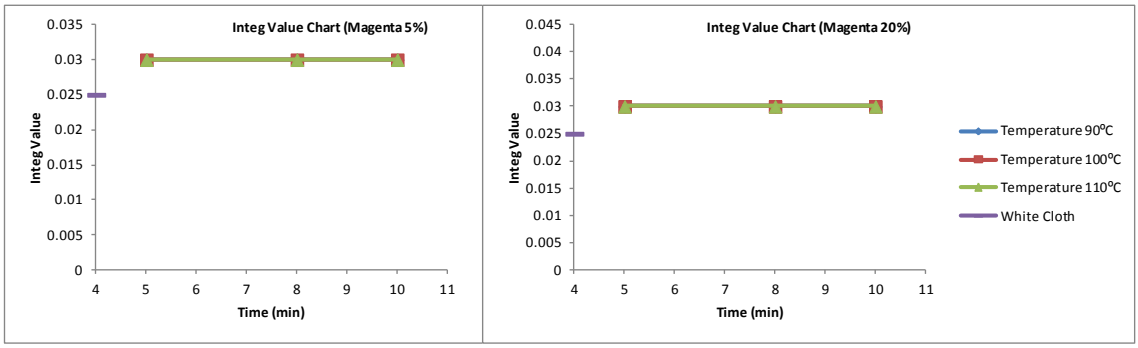

(d) Dry rubbing

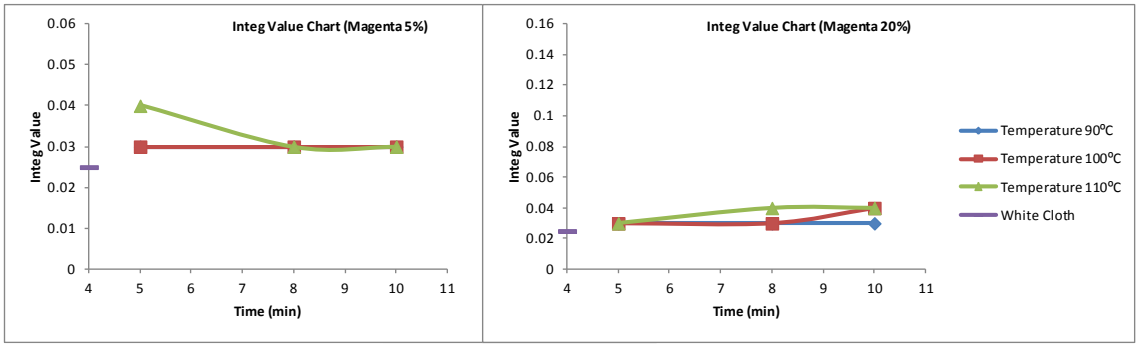

(e) Wet rubbing

Figure 4.15 Integ values charts of Thermostar binder

4.1.4 Colour Concentration

Normally, traditional pigments available in the market give the highest colour strength at up to 3-4% of their concentrations on the weight of the paste. Beyond these concentrations, any further addition of pigment does not affect the colour depth and therefore, it is useless to add more, raising the cost with no additional value. The extra pigment, which does not increase colour strength, may reduce the fastness properties such as dry and wet rub fastness. The leuco dye based thermochromic pigments consist of several components, microencapsulated to protect their compositions and to facilitate application on substrates such as textiles. Therefore, the available colour strength is significantly reduced due to lower amounts of colour-producing substances compared to normal pigments. In the case of thermochromic pigments in slurry form, water is present, further reducing their ability to develop colour strength. Therefore, it was anticipated that high colour strength would require using a higher concentration of these pigments than normal pigments and it has been suggested as 15%-30% on the weight of the paste [9].

To establish the amounts of pigments required to obtain saturated colours on textile substrates, using thermochromic pigments in slurry form, the fabric samples were printed with pigment concentrations of 2%, 5%, 10%, 20%, 30%, 40% and 50% by

weight of the paste. The four colours used were magenta, orange, green and blue. Initially, these pigments were printed using Bricoprint SF20E binder which is commonly used for printing pigments on textiles at Heriot Watt University. After establishing that the Thermostar binder was the most suitable for printing these pigments, as discussed in section 4.1.3, the samples were reprinted using this binder. To avoid loss in colour depth due to high temperatures, these printed samples were not cured. The integ values were plotted in graphs to evaluate the trends in colour strengths.

In Figures 4.16-4.19, the prints using SF20E binder show that the integ values increase progressively up to 30% concentrations for magenta and orange while for green and blue, they increase up to 40%, although the increase from 30% to 40% is small. After achieving the maximum, the integ values show a subsequent decrease in colour strength. The prints using Thermostar binder show that the integ values gradually increase up to 30% concentrations for magenta and blue, up to 20% colour concentration for orange and, for green, the same highest colour strength is achieved at 20% and 30% colour concentrations. After achieving the maximum colour strength, the integ values again show a gradual decrease with increase in concentrations. Thus, after the highest colour strength has been achieved, there is no value in further increasing the concentration. However, a further increase in concentration of the microcapsules, consisting of the wall construction and other components, which may not be completely transparent, may cause a decrease in colour strength due to an increase in opacity of the printed film. The colour strengths of magenta, orange and blue show higher values for Thermostar binder than Bricoprint SF20E binder, up to 20%, while for green prints it is similar and for concentrations higher than 20% of all colours, the colour strength is lower for Thermostar binder. With the Thermostar binder, the highest colour strength is achieved at lower concentrations than for Bricoprint SF20E binder. Thus, it is concluded that the highest colour strength available from the different leuco dye based thermochromic pigments vary with the colour and the binder. However, normally the maximum can be achieved between 20% and 30% concentrations.

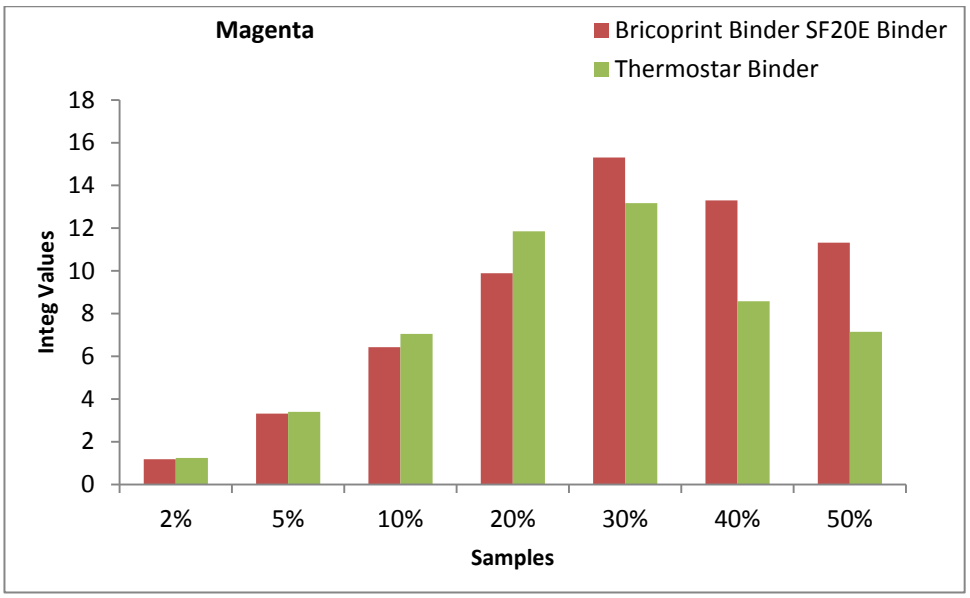

Figure 4.16 Variation of integ values with concentration of magenta

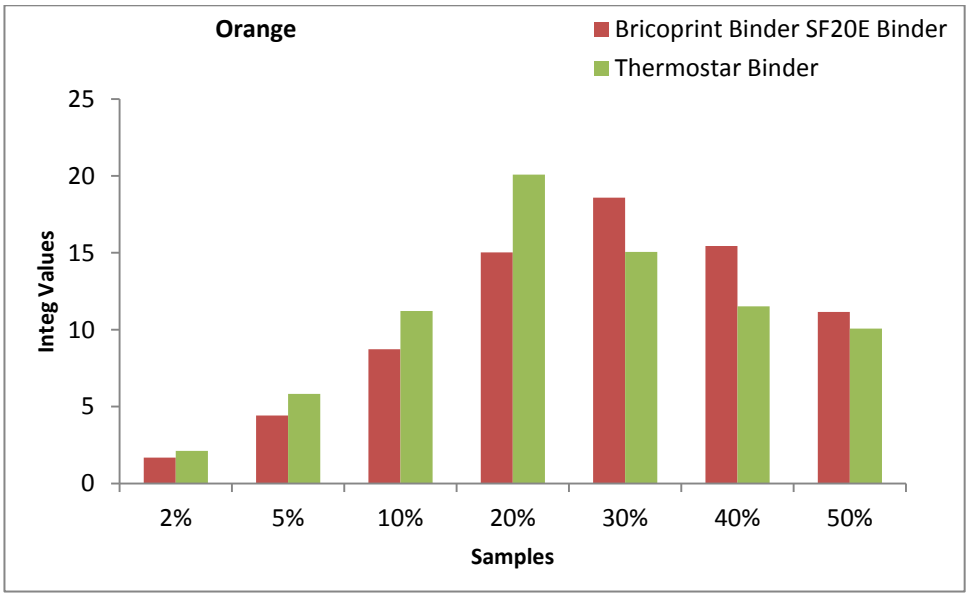

Figure 4.17 Variation of integ values with concentration of orange

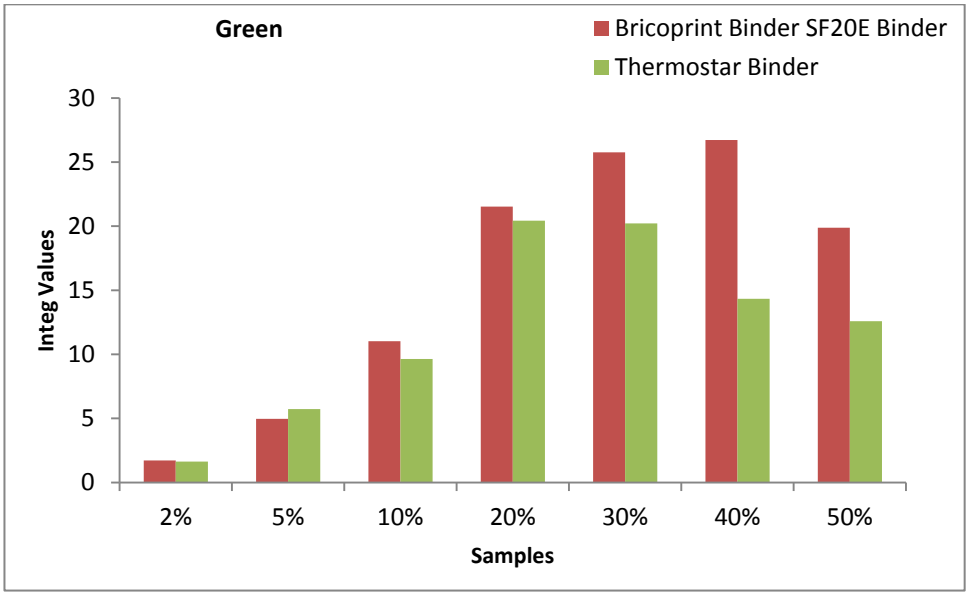

Figure 4.18 Variation of integ values with concentration of green

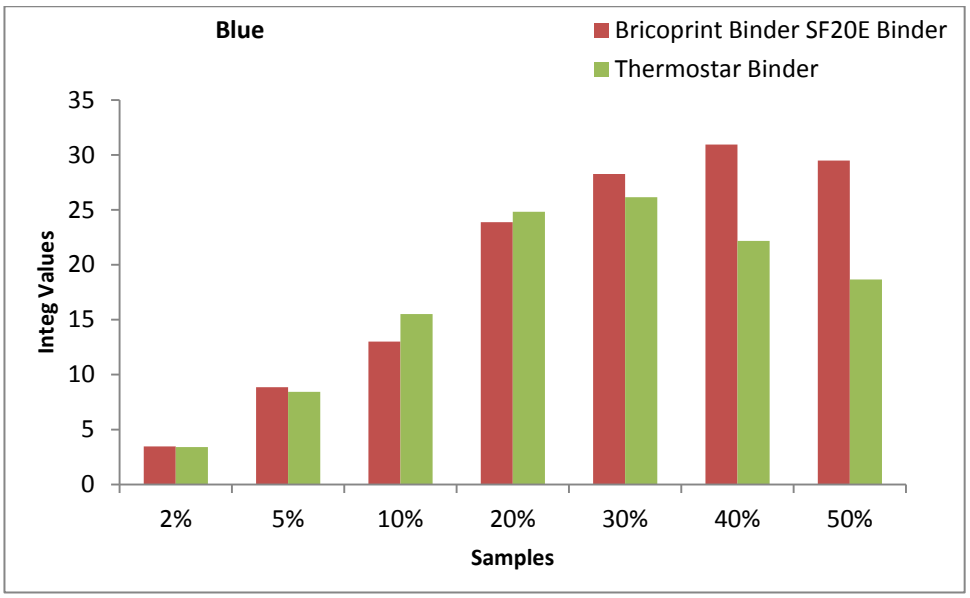

Figure 4.19 Variation of integ values with concentration of blue

4.1.5 Lightfastness Enhancement

The lightfastness properties of leuco dye based thermochromic pigments are generally only modest and therefore, selected additives are used to improve their lightfastness. Normally, these additives are incorporated by the pigment manufacturer prior to microencapsulation, so that they can minimise colour loss due to light exposure by direct interaction with the colour former and other components of thermochromic pigments. In this research, an investigation was carried out to determine whether action by the end user or processor of these pigments might improve lightfastness at the application stage. For this purpose, three lightfast enhancers from different classes, UV absorbers, hindered amine light stabilisers (HALS) and antioxidants were selected.

Tinuvin 144 (Ciba Speciality Chemicals) is a highly efficient hindered amine light stabiliser (HALS). It is chemically bis(1,2,2,6,6-pentamethyl-4-piperidinyl)-2-butyl-2-(4-hydroxy-3,5-di-tert-butylbenzyl)propanedioate. Stabilon AO (Huntsman Textile Effects) is a water soluble anionic phenolic antioxidant. Tinuvin P (Ciba Speciality Chemicals) is an ultraviolet light absorber (UVA) of the hydroxyphenylbenzotriazole class. Chemically, it is 2-(2H-benzotriazole-2-yl)-p-cresol. It is reported that it has strong absorption in the 300-400 nm region and releases the absorbed energy in non sensitizing ways.

Blue and magenta leuco dye based thermochromic pigments were selected for this study, used at a concentration of 5% on the weight of the printing paste. The lightfastness enhancers were used in two ways; by mixing directly into the pigment

print pastes and printing on white fabric, and by incorporating separately into print pastes and then coating them over the printed fabrics, covering the thermochromic pigments as protective layers. The concentration of lightfastness enhancers used was 3% by weight in both coloured and colourless printing pastes. The layer of lightfastness enhancer produced a visual effect of slight creaminess over the colours. The printed samples were cured at 110°C for 10 minutes, as discussed in section 4.1.3.

These printed and cured samples were exposed to light on the Heraeus Xenotest 150S fadeometer for 1, 2, 3, 4, 6, 8, 12, 18 and 24 hours. Normally, a blue wool scale is exposed in Xenotest together with the samples, and the samples compared visually after exposure with the blue wool scale to assess the grades of lightfastness. However, the leuco dye based thermochromic pigments were found to have poor lightfastness and faded so quickly when exposed to light that, instead of using the blue wool scale, colour measurements were taken on the spectrophotometer with the calibration conditions discussed in section 4.1.1. The integ values of samples at different exposure times were plotted against time.

In the case of lightfastness enhancers mixed with magenta pigment, as shown in Figure 4.20, antioxidant and HALS show a slight improvement in lightfastness, while the UV absorber shows a more significant improvement in lightfastness when compared to the original sample, demonstrated by higher retention of colour strength with time. In the case of lightfastness enhancers coated over magenta, Figure 4.21, antioxidant and HALS show no apparent improvement in lightfastness. However, the UV absorber provides lightfastness enhancement, better than the sample, printed mixed with the UV absorber. In the case of lightfastness enhancers mixed with blue pigment (Figure 4.22), there is no improvement in lightfastness with antioxidant and HALS and only a very slight improvement with UV absorber. In the case of coating over the blue pigment (Figure 4.23), the antioxidant and HALS do not show any enhancement of lightfastness. However, the coated UV absorber shows obvious improvement, better than the printed sample mixed with the UV absorber. In the cases of magenta and blue pigments, mixed and coated with the UV absorber, the colour strengths appear to show an increase after initial exposure. A tentative explanation for this phenomenon may be that the film becomes more transparent initially after absorbing UV light after which the degradation of colour dominates. There are occasional results suggesting an increase in colour strength using antioxidant and HALS as well, but these are not consistent and probably due to experimental error or variation.

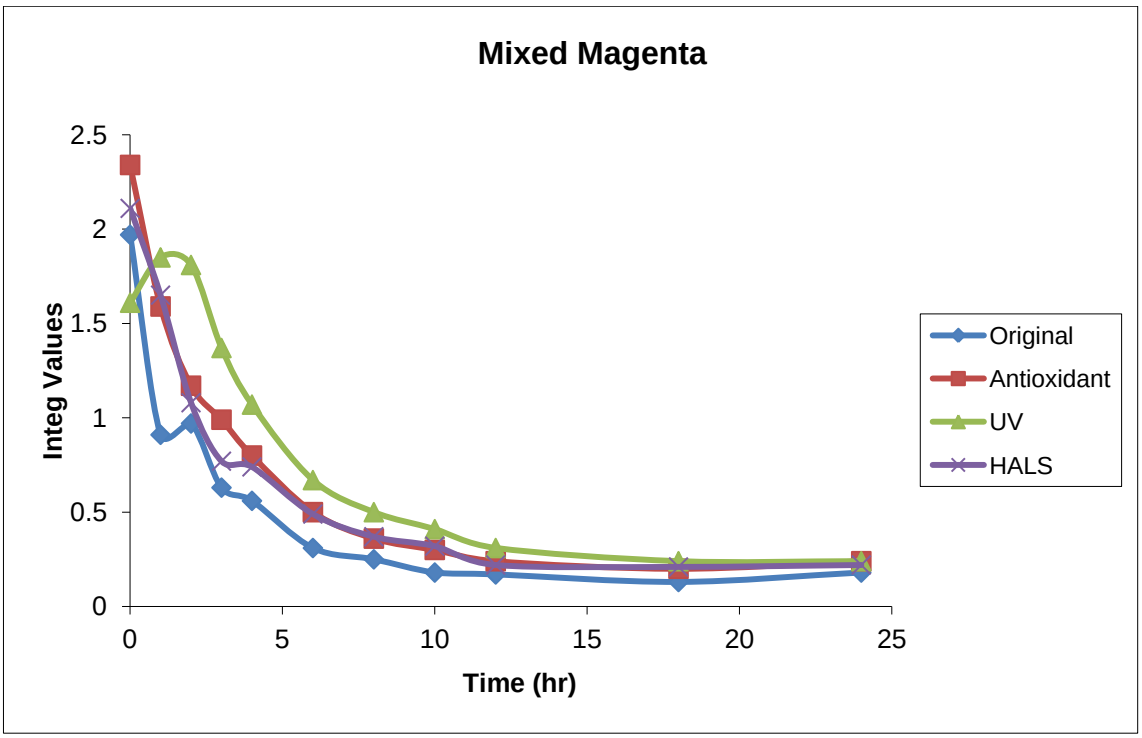

Figure 4.20 Integ values against time for exposure to the Xenotest of the magenta pigment mixed with lightfastness enhancers

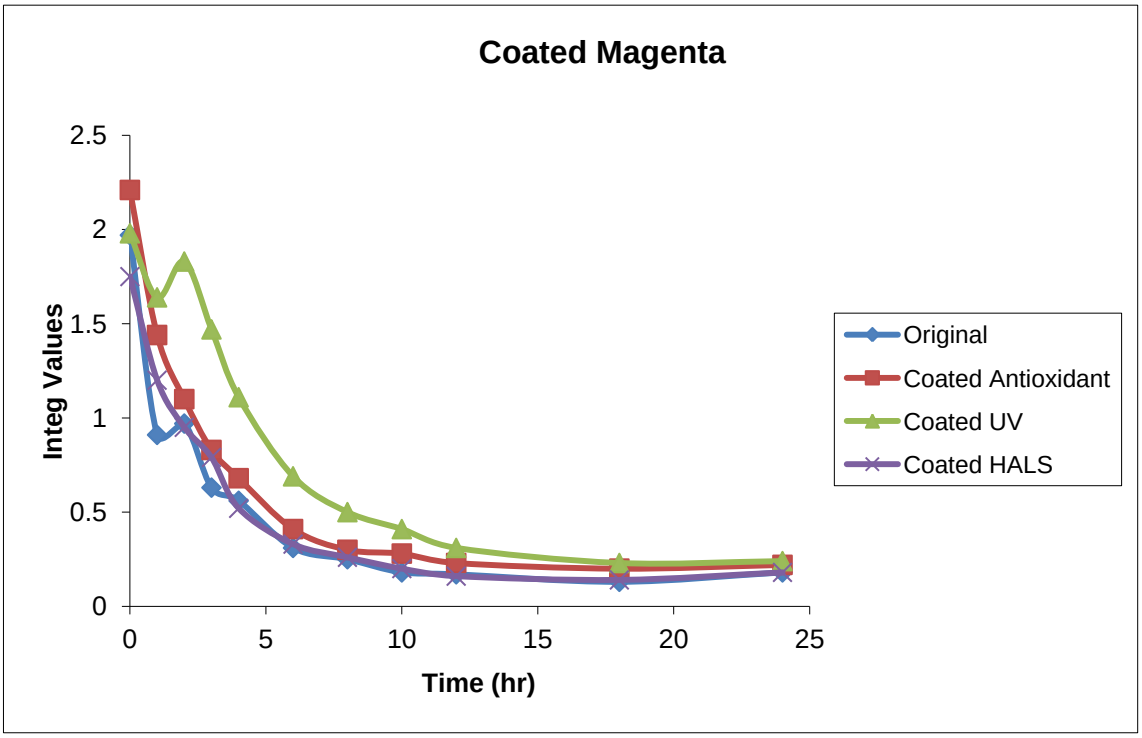

Figure 4.21 Integ values against time for exposure to the Xenotest of the magenta pigment coated with lightfastness enhancers

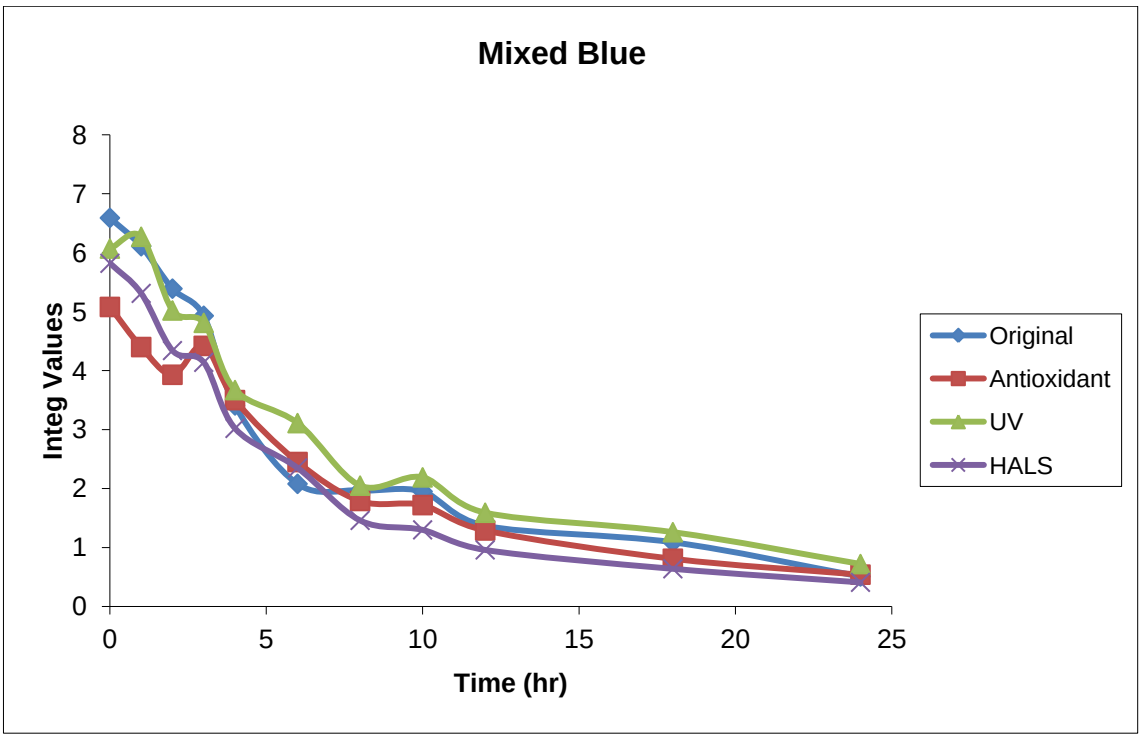

Figure 4.22 Integ values against time for exposure to the Xenotest of the blue pigment mixed with lightfastness enhancers

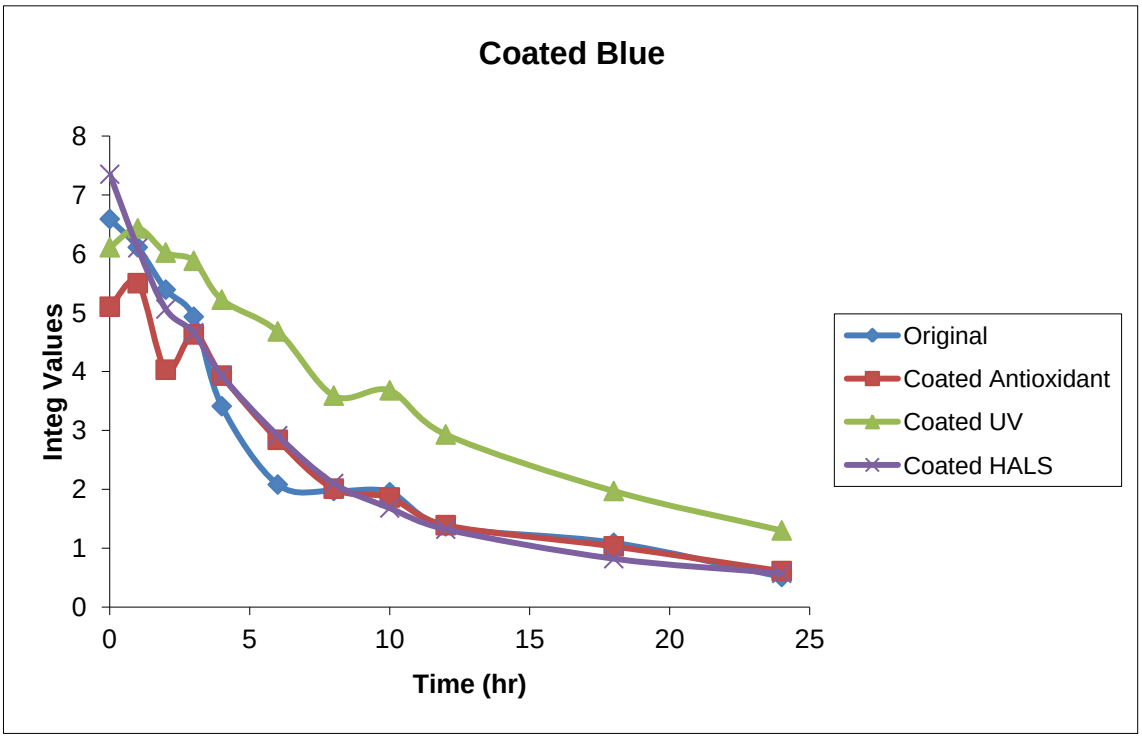

Figure 4.23 Integ values against time for exposure to the Xenotest of the blue pigment coated with lightfastness enhancers

Thus, it is clear that the UV absorber shows significant lightfastness enhancement of the thermochromic pigments in textile prints, much better than using the antioxidant or HALS. This is consistent with the differences in their actions. Exposure to UV light causes the chromophore developed by the colour former to degrade, and hence the

colour. The UV absorber protects the chromophore by absorbing UV light. In contrast, antioxidants and HALS protect the chromophore by interacting with the colorant or intermediate species produced during chromophore degradation. As these thermochromic pigments are microencapsulated and lightfastness enhancers can only come into contact with the walls of microcapsules, antioxidant and HALS are unable to interact with the colour formers. On the other hand, the UV absorber is able to perform its function to absorb UV light, when located outside the microcapsules, by reducing the level of damaging UV light which reaches the colour formers and other components. It is also clear that the UV absorber coated over the pigments works better than UV absorber mixed with them. Hence, it is concluded that the UV absorber is a useful lightfastness enhancer for improving the performance of textile prints based on microencapsulated leuco dye based thermochromic pigments.

In view of these results, the range of UV absorbers available was further investigated for their potential to effect lightfastness enhancement. For this purpose Tinuvin P, Tinuvin 1577, Uvinul 3049 and UV Titan L181 were selected. Tinuvin 1577 (Ciba Speciality Chemicals) is a low volatility hydroxyphenyl-triazine UV absorber. Its chemical name is 2-(4,6-diphenyl-1,3,5-triazin-2-yl)-5-hexyloxyphenol. Uvinul 3049 (BASF) is 2,2-dihydroxy-4,4-dimethoxybenzophenone. UV Titan L181 (Kemira Chemicals (UK) Ltd.) is an ultrafine titanium dioxide, which scatters UV light and transmits visible light and is commonly used in cosmetics and sun-screening preparations. Tinuvin P, Tinuvin 1577 and Uvinul 3049 are reported to have strong absorption in the 300-400 nm region with UV Titan L181 in the range 350-370 nm.

These UV absorbers were used with four thermochromic pigments; blue, magenta, orange and green, at 5% pigment concentration. The samples were again prepared both by mixing the UV absorbers directly in the pigment paste and by coating on the printed fabric. To investigate the effect of the level of UV absorbers, two concentrations were used; 3% and 5% by weight in both coloured and colourless printing pastes. The printed samples were again cured at 110°C for 10 minutes and exposed on the Heraeus Xenotest 150S fadeometer for 1, 2, 3, 4, 6, 8, 12 and 24 hours. The integ values were plotted against time.

In Figures 4.24-4.27, the integ values for the blue prints show that Tinuvin 1577 decreases colour strength probably by imparting yellowness or opacity in the prints. However, it shows lightfastness enhancement compared with the original sample. The

lightfastness improves considerably as the amount of Tinuvin 1577 is increased, when applied in mixture form. Uvinul 3049 is most effective as a lightfastness enhancer for the blue pigment. It also shows an increase in lightfastness with an increase in concentration. Tinuvin P shows greater colour strength with blue pigment when mixed and a little less, when coated on the colour. It also provides lightfastness enhancement but less than Uvinul 3049 and Tinuvin 1577, especially for longer light exposure times. UV Titan L181 reduces colour strength, probably by imparting whiteness or opacity and does not provide significant lightfastness enhancement. In the case of blue leuco dye based thermochromic pigments, it may be concluded that the non-phenolic UV absorber Uvinul 3049 is more effective than phenolic UV absorbers Tinuvin 1577 and Tinuvin P or ultrafine titanium dioxide.

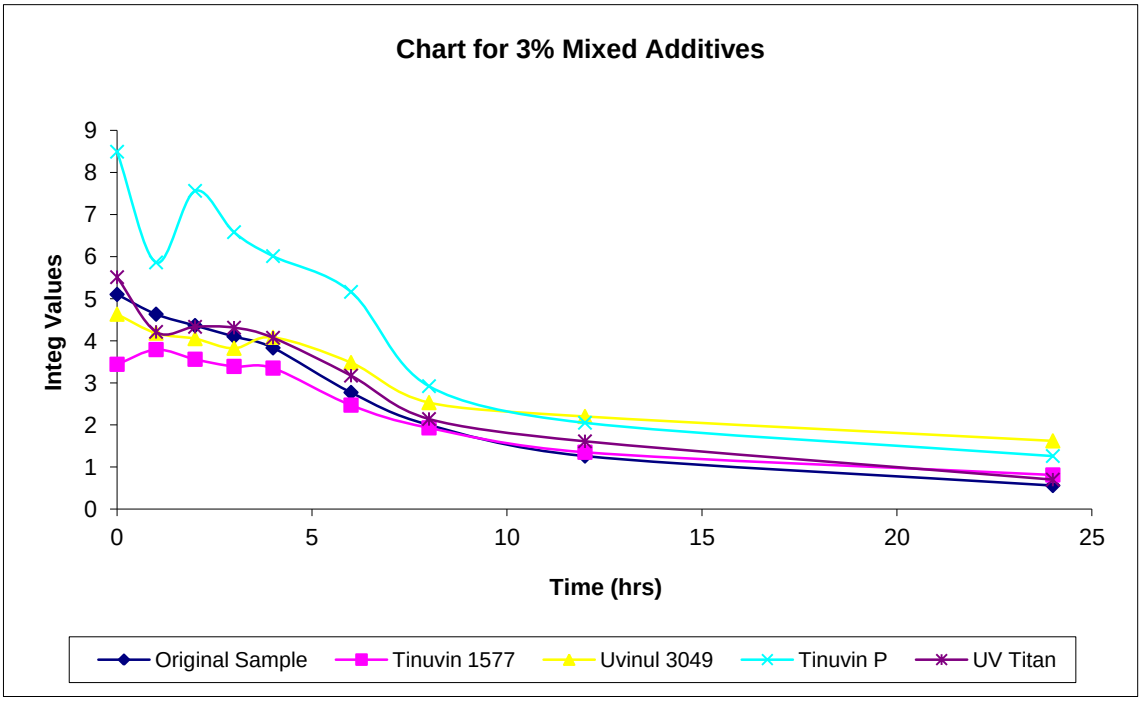

Figure 4.24 Integ values of blue prints against time of exposure to the Xenotest when mixed with 3% of different UV absorbers

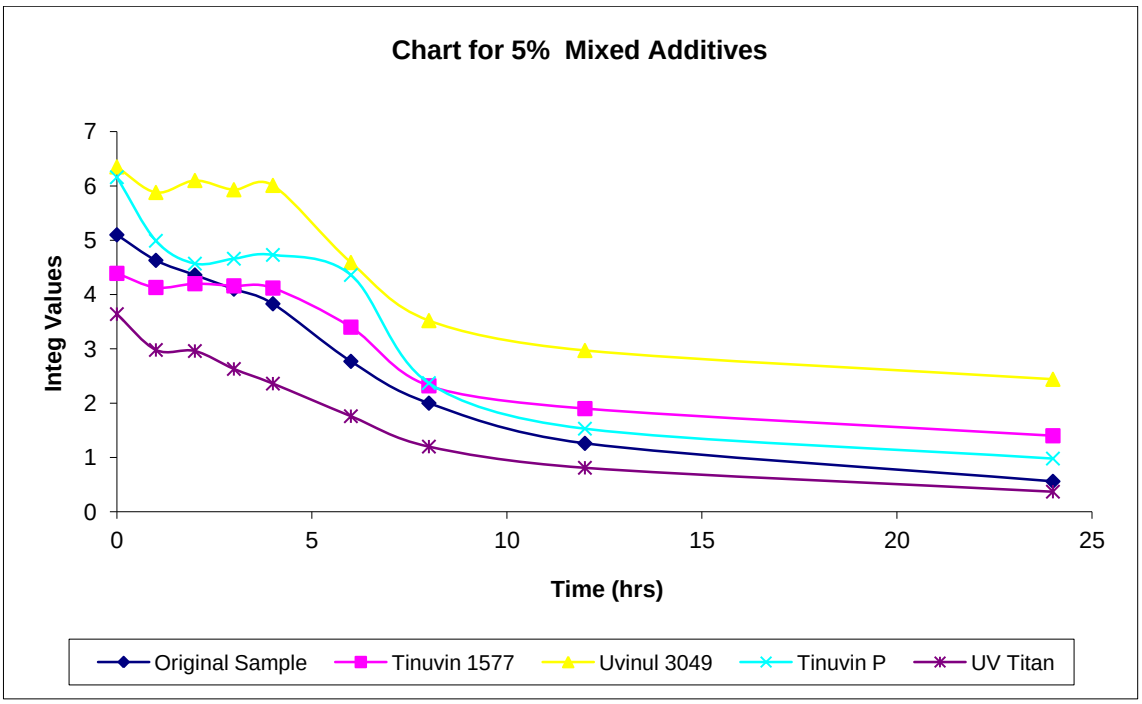

Figure 4.25 Integ values of blue prints against time of exposure to the Xenotest when mixed with 5% of different UV absorbers

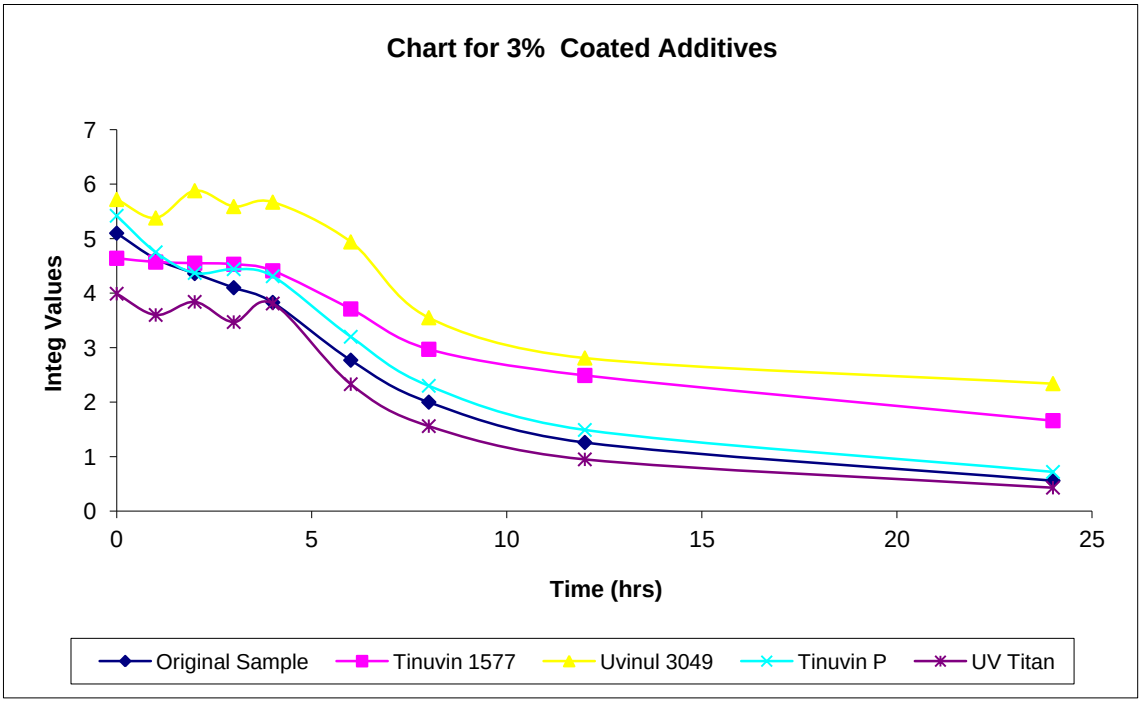

Figure 4.26 Integ values of blue prints against time of exposure to the Xenotest when coated with 3% of different UV absorbers

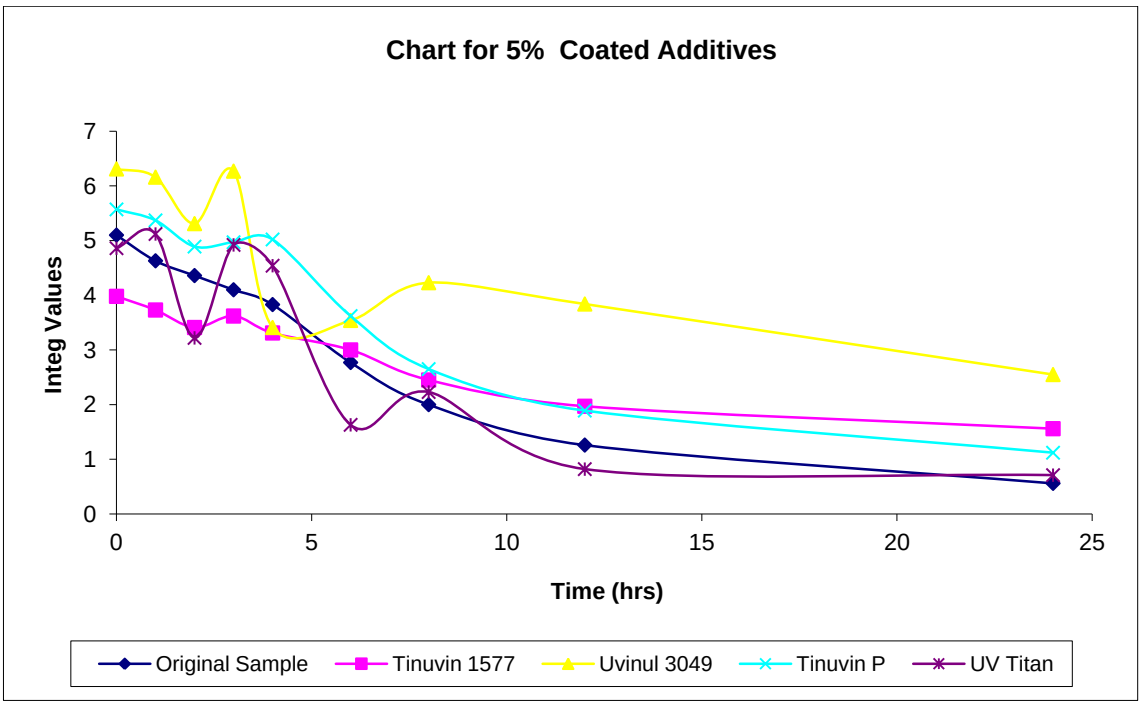

Figure 4.27 Integ values of blue prints against time of exposure to the Xenotest when coated with 5% of different UV absorbers

In Figures 4.28-4.31, the integ values for the green prints show that Tinuvin 1577, possibly by imparting a slight yellowness or opacity, are less than for the original sample. However, it shows lightfastness enhancement, improving considerably as the amount of Tinuvin 1577 increases, in the coated form. Uvinul 3049 is also the most effective lightfastness enhancer for the green pigment, and shows an increase in lightfastness with increase in concentration, especially for coated samples. Tinuvin P shows lightfastness enhancement but less than Uvinul 3049 and Tinuvin 1577, and is especially less effective for long exposure. UV Titan L181 does not affect the colour strength of the green pigment, but it is not an effective lightfastness enhancer. Thus, for the green pigment, the non-phenolic UV absorber Uvinul 3049 is the most effective agent.

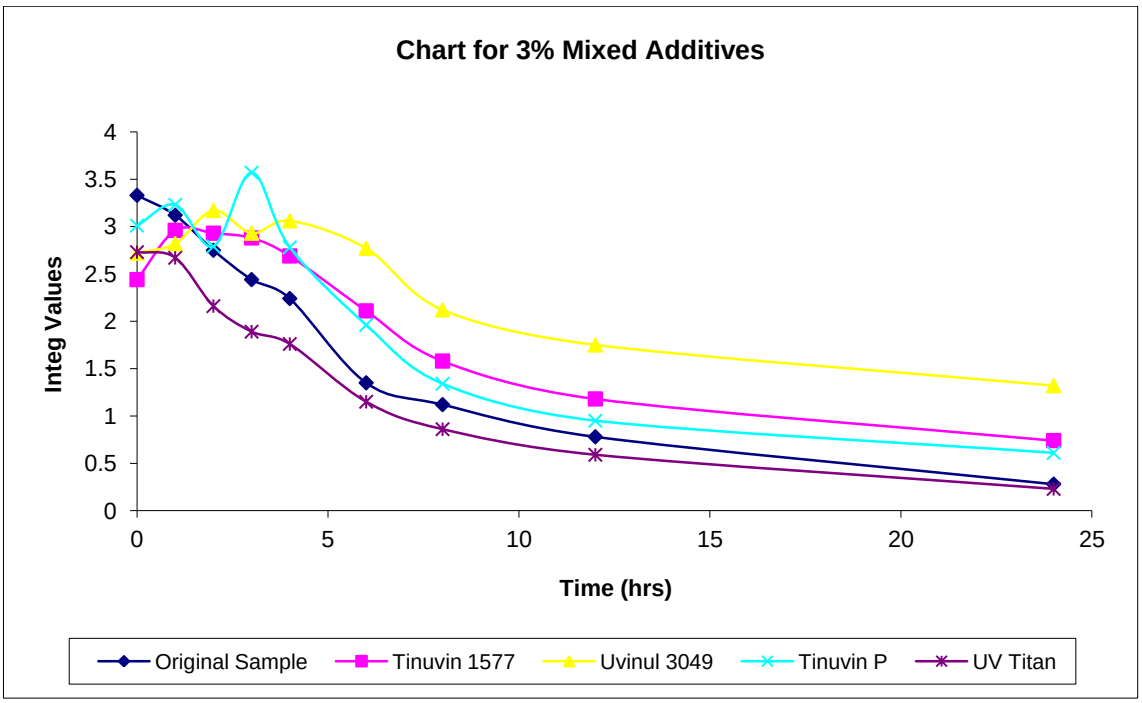

Figure 4.28 Integ values of green prints against time of exposure to the Xenotest when mixed with 3% of different UV absorbers

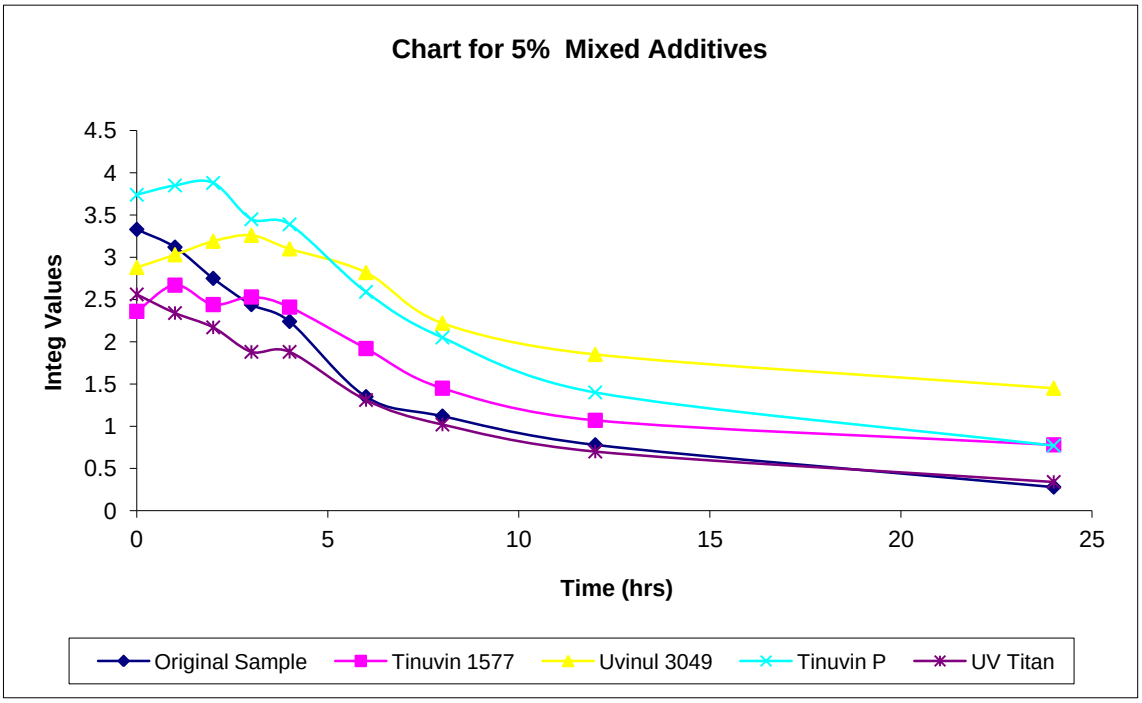

Figure 4.29 Integ values of green prints against time of exposure to the Xenotest when mixed with 5% of different UV absorbers

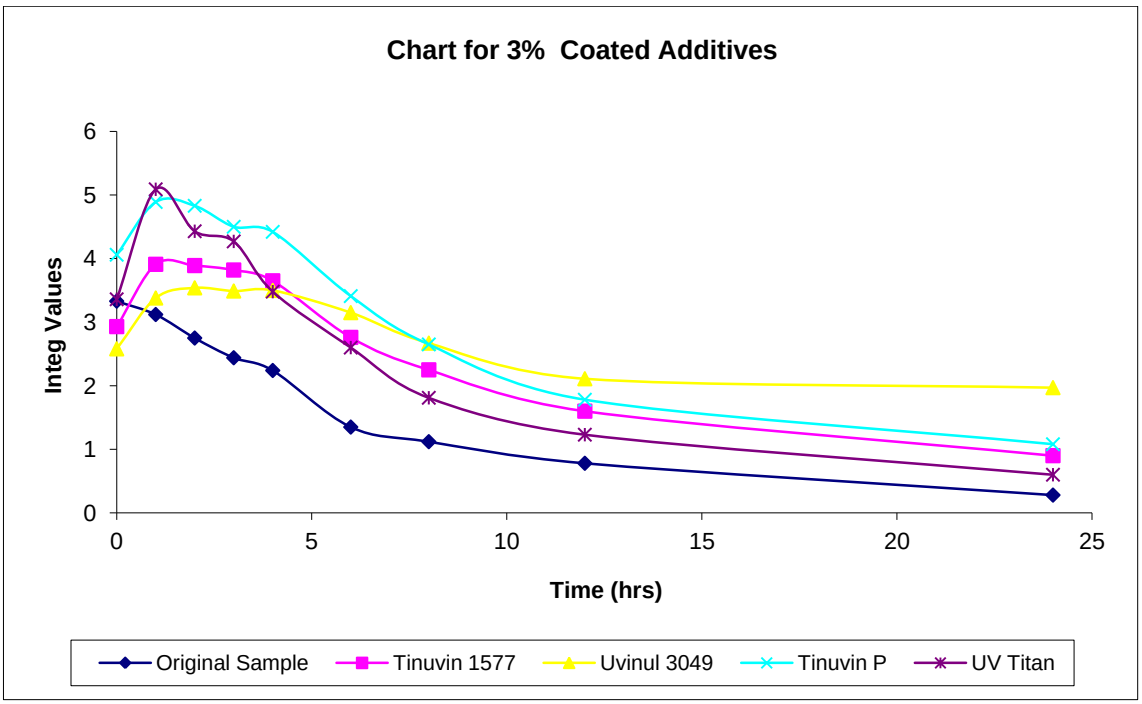

Figure 4.30 Integ values of green prints against time of exposure to the Xenotest when coated with 3% of different UV absorbers

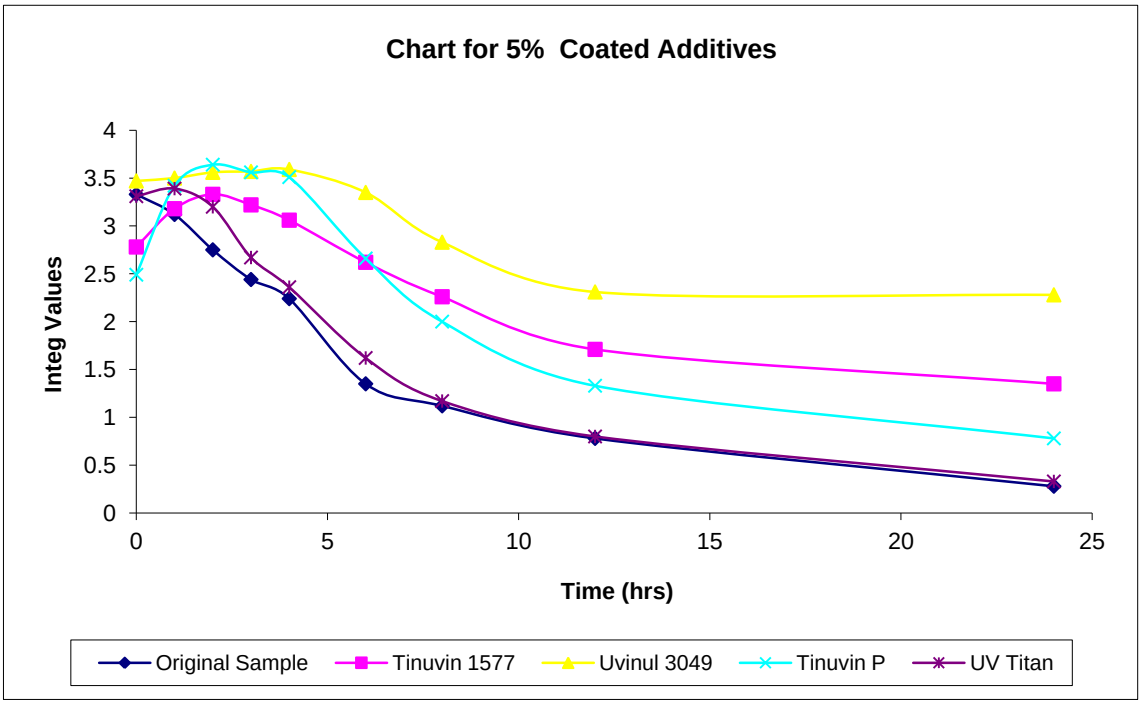

Figure 4.31 Integ values of green prints against time of exposure to the Xenotest when coated with 5% of different UV absorbers

In Figures 4.32-4.35, the integ values for magenta show that Tinuvin 1577 does not reduce the colour depth except at 5% concentration in the case of coating. There is lightfastness enhancement with Tinuvin 1577 and it is consistent when used both mixed and coated. Uvinul 3049 also proves to be the most effective for magenta, also showing an increase in lightfastness with an increase in level. Tinuvin P shows less effective

lightfastness enhancement than Uvinul 3049 and Tinuvin 1577. UV Titan L181 does not affect the colour strength of magenta, but it does not give better lightfastness. Thus, for magenta also, the non-phenolic UV absorber is the most effective.

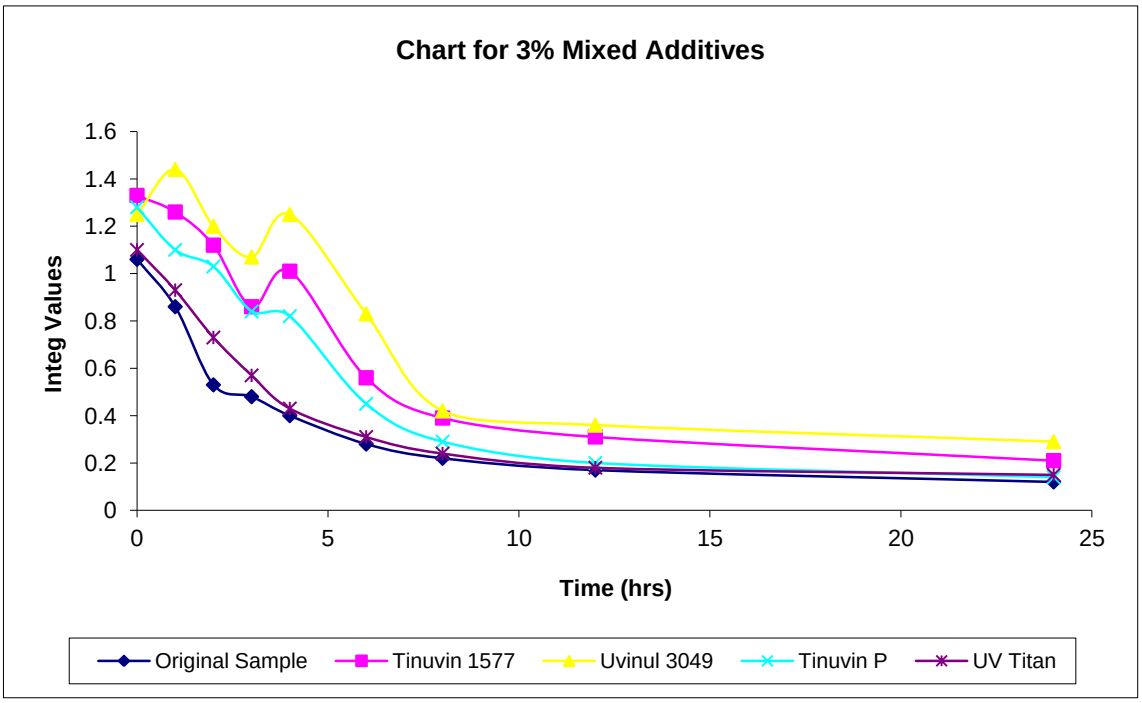

Figure 4.32 Integ values of magenta prints against time of exposure to the Xenotest when mixed with 3% of different UV absorbers

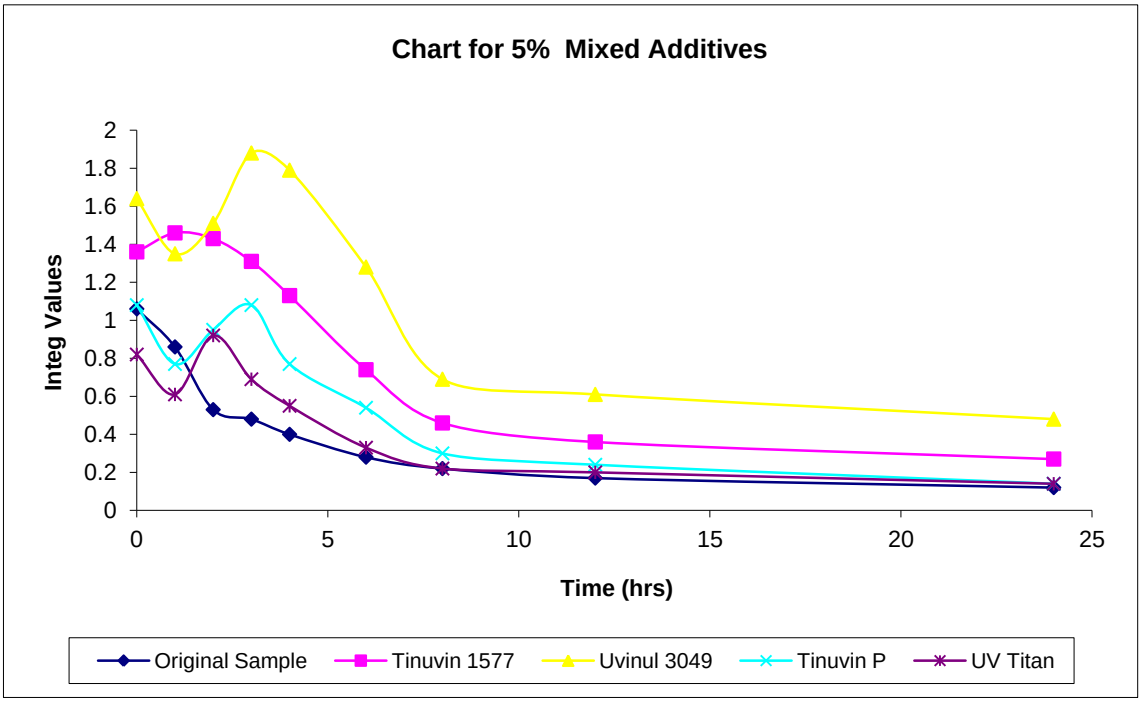

Figure 4.33 Integ values of magenta prints against time of exposure to the Xenotest when mixed with 5% of different UV absorbers

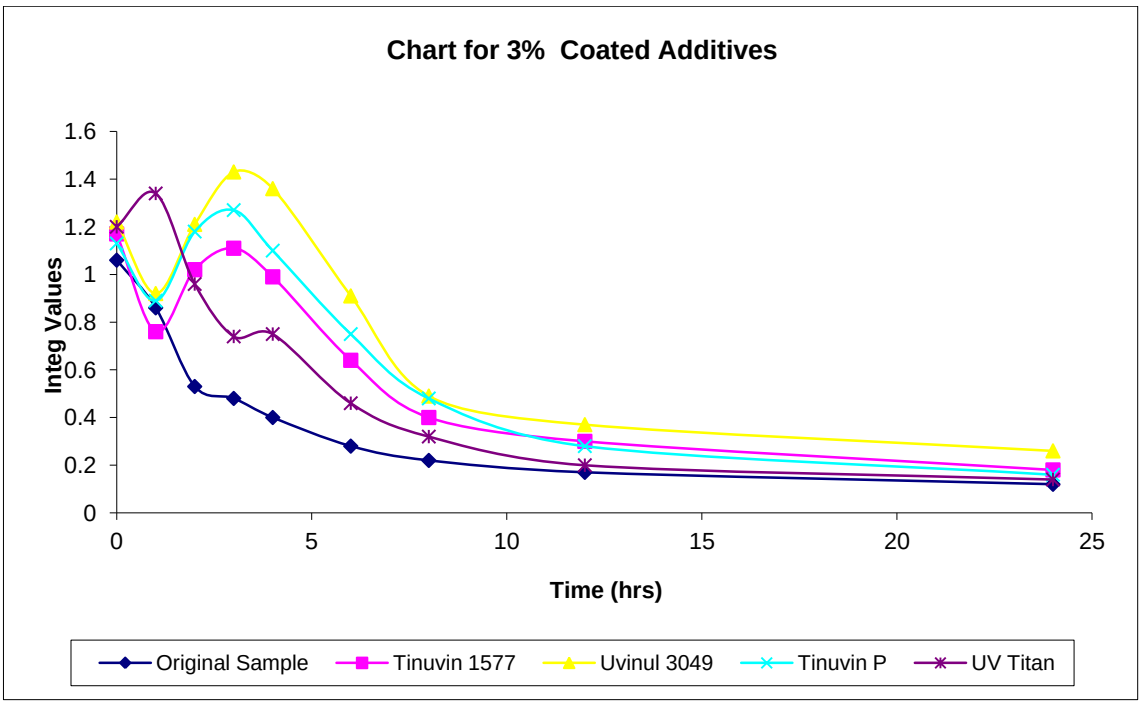

Figure 4.34 Integ values of magenta prints against time of exposure to the Xenotest when coated with 3% of different UV absorbers

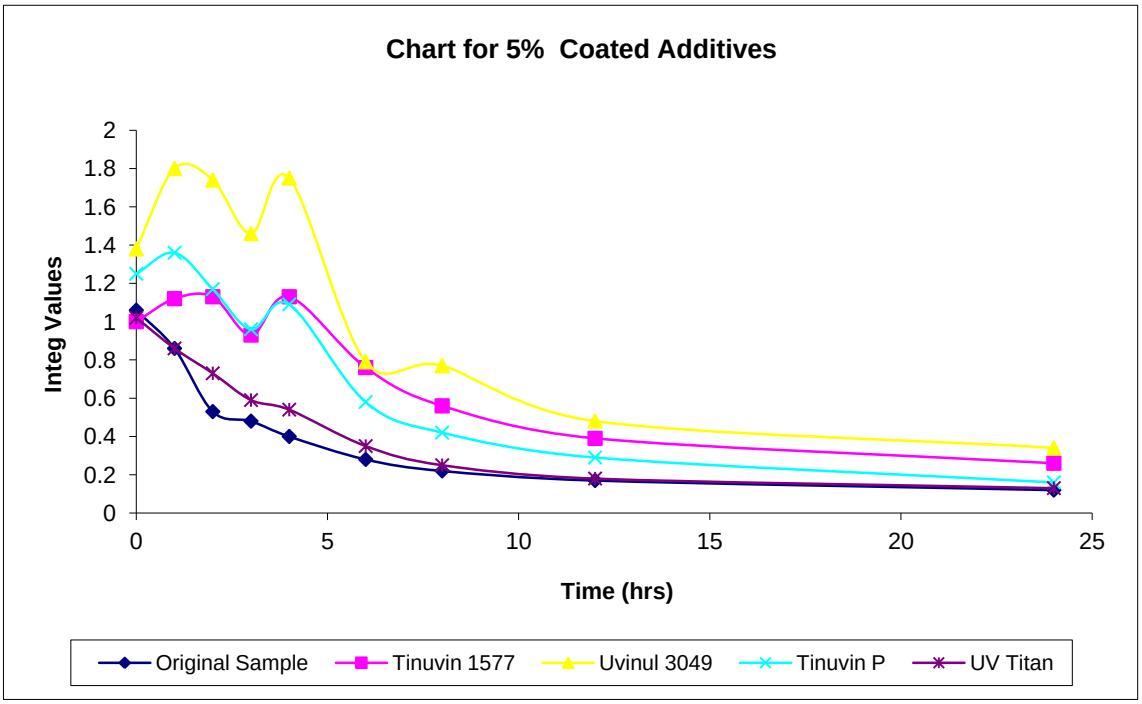

Figure 4.35 Integ values of magenta prints against time of exposure to the Xenotest when coated with 5% of different UV absorbers

Figures 4.36-4.39 show that the colour strength of the orange print is affected by all the UV absorbers except in the case of 3% concentration of Tinuvin 1577 in mixed form. Uvinul 3049 and Tinuvin 1577 show lightfastness enhancement, but it is not significant. As the UV absorbers reduce the colour strength of orange and lightfastness enhancement is also low, they are not as effective for orange as for the other pigments.

From the above analysis, it can be concluded that a UV absorber with a non-phenolic chemical structure is more effective in lightfastness enhancement than UV absorbers with phenolic chemical structures and ultra fine titanium dioxide. It is also important to note that the additive may reduce the colour strength of the pigment, possibly by imparting colour or opacity. In this investigation, Uvinul 3049 is found to be the best lightfastness enhancer for leuco dye based thermochromic pigments, with Tinuvin 1577 also effective but less than Uvinul 3049. Tinuvin P is not effective especially for long exposure to light. UV Titan L181 is not effective as a lightfastness enhancer for the pigments and it also considerably reduces the colour strength presumably by imparting opacity.

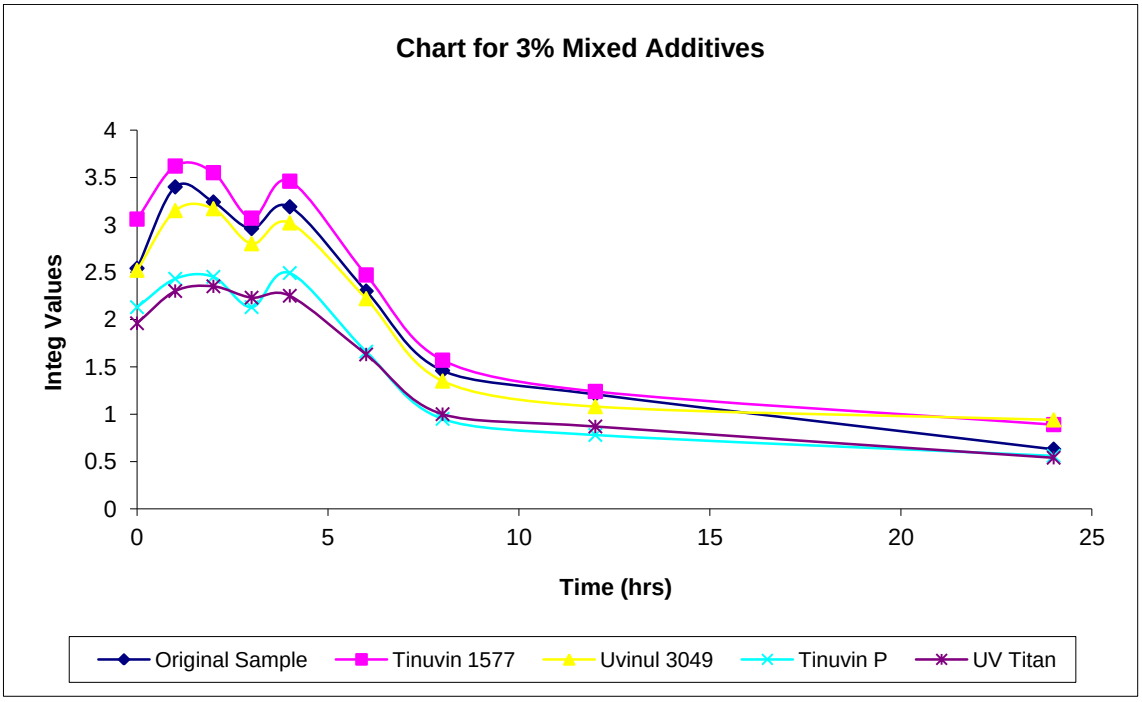

Figure 4.36 Integ values of orange prints against time of exposure to the Xenotest when mixed with 3% of different UV absorbers

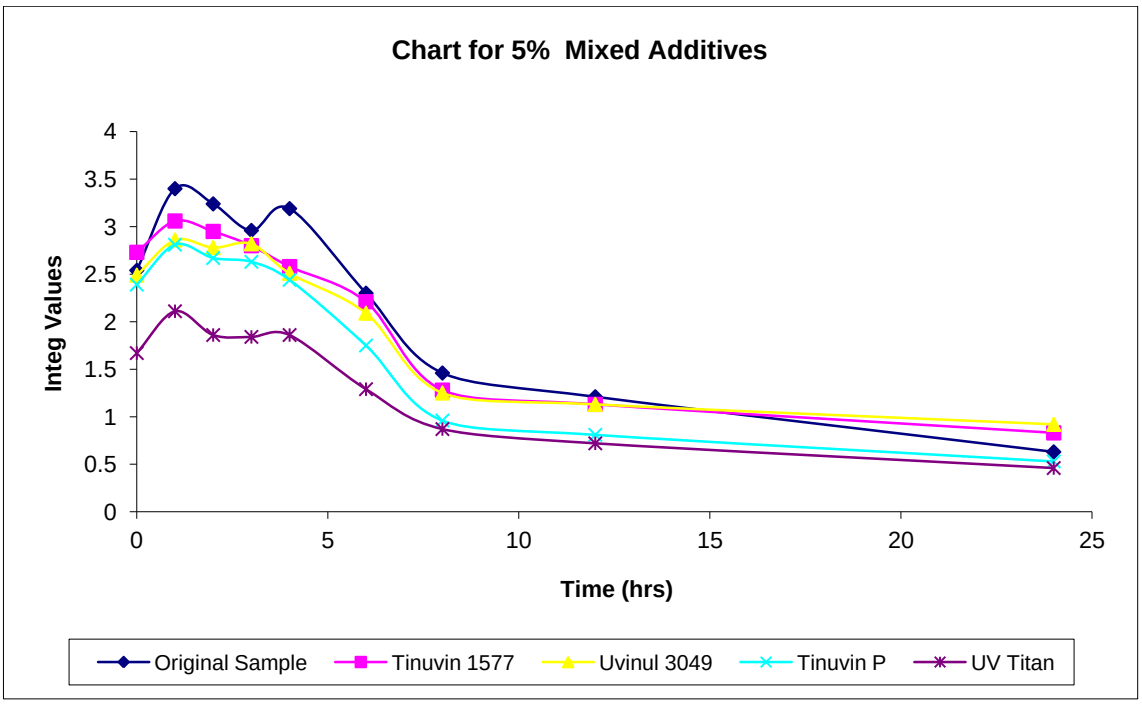

Figure 4.37 Integ values of orange prints against time of exposure to the Xenotest when mixed with 5% of different UV absorbers

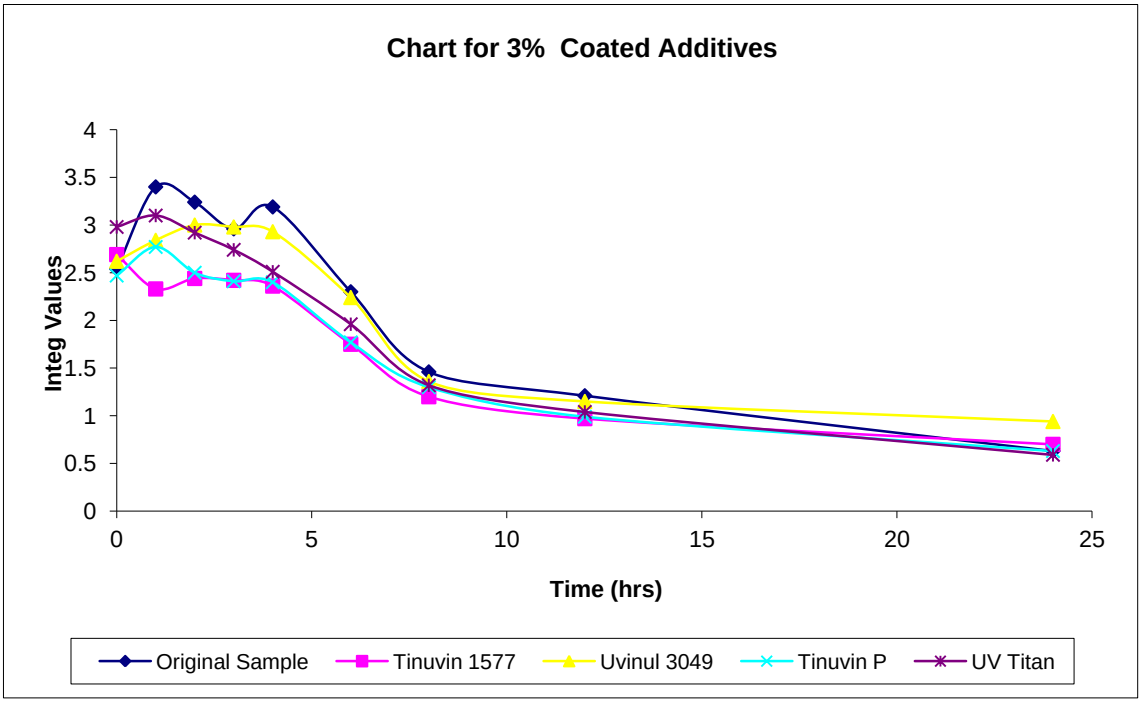

Figure 4.38 Integ values of orange prints against time of exposure to the Xenotest when coated with 3% of different UV absorbers

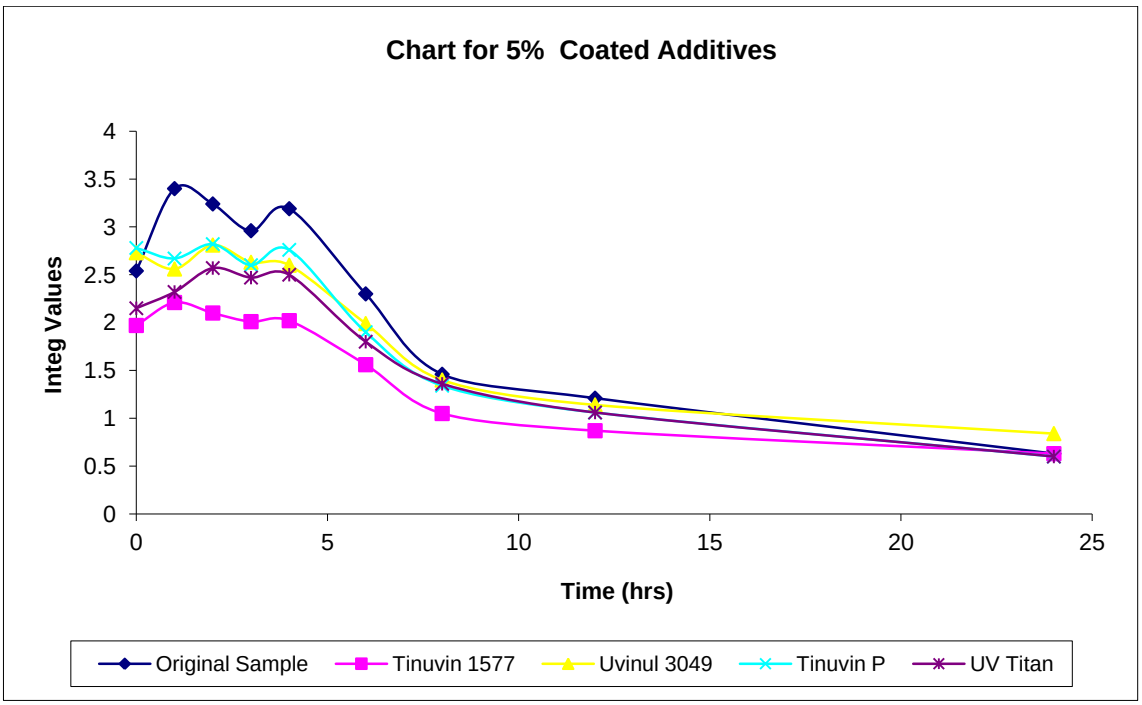

Figure 4.39 Integ values of orange prints against time of exposure to the Xenotest when coated with 5% of different UV absorbers

4.2 Extrusion

The leuco dye based thermochromic pigments were available in two forms; slurry and powder form. It has been reported and observed that these pigments are sensitive towards heat and may be degraded at high temperatures as discussed in section 4.1.2. Normally, for textile applications, these pigments are printed in slurry form on the fabric incorporated into a binder which is fixed through curing. It has been demonstrated that the curing at high temperatures may degrade these pigments and this causes loss of colour strength. The fastness to washing and rubbing of these pigments in printed form are inferior, due in part to the need for fixation at a low temperature meaning that the film may not be completely cured and there is a need for a high concentration of pigment to acquire the required colour depth as discussed in section 4.1.3. When incorporated from a slurry form, the highest colour strength was obtained with a 30% colour concentration on the weight of the print paste as discussed in section 4.1.4. The lightfastness of these pigments is also inferior when printed on the fabric as discussed in section 4.1.5.

Considering these conclusions, it was anticipated that some of the properties might prove to be better when they were incorporated into filaments during melt extrusion. For this purpose, it was decided to extrude filaments of different polymers with incorporation of the powder form of the leuco dye based thermochromic pigments,

provided by LCR Hallcrest. The microencapsulated thermochromic pigments are sensitive towards heat, so it was envisaged that maximum performance in terms of colour strength would be achieved at lower processing temperatures. To investigate the possibility of colour loss due to high temperatures and other aspects of the properties of thermochromic pigments, polypropylene, linear low density polyethylene, a copolymer of ethylene with vinyl acetate (EVA) and polycaprolactone were selected for the investigation. These polymers have different extrusion processing temperatures which cover the temperature range from 130°C to 260°C. Polypropylene was provided by Basell Polyolefins (UK) Ltd. The melt flow index (MFI) was 13g/10min, measured with a 2.16kg weight at 230°C. Linear low density polyethylene was provided by Basell Polyolefins (UK) Ltd. The MFI was 18g/10min, measured with a 2.16kg weight at 160°C. Ethylene vinyl acetate copolymer (EVA) was provided by Dupont Engineering Polymers and DuPont Packaging & Industrial Polymers, branded as Elvax 450 with MFI (190°C, 2.16kg) of 8g/10min. and Elvax 3175LGA with MFI (190°C, 2.16kg) of 6g/10min. Polycaprolactone provided by Perstorp, was branded as Capa 6500. Its MFI was 7g/10min, measured with 2.16kg weight at 160°C. These polymers and thermochromic pigments in powder form were investigated by differential scanning colorimetery (DSC) to determine their melting and degradation characteristics and hot stage microscopy was carried out to observe their melting behaviour before extrusion was carried out. The DSC was carried out both in nitrogen and air environment and scans are shown in Figures 4.40-4.46. The hot stage observations were consistent with the results obtained by DSC. These observations were used to assess the appropriate processing temperatures of the polymers.

Figures 4.40-4.46 show DSC traces for PP, LLDPE, EVA (450), EVA (3175LGA), PCL, blue and red pigments respectively, in nitrogen and air, while their respective melting, degradation onset and degradation peak temperatures are illustrated in Table 4.4. The melting temperature of all polymers and pigments are almost same in both nitrogen and air environments except for blue pigment where it is slightly lower in nitrogen. In the case of red pigment, some minor peaks are also observed in the air environment. These peaks for blue and red pigments are likely to be due to the melting of the solvent inside the microcapsules.

The degradation onset temperature of PP is slightly higher in nitrogen than in air. The degradation onset temperatures for LLDPE and EVA (450 and 3175LGA) are almost

the same in both environments with minor variations probably within experimental error. The degradation peak temperature for PP is considerably lower in an air environment than in nitrogen. The degradation peaks for LLDPE and EVA (450) are similar in nitrogen and air, while EVA (3175LGA) does not show a degradation peak within the scan temperature range used. Degradation onsets and peaks for PCL and blue and red pigments were also not found in the scan temperature range. The DSC traces for thermochromic pigments were recorded up to 250°C because these were to be incorporated into polymers, extruded up to around that temperature. No obvious degradation of pigments was observed up to 250°C. Therefore, it can be concluded that the microcapsules of both blue and red thermochromics are stable up to the highest extruded temperatures, which in the case of this study is about 240°C although this will also be dependent on time of exposure.

Table 4.4 DSC results of polymers and thermochromic pigments in °C

	Melting point		Degradation onset		Degradation peak	
	Nitrogen	Air	Nitrogen	Air	Nitrogen	Air
PP	164.2	163.2	207.6	203.4	283.3	235.9
LLDPE	125.0	124.9	212.4	210.1	229.2	225.9
EVA 450	82.8	85.0	200.8	203.7	228.9	232.9
EVA 3175	74.1	74.3	228.0	228.9	-	-
PCL	60.9	61.0	-	-	-	-
Blue Pigment	34.1	38.8	-	-	-	-
Red Pigment	39.6	40.6	-	-	-	-

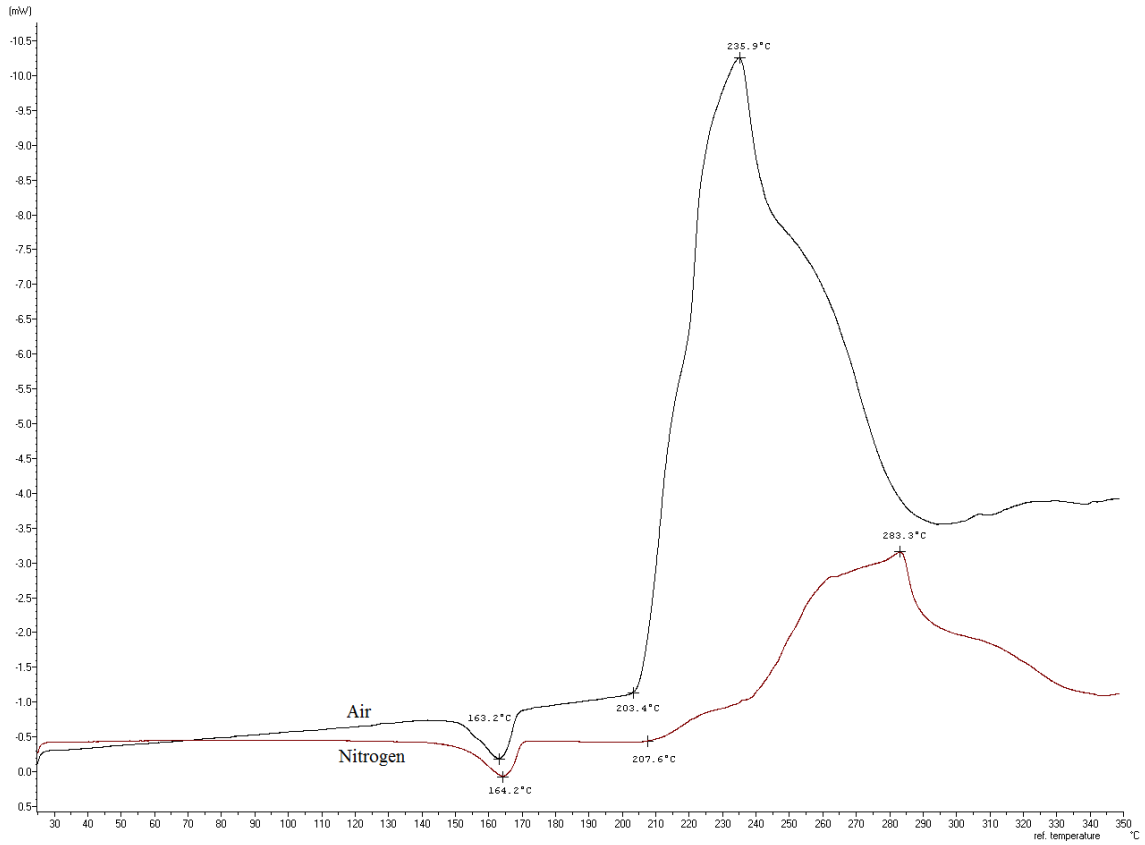

Figure 4.40 DSC of PP in nitrogen and air atmospheres

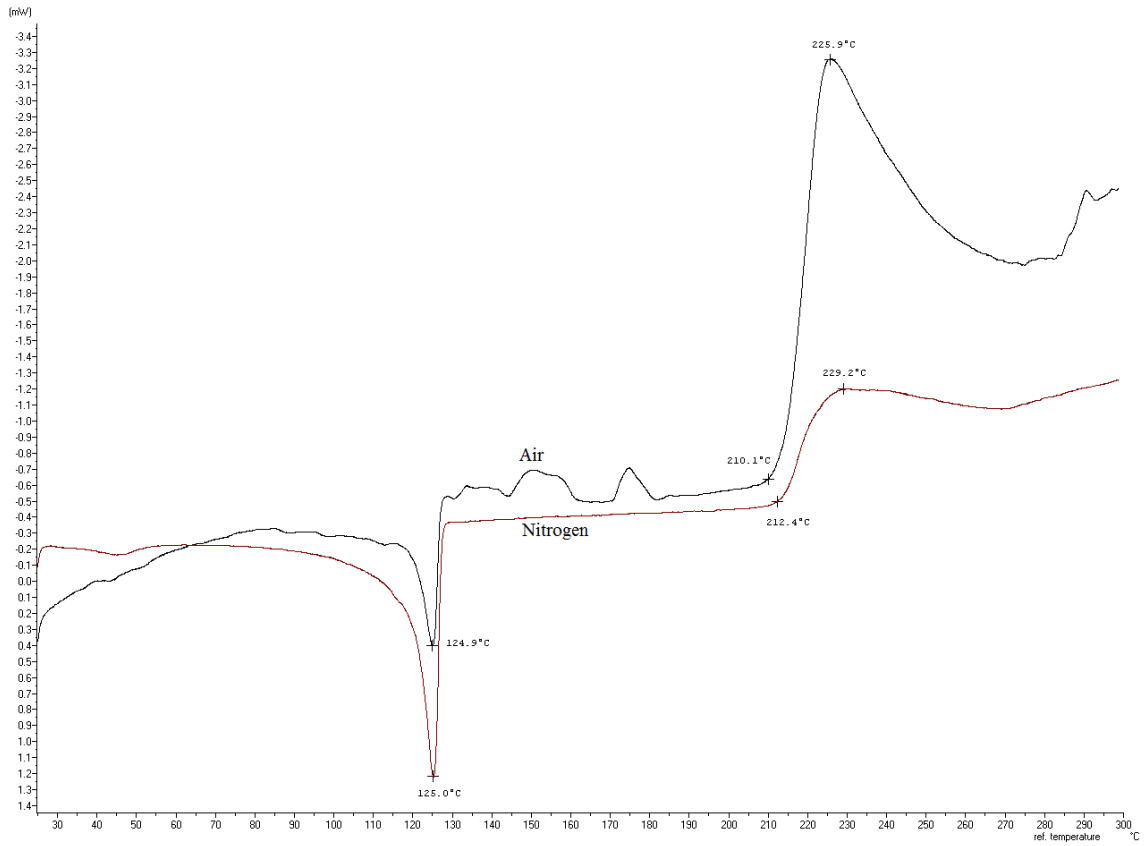

Figure 4.41 DSC of LLDPE in nitrogen and air atmospheres

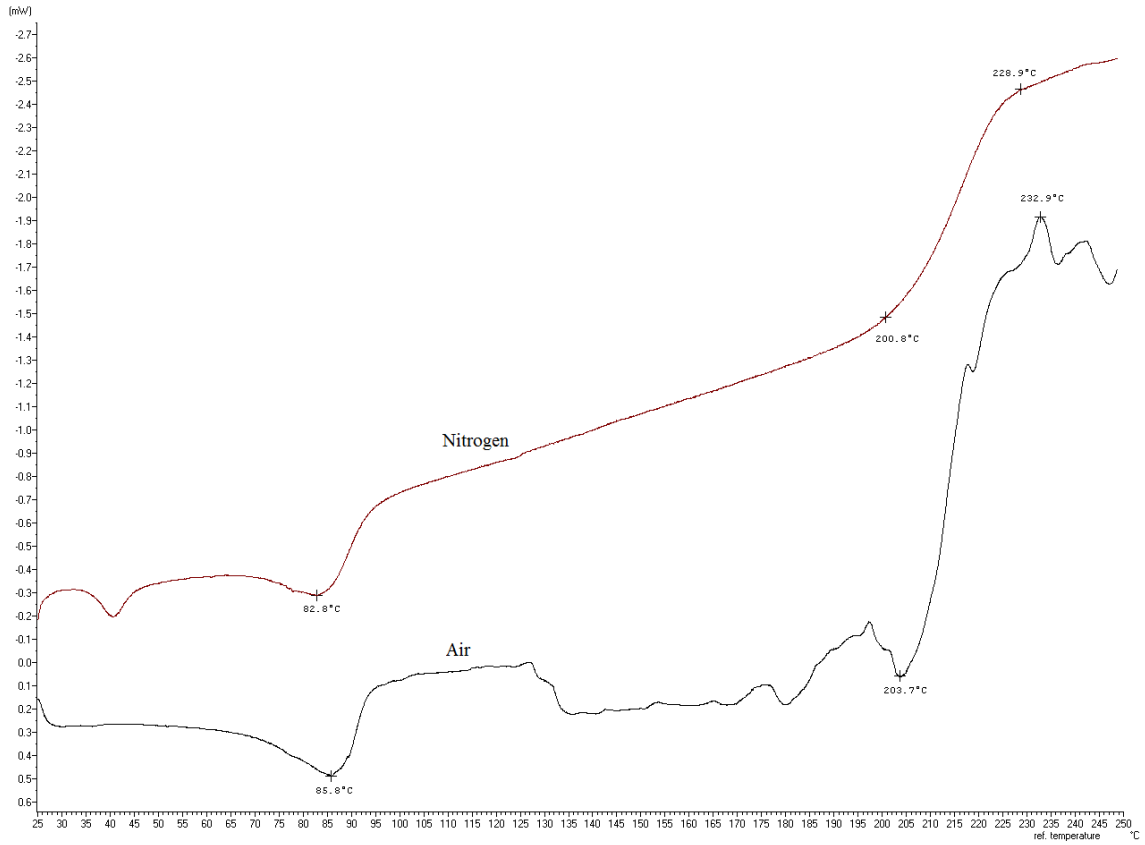

Figure 4.42 DSC of EVA(450) in nitrogen and air atmospheres

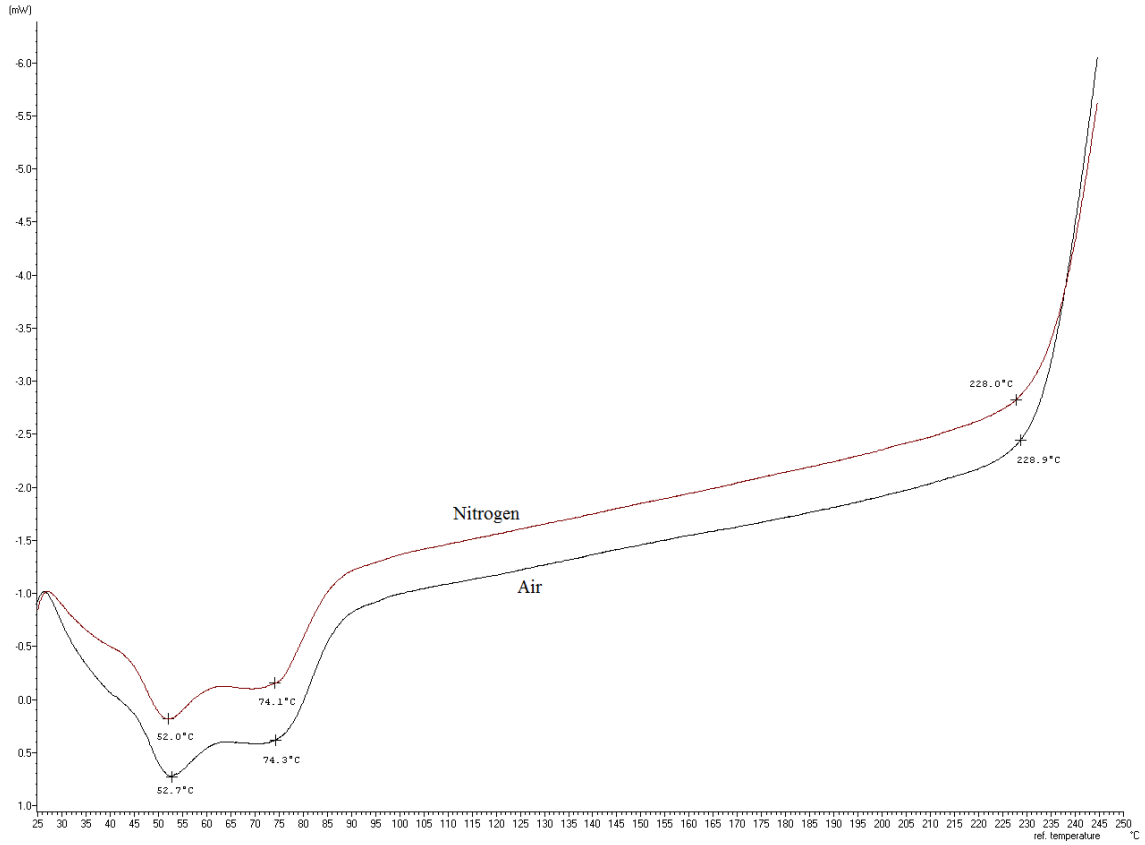

Figure 4.43 DSC of EVA(3175LGA) in nitrogen and air atmospheres

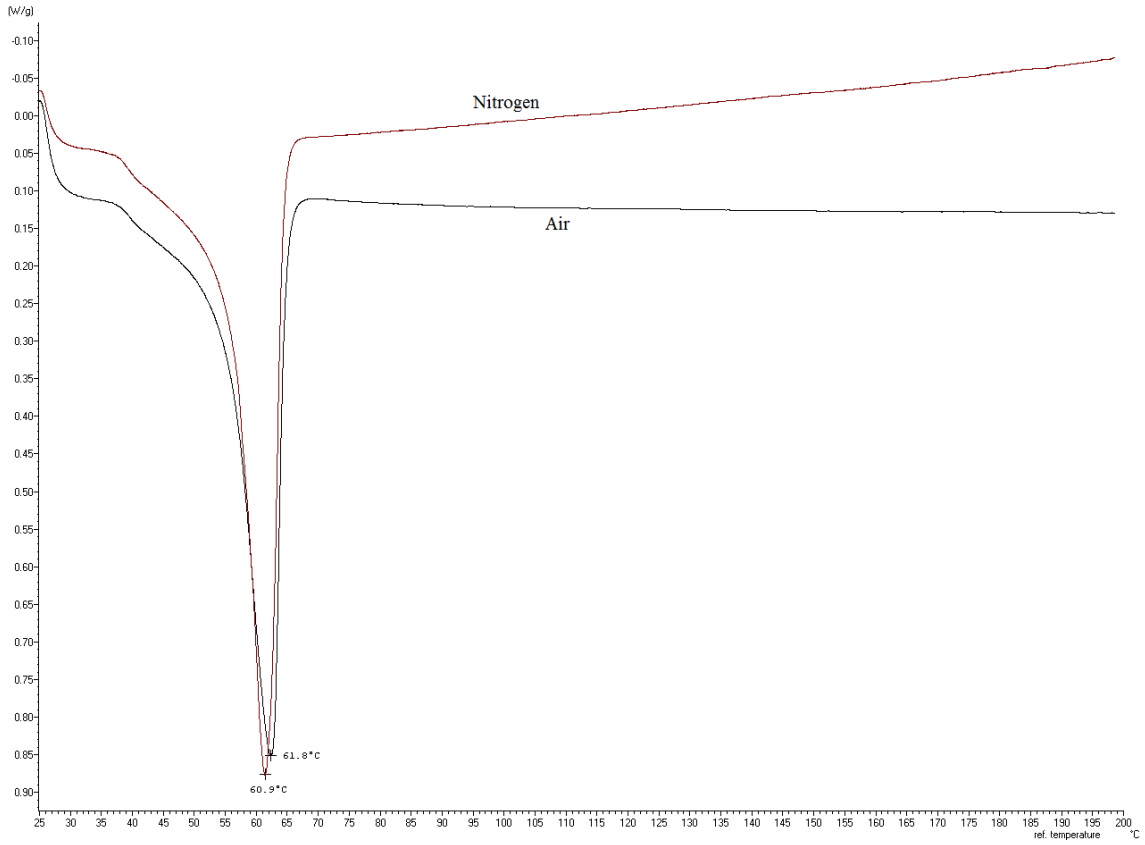

Figure 4.44 DSC of PCL in nitrogen and air atmospheres

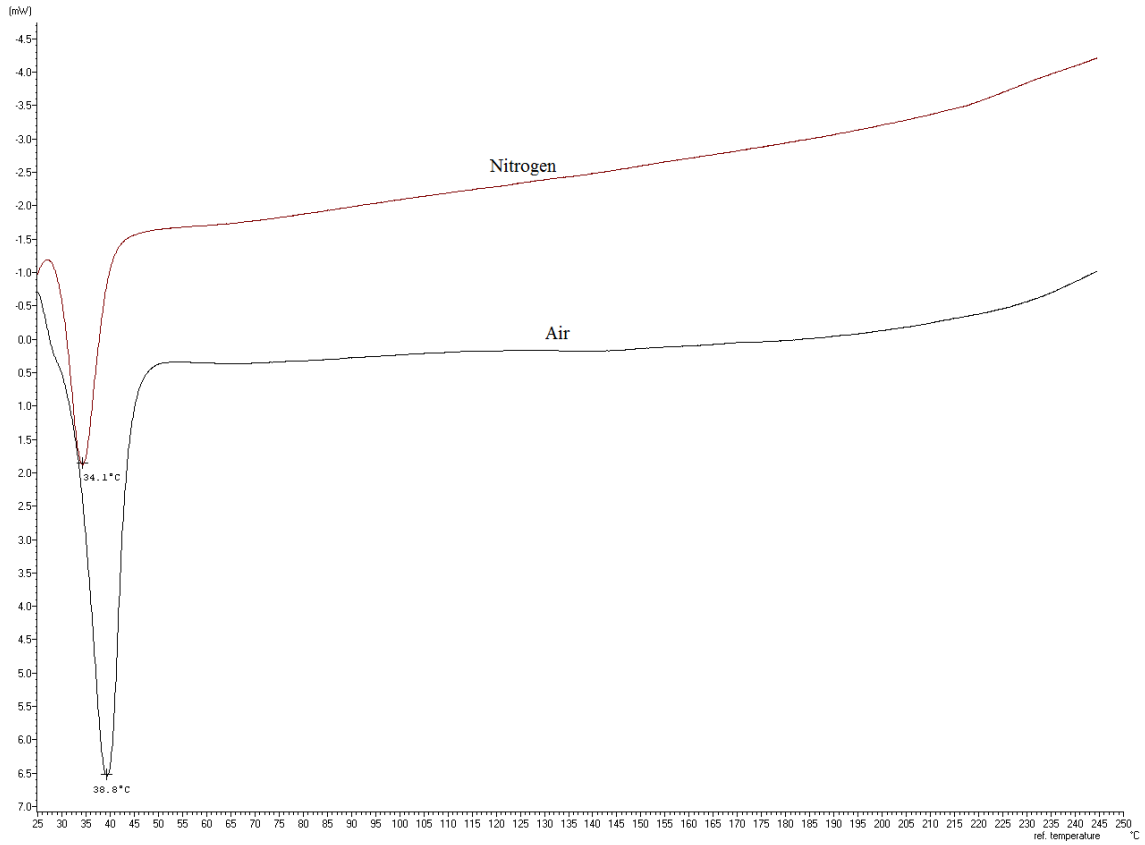

Figure 4.45 DSC of blue thermochromic pigment in nitrogen and air atmospheres

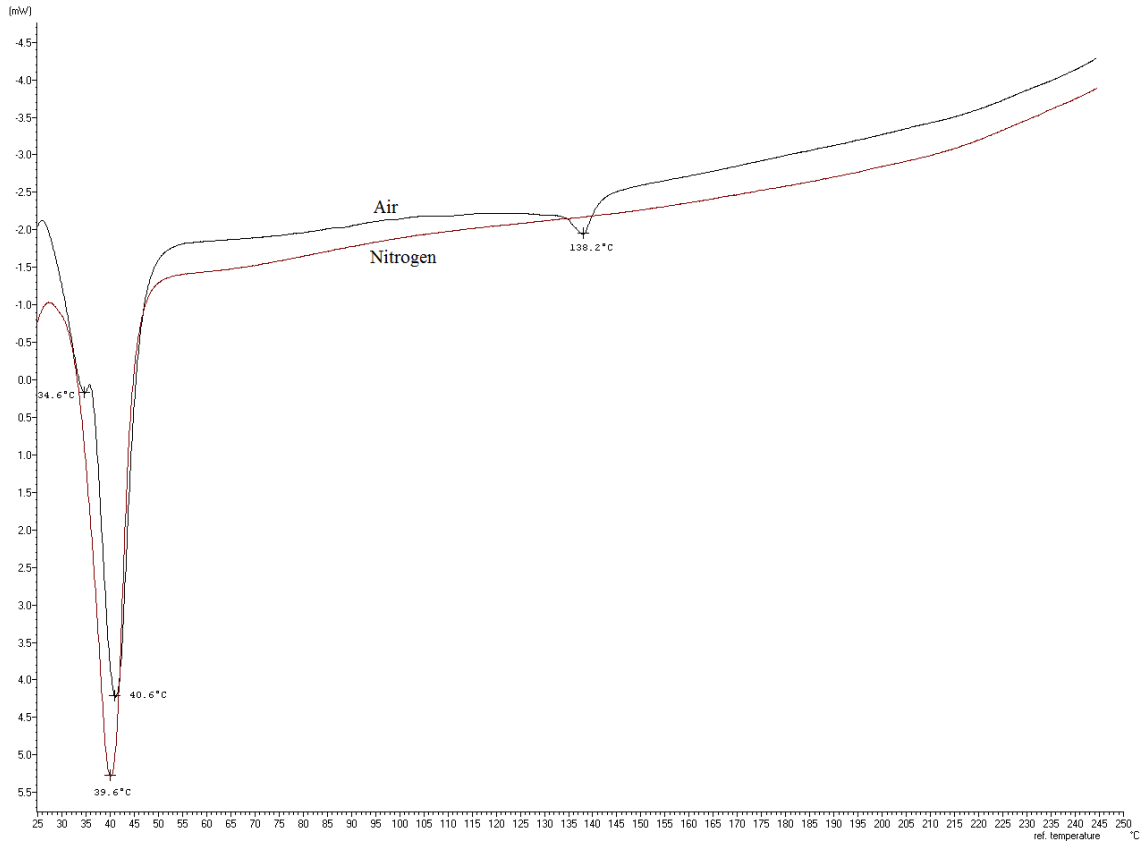

Figure 4.46 DSC of red thermochromic pigment in nitrogen and air atmospheres

Initially, each of these polymers was extruded without pigment to establish the optimum processing conditions such as temperature, pressure, and speed on the ram extrusion and screw extrusion machines. Once the parameters for extrusion had been established for extrusion of prototype filaments, the thermochromic pigment powders were mixed homogenously with the polymer chips and extrusion was carried out.

4.2.1 Extrusion on the Ram Extrusion Machine

The ram extrusion machine works on the simple principle of forcing the material through a narrow hole of the required shape as discussed in section 2.11.1. In this machine, heaters are used to melt the polymer and then the polymer is forced through a die hole with immediate cooling afterwards by quenching into water at room temperature. In this way, the polymer is converted into a filament with the required shape and cross section. However, after initial experiments, as discussed later, this machine was not found to be suitable for incorporation of leuco dye based thermochromic pigments due to the serious issue of inhomogeneous mixing of polymers with the pigments, although there were advantages in that the sample sizes were smaller and experiment times on this machine were shorter than with the screw extrusion machine. Therefore, all of the polymers were first extruded using the ram extrusion

machine to determine the required processing temperature and to observe the behaviour of the polymers under pressure. As the thermochromic pigments were known to be sensitive towards heat, it was anticipated to attempt to produce the prototype filaments at the lowest possible processing temperature.

Polypropylene was processed on a trial basis at 220°C, 225°C, 230°C, 235°C, 240°C and 245°C temperatures. The speed and pressure of the machine was maintained in such a way that the pressure did not exceed 800psi, beyond which the machine cut off the operation to prevent damage that might be caused due to high pressure. The most successful prototype filaments were extruded at the lowest temperature of 230°C and a pressure of 700psi where the lowest number of breakages occurred. These filaments were collected on a small cone using a winder.

In attempts to prepare thermochromic polypropylene, 15g of the polymer in a bottle was mixed with 0.30g of thermochromic pigment. The mixture was shaken vigorously for 5 minutes by hand to ensure homogeneous mixing as far as possible. This mixture was placed into the ram extrusion machine and the filament was produced at the optimum temperature and pressure. The filament produced contained the thermochromic pigment and showed colour change behaviour but the colour was not homogeneous. Areas rich and poor in colour in the filament were quite visible and this situation was not acceptable. Non-homogeneity was attributed to the fact that there is no facility to mix the molten chips of the polymer with pigment in the machine. Therefore, the ram extrusion machine was not found to be suitable to extrude thermochromic pigments incorporated into filaments.

Linear low density polyethylene (LLDPE) was processed at 125°C, 130°C, 135°C, 140°C, 145°C and 150°C temperatures using the ram extrusion machine. The speed and pressure of the machine was again maintained in such a way that the pressure did not exceed 800psi. The prototype filaments were extruded most successfully in this case at the lowest temperature of 145°C with 700psi pressure, based on a low number of breakages.

Two grades of co-polymer of ethylene vinyl acetate (EVA), (Elvax 450 and Elvax 3175LGA, provided by DuPont) were processed at 110°C, 115°C, 120°C, 125°C, 130°C and 135°C temperatures, again ensuring the pressure did not exceed 800psi. The prototype filaments were extruded most successfully at the lowest temperature of 125°C

with 700psi pressure. It was observed that the Elvax 450 was extruded more smoothly and with less breakage of filaments than Elvax 3175LGA. Therefore, Elvax 450 was used further to carry out extrusion on the screw extrusion machine.

Polycaprolactone has a melting point of 58-60°C, and it was expected that it would be extruded at a slightly higher temperature than that. However, on both ram and screw extrusion machines, the grade of polycaprolactone provided could not be extruded at a temperature lower than 160°C. At lower temperatures, the polymer was behaving like a glue and consequently stopping the machine by creating a high pressure, especially when processing on the screw extrusion machine. As a 160°C processing temperature was already covered by the linear low density polyethylene and because of these unsuccessful preliminary trials, it was decided not to proceed further with this polymer.

4.2.2 Extrusion on the Screw Extrusion Machine

In the screw extrusion machine, the screw is responsible for taking material from the feed section to the metering pump and die head. In the screw section, the material is not only pushed forward towards the metering pump but melting and compression of the polymer also take place. The metering zone regulates the quantity of the molten polymer delivered to the die head at the same time keeping it in molten form. In this way, the die head receives the material on a continuous basis and no air gaps are created in the molten polymer which can cause thin and thick places in the filament and thus breakage of filaments during extrusion. The die head of the machine consists of a number of components such as the breaker plate, filters, die with orifices etc. as described in section 2.11.2 (c). The temperature at the die head is kept high enough to maintain the polymer in its molten state. The rotational speed of the screw is normally adjusted in such a way that the polymer is melted up to the metering zone of the screw, and so that mixing can be carried out in that zone. The screw extrusion machine used in this study was a bench top Screw Extrusion Machine in which the screw also has a mixing head, which makes it more competent for the homogeneous mixing of thermochromic pigments with polymers. The speed of the metering pump depends on the feed of the molten polymer from the screw and, therefore, the ratio of the speed of the screw to the speed of the metering pump is normally adjusted in such a way that a continuous supply of the polymer at optimum pressure is maintained to the die head. As before, it was anticipated that the processing temperatures of the polymers should be as low as possible. The lowest possible temperatures cause the polymers to melt slowly

and so the speed of the machine is slower relatively than when high temperatures are used. A schematic diagram of the bench top extrusion machine is shown in Figure 4.47.

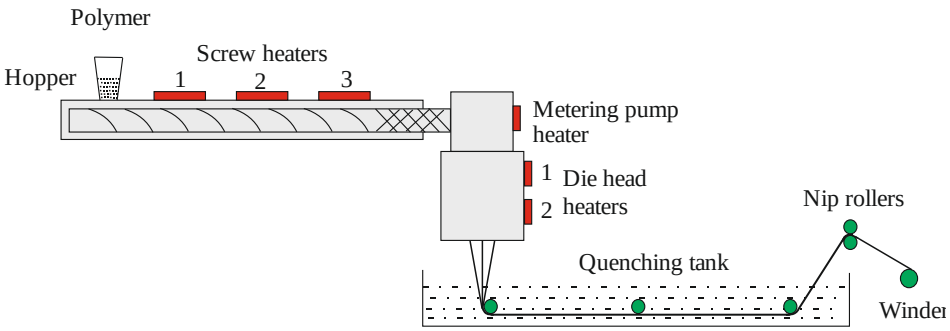

Figure 4.47 Schematic diagram of the bench top screw extrusion machine

The bench top Extrusion Machine has screw, metering and die head sections. Three temperatures zone with respect to the three screw zones; feed zone, compression zone, and metering zone, can be controlled independently. The temperatures of the feed zone were kept lower than the melting points of the polymers so that the solid polymer could resist backward movement pressure of the polymer and push the polymer forward towards the die head where the pressure is high due to the narrow die orifice. The temperatures in the compression and metering zones were kept high enough to ensure melting of the polymers. Trapped air was removed by the compression zone where polymers were compressed in molten form. The temperature of the metering zone was controlled individually and maintained high enough to keep polymers in molten form. The ratios between the speeds of the screw and the metering pump were different for the different polymers. The temperature at the die head was also maintained high enough to keep the polymers in molten state and to avoid solidification of the polymer. The breaker plate ensures smooth flow of the polymers and filters prevent blockage of die orifice or damage to the filament, due to impurities present. A single orifice die was used to extrude the polymers. The hot filaments were quenched in water at room temperature to solidify them and filaments were taken up on cones using a winder. The air gap between die and water, quenching length and take up speeds of different polymers were different. As the polymers had previously been extruded successfully on the ram extrusion machine, their processing temperatures provided a guide for processing temperatures on the screw extrusion machine. However, prototype filaments were produced on this machine on the basis of a further optimising process involving adjusting the conditions after a number of trials for each polymer. The optimum conditions used to produce the most successful prototype filaments of each polymer on

the basis of lowest number of breakages at the lowest temperatures are given Tables 4.5 and 4.6.

After establishing the extrusion parameters on the screw extrusion machine, the red and blue thermochromic pigments were incorporated into the polymers and filaments were extruded using the established conditions for each polymer. The sample size for the extrusion was 200g which was the lowest possible working sample size on this machine, established after trials. The concentrations of pigments were 0.5%, 1% and 2% on the weight of the polymer for each polymer.

Table 4.5 Temperatures in $^{\circ}$C at different zones of the screw extrusion machine

Polymer	**Screw Zones**			**Metering pump**	**Die Head**	
	Feed	**Compression**	**Mixer**		**1**	**2**
PP	190	221	231	231	242	236
LLDPE	141	140	152	151	162	150
EVA	111	126	131	131	131	132

Table 4.6 Optimized parameters on the screw extrusion machine

Polymer	Screw to pump speed ratio	Die orifice (mm)	Air gap b/w die and water (cm)	Quenching length (cm)	Take up speed (rpm)	Flow rate (g $10min^{-1}$)
PP	5 : 12.8	0.3	4.5	90	50	28.5
LLDPE	6 : 7.9	0.3	4.3	60	75	35.3
EVA	6 : 10.0	0.3	5.8	64	32	37.5

4.2.3 Drawing of Extruded Filaments

Drawing of filaments of polypropylene, linear low density polyethylene and EVA was carried out on cold and hot drawing machines. The drawing of filaments is normally carried out to strengthen and increase the fineness of filaments by straightening polymer chains and reducing the number of amorphous regions as discussed in section 2.12. The trials on the cold drawing machine which has no mechanism to heat the filament, were not successful because breakages of filaments were high in numbers. The drawing is carried out at room temperature and the filament sample size is small. In cold drawing, the filaments are stretched and the polymer chains resist stretching and thus, breakages during drawing tend to increase.

After unsuccessful trials on the cold drawing machine, drawing was carried out using a hot drawing machine. A schematic diagram of the hot drawing machine is shown in Figure 4.48. The hot draw frame consists of four hot rollers, three hot plates, a guide roller and a winder. Each roller has a diameter of 160mm with a freely rotating separator of 35mm diameter which is used to separate the wraps of filaments. Each hot plate has a length of 495mm and width of 30mm. The speed and temperature of rollers were different for each polymer. The filaments were carried through the guide roller to roller 1, where filaments were wrapped around the roller and the separator five times to avoid slippage. These filaments were then taken through hot plate 1 to roller 2 where the same procedure as roller 1 was repeated. The filaments were taken up in the same way through the rest of the rollers and hot plates. The drawn filaments were then taken up on cone packages using a winder. The hot drawing machine was run slowly initially and the speed was then increased gradually to that required.

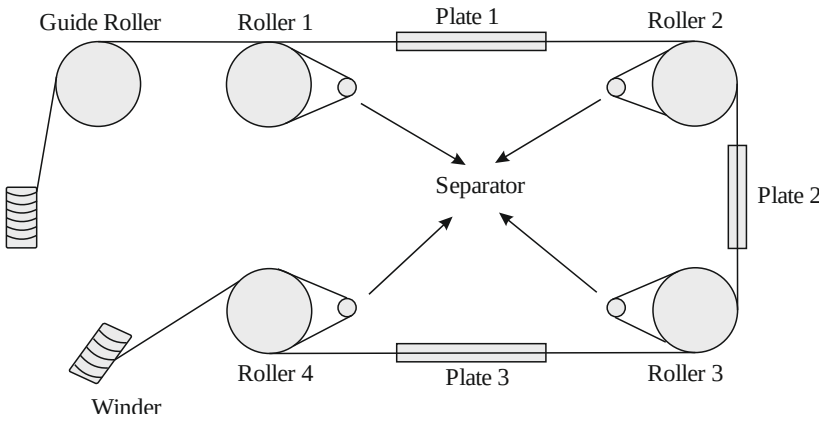

Figure 4.48 Schematic diagram of hot drawing machine

Hot drawing of the polymers was successful after a number of trials to establish the optimum speeds and temperatures of the rollers. For polypropylene, the speeds of rollers 1-4 were 60m min^{-1}, 120m min^{-1}, 180m min^{-1} and 180m min^{-1}, respectively. The temperatures of rollers 1 and 2 were 60°C and 120°C respectively while rollers 3 and 4 were kept at room temperature. For linear low density polyethylene, the speeds of rollers 1-4 were 60m min^{-1}, 130m min^{-1}, 200m min^{-1} and 200m min^{-1}, respectively. The temperatures of rollers 1 and 2 were 40°C and 70°C respectively while rollers 3 and 4 were kept at room temperature. For EVA, the speeds of rollers 1-4 were 60m min^{-1}, 150m min^{-1}, 210m min^{-1} and 210m min^{-1}, respectively. The temperatures of rollers 1 and 2 were 30°C and 50°C respectively while rollers 3 and 4 were kept at room temperature. In all three cases, the hot plates were not heated as the required softening temperature was maintained by the hot rollers.

4.2.4 Properties of Extruded Samples

The prototype filaments were subjected to a number of tests to evaluate their properties.

(a) Thermochromism of Extruded Filaments

The three polymers were extruded with incorporation of blue and red thermochromic pigment powder, incorporated at 0.5%, 1% and 2% concentrations. The colours of the filaments were observed immediately after cooling of the filaments. However, in order to observe whether there was an effect of the extrusion process on the thermochromism phenomena, the extruded filaments were heated with a hair dryer and cooled a number of times. The colour change was observed consistently in the filaments in response to heating and cooling. The thermochromism of pigmented filaments with 2% colour concentration for all three polymers is shown in Figures 4.49-4.50.

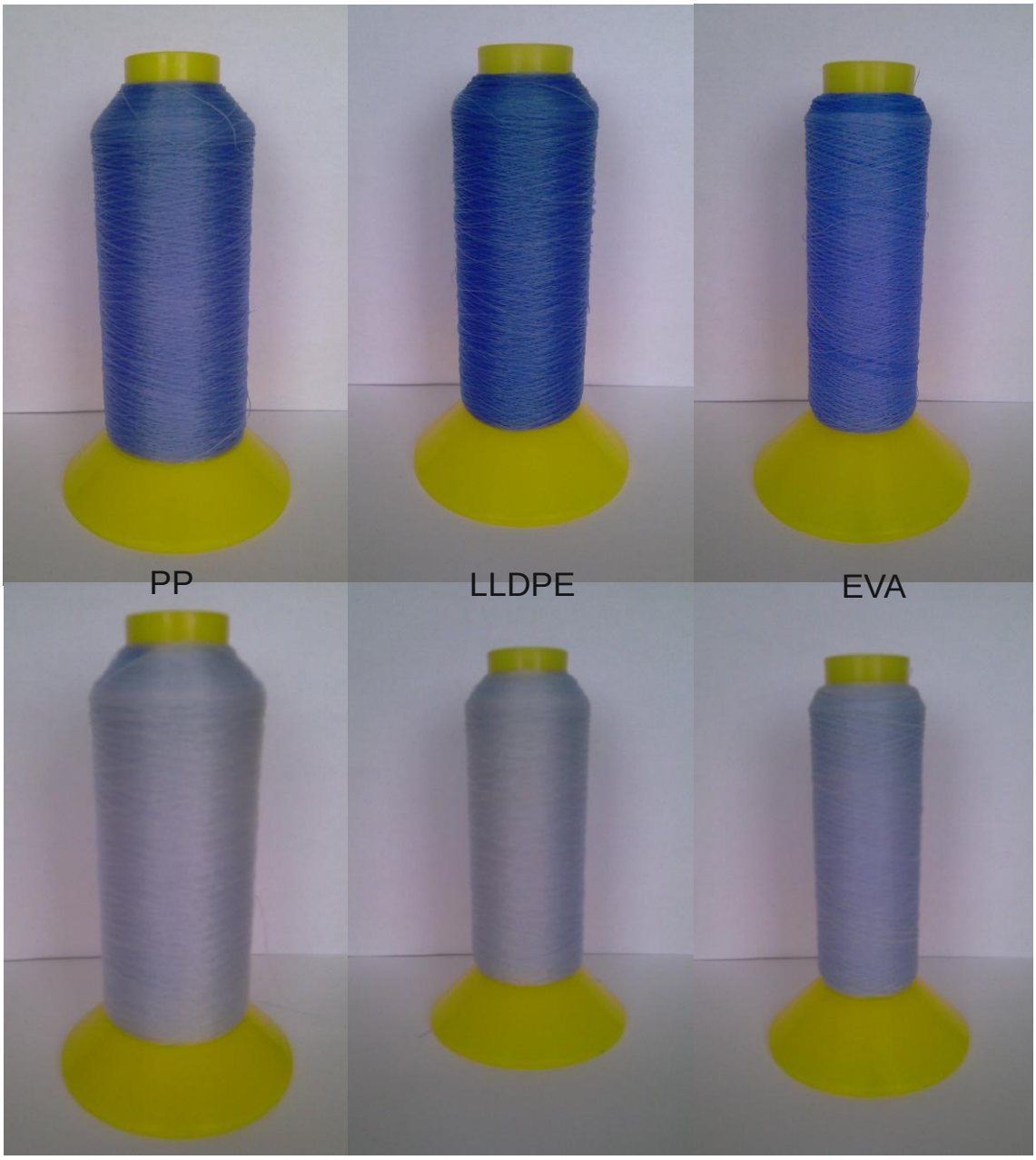

Figure 4.49 Thermochromism of polymers containing the blue pigment

Figure 4.50 Thermochromism of polymers containing the red pigment

(b) Scanning Electron Microscopy

Scanning electron microscopy (SEM) was used to visualise the filaments and thermochromic pigment powders. The SEM investigation of filaments used longitudinal views to examine the surface structure of the drawn filaments, while the SEM of thermochromic powders and cross section of filaments was carried out to examine the nature of the microcapsules in powder form and also their distribution within the filaments. The white, blue and red filaments were used from all three polymers i.e., PP, LLDPE and EVA. The blue and red thermochromic filaments, selected for this study, have 2% concentrations.

For the longitudinal views, three samples from each drawn filament of PP, LLDPE and EVA, both with and without thermochromic pigment were cut by scissors and mounted on stubs. For the cross sectional view of the thermochromic pigments incorporated into filaments, a sharp razor blade was used. The cross sections obtained using this technique showed a small shear effect at one end which was visible only in SEM examination, but it did not appear to have a serious effect in assessing the distribution of the microcapsules within the filaments. For the SEM examination of the thermochromic pigments, the powder container was shaken gently to produce a fine dust of pigment in the air and the stub was passed through it. The dust on the stub was not visible to the naked eye but it gave good results using SEM. All of the stubs with samples were sputter coated with gold before SEM examination using a Polaron SC7620 Sputter Coater. Sputter coating of samples gave good images using the SEM by providing a protective layer against the high voltage used in the SEM.

Scanning electron microscopy was carried out using the Hitachi S-4300 Field Emission instrument. Details of the operating procedure have been given in section 3.17.3. The images were captured at different magnifications according to the nature of the samples. For example, in the case of longitudinal view, the samples were magnified up to 250 times. The voltage of the SEM was kept low to take outer surface images and to avoid beam damage to the sample. After clear focus was obtained for each sample, the images were captured. A number of images were taken for different samples from which only representative images were selected as shown in Figures 4.51-4.56.

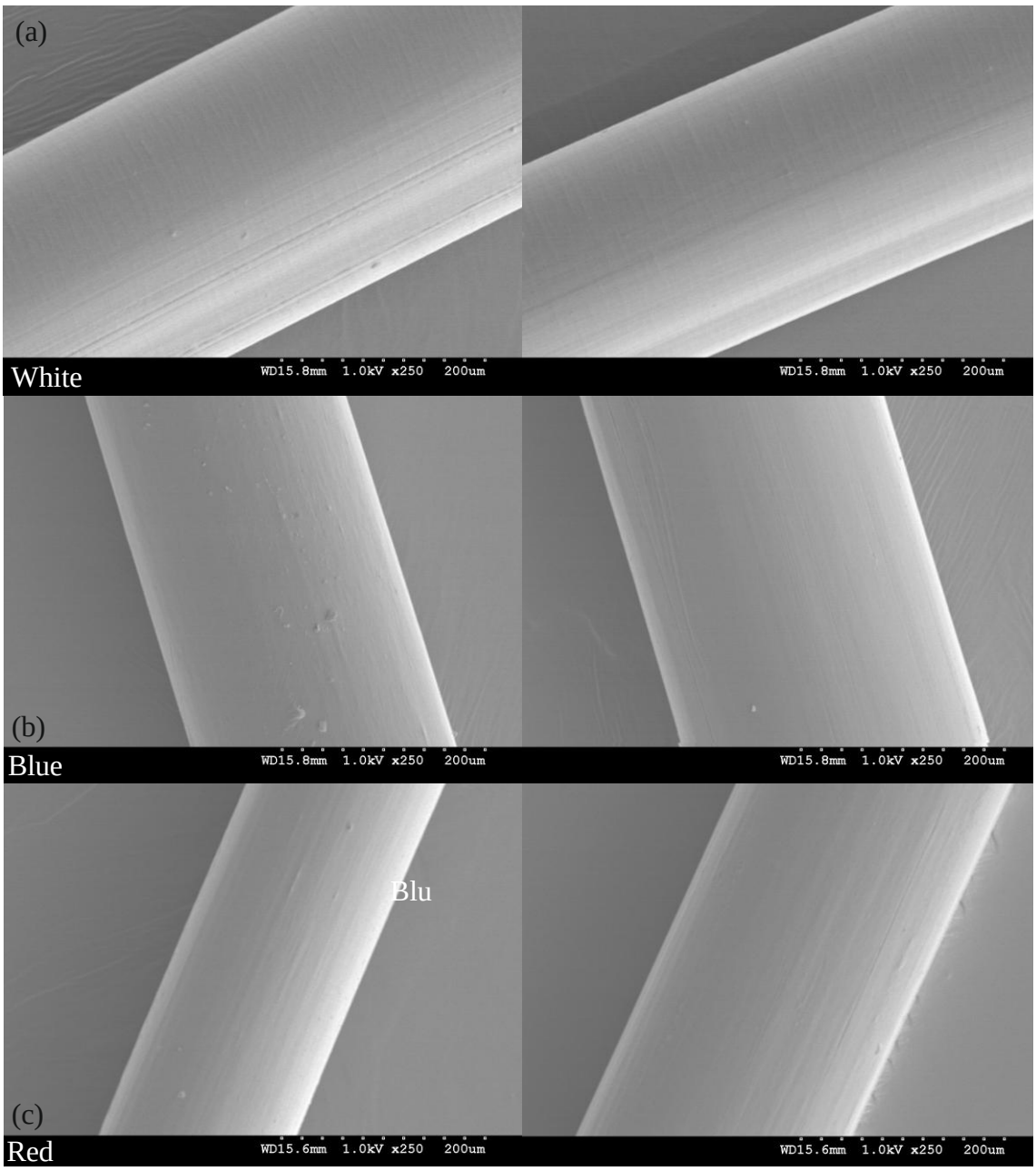

Figure 4.51 Polypropylene filaments: (a) unpigmented; (b) containing 2% blue pigment; (c) containing 2% red pigment

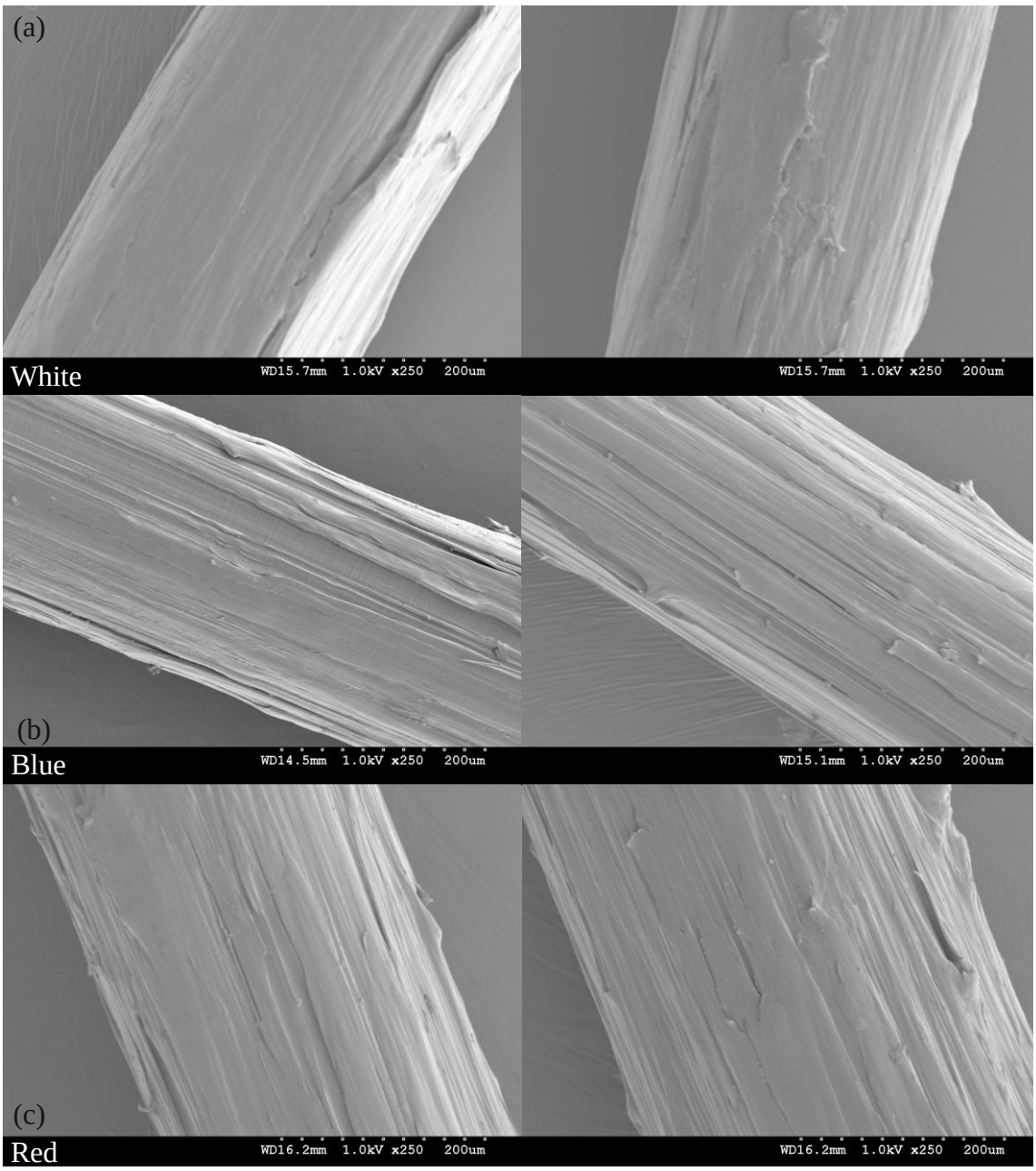

Figure 4.52 Linear low density polyethylene filaments: (a) unpigmented; (b) containing 2% blue pigment; (c) containing 2% red pigment

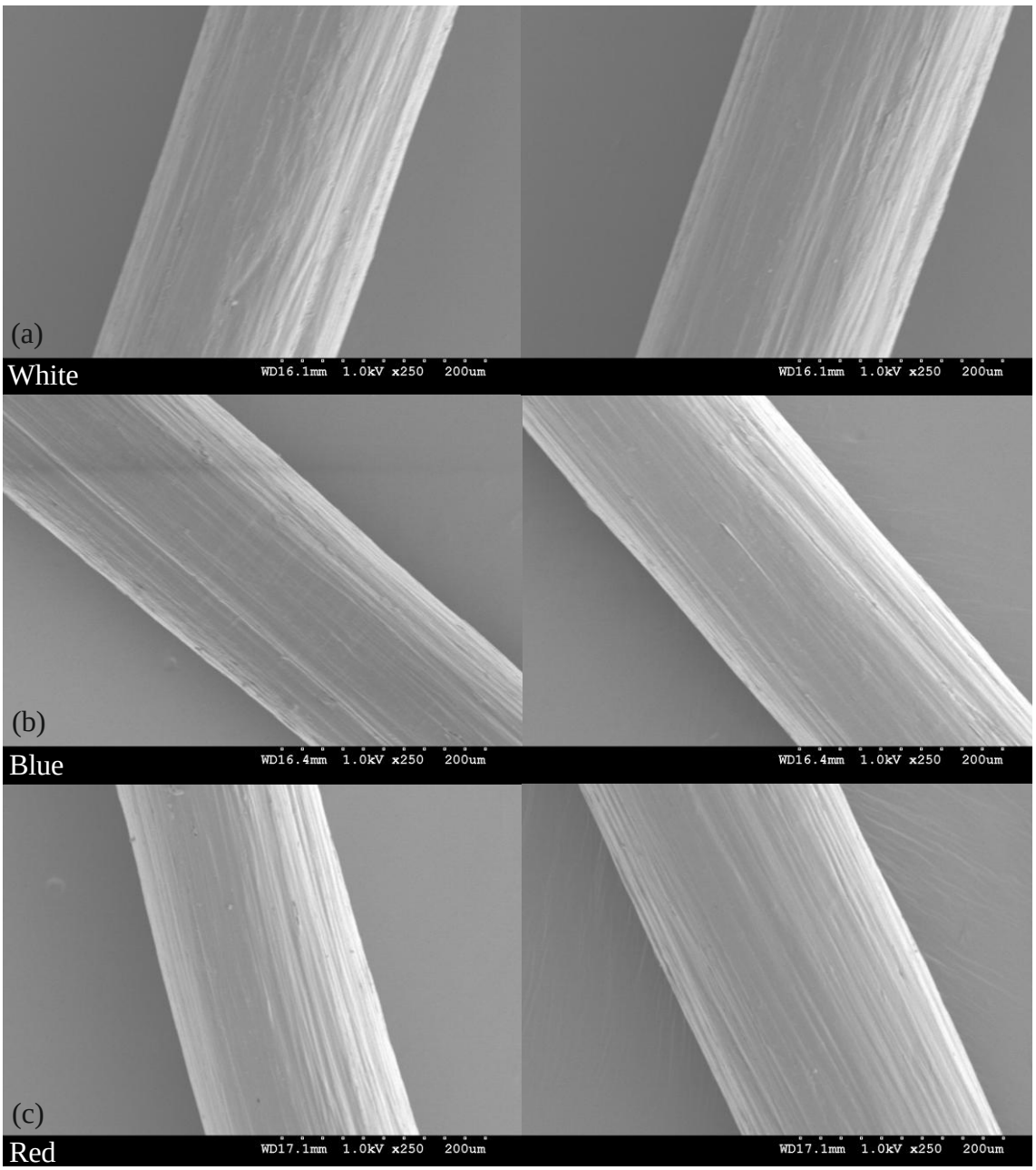

Figure 4.53 Copolymer of ethylene with vinyl acetate filaments: (a) unpigmented; (b) containing 2% blue pigment; (c) containing 2% red pigment

In Figure 4.51, the longitudinal views of unpigmented, blue and red polypropylene filaments are shown. The outer surface of PP filaments appears quite smooth. The blue and red thermochromic pigments do not appear to cause significant changes to the outer surface because the pigmented filaments are similar to the unpigmented filaments. Figure 4.52 shows the longitudinal view of unpigmented, blue and red linear low density polyethylene filaments. The outer surface of the white, blue and red filaments is uneven and striated although this is not visible to the naked eye. This surface structure may be formed during the drawing of the filaments. Again, there is no significant indication of thermochromic pigment on the outer surface. In Figure 4.53, the

longitudinal views of unpigmented, blue and red EVA filaments are shown. The outer surface of the filaments shows a little unevenness but there is no indication of striations. It also appears that the thermochromic pigment is not on the surface of the filament in the cases of both blue and red pigments. The smooth surface of PP filaments and a slightly uneven surface of EVA filaments are indicative of smooth slippage of polymer chains during the drawing process. However, in the case of LLDPE, the striated surface may indicate the resistance of polymer chains during the drawing process, causing surface roughness. As there is no indication of thermochromic capsules on the surface of the filaments in all polymers, it is a reasonable conclusion that the thermochromic pigment is essentially all inside the filament. This is positive feature as there is little chance of release of pigment from the filament unless damaged and the pigment is likely to have become an integral part of the filament for its lifetime. Hence, it is anticipated that fastness properties, such as wash and rub fastness may be better than that of printed samples where the pigment is in a binder on the surface.

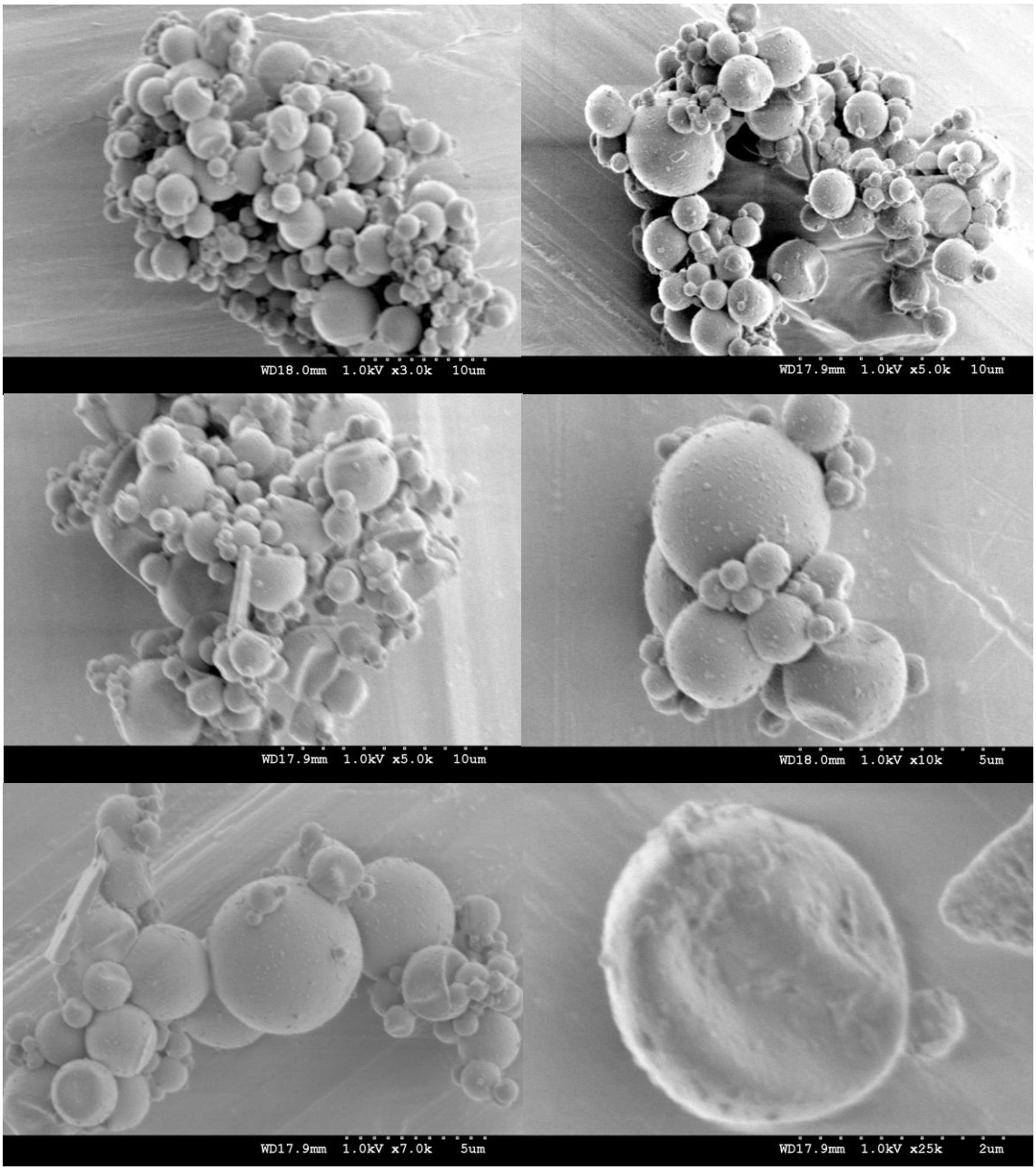

Figure 4.54 Blue thermochromic pigment microcapsules in powder form at magnifications 3K, 5K, 7K, 10K and 25K, as indicated in the individual photomicrographs

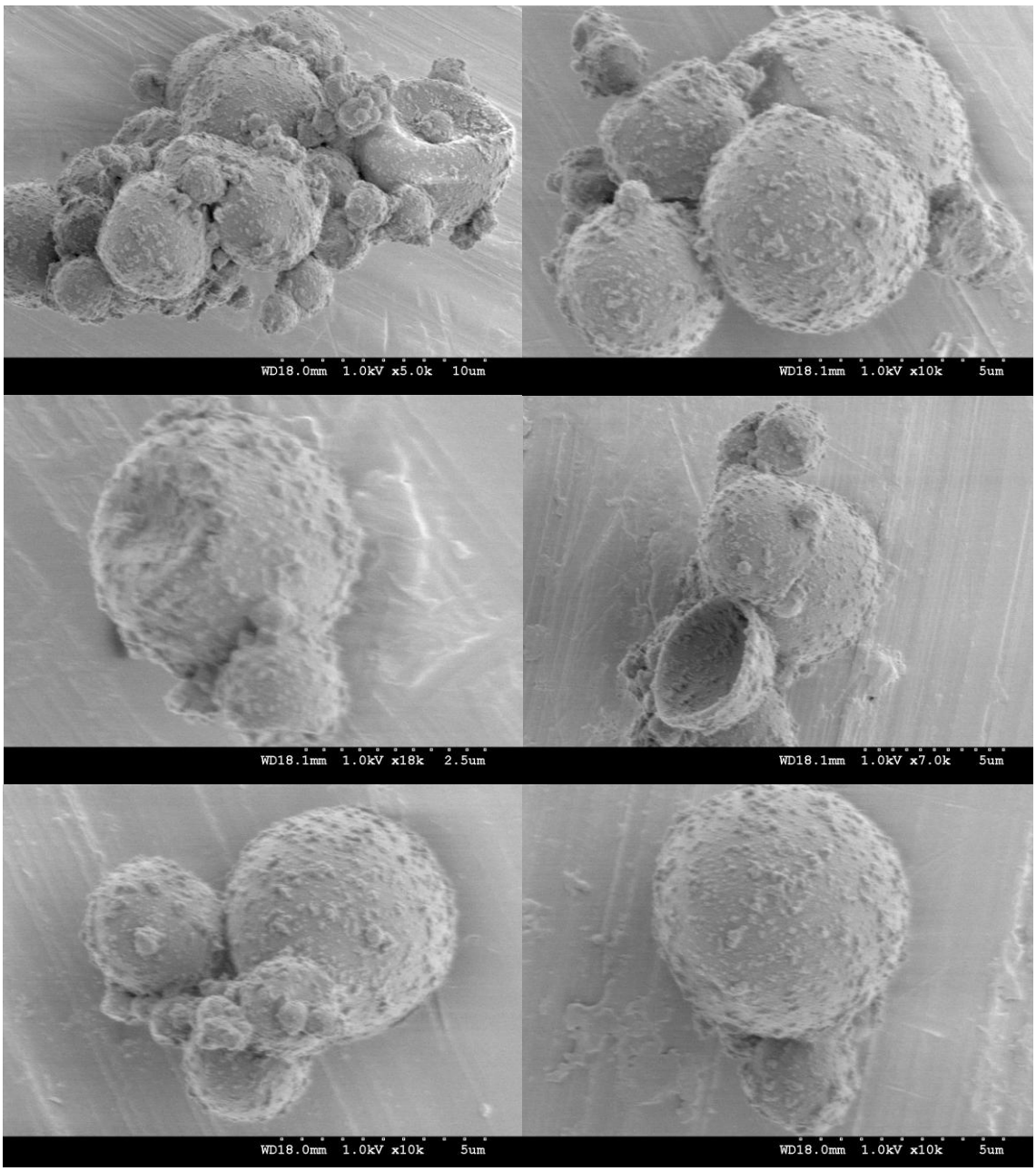

Figure 4.55 Red thermochromic pigment microcapsules in powder form at magnifications 5K, 7K, 10K and 18K, as indicated in the individual photomicrographs

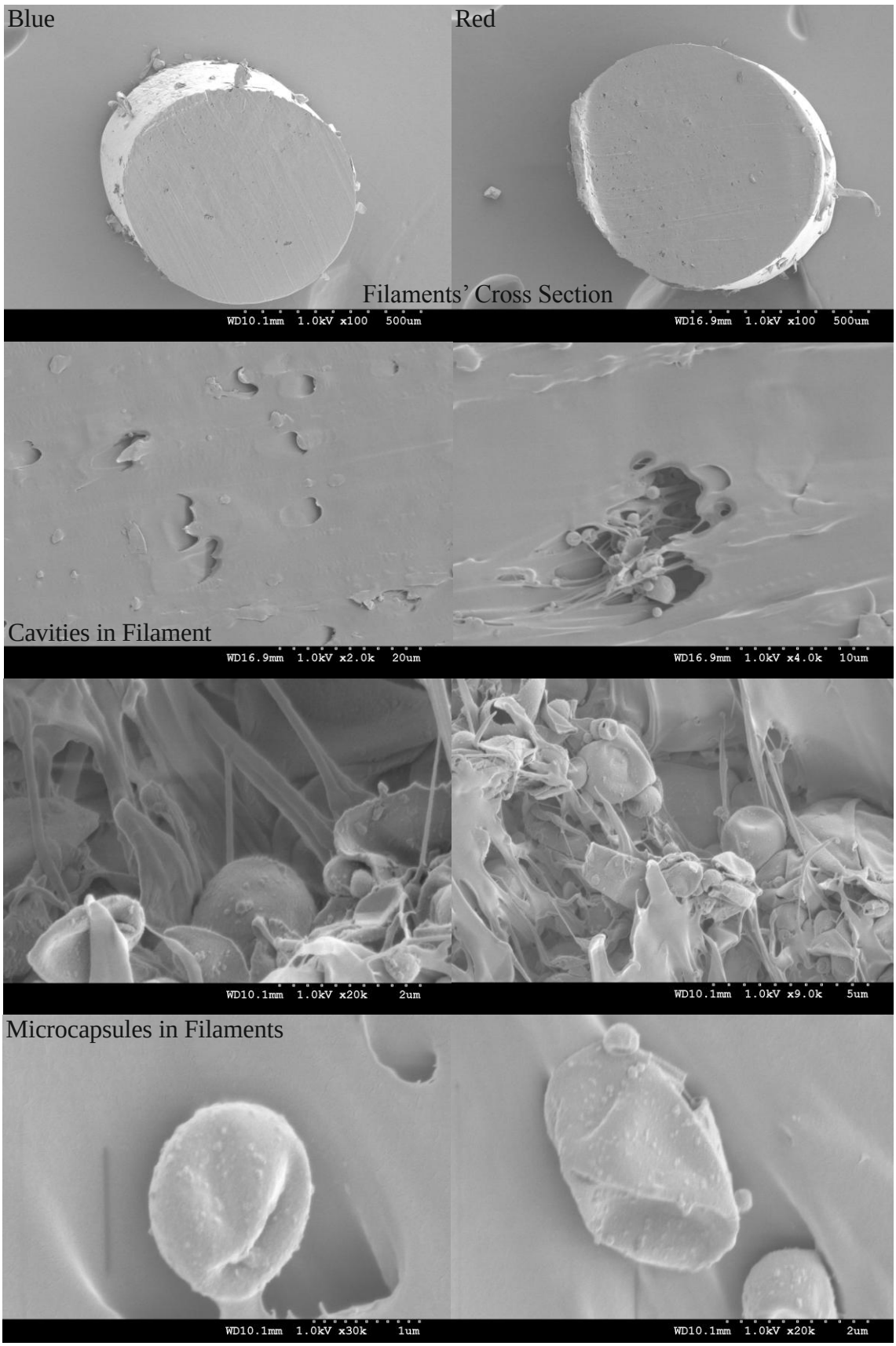

Figure 4.56 Thermochromic pigment microcapsules in cross sections of filaments at magnifications 100, 2K, 4K, 9K, 20K and 30K, as indicated in the individual photomicrographs

Figures 4.54 and 4.55 show microcapsules of the blue and red thermochromic pigments. It is clear that the microcapsules are present as aggregates, sticking to each other. Some of them are not perfectly round and appear as if they have a pinched surface. The blue thermochromic microcapsules are more clean and smooth on the surface than the red microcapsules. The microcapsules show variation in sizes approximately from 1μm to 5μm. The cross sectional views which attempt to illustrate the distribution of microcapsules of the pigments in the filaments, are shown in Figure 4.56. The cross sections of filaments show some small cavities. Some microcapsules appear to lie in these cavities in the form of aggregates. Some of the microcapsules show the pinched surfaces observed in the pigment samples. The microcapsules are aggregated in their powder form, most probably arising during their manufacture and mostly are spherical. Comparing microcapsules in the powder form and after incorporation into the filaments, it appears that during extrusion, these microcapsules probably survived with no obvious damage has been done to them although this cannot be concluded with certainty. Their dispersion into the polymers is not to individual microcapsule level, but the aggregates are small and do not appear to affect overall visual homogeneity in the filaments. The blue thermochromic filaments show higher colour strength assessed visually than the red filaments as discussed in section 4.2.4 (c). One factor may be the cleaner and smoother surface of the blue thermochromic microcapsules compared with the red microcapsules which ensures higher transparency, but there will be other factors.

(c) Colour Strength

The blue and red thermochromic pigments were extruded into filaments at 0.5%, 1% and 2% concentrations in the polymers processed at relatively high temperatures. As thermochromic pigments are sensitive towards heat, some colour loss might be expected. It has already been established (section 4.1.2) that these pigments in printed form lose some colour strength at a high temperature. It was also considered a possibility that the microcapsules of thermochromic pigments might rupture during extrusion and that this would adversely affect colour. Nevertheless, the filaments of polymers, with thermochromic capsules incorporated were successfully extruded giving colours with thermochromic properties and there is no obvious sign of ruptured microcapsules as discussed in sections 4.2.4 (a) and (b). Therefore, an investigation was carried out to study the colour strength of these filaments. For colour measurement, the filaments were wrapped around white paper card to make strips and the samples

were measured by the spectrophotometer with the calibration conditions as discussed in section 4.1.1. The integ values were plotted in graphs.

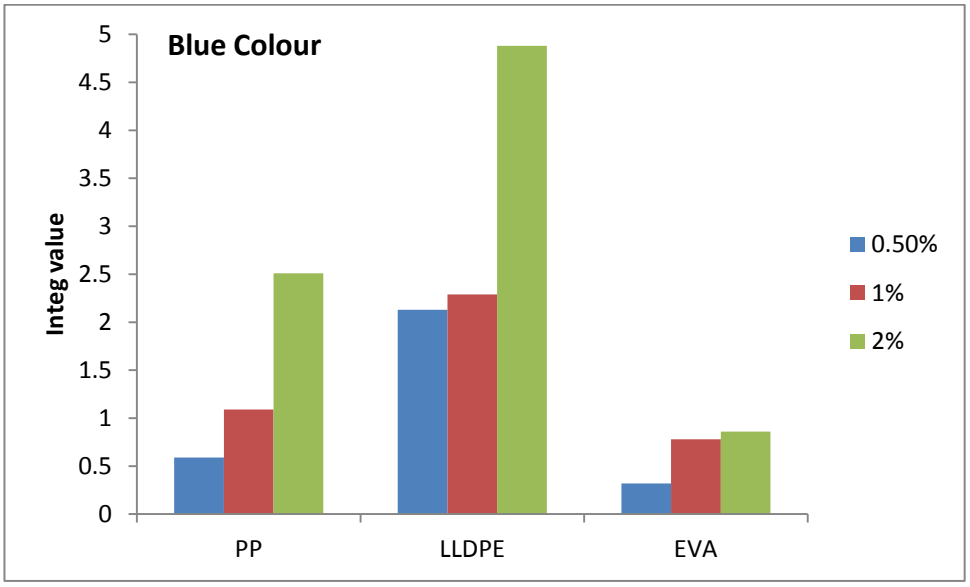

Figure 4.57 Comparative colour strength of blue thermochromic filaments

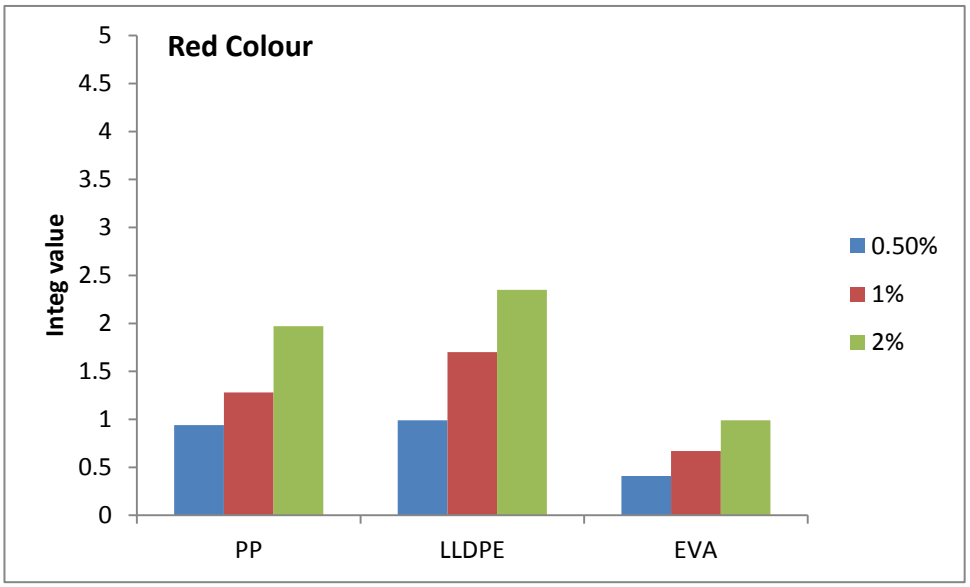

Figure 4.58 Comparative colour strength of red thermochromic filaments

The integ values for the blue pigment in PP, LLDPE and EVA filaments are shown in Figure 4.57. The integ values shown by LLDPE are higher than those given by the pigment in PP and EVA. It was anticipated that higher colour strength might be given by the polymer processed at the lowest temperature, which is EVA, and the lowest colour strength would be from the polymer with the highest processing temperature, which in this case is PP, on the basis of thermal instability of the pigments. However, EVA gives the lowest colour strength. Another factor may be the optical properties of

polymers, which may be glossy, opaque, translucent or transparent. It was observed that the filaments of EVA and PP are relatively translucent while LLDPE is opaque. EVA is also a glossy material and may reflect a major portion of incident light before allowing it to approach the thermochromic pigment, inside the filaments [95,118]. Therefore, the low colour strength shown by the EVA may be lowered by its gloss property. However, in the case of PP, there may be a loss of colour strength due to the high processing temperature. Another important factor may be the efficiency of the dispersion of the pigment, which will influence the colour strength and may vary with the polymer.

The integ values given by the red thermochromic filaments are shown in Figure 4.58. The integ values for the red colour are lower than those of the blue colour which may be due to weaker intensity of the dye molecule. However, in section 4.2.4 (b), SEM images show that the red thermochromic capsules are covered with some dusty material while blue thermochromic capsules have a relatively clean surface. Therefore, the dusty surface properties of the red thermochromic microcapsules may also affect the colour value of the pigment. In the case of red thermochromics, again EVA shows the lowest integ values but PP filaments gives colour strength values closer to that of LLDPE. However, the LLDPE also gives the highest colour strength in red. More experiments may be conducted to verify the effectiveness of these results or to investigate any anomalies.

(d) Wash and Rub Fastness

The extruded filaments of all polymers with 2% blue and red pigment, were subjected to washing according to 'ISO 105, part C10: colour fastness to washing with soap or soap and soda, method A(1)' as for the printed samples described in section 4.1.3. The test specimens were prepared by making a lee of 100mm × 40mm and attaching this to the SDC multifibre fabric with the same dimensions by means of staple pins. Dry and wet rubbing tests were also performed on filament samples in the form of lee as in section 4.1.3. The colour of filament samples were measured as discussed in section 4.1.1, with integ values plotted as shown in Figures 4.59-4.60.

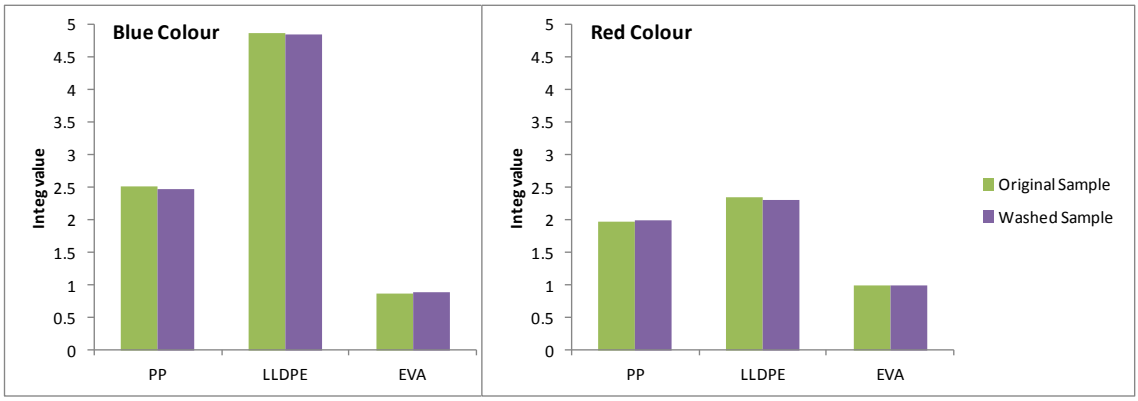

Figure 4.59 Comparison of integ values of extruded filament with 2% colour concentration before and after washing

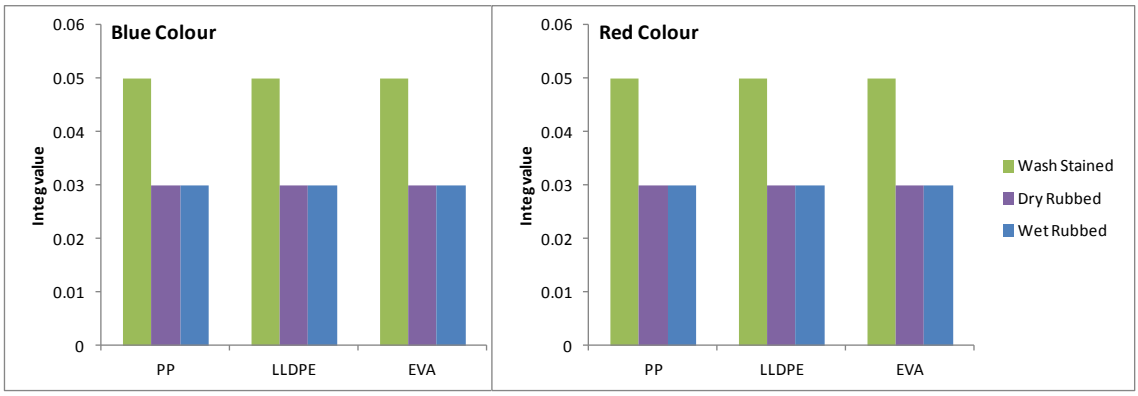

Figure 4.60 Integ values of stained cloth obtained during washing, and dry and wet rubbing

Figure 4.59 shows that the integ values of blue and red pigmented filaments of PP, LLDPE and EVA, show no difference in integ values before and after washing. This indicates that the thermochromic pigments have become contained in the filaments as anticipated in section 4.2.4 (b). Figure 4.60 shows the most stained part of multifibre fabric used for washing and on white cloth used for dry and wet rubbing. The integ values for stained cloth from dry and wet rubbing show very small values for all filaments, the same as the integ value of white cloth used for rubbing so there is no colour stripped during rub fastness. The rub fastness of extruded and printed samples is similar (section 4.1.3), however, the wash fastness of extruded samples is excellent and better than thermochromic prints.

(e) Lightfastness

The lightfastness of leuco dye based thermochromic pigments in printed samples has been discussed in section 4.1.5. To investigate the lightfastness in extruded thermochromic filaments, the filaments at all concentrations and in each polymer were wrapped around a white paper card along with printed sample of blue pigment. These

samples were, as before, exposed on the Heraeus Xenotest 150S fadeometer for 1, 2, 3, 4, 6, 8, 12, and 24 hours and evaluated using colour measurement.

Figures 4.61-4.63 show the lightfastness of blue thermochromic filaments at different concentrations together with the printed blue thermochromic sample. All of the thermochromic polymers show a decrease in colour strength with exposure time. The integ values of LLDPE show a larger decrease with exposure time than PP and EVA which indicates better lightfastness of the pigment in PP and EVA than in LLDPE. There is some abnormal variation in integ values with exposure which may be within the limits of experimental error. The lightfastness trends of all three polymers are similar with no significant effect of concentration. In Figure 4.63, the lightfastness of thermochromic filaments are compared with the lightfastness of the printed sample. The 5% concentration in the printed sample shows comparable colour strength to that of thermochromic filaments with 2% concentrations, so this concentration of blue print was selected for comparison of lightfastness. The printed sample shows higher colour loss with exposure time than the thermochromic filaments of all polymers. Thus, the thermochromic filaments have better lightfastness than the printed sample. The lightfastness of red thermochromic filaments is shown in Figures 4.64-4.66. At 0.5% concentrations, the LLDPE and PP give similar initial colour strength. The pigmented LLDPE shows more rapid colour loss with exposure than PP. At 1% and 2% concentrations, although the initial colour strengths in PP and EVA are less than in LLDPE, they show reduced colour loss than in LLDPE. From this discussion, it can be concluded that the polymers play a role in determining the lightfastness of leuco dye based thermochromic pigments. The lightfastness shown by the pigments incorporated into PP and EVA are better than in LLDPE. These polymers are thus providing some protection for the pigments which may be due to UV absorption properties. It can also be concluded that the thermochromic filaments have better lightfastness than printed samples. This may be due to presence of thermochromic microcapsules embedded inside the polymer compared with location within a binder on the surface as in the case of printed samples, and possibly some improved protection of the thermochromic pigments from UV light absorption.

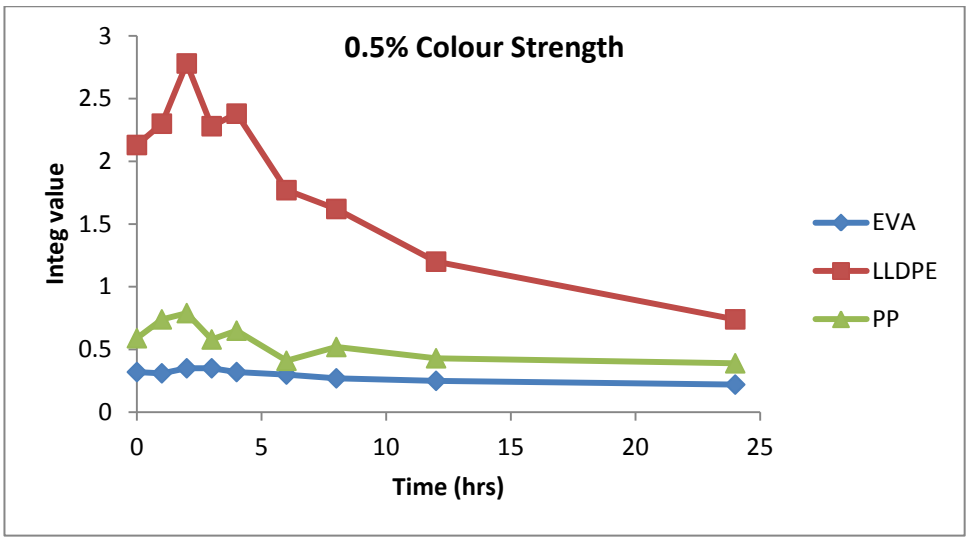

Figure 4.61 Lightfastness of extruded 0.5% blue filaments

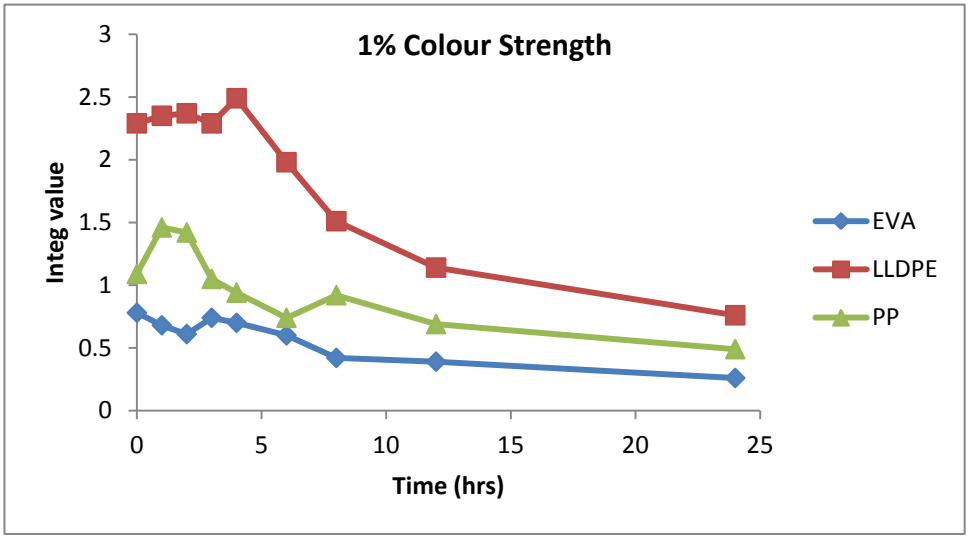

Figure 4.62 Lightfastness of extruded 1% blue filaments

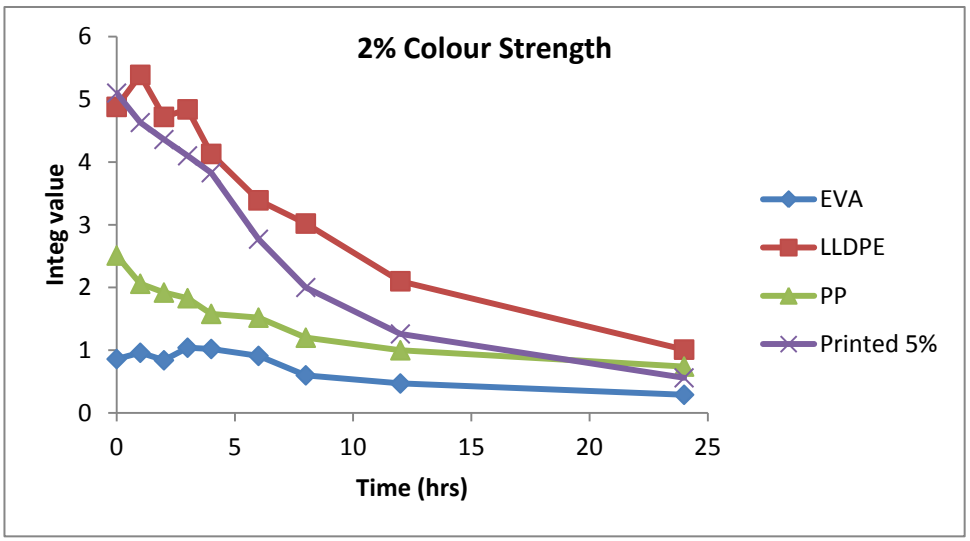

Figure 4.63 Lightfastness of extruded 2% blue filaments and printed sample

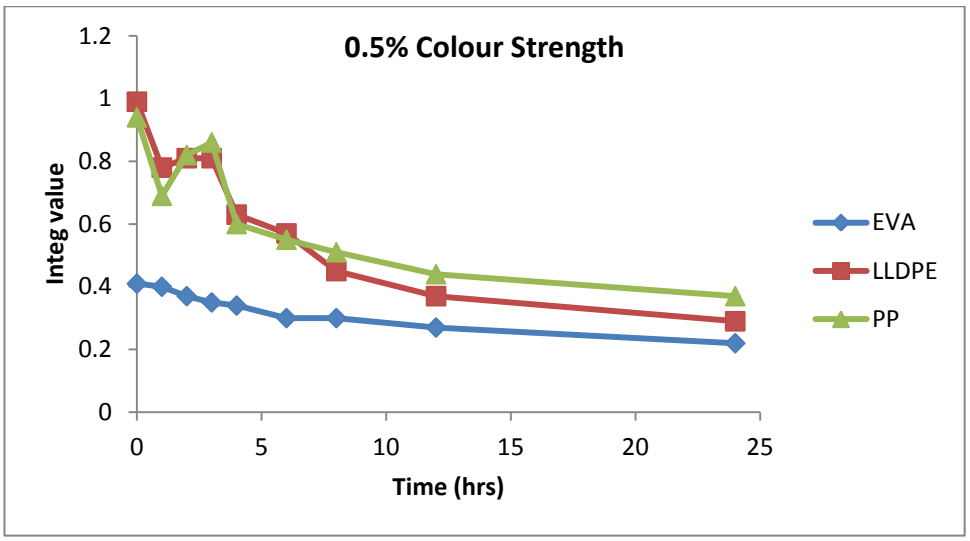

Figure 4.64 Lightfastness of extruded 0.5% red filaments

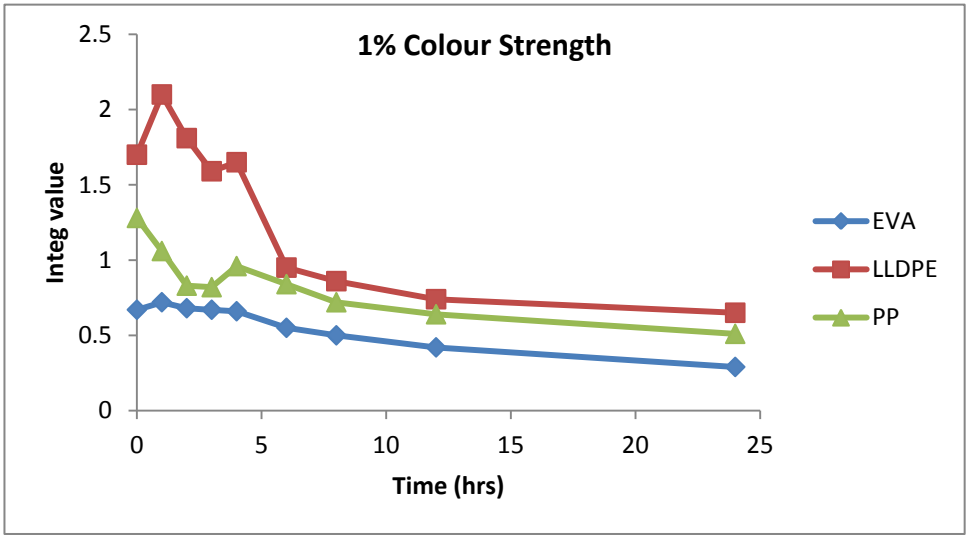

Figure 4.65 Lightfastness of extruded 1% red filaments

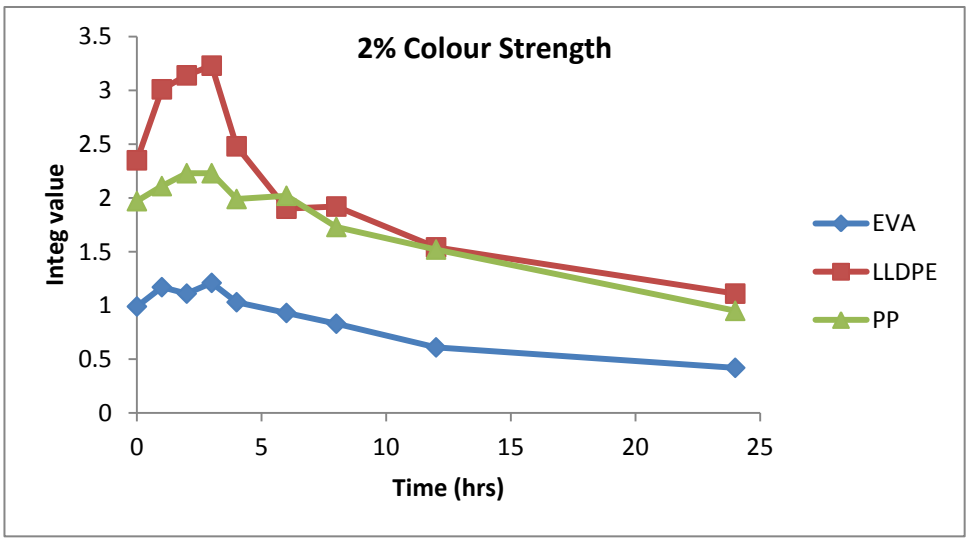

Figure 4.66 Lightfastness of extruded 2% red filaments

(f) Differential Scanning Colorimetry (DSC)

Differential scanning colorimetry (DSC) was carried out on filaments of all three polymers both with and without thermochromic pigments at 2% concentration. The DSC investigation was carried out both in nitrogen and air environments. In the nitrogen environment, the samples cannot undergo oxidation and more consistent curves can be obtained. In air, there is a possibility of oxidation of samples during heating and the level of oxygen in the pan may vary, causing inconsistent curves. However, it is closer to the actual process of extrusion in air as carried out in this study.

Table 4.7 DSC results for unpigmented and pigmented polymers in $^{\circ}$C

	Melting point		Degradation onset		Degradation on peak	
	Nitrogen	Air	Nitrogen	Air	Nitrogen	Air
PP White	164.0	162.6	207.1	203.6	283.3	235.6
PP Blue	163.4	167.5	233.9	213.8	292.5	251.9
PP Red	164.7	165.8	241.7	218.6	311.1	254.3
LLDPE White	125.3	124.7	211.2	210.1	229.0	225.9
LLDPE Blue	124.6	125.6	232.5	231.0	244.4	240.4
LLDPE Red	125.7	125.1	245.6	235.5	251.8	242.9
EVA White	82.8	85.8	199.0	203.8	229.4	233.1
EVA Blue	84.5	84.1	218.0	209.8	237.6	248.7
EVA Red	84.5	85.8	231.8	222.6	245.9	243.1

Figures 4.67-4.72 show the DSC traces of PP, LLDPE and EVA (unpigmented and pigmented) filaments in nitrogen and air environments. The melting points, degradation onsets and degradation peaks are given in Table 4.7. The melting temperatures of PP, LLDPE and EVA are similar in nitrogen and air environments with only minor variations; however, EVA unpigmented shows a slightly higher melting temperature in an air environment than in a nitrogen environment. In both environments, the melting temperatures of unpigmented and pigmented filaments are similar.

The degradation onset temperatures of pigmented PP, LLDPE and EVA are higher than of their corresponding unpigmented filaments in a nitrogen environment. In an air environment, these temperatures show a similar trend for pigmented filaments with the values generally lower than a nitrogen environment except in the case of LLDPE unpigmented and blue, and EVA unpigmented, where these values are similar. The degradation peaks for all polymers also show the same trend, with increased values for pigmented filaments than unpigmented filaments in both environments. The degradation peaks are significantly lower for PP and LLDPE in air than in nitrogen. However, for EVA unpigmented and blue, these are higher in air, and for EVA red, it is similar in both environments.

Thus, incorporation of the thermochromic pigments increases the degradation onset and degradation peak temperatures of polymers but has almost no effect on melting temperatures. The inhibition of degradation may be due to the high degradation temperature of the polymer used in wall construction of microcapsules which in this case is mostly cross-linked melamine formaldehyde, as reported by LCR Hallcrest. It is also noted that the red filaments give higher degradation onset and degradation temperatures than blue filaments. The reason for this is not obvious, but it was noted that the red microcapsules have a more ‘dusty’ surface as discussed in section 4.2.4 (b) than blue microcapsules and that material may increase the temperature required for degradation. Generally, the filaments are thermally more stable in a nitrogen environment than in an air environment as expected, except in the case of EVA, where the opposite is observed.

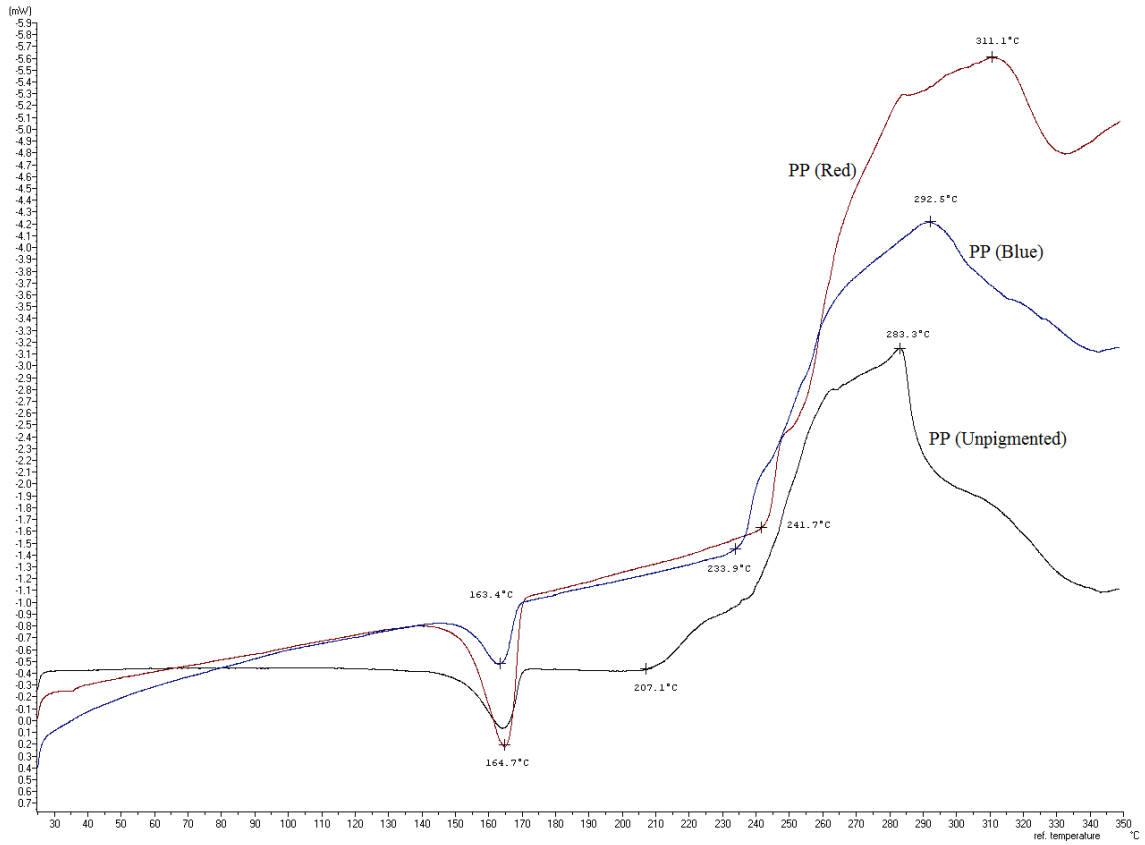

Figure 4.67 DSC of polypropylene with and without thermochromics in nitrogen environment

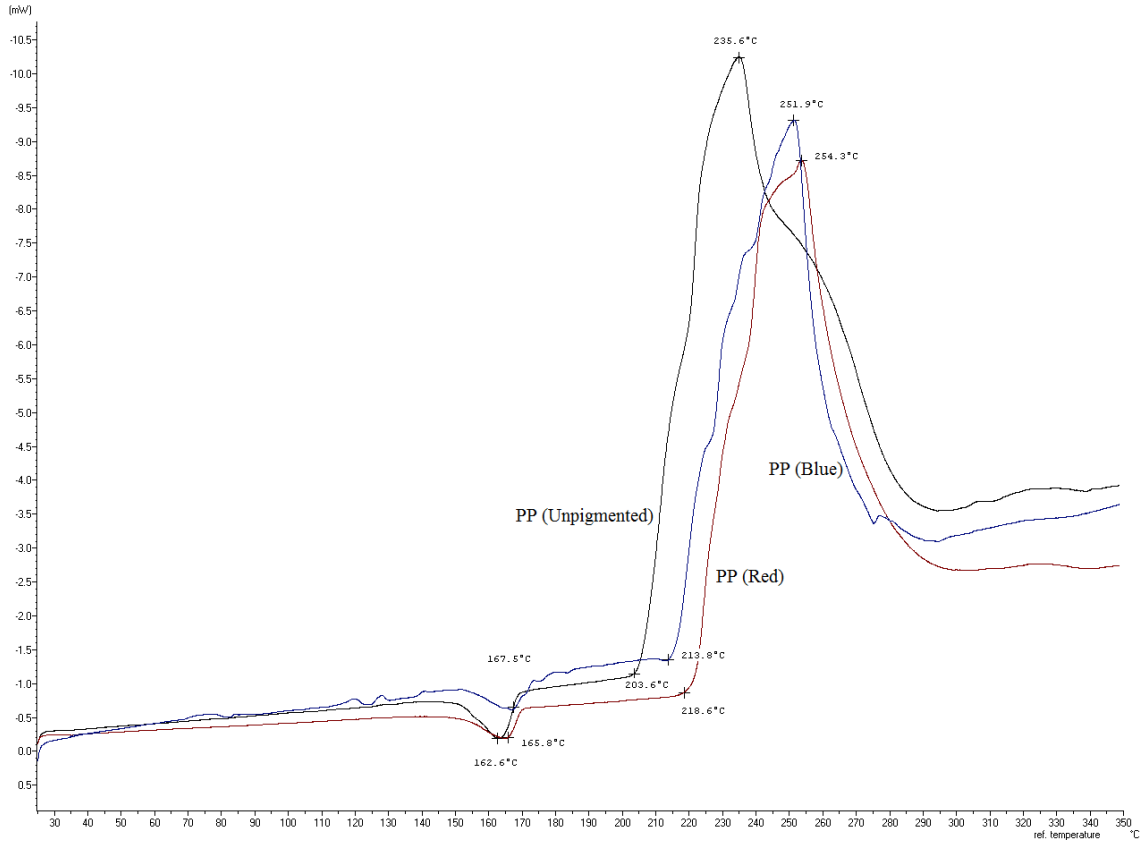

Figure 4.68 DSC of polypropylene with and without thermochromics in an air environment

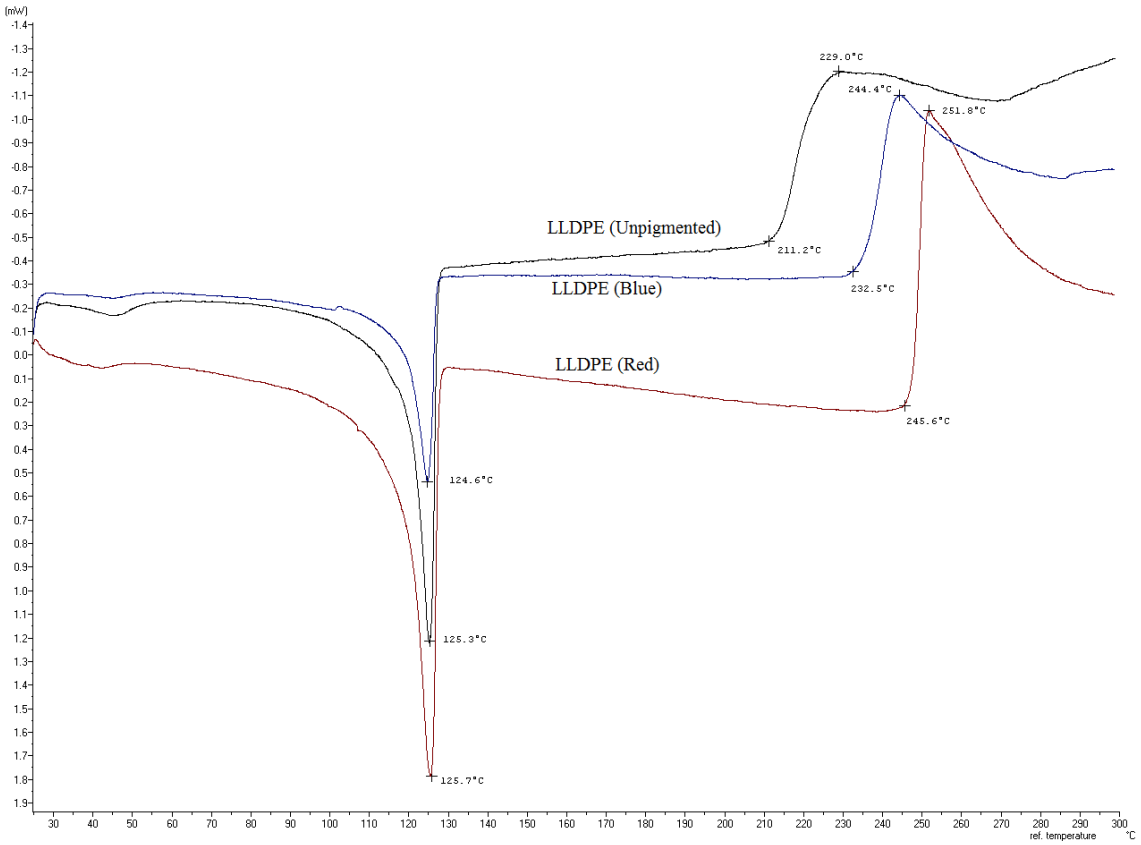

Figure 4.69 DSC of LLDPE with and without thermochromics in nitrogen environment

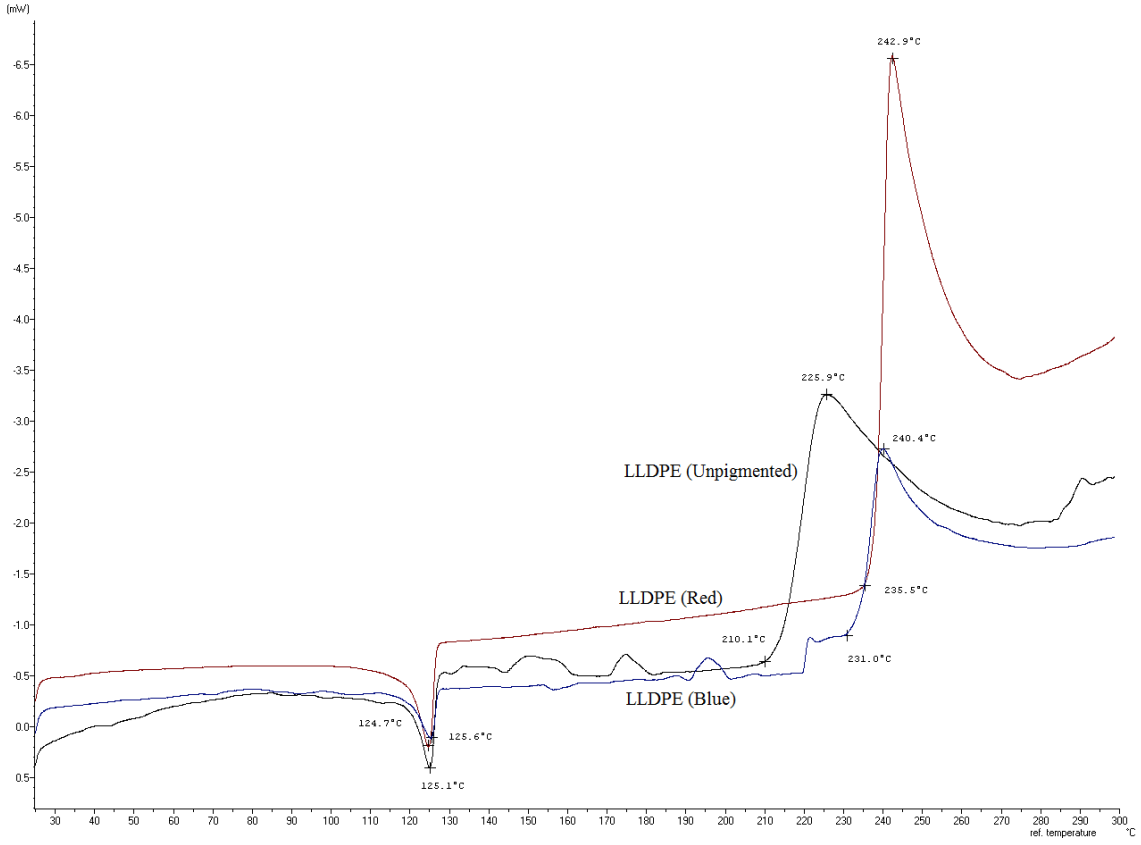

Figure 4.70 DSC of LLDPE with and without thermochromics in an air environment

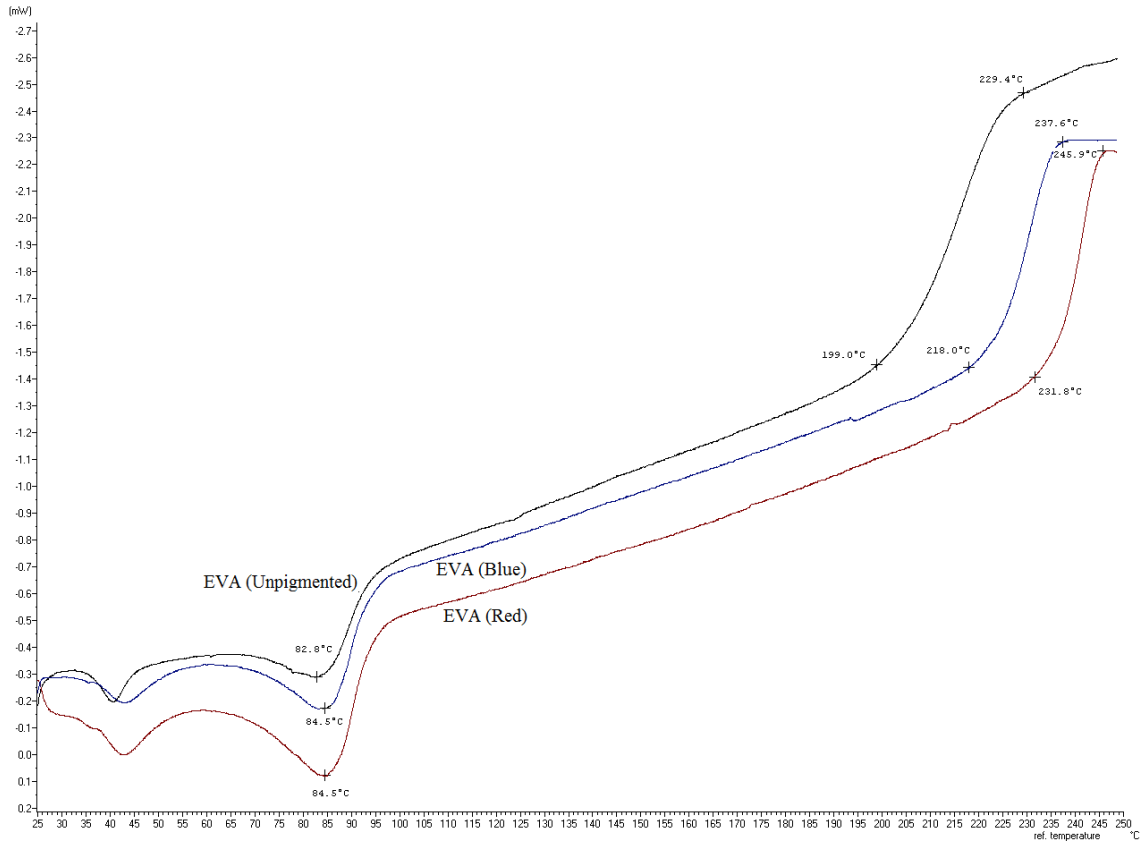

Figure 4.71 DSC of EVA with and without thermochromics in nitrogen environment

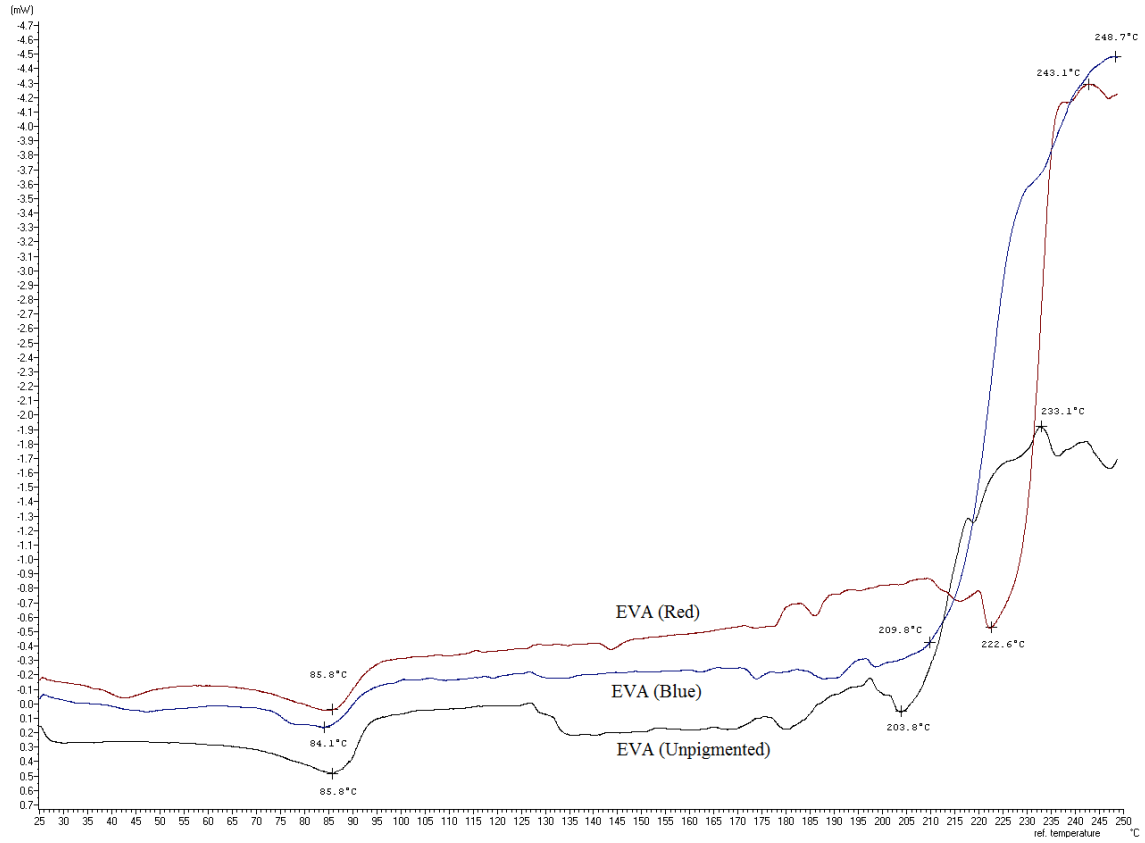

Figure 4.72 DSC of EVA with and without thermochromics in an air environment

(g) Tensile Properties

The mechanical properties of fibres have an important role in textile applications. In the textile industry, the fibres are commonly evaluated for tensile properties, together with other mechanical properties. In this study, the tensile properties of filaments of the three polymers containing the leuco dye based thermochromic pigments i.e., PP, LLDPE and EVA were studied.

Tensile testing of filaments was carried out using an Instron 3345K7484. The test method BS EN ISO 2062:1995 (textiles-yarn from packages-determination of single-end breaking force and elongation at break) was used. The test was performed for coloured and colourless filaments to provide a comparison. The gauge length was kept at 100mm and the test was performed at a constant rate of stretching of 250mm min^{-1}. The test was carried out using filaments with a 2% concentration of blue and red pigments, and uncoloured for each polymer. The symbols (B) and (R) refer to blue and red filaments respectively. The load applied was recorded as a function of extension. The maximum load is measured in Newtons (N) and extension at break was measured in millimetres (mm). Using the area and denier of the filaments, strength and tenacity of fibres were calculated in MPa and N tex^{-1}, respectively.

Figure 4.73 shows the maximum load borne by the filaments. The maximum load for PP filaments is greater for LLDPE filaments which is greater than for EVA. In each polymer, the maximum load decreases when pigment is incorporated into the filaments which indicates reduced strength. The extension at break is shown in Figure 4.74. The maximum extension is given by EVA and the minimum by PP filaments. Hence, EVA is more stretchable and PP filaments are least stretchable and more rigid as compared to EVA and LLDPE. The filaments with thermochromic pigments incorporated show more extension and thus are more stretchable than unpigmented filaments for all polymers. It is likely that the pigments are facilitating the polymer chains sliding over each other before breakage. Figures 4.75 and 4.76 show the strength and tenacity of the filaments. The PP filaments have higher tensile strength and tenacity than LLDPE, and LLDPE filaments have more than EVA. The unpigmented filaments show higher tensile strength and tenacity than blue and red filaments in the case of all three polymers. Therefore, it may be concluded that by incorporating thermochromic pigments in the polymers, their tensile properties such as maximum load, strength and tenacity decrease but filaments become more stretchable. It is normal that incorporation

of pigments weakens fibres as the particles disrupt the structure and introduce weak points.

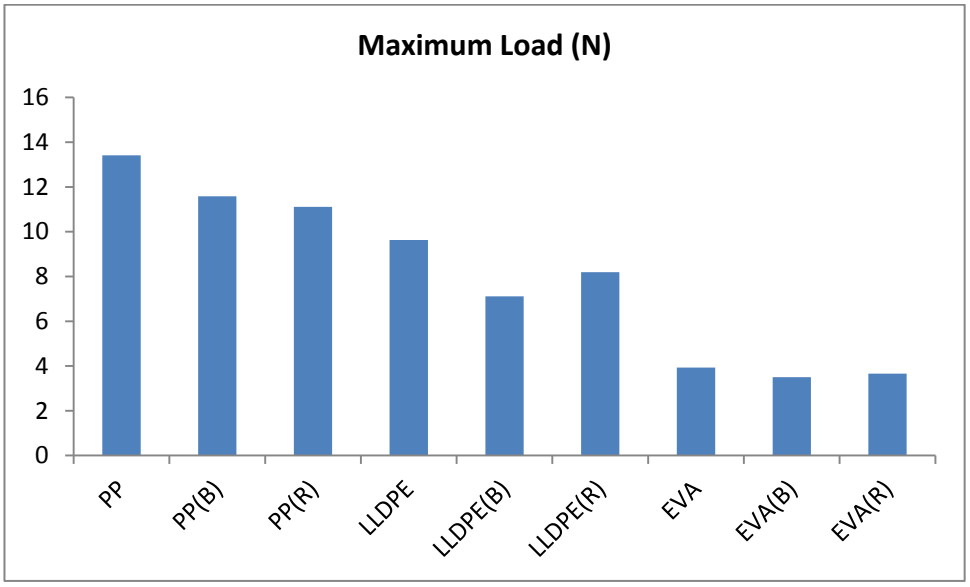

Figure 4.73 Maximum load for different filaments

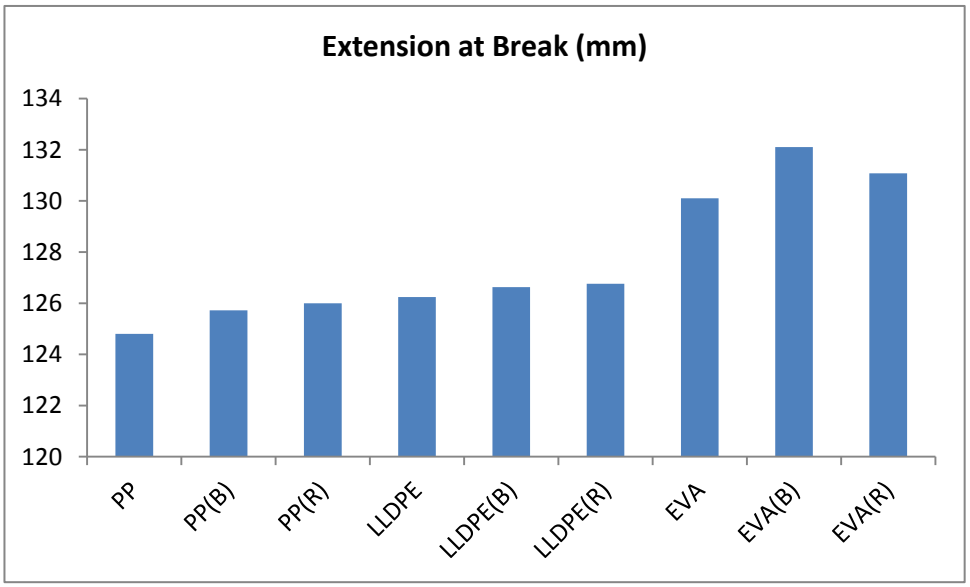

Figure 4.74 Extension at break for different filaments

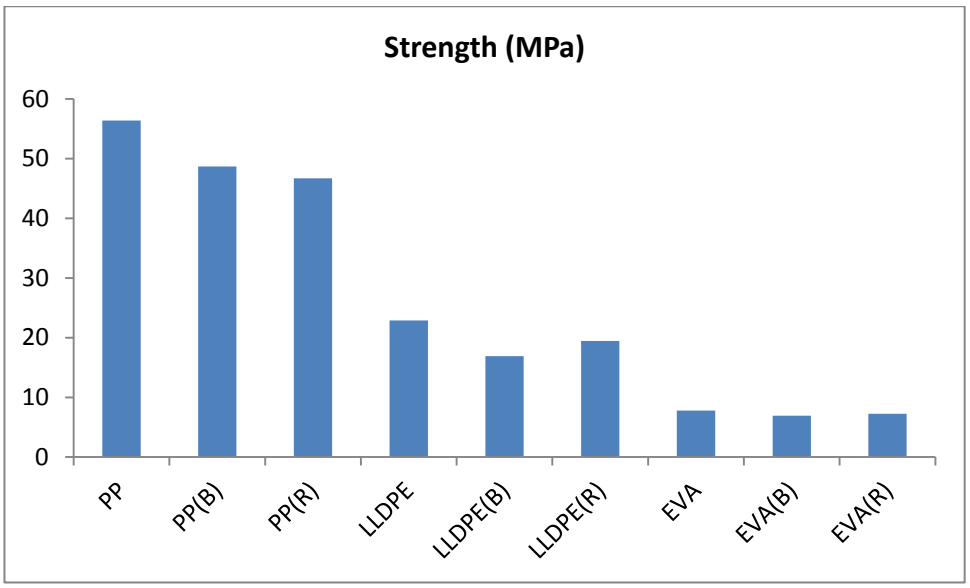

Figure 4.75 Strength of different filaments (MPa)

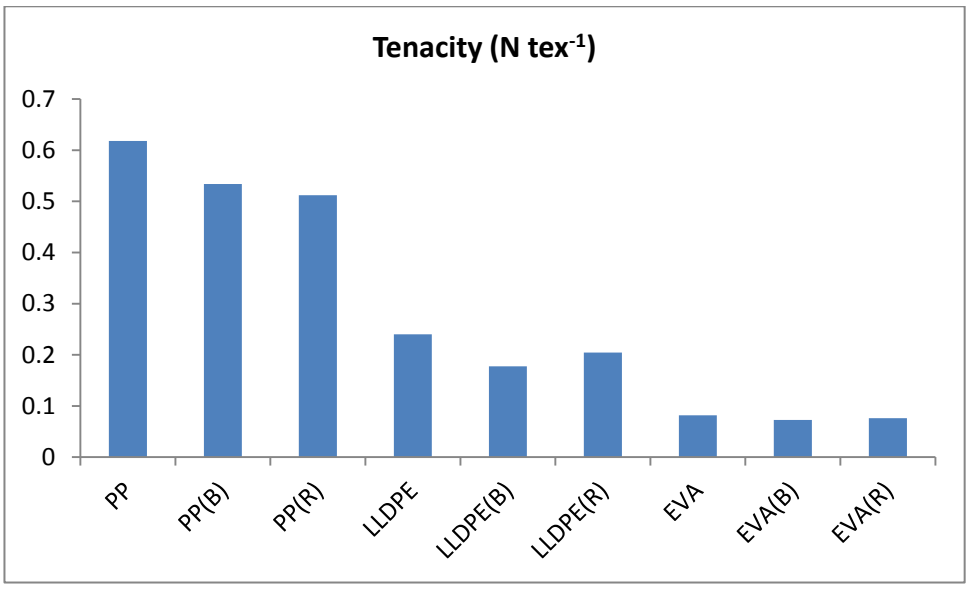

Figure 4.76 Tenacity of different filaments N tex^{-1}

4.3 Colour Measurement of Leuco Dye based Thermochromic Prints with varying Temperature

The leuco dye based thermochromic pigments change from coloured to colourless as a function of temperature. It was anticipated that the colour change may not be sharp as LCR Hallcrest, provider of thermochromic pigments, provided information that the colour may start to change 4°C below the quoted activation temperature. Therefore, an investigation was carried out to establish the dynamic colorimetric properties, the nature of the colour change and the possibility of colour hysteresis effects with heating and cooling cycles.

The colour measurement with varying temperature was carried out using a hot stage in conjunction with the spectrophotometer, established as discussed in section 3.18.2. The hot stage was insulated with glass fibres from the sides and behind, and the front side was kept clear to allow contact of the printed thermochromic samples against the spectrophotometer. The colour measurements were taken according to the optimized calibration conditions as discussed in section 4.1.1. The selected start temperature was 26°C for leuco dye based thermochromic pigments with a reported colour change temperature of 31°C. The colour measurements were taken with either an increase or decrease of 1°C intervals in both heating and cooling cycles. The measurements for the blue colour were taken up to 50°C. After observing that the printed sample did not become completely colourless but retained some colour at high temperatures, the rest of the printed samples were measured up to 40°C. An a^*b^* diagram was constructed, and integ and L^* values were plotted against temperature for both heating and cooling cycles.

Figures 4.77-4.78 show the integ values of blue thermochromic prints in heating and cooling mode, respectively. In heating, the integ values start decreasing with temperature below the reported activation temperature. The decrease is rapid, up to the reported activation temperature, i.e., 31°C in this case, and then there is very little decrease with temperature. Unexpectedly, the printed sample retained some residual colour at higher temperatures, measured up to 50°C. On cooling the printed sample, the integ values show a slight increase around 29°C which is below the reported activation temperature, after which a more pronounced increase leads to the complete reversible colour change. The colour build up on cooling is different from colour loss in heating. Figures 4.79-4.80 show the colour change in magenta prints with varying temperature. Again, the change in colour with temperature is rapid up to 31°C but after that it slows and then remains at a level beyond which no colour loss is observed. On cooling the print sample, the reverse colour change is observed after 30°C and then increases progressively up to 26°C. Figures 4.81-4.82 show the colour change of orange print. On heating, the colour change occurs gradually up to 35°C and then it retains its constant value. On cooling, the colour change occurs after 28°C and complete reversible colour development is seen at 26°C. Figures 4.83-4.84 show the colour change in the green print. Again on heating, a gradual colour change is observed up to

35°C and then remains constant, and on cooling, there is no change to 29°C, after which rapid colour build occurs.

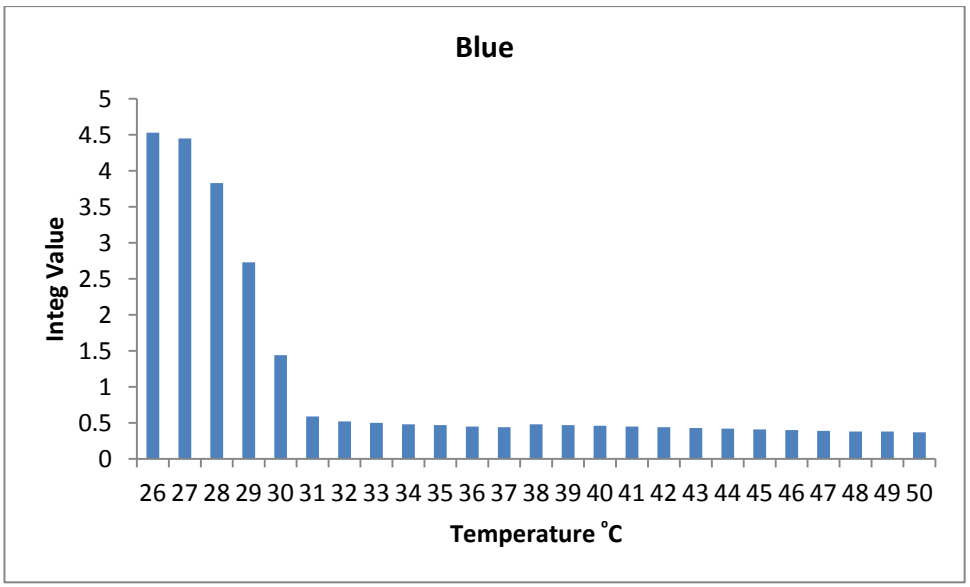

Figure 4.77 Integ values of blue leuco dye based thermochromic at increasing temperature

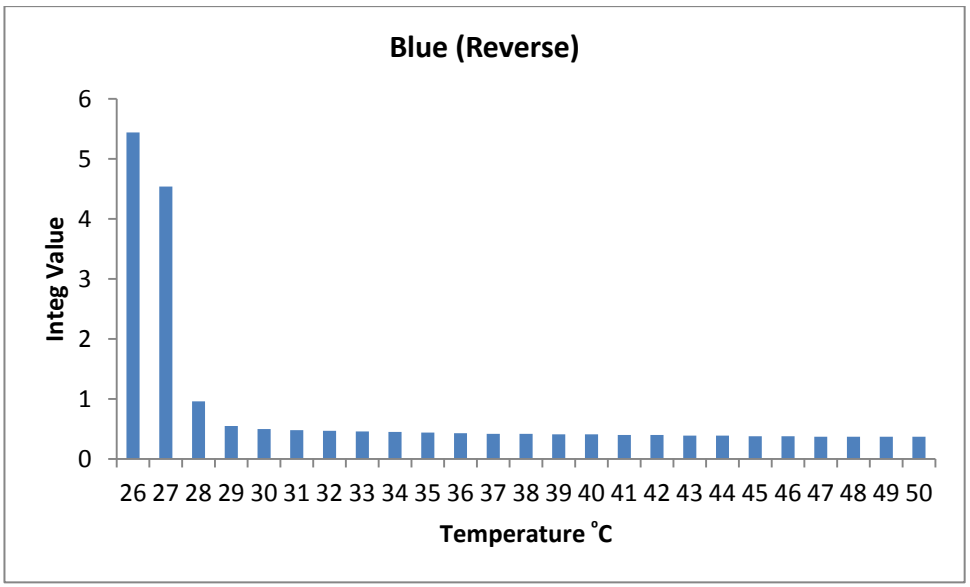

Figure 4.78 Integ values of blue leuco dye based thermochromic at decreasing temperature

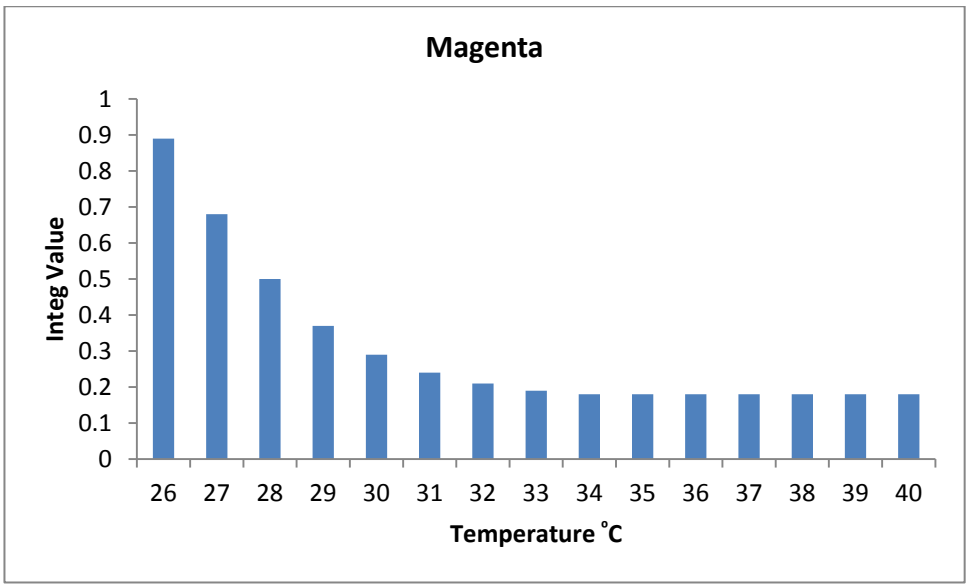

Figure 4.79 Integ values of magenta leuco dye based thermochromic at increasing temperature

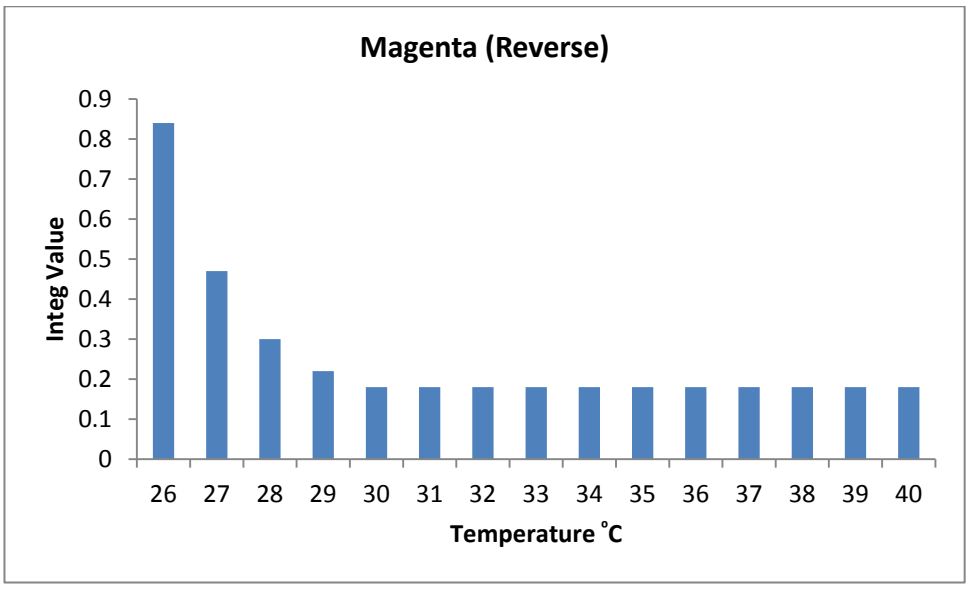

Figure 4.80 Integ values of magenta leuco dye based thermochromic at decreasing temperature

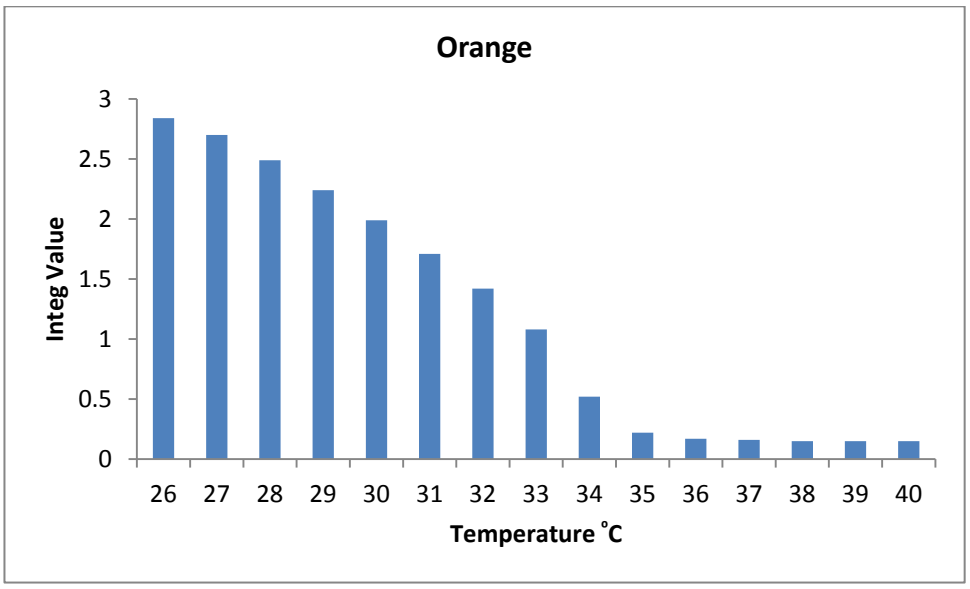

Figure 4.81 Integ values of orange leuco dye based thermochromic at increasing temperature

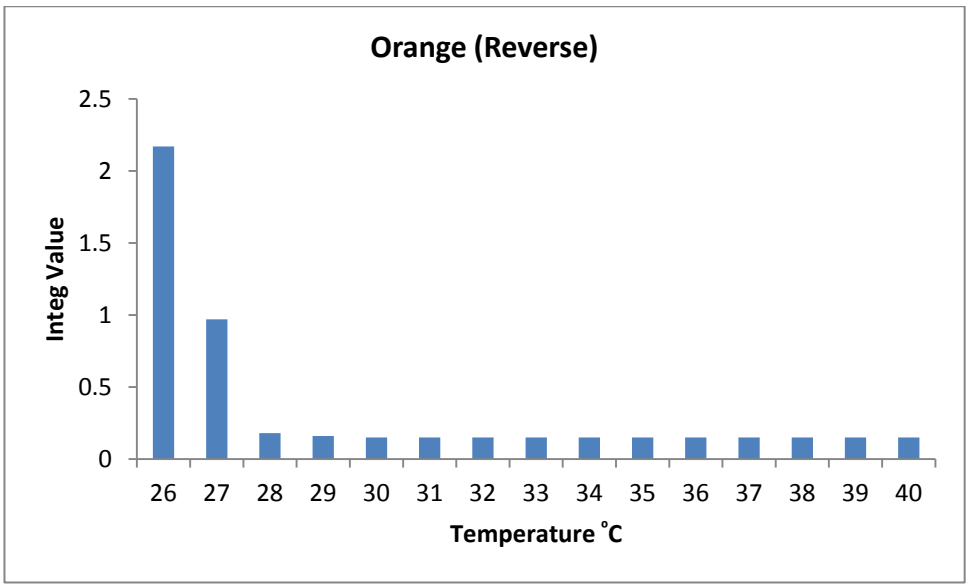

Figure 4.82 Integ values of orange leuco dye based thermochromic at decreasing temperature

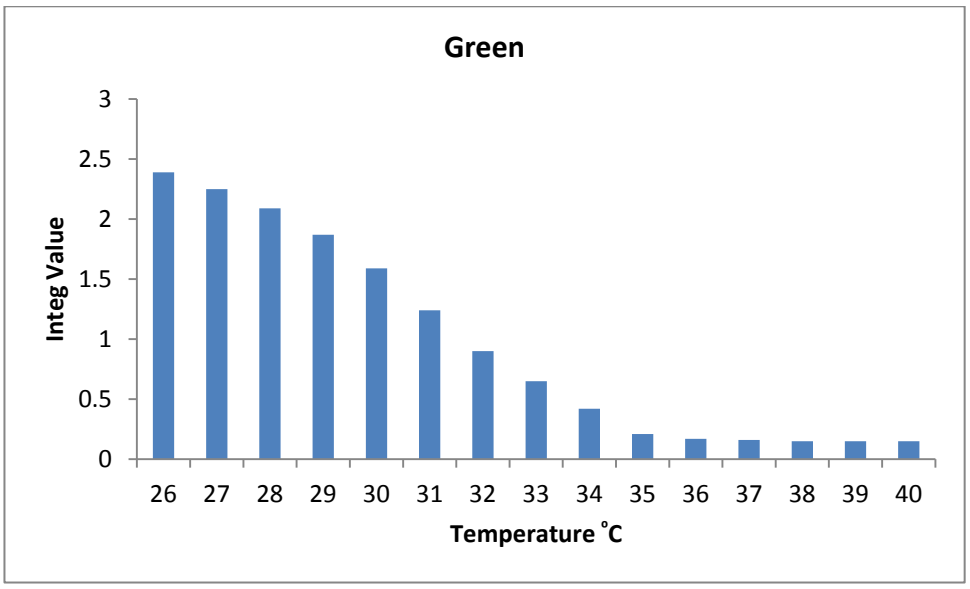

Figure 4.83 Integ values of green leuco dye based thermochromic at increasing temperature

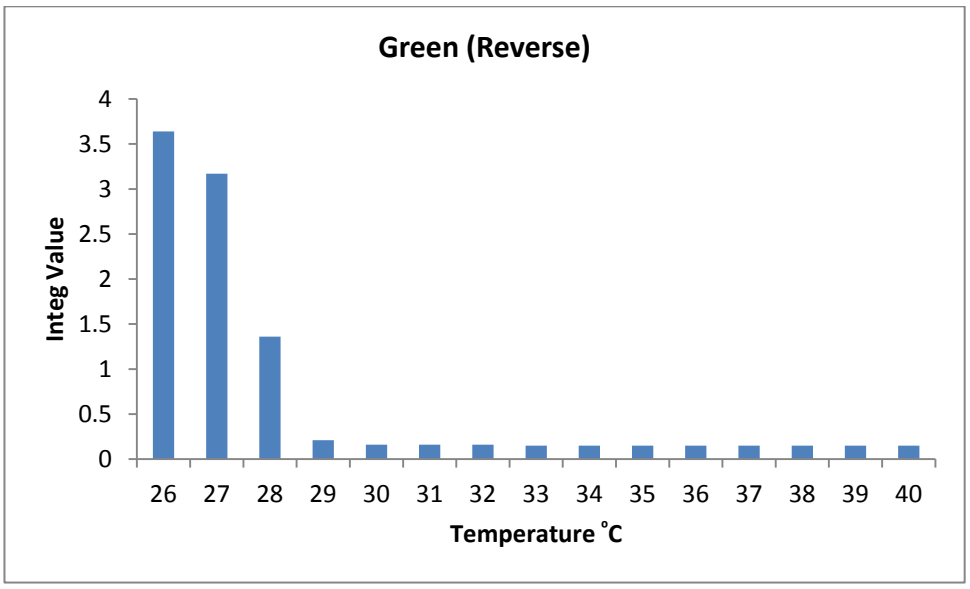

Figure 4.84 Integ values of green leuco dye based thermochromic at decreasing temperature

Figure 4.85 shows the a^*b^* diagram for prints containing leuco dye based thermochromic pigments, blue, magenta, orange and green, with heating and cooling. Each point in the diagram represents a measurement at a single temperature. The thermochromic colour change in respect of hue and saturation, but excluding lightness shows similar trajectories for heating and cooling. Every colour shows a closed loop made by a^*b^* values during a heating and cooling cycle. Figure 4.86 shows L^* values of the thermochromic prints, plotted against temperature. The L^* values increase with temperature for all colours as the colour change proceeds from coloured to colourless. On cooling, L^* values decrease with decrease in temperature until the complete colour is regained. The colour hysteresis obtained by heating and cooling the prints, is again a closed loop. The trajectories followed during heating and cooling in term of lightness are different as shown in Figure 4.86. These pigments give colour in the solid form and colourless in a liquid solution form of the solvent, present in the microcapsules. As discussed in section 2.3.3 (b) , the developer interacts with the colour former in the solid state, probably leading to an ion-pair complex form [1]. The melting of the solvent breaks up this ion-pair complex, resulting in a transition from coloured to colourless. A likely explanation is that the disintegration of the ion-pair complex occurs gradually on heating at specific temperatures and that re-formation on cooling occurs at lower temperatures as the solvent solidifies, causing the colour hysteresis. It is possible that the solvent (or a mixture of solvents) melts gradually rather than sharply, causing the colour change over a range of temperatures rather than a sharp colour change at the reported activation temperature. The residual colour may indicate that the disintegration of the ion-pair complex is not complete even at high temperatures, so that there is also some colour former and developer interaction in solution form in the solvent as well. Thus, it can be concluded that the colour strength profile of leuco dye based thermochromic pigments in heating will be different from that on cooling, and that the colour of the pigment at a specific temperature will not only depend on the temperature but also on the thermal history of the sample.

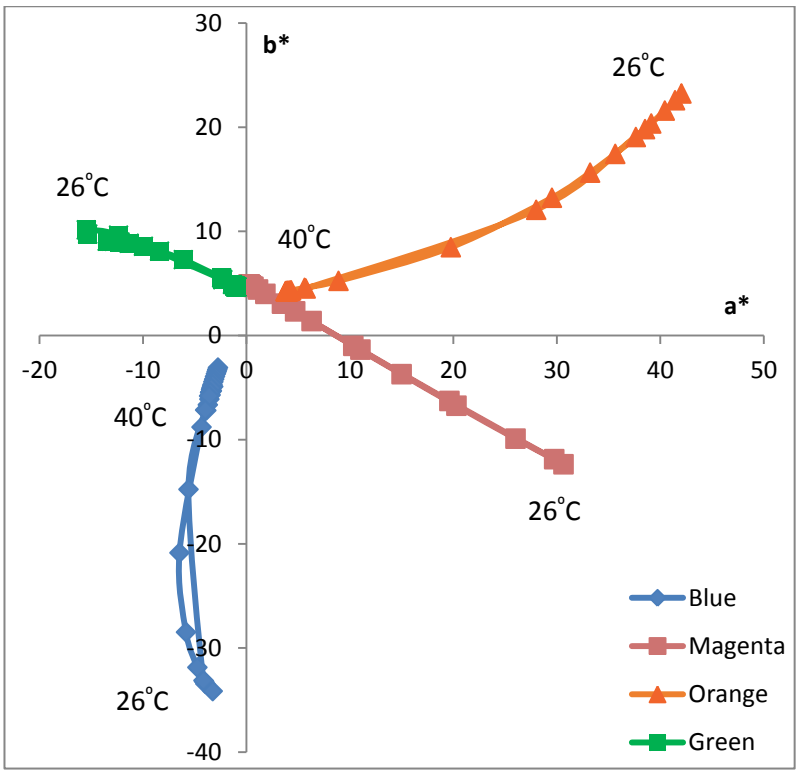

Figure 4.85 a^*b^* diagram of leuco dye based thermochromic prints, measured at increasing and decreasing temperature

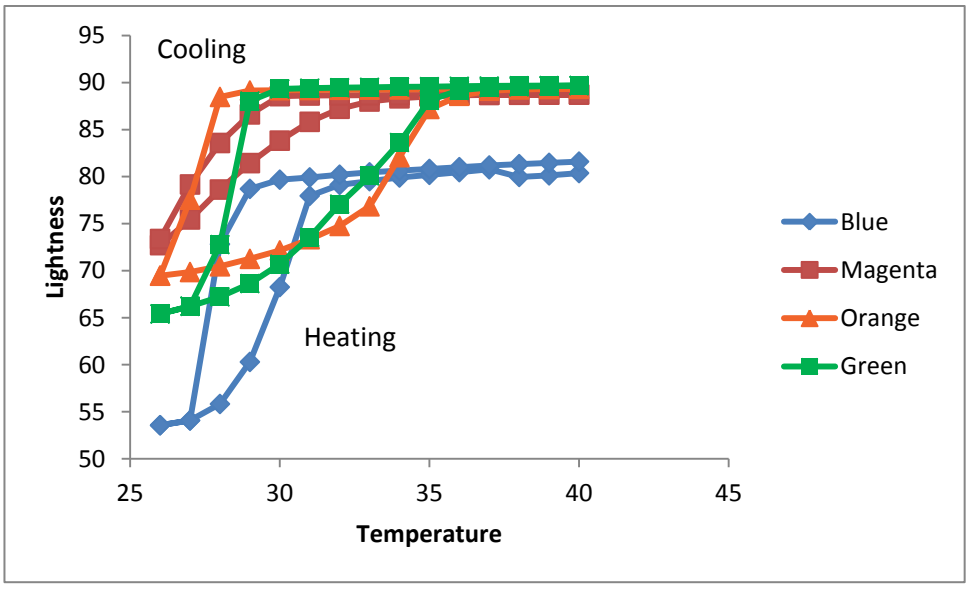

Figure 4.86 Lightness of leuco dye based thermochromic prints, measured at increasing and decreasing temperature

4.4 Investigation of the Application of Liquid Crystal Thermochromics

Liquid crystals form a fourth state of matter, between solid and liquid. They move like liquids, but keep a specific arrangement or pattern between the molecules. Certain liquid crystals interact with light and provide different colours by selective reflection of specific wavelengths of light, a phenomenon known as 'colour play'. Cholesteric liquid

crystals exhibit colour play with variation in temperature and are suitable for use on textiles as discussed in sections 2.5 and 2.7.1. Their colour play has been studied previously in our laboratories by colour measurement using a spectrophotometer and a hot stage [25]. In a fashion-based research project, also conducted in our laboratories, it was found unexpectedly that an unusual range of bright and intense colours, including orange, lilac, purple, pink etc., were obtained by layering of liquid crystals of different activation and bandwidth temperatures [70]. These colours were completely different from the rather dull greens and blues given when a single liquid crystal is subjected to heat and offer the potential for extending significantly the colour range and colour change effects available, which is particularly interesting for design and fashion applications. Therefore, a programme of research was initiated to measure different combinations of over-layered liquid crystals, using the spectrophotometer and the hot stage with a view to understanding the scientific basis of the phenomena.

The liquid crystals used were provided by LCR Hallcrest, as Chiral Nematic TLC Sprayable Coatings. The liquid crystals provided were specially made for research purposes and provide different starting colour play temperatures and temperature bandwidths. The liquid crystals used were known as R25C20W, R30C20W, R35C1W, R35C5W and R40C5W where the numeral following R indicates the starting temperature of colour play in $^{\circ}$C while the numeral following C is the temperature bandwidth, in $^{\circ}$C, over which the liquid crystals change colour from red through to blue. These liquid crystals were supplied with polyvinyl alcohol (PVA) in their compositions, so that no additional binder was used. The solid content of these liquid crystals was 37.9% as discussed in section 3.1.3.

The liquid crystals were applied on both black and transparent polyester sheets and also on printed leuco dye based thermochromic fabric by a method developed for this purpose as discussed in section 3.7.4. The liquid crystal coated polyester sheets and fabric were dried at room temperature, avoiding the need for high temperature curing. Initially, the liquid crystals were coated on transparent sheets individually. To make over-layered liquid crystal combinations, the individually coated sheets were layered over each other with a black sheet behind as required to absorb the transmitted wavelengths of light, (see section 2.5) for colour measurement purposes. It was envisaged that this method to make combinations would be easy and versatile, assuming that the transparent sheets would not have a significant effect on results. However, later

on, major differences were found in brightness and intensity of colours compared with a method involving over-layering liquid crystals on one another on a black sheet. On black polyester sheets, combinations of two liquid crystals were made by applying the first liquid crystal, drying with a hair dryer and then applying the second liquid crystal over it. Therefore, in this discussion, the term 'first liquid crystal' is used to refer to the liquid crystal on the ground or lower layer while, 'second liquid crystal' is used for the liquid crystal in the upper layer. The colour measurements were taken with a spectrophotometer in conjunction with a hot stage as discussed in section 3.18.2. The colour measurements were carried out at 0.2°C intervals for a temperature bandwidth of 5°C or less until a clear blue colour was achieved. The colour measurements after achieving the blue colour and for liquid crystals with a temperature bandwidth of 20°C, were taken at 0.5°C increments. Measurements were started from the smectic A phase, below the transition, and ended at a clear sign of the isotropic phase, which was assured when liquid crystals became transparent. The samples were also measured during cooling with the same temperature intervals (0.2°C or 0.5°C) as for heating.

The hot stage was calibrated according to manufacturer's instructions. The spectrophotometer was calibrated as for leuco dye based thermochromic pigments as discussed in section 4.1.1. The colour measurements processed by the DataColor software were represented in a number of ways. For colour space representation, a^*b^* values were plotted and selectively labelled according to the corresponding temperatures in °C. As the a^*b^* diagram does not include lightness, L^* values were also plotted against temperature. In addition, it was considered important to develop a method to provide an actual colour display of the over-layered liquid crystals as a potential tool for designers for creative applications. For this purpose, a computer program provided by DataColor was used in conjunction with the DataColor software to calculate RGB values for every colour measurement. These RGB values were used in a program to display the colours of the liquid crystals at specific temperatures. The program was written in visual basic and used in conjunction with Microsoft Excel 2007. The reflectance values, measured at varying temperatures, were also plotted against wavelength.

4.4.1 R25C20W layered over R30C20W

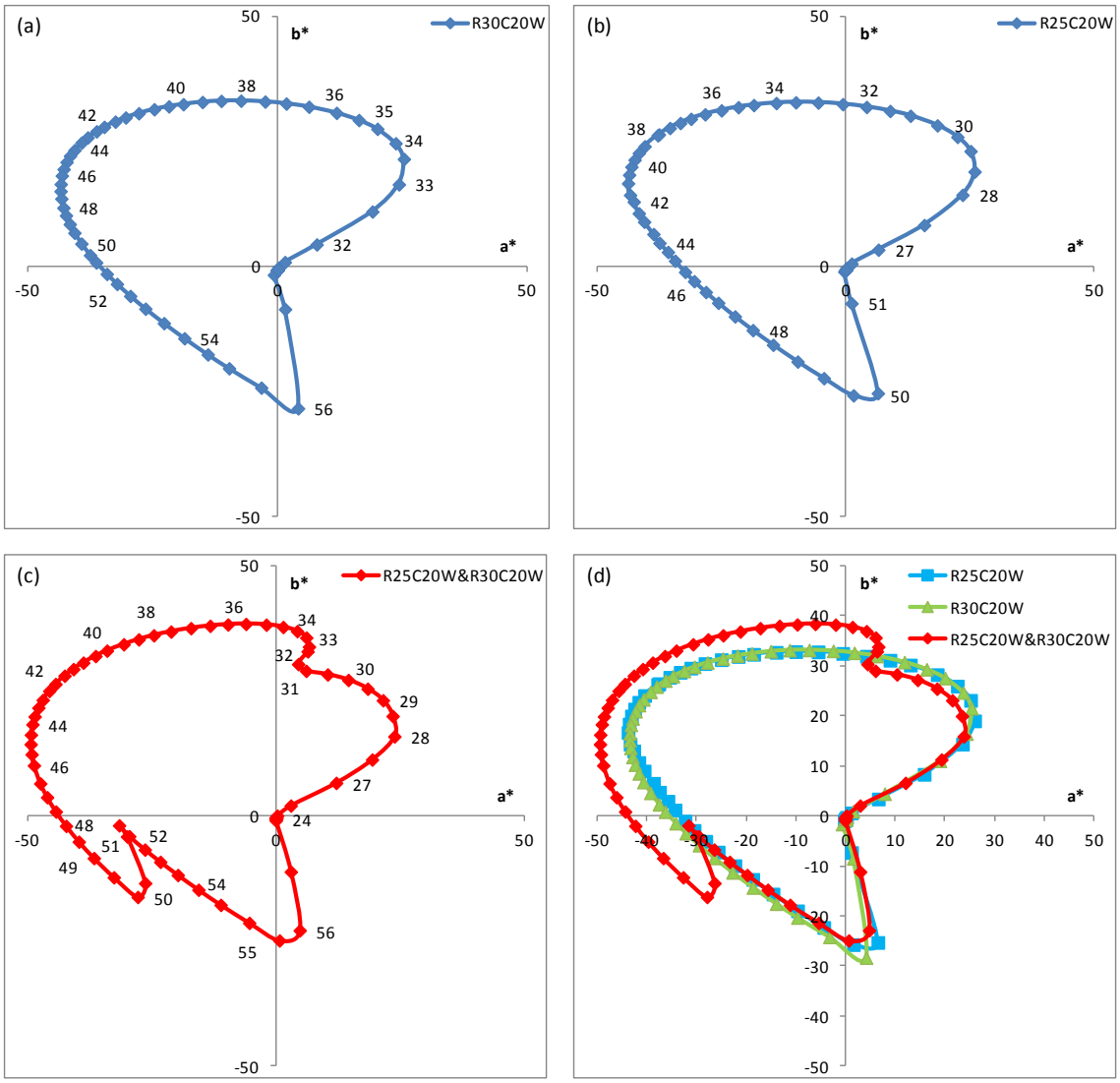

Figure 4.87 a*b* diagram of R25C20W&R30C20W, with data labels in °C, coated on a black sheet

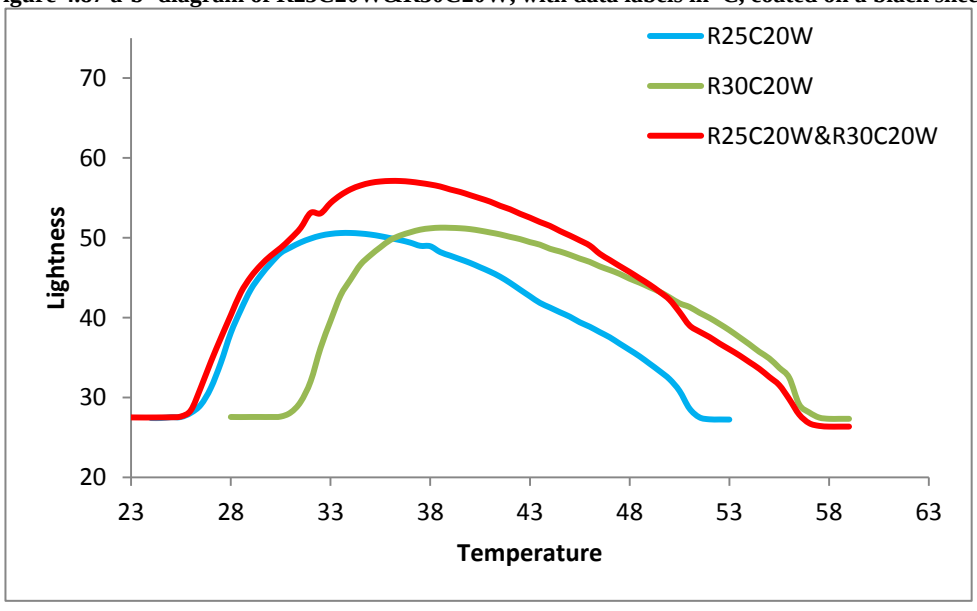

Figure 4.88 Effect of temperature on lightness of R25C20W&R30C20W, coated on a black sheet

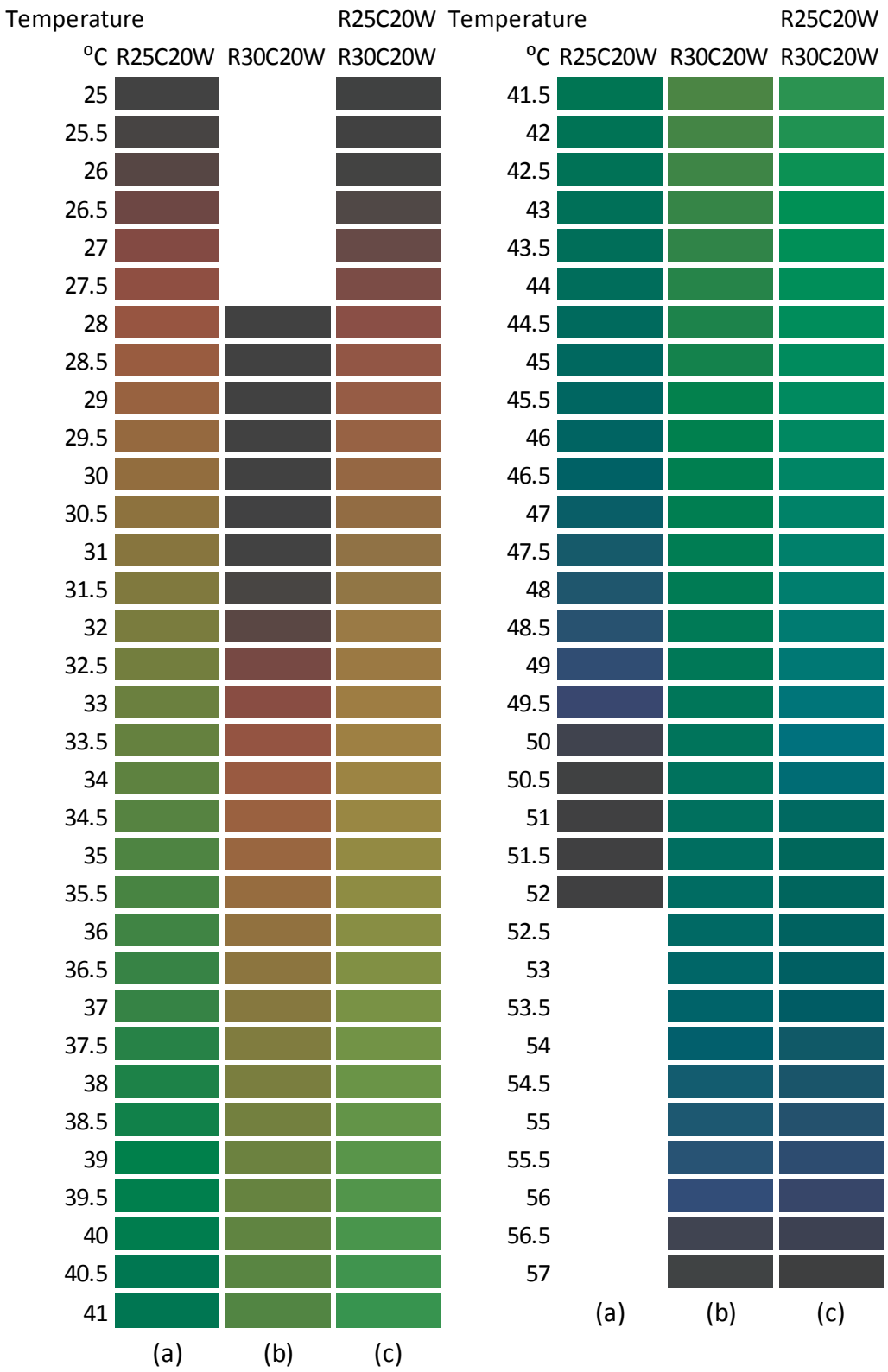

Figure 4.89 RGB colour display of R25C20W&R30C20W, coated on a black sheet

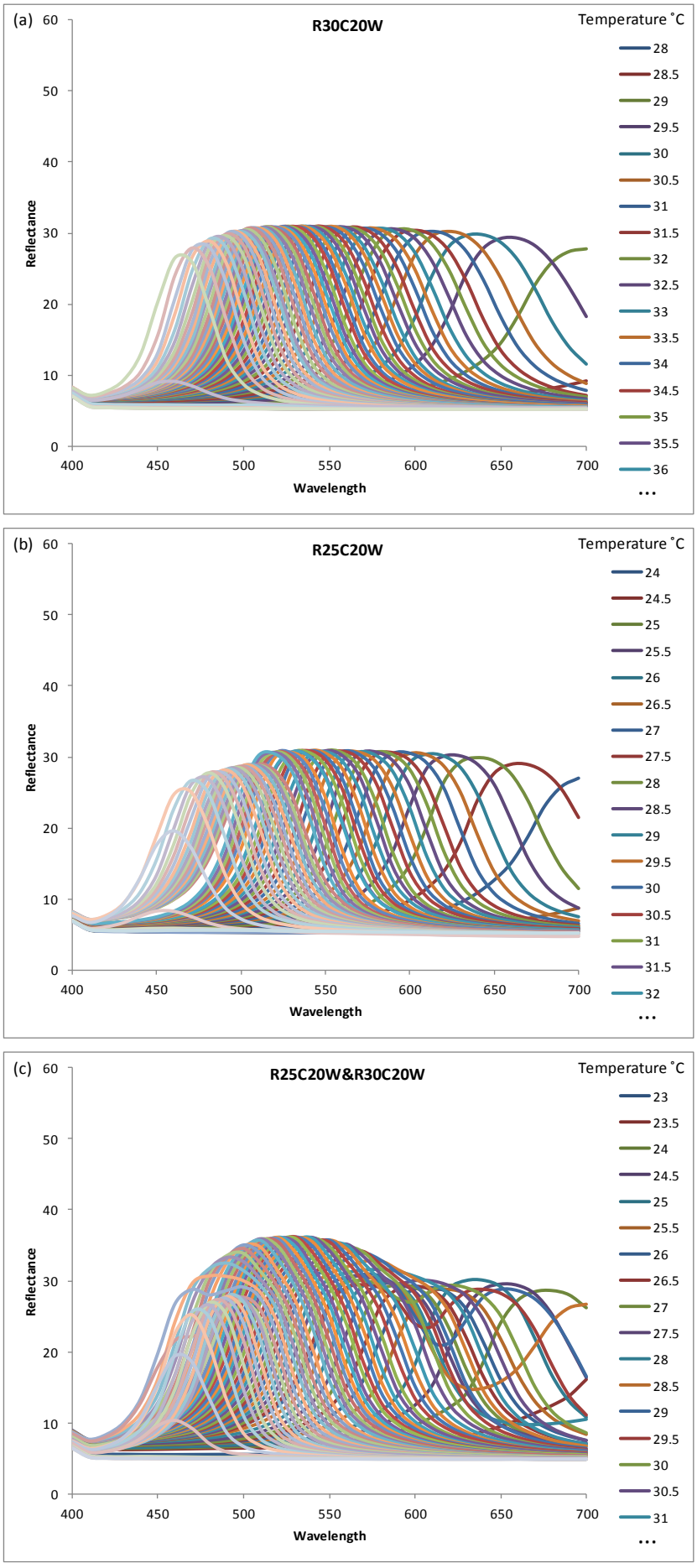

Figure 4.90 Reflectance curves of R25C20W&R30C20W, coated on a black sheet

The colour measurements were taken for R25C20W layered over R30C20W, coated on a black polyester sheet. Figures 4.87 (a)-(d) show a^*b^* diagrams of the liquid crystals, individually and overlaid, labelled with their corresponding temperatures. The R30C20W (a) and R25C20W (b) individually show the start of colour play a little above their reported initial temperatures. In both liquid crystals, the colour continues to build with temperature in the first quadrant of the a^*b^* diagram, which represents red ($+a^*$) to yellow ($+b^*$) colours, as a progressive colour change occur from red to yellow, through orange, with increasing temperature. The colour change becomes slower in the second quadrant which represents yellow to green ($-a^*$) colour. The colour changes quite slowly with temperature when a green colour has been developed. In the third quadrant, which represents green to blue ($-b^*$) colours, a gradual progressive colour change is observed with temperature, from green to blue. In the fourth quadrant which represents blue to red colours, there is a rapid change from blue to black i.e., the liquid crystals become transparent and enter into an isotropic phase from an anisotropic phase so that only the black background is observed.

On the basis that the liquid crystal layers act effectively as a source of light, unusually, the principles of additive colour mixing apply to the over-layered combinations (section 2.13.5). The a^*b^* diagrams of R25C20W layered over R30C20W, (c)-(d), show a similar colour start as R25C20W. However, the colour saturation is a little less in the first quadrant, from 28°C to 31°C, which may be due to a coated layer of R30C20W that is not completely transparent, thus decreasing the saturation by reflecting a portion of light, transmitted by the upper layer of R25C20W, and making the background less black which is also observed as an increase in lightness, as discussed later. At 31°C the colour play of the first liquid crystal i.e., R30C20W starts, a little higher than 30°C. The curve at this point shows a slight colour change with temperature, which is not shown by the individual liquid crystals. The red colour developed by the first liquid crystal moves the curve from the yellow of the second layer towards the red. Thus a cumulative colour effect is observed. The measured cumulative effect shows that the wavelengths reflected by the first and second liquid crystals have added (the additive colour mixing phenomenon), illustrated by an increase in saturation and also lightness as discussed later. Therefore, more saturated and brighter colours are observed. This additive colour mixing effect retains brighter colours until 50°C, where the second liquid crystal, R25C20W, shows a rapid transition towards the isotropic phase and ends the colour play. At this point, the a^*b^* values, rather than progressing towards the blue

and to the origin, diverts back towards green, which is due to the first liquid crystal i.e., R30C20W, which is still far from the isotropic phase and reflecting green. From this point to the isotropic phase, the over-layered liquid crystals follow almost the same trajectory as the first liquid crystal, as the second liquid crystal is colourless.

Figure 4.88 shows L^* values of over-layered and individual liquid crystals plotted against temperature. In each case, lightness increases rapidly with temperature as soon as colour play starts. It reaches its maximum values at temperatures giving greenish yellow for both liquid crystals measured individually. In over-layered form, the cumulative lightness effect of both liquid crystals is observed. The maximum lightness remains in the greenish yellow region and is at a temperature between the peak temperatures of both individually measured liquid crystals. A small 'bump' in the lightness curve of over-layered liquid crystals is observed when the first liquid crystal starts colour play. The enhanced lightness of the over-layered sample is observed from the start of colour play of the first liquid crystal almost to the end of colour play of the second liquid crystal. The lightness of over-layered liquid crystals at the start, from 26°C to 31°C, before the transition of the first liquid crystal, is slightly higher than the second, possibly because of additional reflection due to slight opacity of the layer of first liquid crystal, in the smectic A phase. The lightness of the over-layered liquid crystals becomes lower than the first liquid crystal, measured individually, at the end of colour play of the second liquid crystal which is around 50°C. However, the colour saturation is not affected above this temperature as shown in the a^*b^* diagram. When the second liquid crystal enters the isotropic phase, layered over the first liquid crystal, it is likely to become transparent which would not affect saturation but would not be expected to reduce lightness provided by the first liquid crystal. This feature thus remains unexplained. It is also observed in the case of over-layered liquid crystals that lightness in the isotropic phase is slightly lower than in the smectic A phase. This may be due to liquid crystals reflecting some light in the smectic A phase where molecules are aligned and in isotropic phase they become transparent due to random orientation of molecules.

It is known that cholesteric liquid crystals may experience an intermediate state in the transition from cholesteric to isotropic phase. The cholesteric liquid crystals show an unusual packing structure of helices over a narrow temperature range, just before the isotropic phase. This phenomenon is known as blue phase because it was first observed

as a flash of bright blue colour. However, flashes of other colours such as green or red may be observed, depending on the type of material. Blue phases are found in three types of cubic lattice structures, normally referred to as BP(I), BP(II) and BP(III) [20,25,128]. In Figure 4.88, the lightness curves for all liquid crystals, individual and over-layered, show a dip to the isotropic phase which may be due to a rapid change from blue to colourless or may be an indication of the blue phase.

Figure 4.89 shows RGB colour displays of individual and over-layered liquid crystals at varying temperatures. In the case of both individual liquid crystals, the colour changes progressively from red to green with temperature. The green colour persists longer with increasing temperature and then rapidly changes to black, in the isotropic phase, through blue. The over-layered liquid crystals show the same colour change behaviour in the red region. However, when the first liquid crystal starts colour play at 31°C, the greenish yellow colour of the second liquid crystal and the red colour of the first liquid crystal mix additively to provide a dull yellowish colour. The colour becomes yellowish green with increasing temperature as the first liquid crystal becomes reddish yellow, around 36°C. Following this point, the combined effect forms a light bright green colour from a dull greenish yellow and dark green of the first and second liquid crystals respectively. This is consistent with additive colour mixing because in subtractive colour mixing, dull colours mix to form an even duller colour. As the second liquid crystal becomes blue and the first is yellowish green at about 49°C, the over-layered liquid crystals show a turquoise or bluish green colour, from additive mixing. As the second liquid crystal enters the isotropic phase, the over-layered liquid crystals change to the dark yellowish green, of the first liquid crystal at this temperature, after which the pattern of the first liquid crystal is followed up to the isotropic phase.

Figures 4.90 (a)-(c) show reflectance curves of individual and over-layered liquid crystals, measured from 400nm to 700 nm at intervals of 10nm at varying temperatures. The centred wavelength ($\lambda_\circ$) of the reflected band of light at a specific temperature, for a liquid crystal with the cholesteric liquid crystal pitch length (p) and average refractive index (n) is given by Equation 4.3.

$$\lambda_\circ = np$$

Equation 4.3

and the bandwidth of the reflected light is as follows:

$$\Delta\lambda = p\,(n_e - n_\circ) = p\Delta n$$

Equation 4.4

where n_e and $n_\circ$ are refractive indices of the liquid crystal phase parallel and normal to the director in the same plane respectively. The reflected wavelengths show peaks progressing from 700nm (red region) to 450nm (blue region) with increasing temperature. The reflectance curves of over-layered liquid crystals show two peaks at some temperatures, due to the individually reflected wavelengths of over-layered liquid crystals. The effect of wavelengths reflected by one liquid crystal can be dominated by the other liquid crystal depending on the sequence of liquid crystal layers, as discussed later in section 4.4.6. It is also observed that the peak reflectance values of over-layered liquid crystals are higher than the reflectance peak values of individually measured liquid crystals. This demonstrates that in the case of over-layered liquid crystals, the reflectances of individual liquid crystals interact constructively giving higher values, consistent with additive colour mixing phenomena.

4.4.2 R35C1W layered over R25C20W

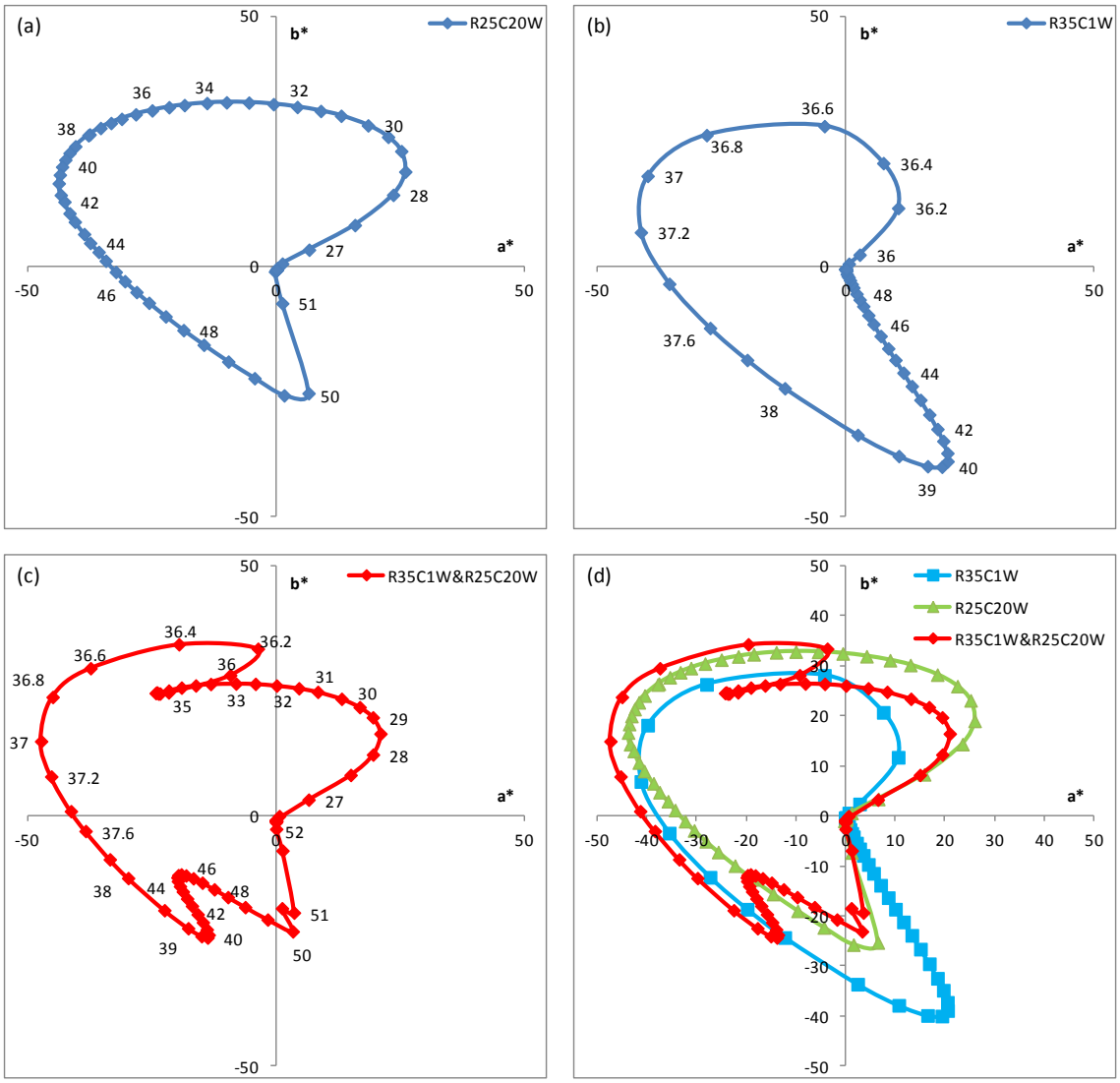

Figure 4.91 a*b* diagram of R35C1W&R25C20W, with data labels in °C, coated on a black sheet

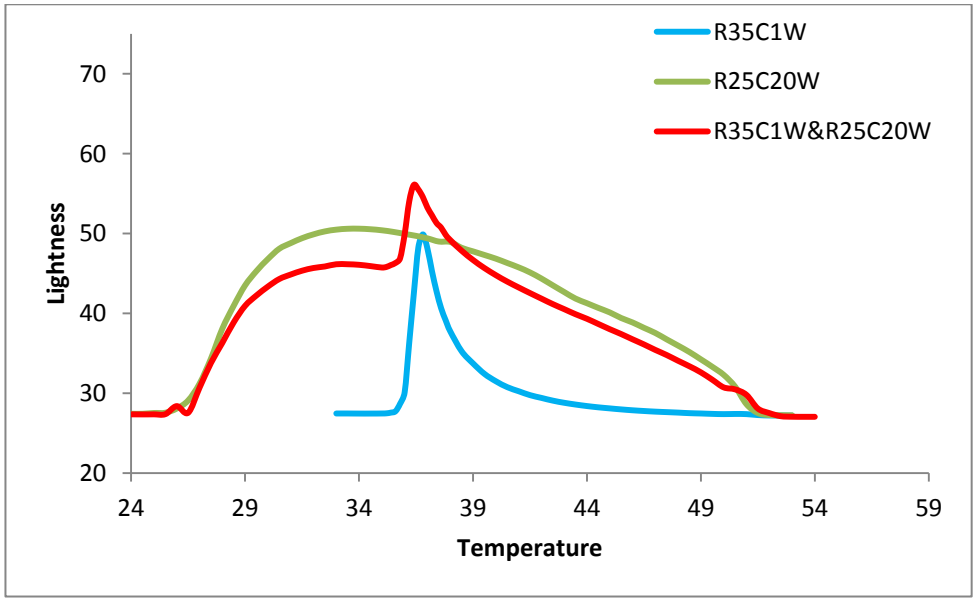

Figure 4.92 Effect of temperature on lightness of R35C1W&R25C20W, coated on a black sheet

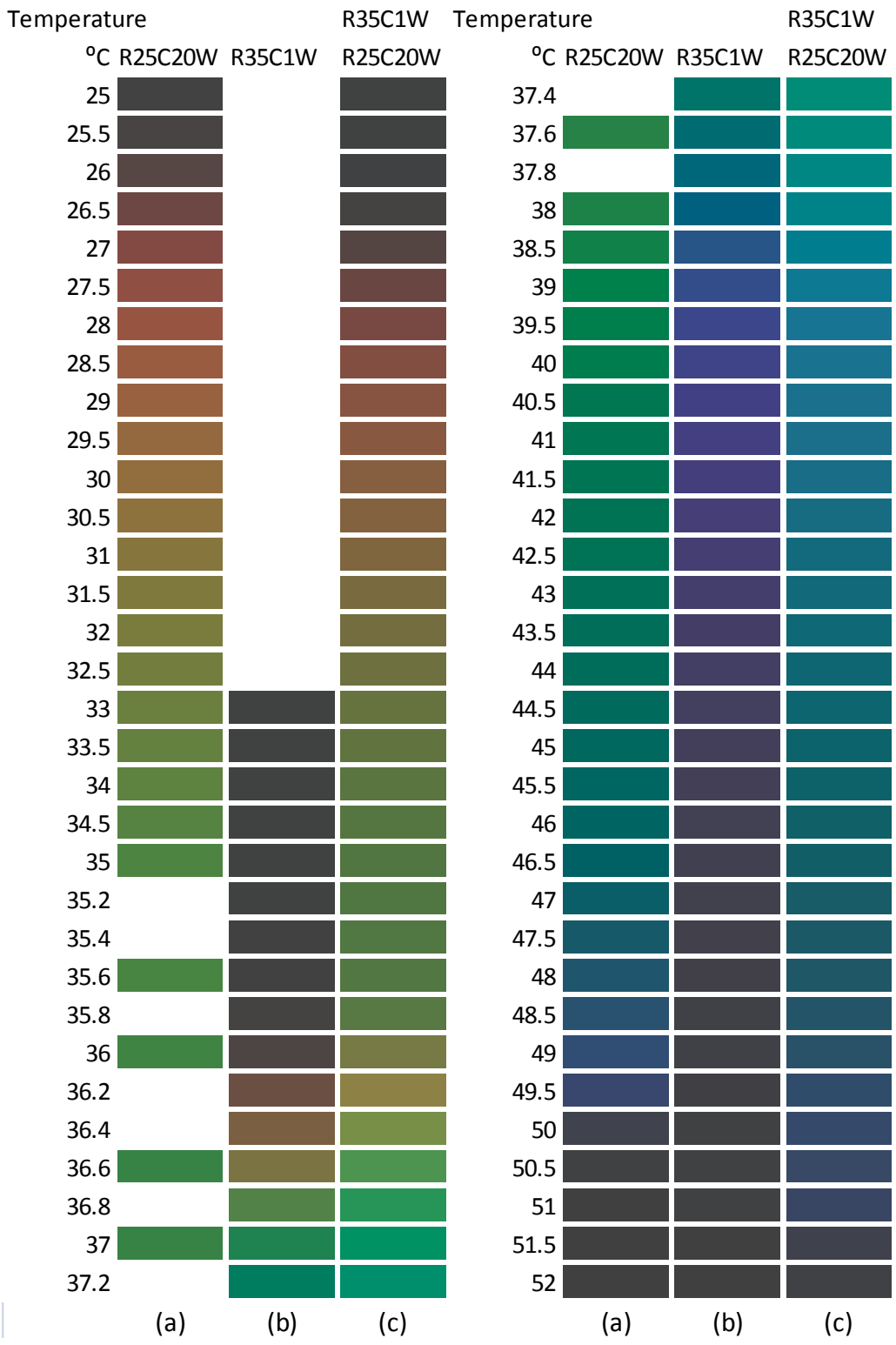

Figure 4.93 RGB colour display of R35C1W&R25C20W, coated on a black sheet

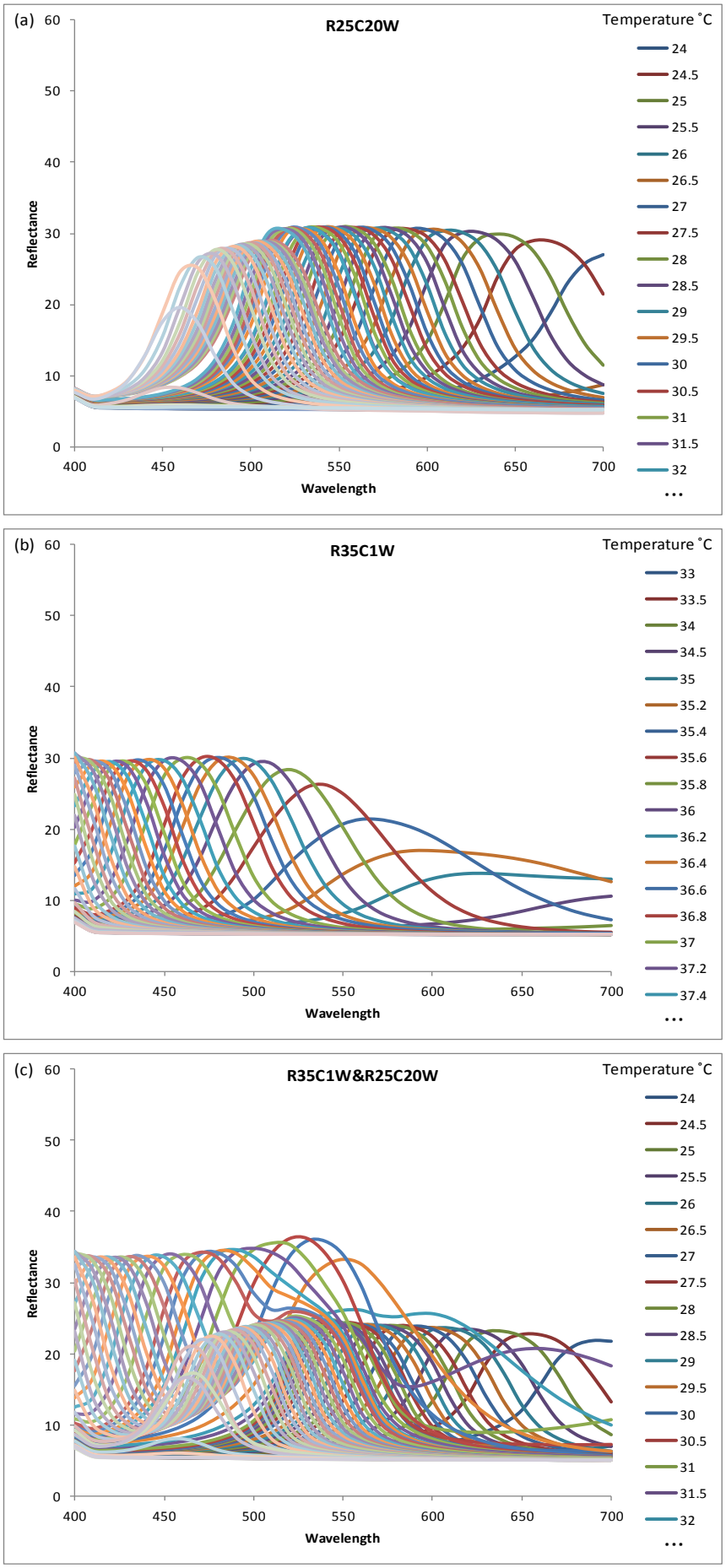

Figure 4.94 Reflectance curves of R35C1W&R25C20W, coated on a black sheet

Figures 4.91 (a)-(d) show a^*b^* diagrams of R35C1W and R25C20W, individually and collectively. R35C1W (b) shows the start of colour play at a temperature of 36°C. The temperature bandwidth is only 1°C, i.e., it changes colour through the whole spectrum from red to blue within 1°C. Due to the small bandwidth, the colour changes rapidly from the first quadrant through to the fourth quadrant. When it achieves the reddish blue colour, it progresses slowly to the origin, i.e., to the isotropic phase. R35C1W shows more colour saturation in the fourth quadrant, in contrast to R25C20W and R30C20W. The a^*b^* diagrams, (c)-(d), of R35C1W layered over R25C20W show a similar colour start as R25C20W. However, the colour saturation is considerably less in the first and second quadrants, from 28°C up to 35°C, which may be due to slight opacity of the upper layer of R35C1W, in the smectic A phase. At 36°C, R35C1W starts its colour play and the colour shows rapid change with temperature. The colour developed by the second liquid crystal moves the curve from the greenish yellow of the first liquid crystal towards the red, due to a cumulative colour effect by additive colour mixing, illustrated by an increase in saturation and brightness. This additive colour mixing phenomenon gives more saturated colours until 40°C, where the second liquid crystal, i.e., R35C1W shows a transition towards the isotropic phase and ends the colour play. At this point, the first liquid crystal causes diversion of the a^*b^* values towards green, as it reflects green and is still far from the isotropic phase. From there to the isotropic phase, the over-layered liquid crystals follow a similar trajectory to the first liquid crystal, with slightly lower colour saturation. A slight reduction in colour saturation from 45°C to 51°C of over-layered liquid crystals is observed. However, this reduction in saturation is less than in the first quadrant, probably because the second liquid crystal in transition, near the isotropic phase, is more transparent than the smectic A phase and only gives a slight diffuse scattering.

L^* values of over-layered and individual liquid crystals plotted against temperature, Figure 4.92, increase rapidly with temperature as colour play starts. In each case, maximum values are reached at temperatures giving greenish yellow. For over-layered form, the peak is at an intermediate temperature, nearer to the second. In over-layered form, the cumulative lightness effect is observed at about 36°C. Enhanced lightness is observed at the peak level due to additive mixing of reflected light from both liquid crystals. The lightness of over-layered liquid crystals at the start, about 27°C, up to the transition of the second liquid crystal at 36°C and after the peak at 38°C, up to the isotropic phase, is lower than the lightness of the first liquid crystal measured

individually. The lightness of over-layered liquid crystals is even lower before the start of colour play of the second liquid crystal than after it is completed. This may indicate that the layer of the second liquid crystal, in the smectic A phase, is slightly opaque and restricts light, whereas in the cholesteric phase or in the isotropic phase it is relatively more transparent. The lightness curve for over-layered liquid crystals shows a small peak before entering the isotropic phase, which is an indication of the blue phase.

Figure 4.93 shows RGB colour displays of individual and over-layered liquid crystals at varying temperatures. The R35C1W shows a rapid change in colour, starting from red to green through yellow and then towards blue, within a very short range of temperatures. The over-layered liquid crystals show the same colour change behaviour as the first liquid crystal up to the start of colour play of the second liquid crystal. When the second liquid crystal starts colour play at 36°C, the green colour of the first liquid crystal and the red colour of the second liquid crystal show a mixing effect in the form of a brownish yellow to yellowish green through yellow. However, the colours are brighter than the colours of individually measured liquid crystals. As the second liquid crystal enters the blue region, around 38°C, the colour of the over-layered liquid crystals becomes greenish blue where the green colour of the first liquid crystal is dominated by the blue colour of the second. As the second liquid crystal approaches the isotropic phase, the over-layered liquid crystals show a bluish green colour, i.e., the first liquid crystal dominates the colour. After that the over-layered liquid crystals follow the same pattern of changing colour as that of the first liquid crystal up to the isotropic phase. The colours exhibited by the over-layered liquid crystals during colour play of both the liquid crystals are brighter and lighter than those of individually measured liquid crystals, indicating additive colour mixing.

In Figure 4.94, the over-layered form shows peaks from 700nm to 400nm with temperature. The peak reflectance values for R25C20W are throughout the 450nm to 700nm range, whilst for R35C1W they are given mainly in the 400nm to 600nm region. The reflectance curves of over-layered liquid crystals show two peaks at temperatures where both liquid crystals change colours. The reflectance curves of the second liquid crystal appear to dominate the first liquid crystal as there is an increase in peak values of the second while a decrease in the first. These may also be a contribution due to reflection of certain wavelengths by the upper layer of second liquid crystal, leaving them unavailable for interaction with the first liquid crystal.

4.4.3 R35C5W layered over R25C20W

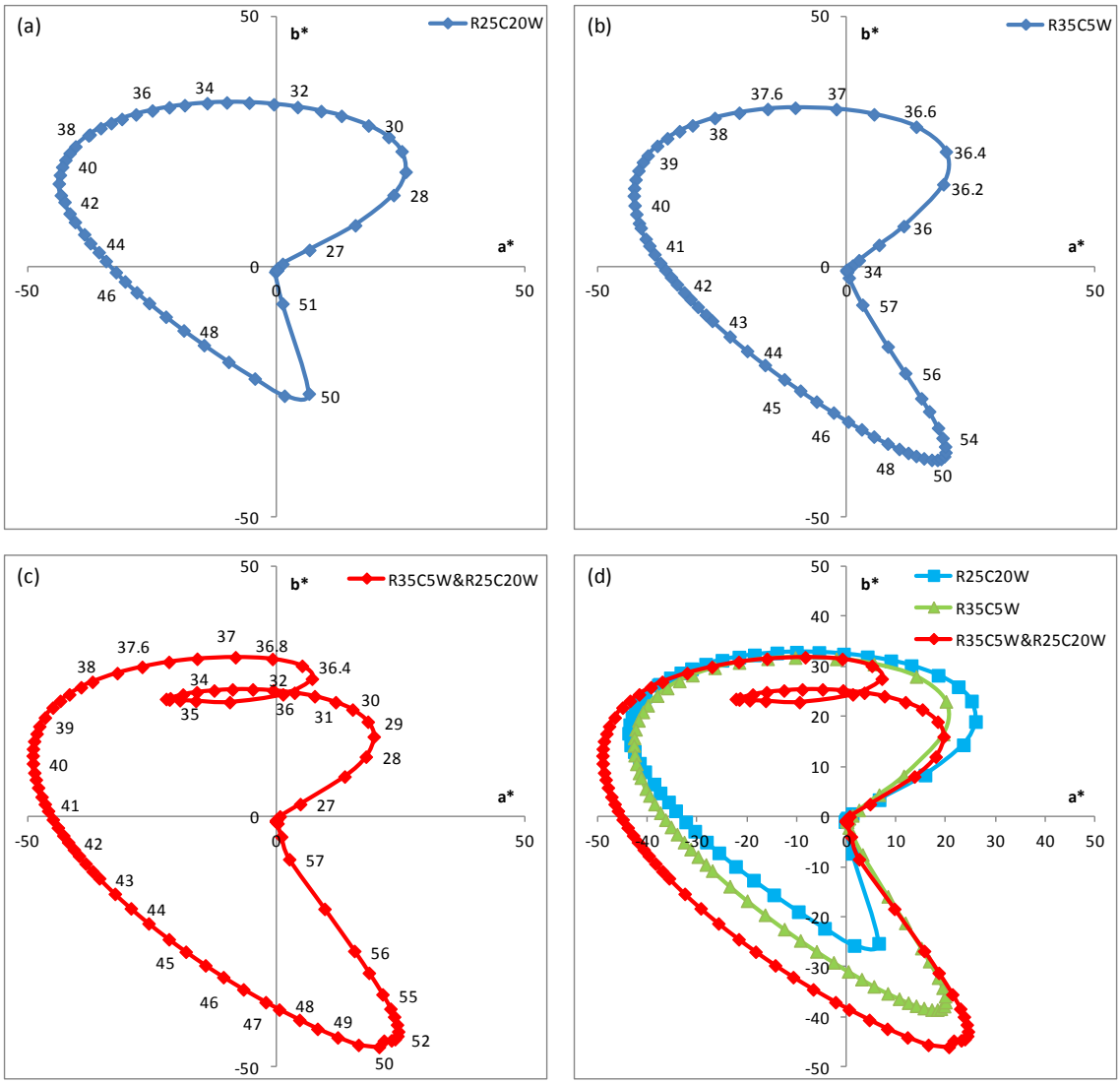

Figure 4.95 a*b* diagram of R35C5W&R25C20W, with data labels in °C, coated on a black sheet

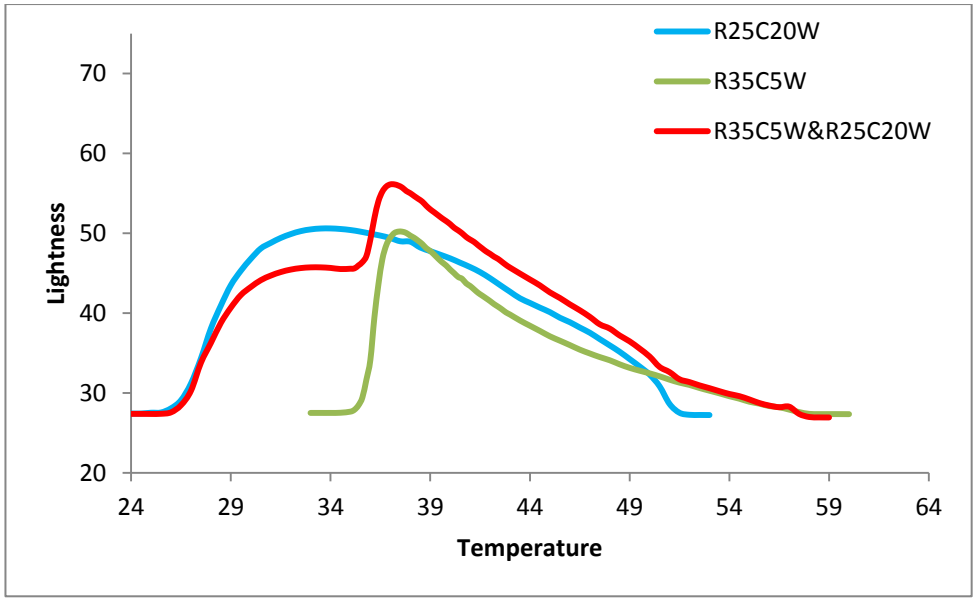

Figure 4.96 Effect of temperature on lightness of R35C5W&R25C20W, coated on a black sheet

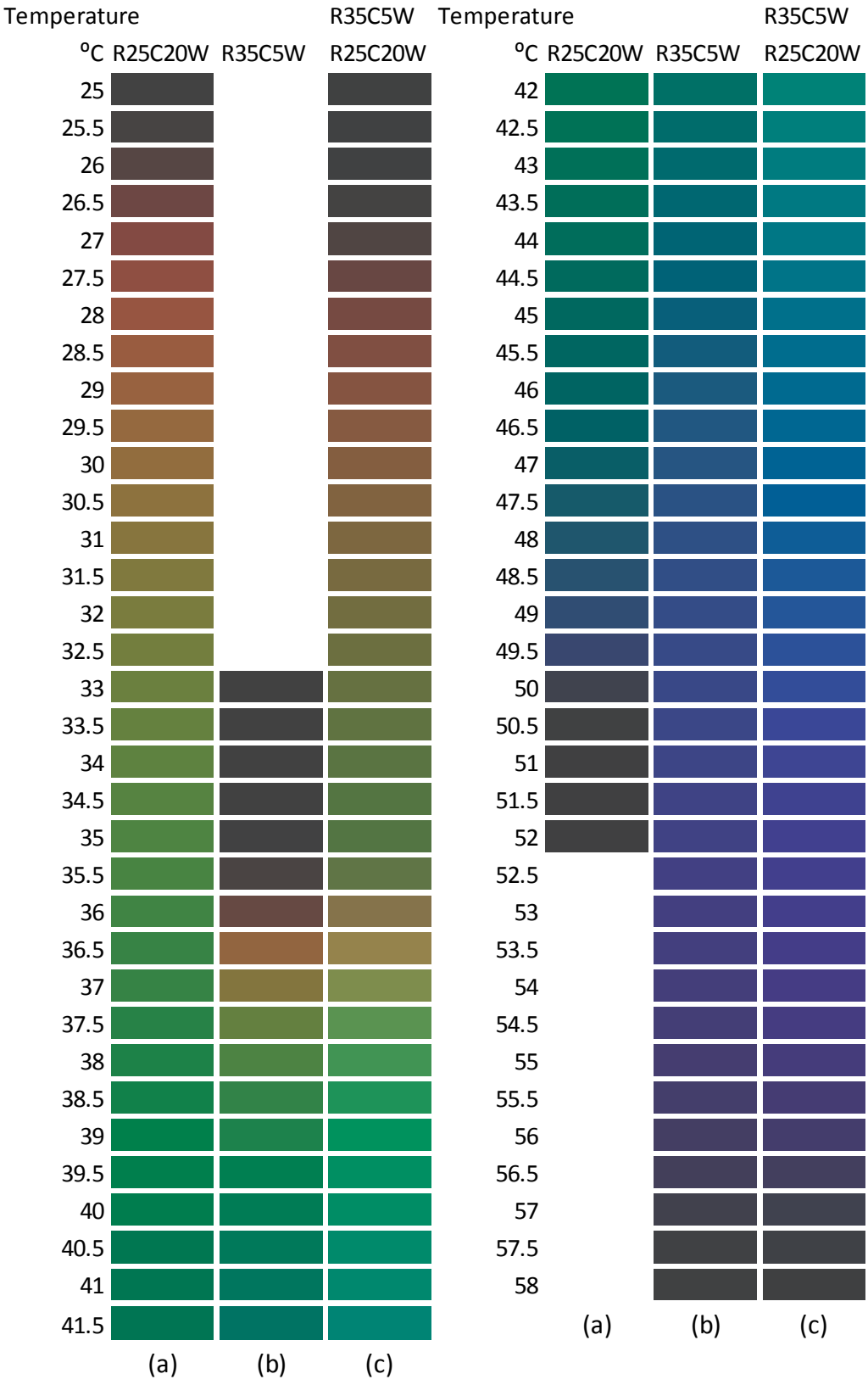

Figure 4.97 RGB colour display of R35C5W&R25C20W, coated on a black sheet

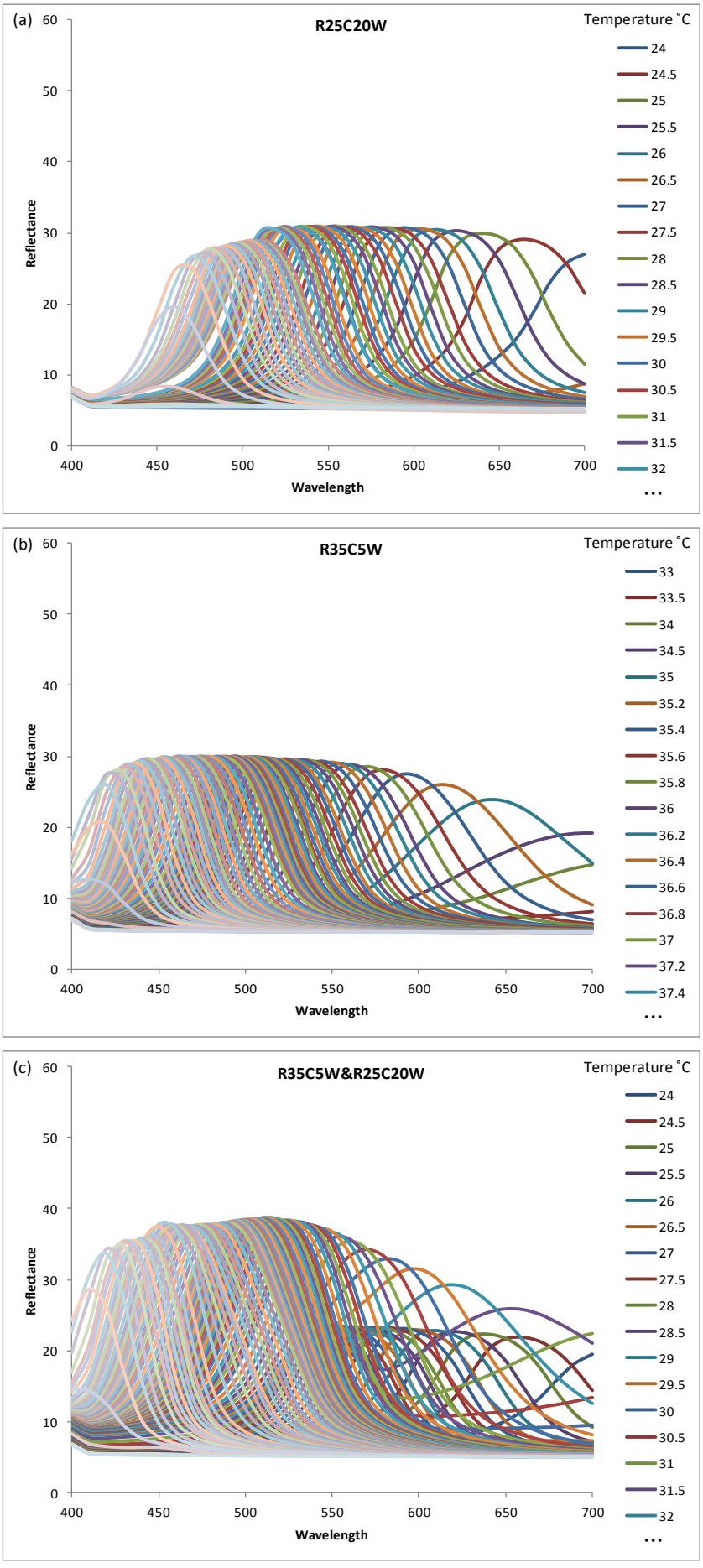

Figure 4.98 Reflectance curves of R35C5W&R25C20W, coated on a black sheet

Figures 4.95 (a)-(d) shows a^*b^* diagrams of the liquid crystals, individually and overlaid. R35C5W (b) starts colour play at 35.6°C. The colour change is fairly rapid in the first quadrant and greenish yellow zone with temperature. R35C5W shows relatively more colour saturation in the fourth quadrant as R35C1W and in contrast to R25C20W and R30C20W. R35C5W layered over R25C20W, (c) and (d), show similar colour change behaviour in the first and second quadrant, as discussed in section 4.4.2. The saturation of the over-layered form is similar to that of the individuals when both liquid crystals are in the cholesteric phase. A pronounced additive colour mixing effect is observed from 38°C to the isotropic phase, resulting in saturated, brighter colours. This high saturation is probably due to the cumulative reflection of similar colours from both individual liquid crystals. In Figure 4.96, L^* values of over-layered form show similar behaviour up to the highest peak at 37°C, as discussed in section 4.4.2. The higher lightness remains up to the isotropic phase of the first liquid crystal at around 51°C and then the curve follows a similar trajectory as the second liquid crystal. A small peak in the curve at about 57°C, near the isotropic phase of the over-layered liquid crystals may indicate the blue phase.

RGB colour displays of individual and over-layered liquid crystals, in Figure 4.97, show similar colour play start phenomena as discussed in section 4.4.2. From 38°C, the over-layered liquid crystals reflect light and bright greens. The second liquid crystal quickly turns to blue at 44°C due to the relatively small temperature bandwidth and causes a change in the colour of the over-layered form into bright cyan which subsequently becomes bright blue as the first liquid crystal also reflects blue. The light and bright colours, obtained from dark and dull colours, indicate additive colour mixing. The brighter blues of over-layered crystal are observed up to the end of the colour play of the first liquid crystal, after which blue is similar to the second liquid crystal. In Figure 4.98, the over-layered form shows a decrease in reflectance in the 550-700 nm range due to restricted reflectance of the first liquid crystal by the upper layer of the second, in the smectic A phase. Larger peaks of the over-layered form in the red region (600-700 nm) are due to dominance by the second liquid crystal. In the 420-550 nm range, the reflectance of the over-layered form shows prominent increases due to additive mixing of reflections with similar wavelengths.

4.4.4 R40C5W layered over R35C1W

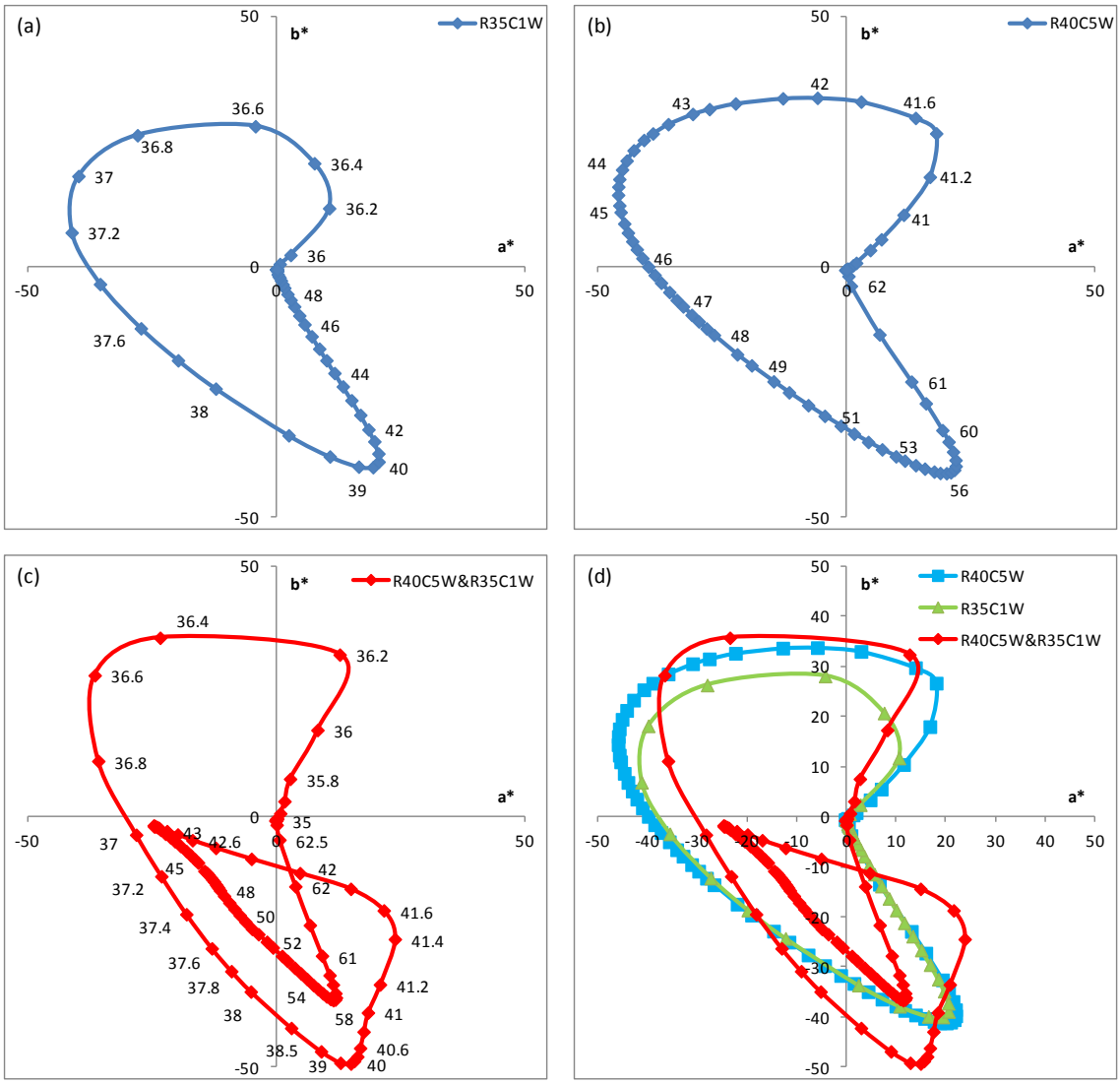

Figure 4.99 a*b* diagram of R40C5W&R35C1W, with data labels in °C, coated on a black sheet

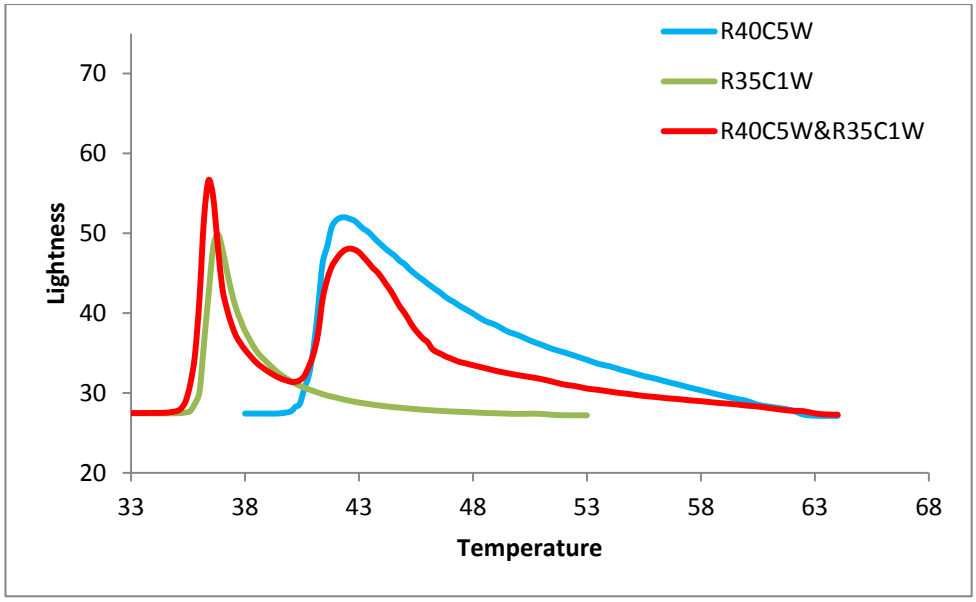

Figure 4.100 Effect of temperature on lightness of R40C5W&R35C1W, coated on a black sheet

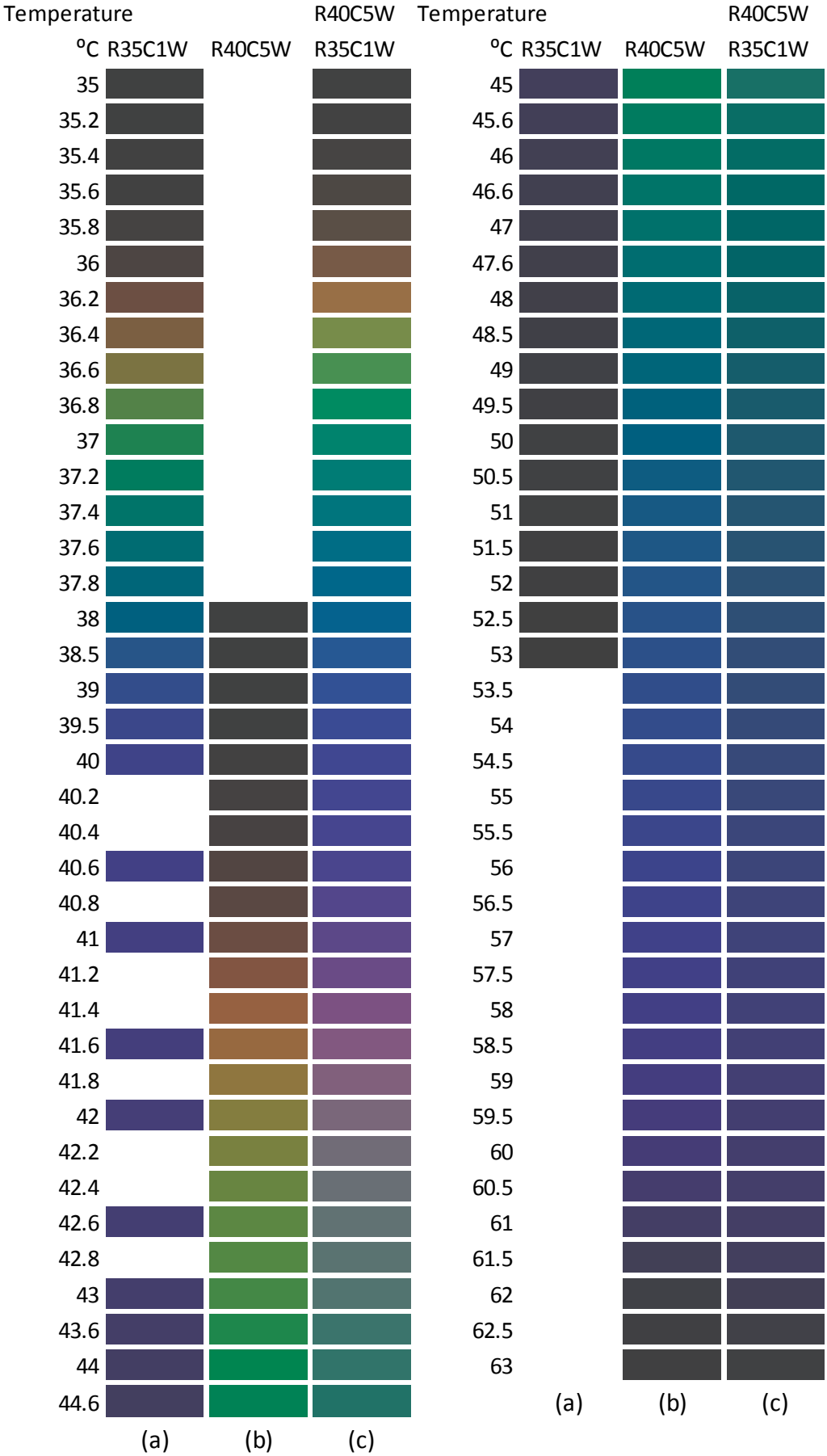

Figure 4.101 RGB colour display of R40C5W&R35C1W, coated on a black sheet

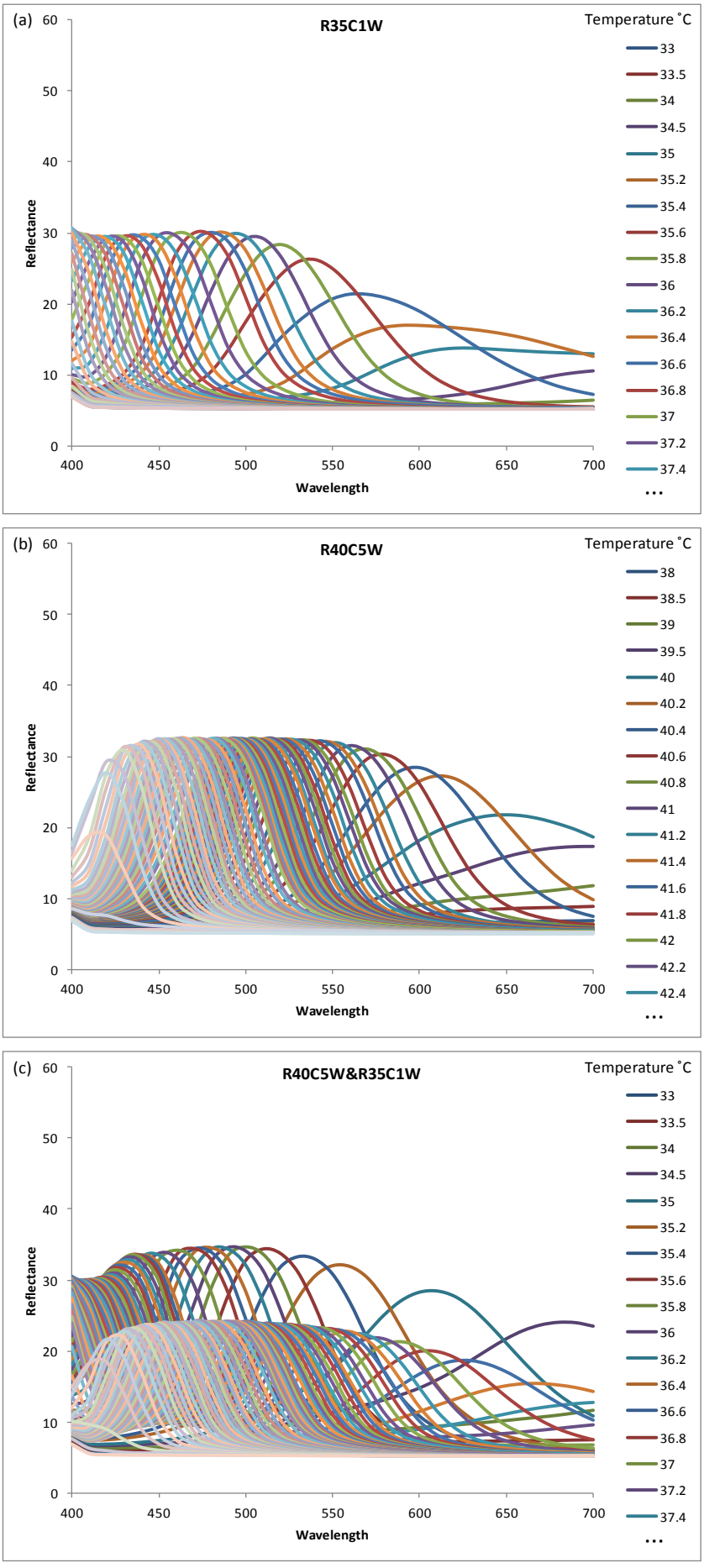

Figure 4.102 Reflectance curves of R40C5W&R35C1W, coated on a black sheet

Figures 4.99 (a)-(d) show a^*b^* diagrams of the liquid crystals, individually and collectively. The colour development of R40C5W (b) starts at 40°C and the colour change is similar to the R35C5W. R40C5W also shows more colour saturation in the fourth quadrant like R35C1W and R35C5W and in contrast to R25C20W and R30C20W. The a^*b^* diagrams of R40C5W layered over R35C1W, (c)-(d), show a start of colour play at 35.4°C, a little earlier than individual R35C1W, possibly due to variation in thickness of the coated layer. Initially, the over-layered form progresses towards yellow more than towards red, in contrast to those individually measured. At 36.2°C, where the maximum $+b^*$ value (yellow) is achieved, the $+a^*$ value (red) is close to the maximum value achieved by the individually measured liquid crystals. The over-layered liquid crystals then change colour quickly to become greenish yellow with the maximum $-a^*$ value (green) achieved at 36.6°C. The over-layered liquid crystals enter the fourth quadrant through the third with a rapid colour change. The maximum $-b^*$ value (blue) for the over-layered form, higher than for individually measured liquid crystals, is achieved at 40°C, the temperature at which the individual first liquid crystal achieves maximum saturation (reddish blue) and moves towards the origin as the second liquid crystal starts colour play. The activity of the first liquid crystal in the over-layered form in yellow and blue region before the second liquid crystal starts its colour play is unusual and there is no obvious explanation. At 40°C, the over-layered liquid crystals progress towards red due to the start of colour play by the second liquid crystal. At 41.4-41.6°C, an unusual bluish-red to purple colour is obtained by additive mixing, which is not shown by individually measured liquid crystals. As the second liquid crystal progresses towards yellow and green zones, the curve of the over-layered form moves towards the third quadrant passing near to the origin due to additive mixing with the blue colour, reflected by the first liquid crystal. The curve of the over-layered form progresses towards the horizontal coordinate in the third quadrant. However, at about 45°C, where the individual second liquid crystal becomes green and entering the third quadrant, the curve diverts back towards the fourth quadrant slowly. This time, the over-layered liquid crystals progress slowly in the fourth quadrant and divert to the origin at 58°C, where the individual second liquid crystal also turns to the origin. The colour saturation of over-layered liquid crystals, from 42°C to the isotropic phase, is low. The first liquid crystal reflects reddish blue and the second yellowish green which combine additively to give broad reflection with low saturation.

In Figure 4.100, the lightness of over-layered form starts to develop a little earlier than individual R35C1W, as discussed previously. In the case of individual liquid crystals, the lightness reaches its maximum values at temperatures giving a greenish yellow colour. In over-layered form, there are two peaks, corresponding to the peaks of the individual liquid crystals. The enhanced lightness in the first peak represents the unusual saturated yellow at about 36.4°C, as identified in the a^*b^* diagram. The second peak of the over-layered form at around 42°C represents the second liquid crystal with lower lightness. There is no clear sign of blue phase in this combination.

The RGB colour displays are shown in Figure 4.101. Up to 41°C, the colour of the over-layered form changes from red to blue through yellow and green as the individual first liquid crystal. However, the colours are brighter as discussed previously. From 41.2°C to 41.8°C, unusual reddish blue to purple colours are observed due to additive colour mixing. In the temperature range 42-43°C, the colours have a greyish tone due to additive mixing of reddish blue of the first liquid crystal, and greenish yellow to yellowish green of the second. After 43°C, the over-layered form follows the colour change pattern of the second liquid crystal. However, colours are duller and darker. In Figure 4.102, the over-layered liquid crystals show two peaks in the reflectance curves. The higher peaks match with the peaks of the individual first liquid crystal and the lower peaks with the second.

The a^*b^* diagrams, L^* values plotted against temperature, RGB colour displays and reflectance curves of a further range of over-layered liquid crystal combinations, having similar colour change phenomena which may be explained in similar ways as discussed in sections 4.4.1-4.4.4, are given in appendix A.

4.4.5 Comparison between Liquid Crystals coated directly on Black Sheet and on Transparent Sheets

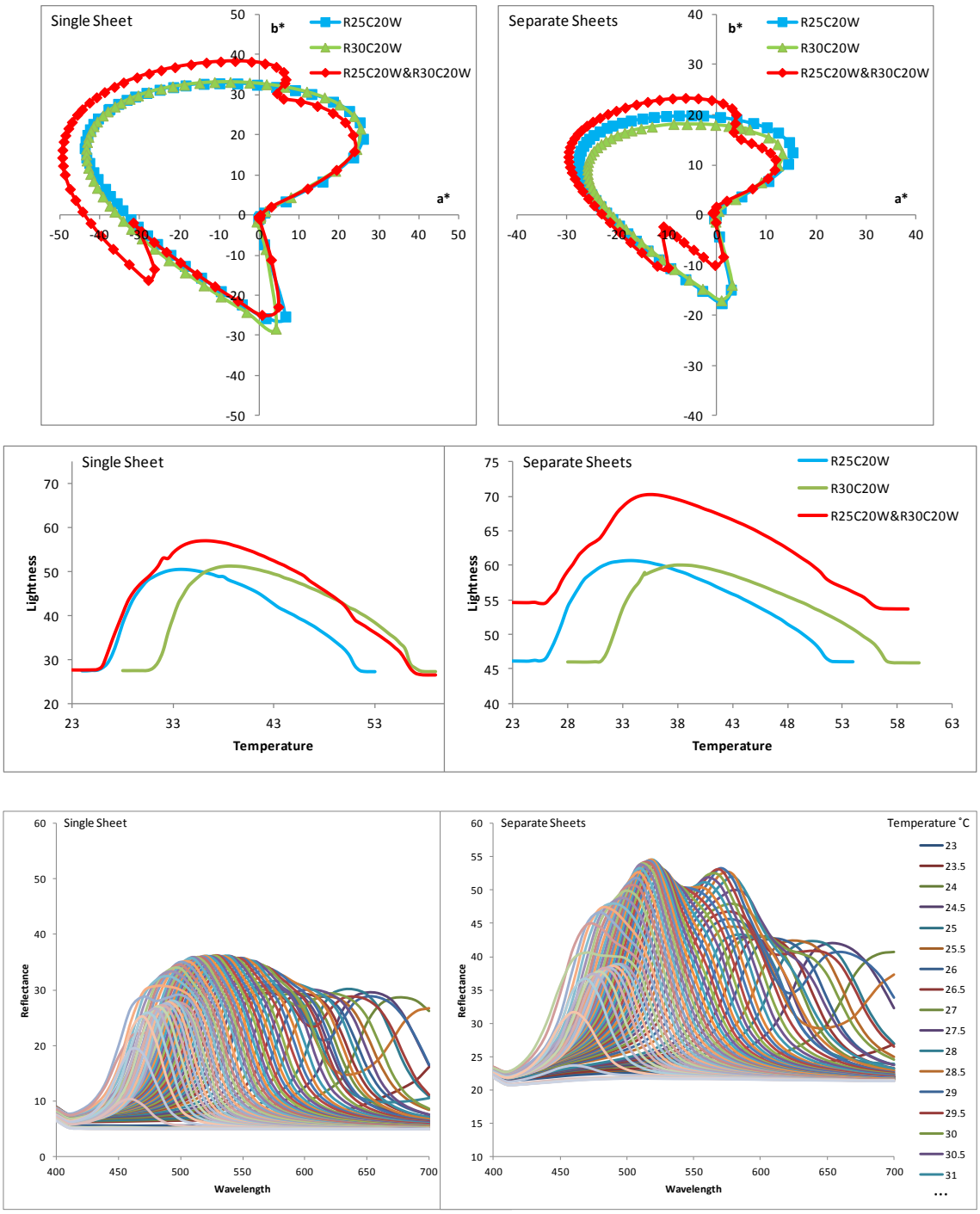

Figure 4.103 Comparison of R25C20W&R30C20W, coated on a black sheet and separate sheets

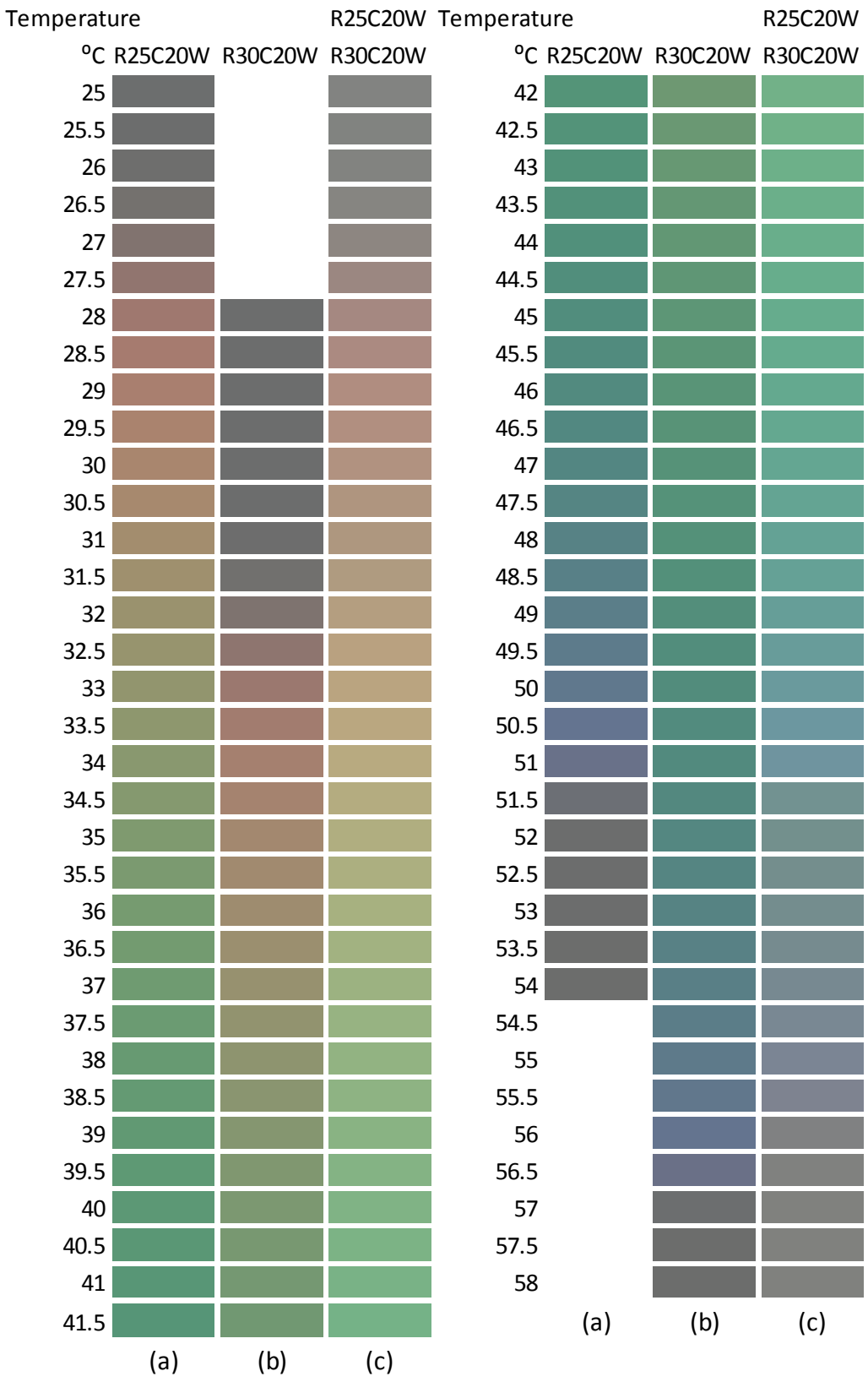

Figure 4.104 RGB colour display of R25C20W&R30C20W, coated on separate sheets

Initially, the liquid crystals were coated on transparent sheets individually and combinations were made by layering these sheets over each other with a black sheet behind to absorb the transmitted light for colour measurement. This method for making

combinations offered the advantages of being easy and versatile, and it was anticipated that it might not have a significant effect on measurements. However, it was found that when liquid crystals were layered over each other directly by coating on a black polyester sheet as discussed in sections 3.7.4 and 4.4, significant differences were observed. Consequently the second method was adopted for the evaluation. However, an example of a comparative study of the liquid crystals coated on a black sheet and on transparent sheets is described here.

Colour measurements were taken for R25C20W layered over R30C20W and individual liquid crystals, coated directly on black sheets, and for those coated on transparent sheets, layered over a black sheet. Figure 4.103 shows the comparison between the two methods. The a^*b^* diagrams show similar trends in colour play for individually and over-layered measured liquid crystals, in both cases. However, the colour saturation, using the transparent sheet method is considerably less than using the black sheet alone. It was also visually observed that the coated liquid crystals showed more cloudiness on transparent sheets as compared to black sheets. The L^* values against temperature, show the same trend in curves for the two methods. However, the lightness using transparent sheets is higher than using the black sheet, even before the start of colour play. The reflectance curves using separate transparent sheets show two clear peaks which are not present using the single black sheet. The initial reflectance values using transparent sheets are higher than using the black sheet. The lower colour saturation, high lightness and reflectance values with transparent sheets compared with black sheets, is consistent with the observed cloudiness of the liquid crystals on the transparent sheets, resulting in light reflected, before reaching the lower layer of liquid crystals, causing in turn an increase in lightness and reflectance, and a decrease in colour saturation. This may also involve an increase in gloss levels of the transparent polyester sheets, due to the presence of multiple sheets.

Figure 4.104 shows the RGB colour displays of individual and over-layered liquid crystals, coated on transparent sheets. The colours demonstrated by liquid crystals coated on transparent sheets are lighter, duller and lower in colour saturation compared to the colours demonstrated by the liquid crystals coated directly on black sheets, as shown in Figure 4.89, both for the individual and the over-layered liquid crystals. However, the colour change trends are similar for the both methods. Therefore, it is apparent that the liquid crystals coated directly on a black polyester sheet show higher colour saturation than when coated on transparent sheets. The lightness and reflectance

values increase with an increase in the number of transparent sheets used. Although it is an easier technique to layer liquid crystals using transparent sheets i.e., a number of combinations can be made using only individually coated liquid crystals, the colours are inferior.

4.4.6 Change in Sequence of Overlaying Liquid Crystals for Single Black Sheet

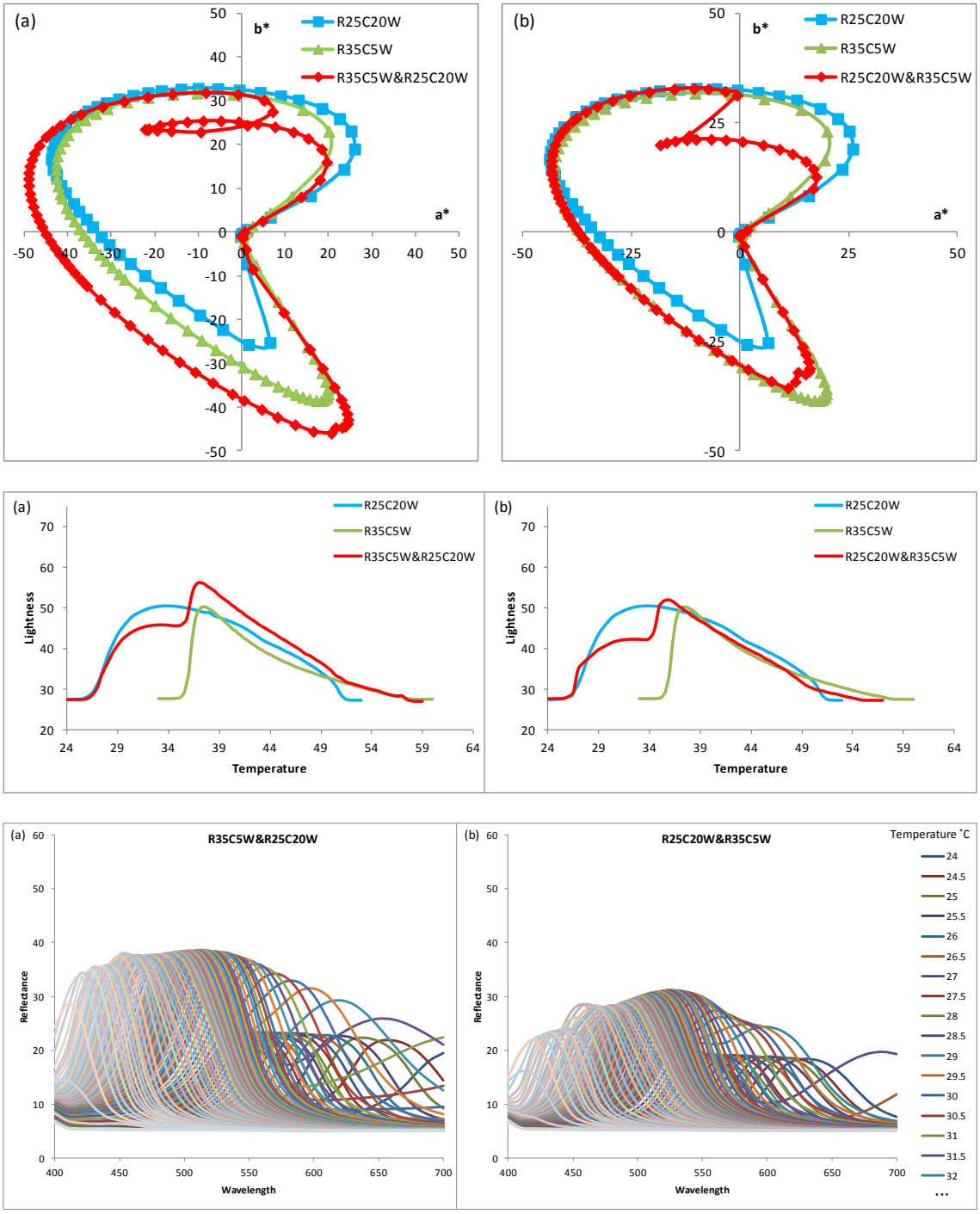

Figure 4.105 Comparison of R35C5W&R25C20W, over-layered on each other, coated on a black sheet (a) R35C5W in upper layer, R25C20W in lower layer (b) R35C5W in lower layer, R25C20W in upper layer

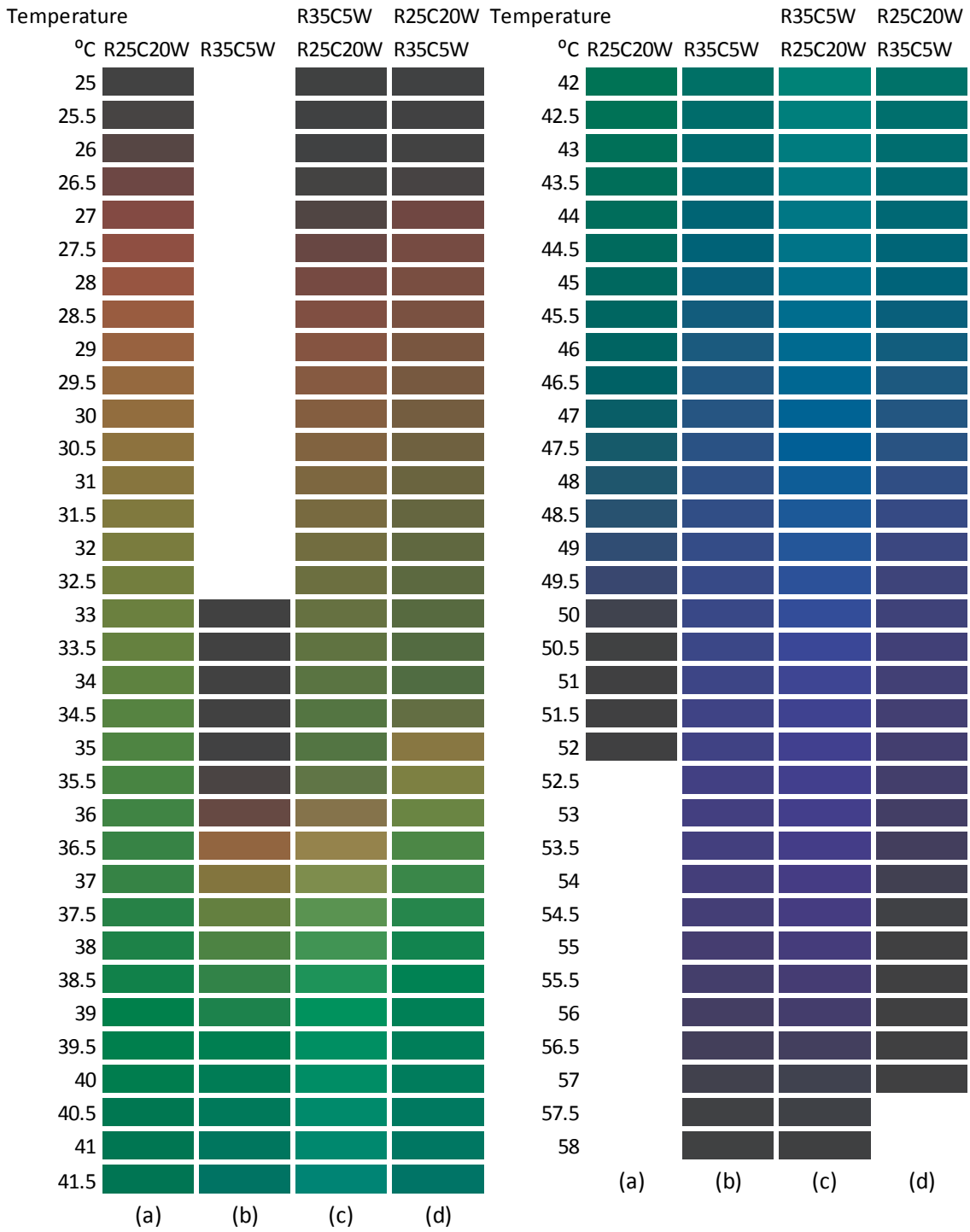

Figure 4.106 RGB colour display of R35C5W&R25C20W, over-layered on each other, coated on a black sheet

The liquid crystals were coated on each other in specific sequences. In most cases investigated, the first liquid crystal, i.e., coated first on black sheet, was that which starts colour play at an early temperature, or in the case of an equivalent colour play start temperature, the liquid crystal with smaller temperature bandwidth was used as the first liquid crystal. The liquid crystal reflects specific wavelengths of visible light according to the pitch length which varies with temperature. The remaining wavelengths are transmitted, to be absorbed by the black background. In the case of completely

transparent over-layered liquid crystals, it is expected that the upper coated layer of the second liquid crystal reflects some wavelengths and these become unavailable to interact with the first liquid crystal underneath. In the case of layers with opacity, the effect of one liquid crystal can dominate the effect of the other. There is thus a possibility of variation in reflected colours by the same over-layered liquid crystal combinations, coated in different sequences. To investigate this effect, over-layered liquid crystals were prepared with alternate sequences of and assessed by colour measurement with varying temperature.

Figure 4.105 shows a^*b^* diagrams, L^* values and reflectance curves of R35C5W layered over (a) and under (b) R25C20W with varying temperatures. Case (a) has been discussed in detail in section 4.4.3. The curves for the two cases are similar but not identical. In a^*b^* diagrams, R35C5W layered over R25C20W, the loop in the second quadrant is associated with the start of the colour play of R35C5W. There is a more pronounced loop in (a) than in (b). This effect may be due to R25C20W in the upper layer, (b), dominating the reflected colours over R35C5W, the red colour of which causes the loop. This is reasonable as the full colour effect operates from the upper layer, while only some wavelengths penetrate to the lower layer. From green through to the blue zone, the colour saturation is higher in (a) than (b). This may be explained since R35C5W reflects more saturated colours in this region as shown by the individual liquid crystals and provides more pronounced additive mixing when it is in the upper layer. In L^* values graphs, the over-layered liquid crystals show higher lightness in (a) than (b) especially at the peak value for R35C5W. This is again consistent with the dominance of R35C5W in the upper layer. A similar explanation accounts for trends observed in the reflectance values. Another comparison example for R30C20W layered over and under R25C20W, describing similar results, is given in appendix B. Therefore, it can probably be concluded that for optimum saturation and brightness in the over-layered form, the individual liquid crystal which reflects more saturated and brighter colours, should be coated in the upper layer. This effect is illustrated in the RGB colour display in Figure 4.106.

4.4.7 Colour Hysteresis of Individual and Over-layered Liquid Crystals during Heating and Cooling

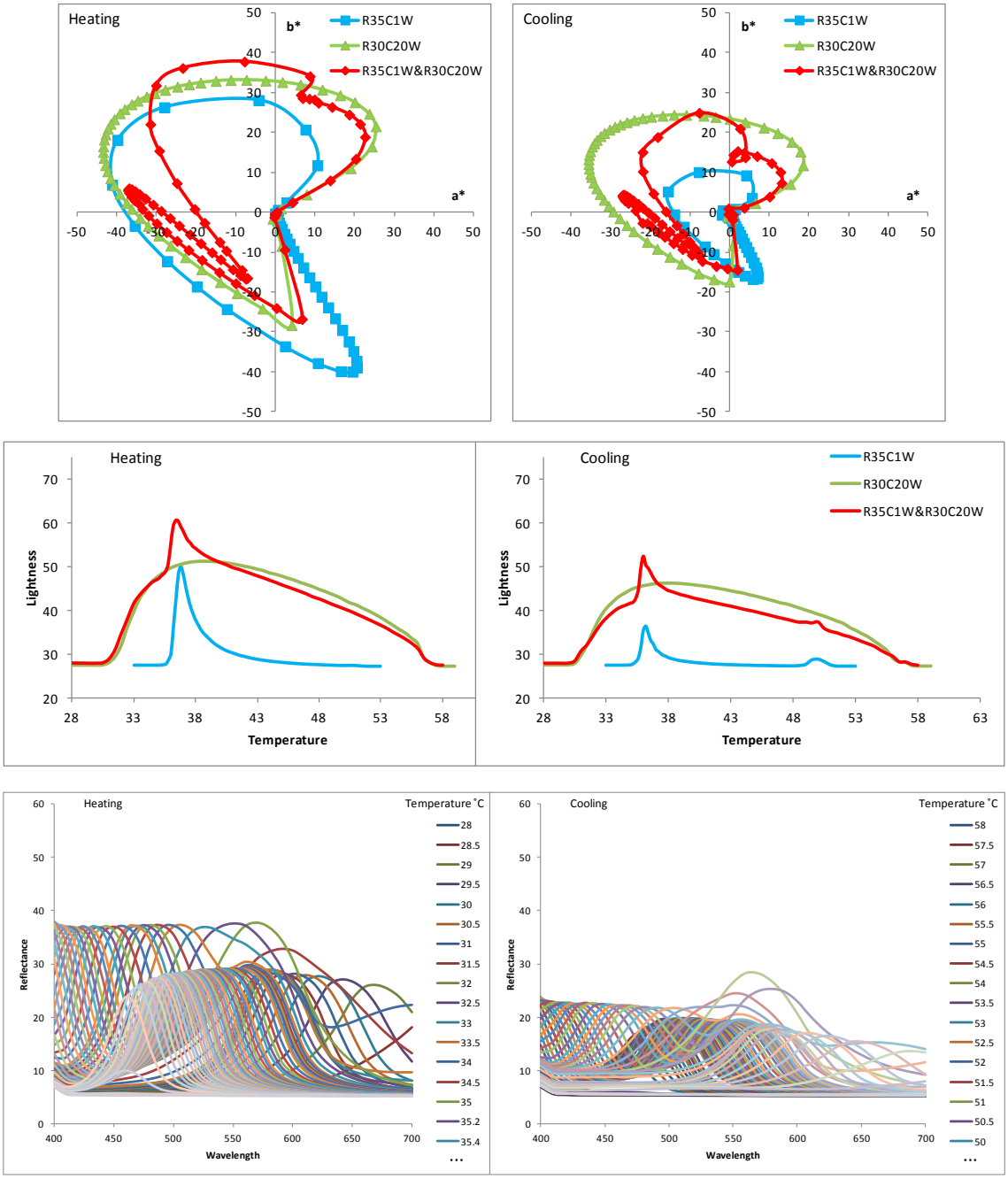

Figure 4.107 Comparison of heating up and cooling down of R35C1W&R30C20W, coated on a black sheet

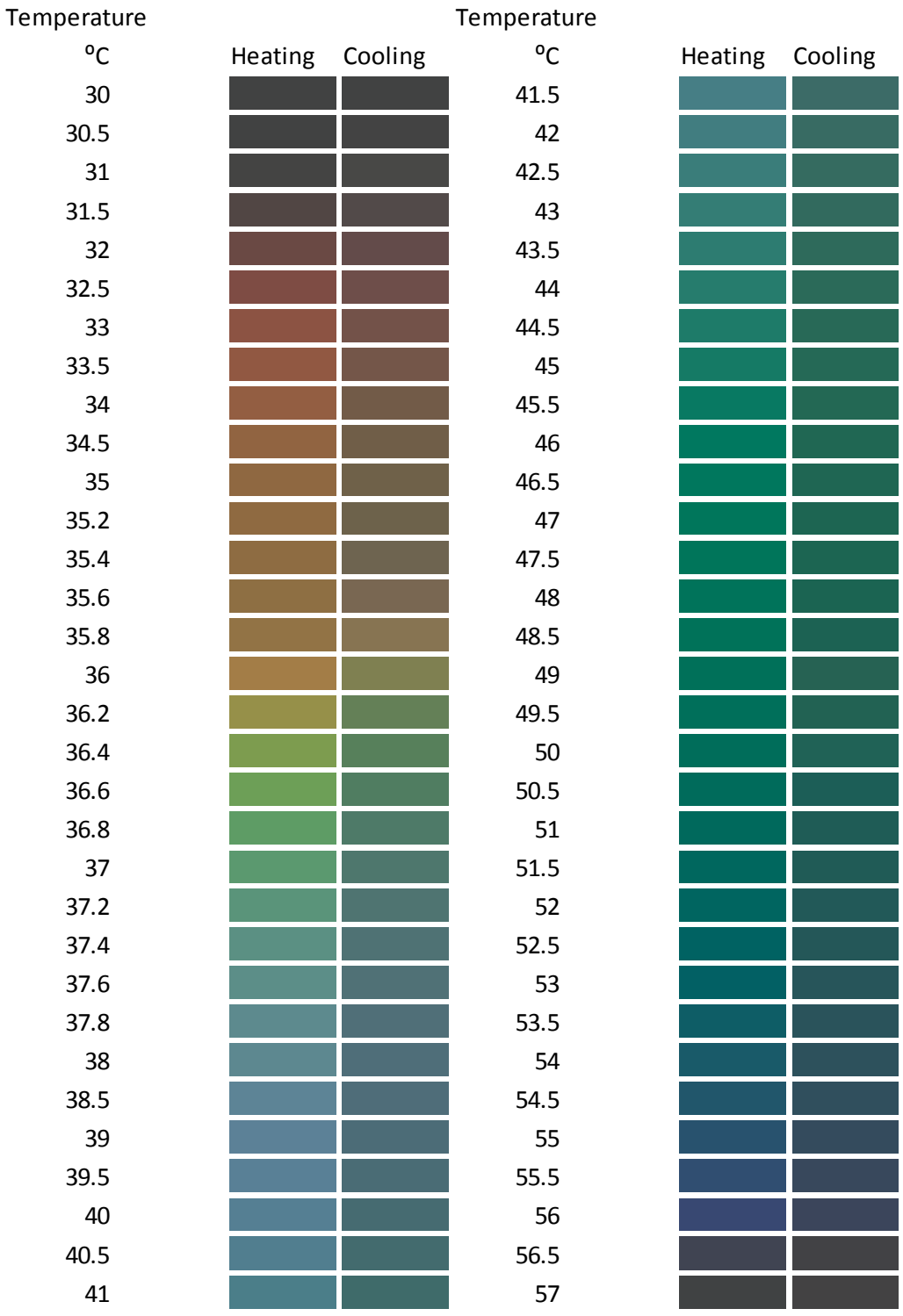

Figure 4.108 RGB colour display of heating up and cooling down of R35C1W&R30C20W, coated on a black sheet

In leuco dye based thermochromic pigments, colour hysteresis was observed during heating and cooling of the printed samples as discussed in section 4.3. Colour hysteresis has also been reported in a previous study of liquid crystals in our laboratories [25]. It was envisaged that the over-layered liquid crystals may also show

some hysteresis. Therefore, to investigate this, colour measurements were also taken during cooling of individual and over-layered liquid crystals. The temperature interval was kept the same as during heating, as discussed in section 4.4.

Figure 4.107 shows a^*b^* diagrams, L^* values and reflectance curves of R35C1W layered over R30C20W, during heating and cooling. In a^*b^* diagrams, the liquid crystals individually and in over-layered form show higher colour saturation during heating than during cooling. However, the individual and over-layered liquid crystals show similar colour change trends in both cases. The L^* values show reduced lightness during cooling as compared to heating. The reflectance curves show depressed phenomena for over-layered liquid crystals during cooling. On heating, the reflectance curves show two clear peaks at most temperatures, indicating the colour play of individual liquid crystals while in cooling, the curves are more complex and it is not easy to differentiate. Figure 4.108 shows colour displays during heating and cooling cycles of over-layered liquid crystals. During heating, the reflected colours are quite bright. However, during cooling, there are duller and darker tones with some greyish tones, such as in the blues around 38-41°C and near the isotropic phase. Some colours notably the yellow, green and blue appear at lower temperatures during cooling than during heating. Therefore, R35C1W and R30C20W, individually and over-layered, show duller and darker colours with less saturation during cooling. However, the trends in colour change are similar in both cases. Some more comparative colour hysteresis illustrations providing similar effects are given in appendix C.

The reason for the differences in reflected colours by the liquid crystals during heating and cooling cycles, is that they exhibit the plane or Grandjean texture when heated i.e., towards the isotropic phase from the cholesteric phase and on cooling, they exhibit the focal-conic texture when cooled i.e., towards the cholesteric phase from the isotropic phase. The plane or Grandjean texture selectively reflects wavelengths, while the focal-conic texture causes diffuse scattering and appears milky. However, the duller and darker reflected colours during cooling suggest that the focal-conic texture is not formed completely in the microcapsules [25]. As a result, the reflected colours during heating are brighter and more saturated than during cooling. The same colour may appear at a higher temperature during heating, as compared to during cooling.

4.4.8 Comparison of Measurements with Specular Included and Excluded

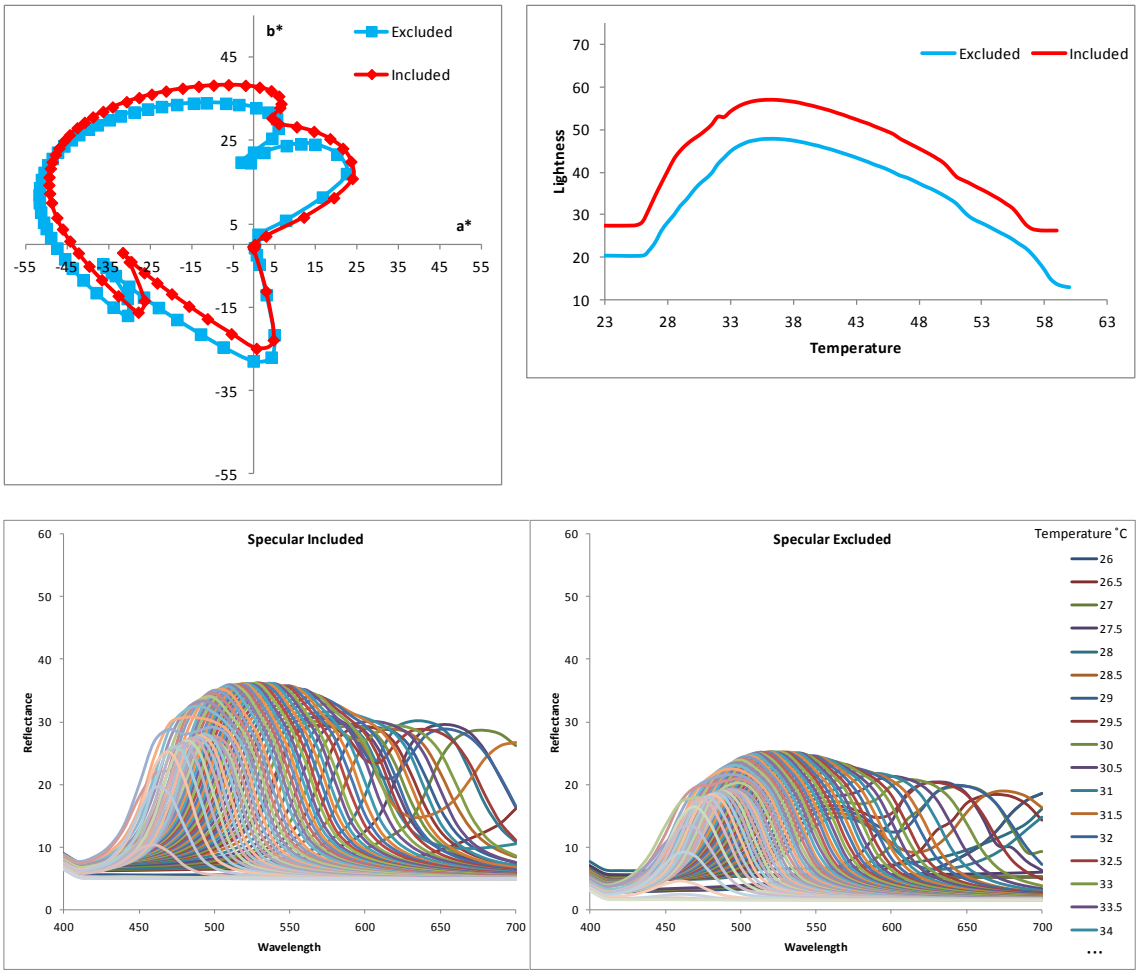

Figure 4.109 Specular included and excluded comparison of R25C20W&R30C20W, coated on a black sheet

It is an ultimate aim of this research programme that the liquid crystals would be used in combination with leuco dye based thermochromic pigments printed on a fabric. Therefore, the colour measurements of liquid crystals in all cases used calibration conditions established for leuco dye based thermochromic pigments i.e., small aperture, specular included, UV light off, with 3 flashes and 3 readings before acceptance, as discussed in section 4.1.1. It was envisaged that the liquid crystals, coated on glossy polyester sheets, might show some differences due to specular included and excluded. However, it was intended to use the liquid crystals in combination with the leuco dye based thermochromic pigments printed on fabric, and therefore, for consistency, the same calibration conditions were used. However, to assess the differences due to specular included and excluded, colour measurements of R25C20W layered over R30C20W, coated on a black sheet, were taken with temperature in both cases.

Figure 4.109 shows a^*b^* diagram, L^* values against temperature and reflectance curves for both specular included and excluded. In the a^*b^* diagram, the specular included and excluded show a similar colour change pattern. The colour saturation with specular included is higher in the first and second quadrant, while specular excluded gives higher saturation in the third and fourth quadrant. In the case of L^* values, the lightness is higher with specular included. The reflectance curves also show higher peaks with specular included. Both features are as expected as there is more reflection when specular is included.

4.5 Liquid Crystal coated on Leuco Dye based Thermochromic Printed Fabric

The leuco dye based themrochromic pigments change from coloured to colourless while the liquid crystals reflects colours through the whole spectrum with temperature. In view of potential design applications, a study of combinations of leuco dye based and liquid crystal thermochromics was carried out. To observe the reflected colour from cholesteric liquid crystals, it is necessary to absorb the transmitted wavelengths of light, using a black background. Therefore, a black leuco dye based thermochromic pigment was selected for the investigation. A black leuco dye based thermochromic pigment with a colour change temperature at 40°C, was selected with liquid crystals with colour play start lower than 40°C. The black pigment was printed by screen printing on the cotton fabric and cured using the optimum conditions i.e., 110°C for 10 minutes as discussed in section 4.1.3. The liquid crystals were coated on the fabric with the method developed as discussed in section 3.7.4. The liquid crystal coated fabrics were assessed using colour measurement at varying temperatures.

4.5.1 Black Leuco Dye based Thermochromic Prints

The colour measurements were taken for black leuco dye based thermochromic print. Figure 4.110 shows integ values plotted against temperature from 30°C to 54°C. The integ values start to decrease as soon as the temperature starts to increase. There is a progressive change in integ values with temperature with the lowest value observed at about 48°C after which some residual black remains. There is no sharp change at the reported activation temperature of 40°C and also complete colour loss does not occur, as discussed in section 4.3. Figure 4.111 shows a colour display of the black thermochromic print with temperature. The colour shows a gradual colour change from deep black to light grey with temperature.

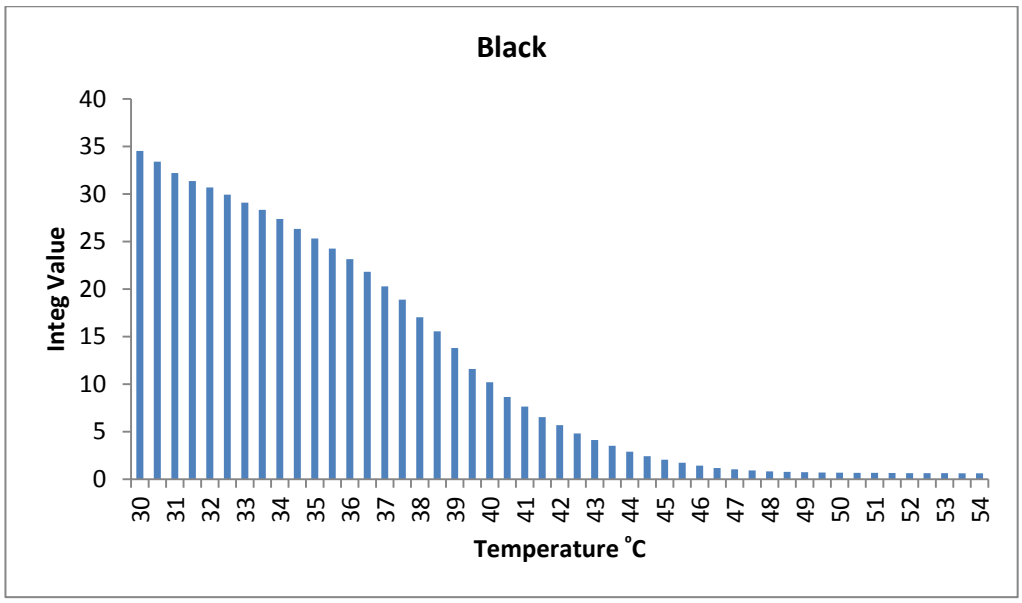

Figure 4.110 Integ values of black leuco dye based thermochromic pigment, printed on cotton fabric

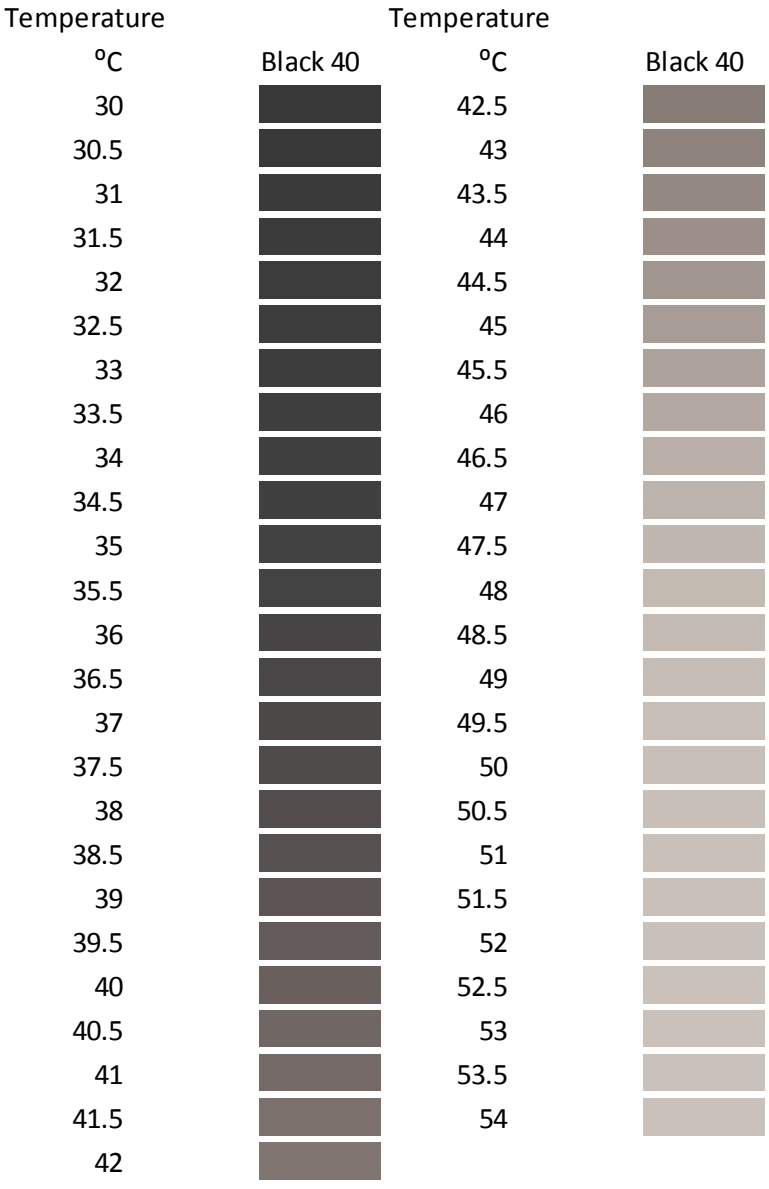

Figure 4.111 RGB colour display of black leuco dye based thermochromic pigment, printed on cotton fabric

4.5.2 R25C20W coated on Black Leuco Dye based Thermochromic Print

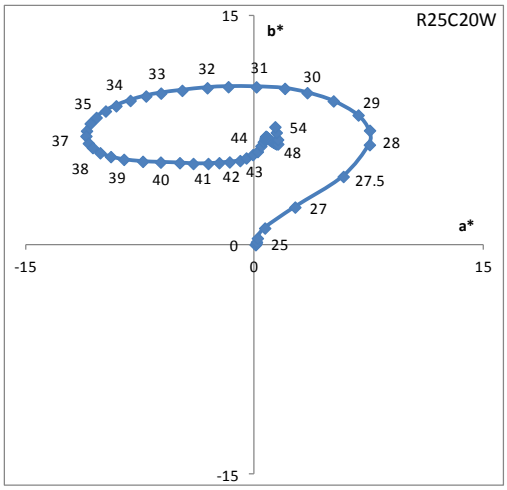

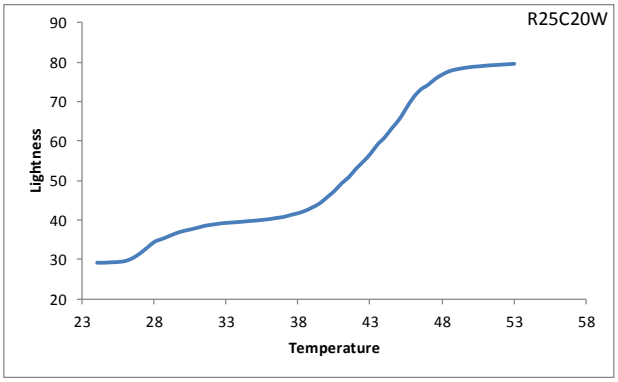

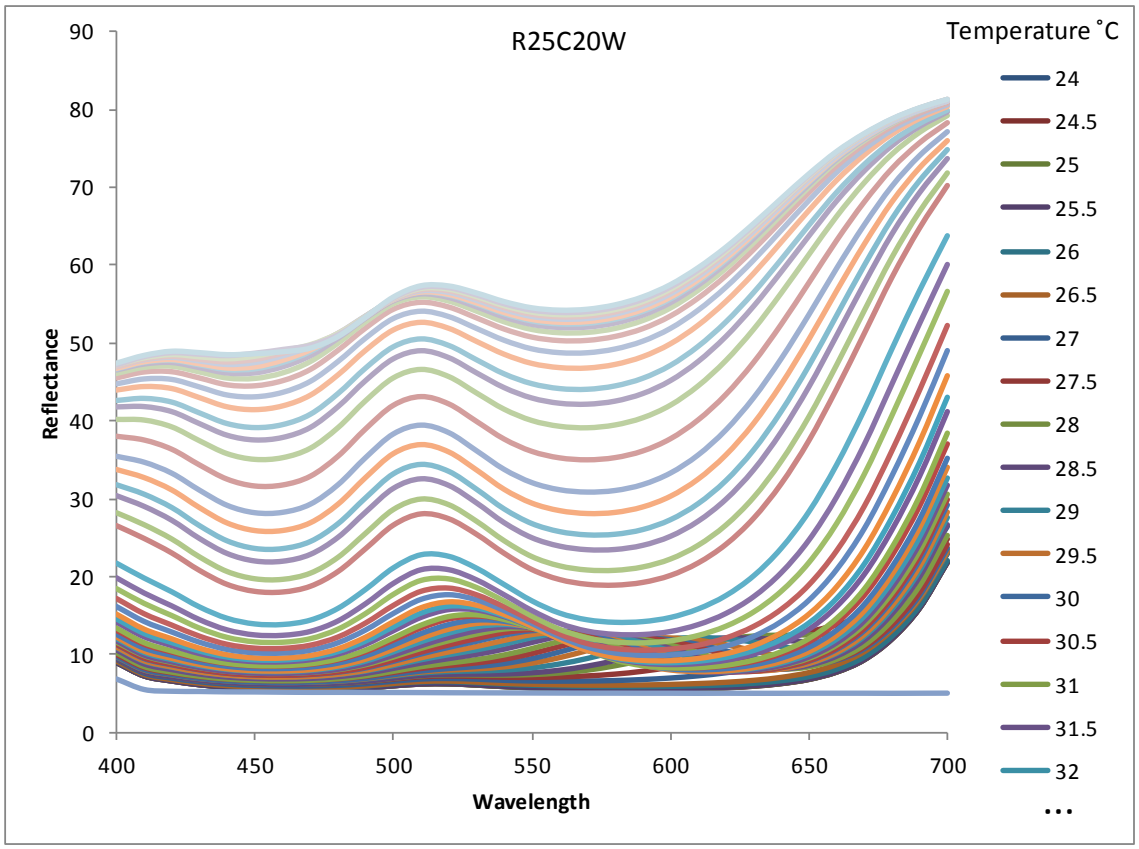

Figure 4.112 a*b* diagram, lightness and reflectance curves of R25C20W, coated on black leuco dye based thermochromic printed fabric

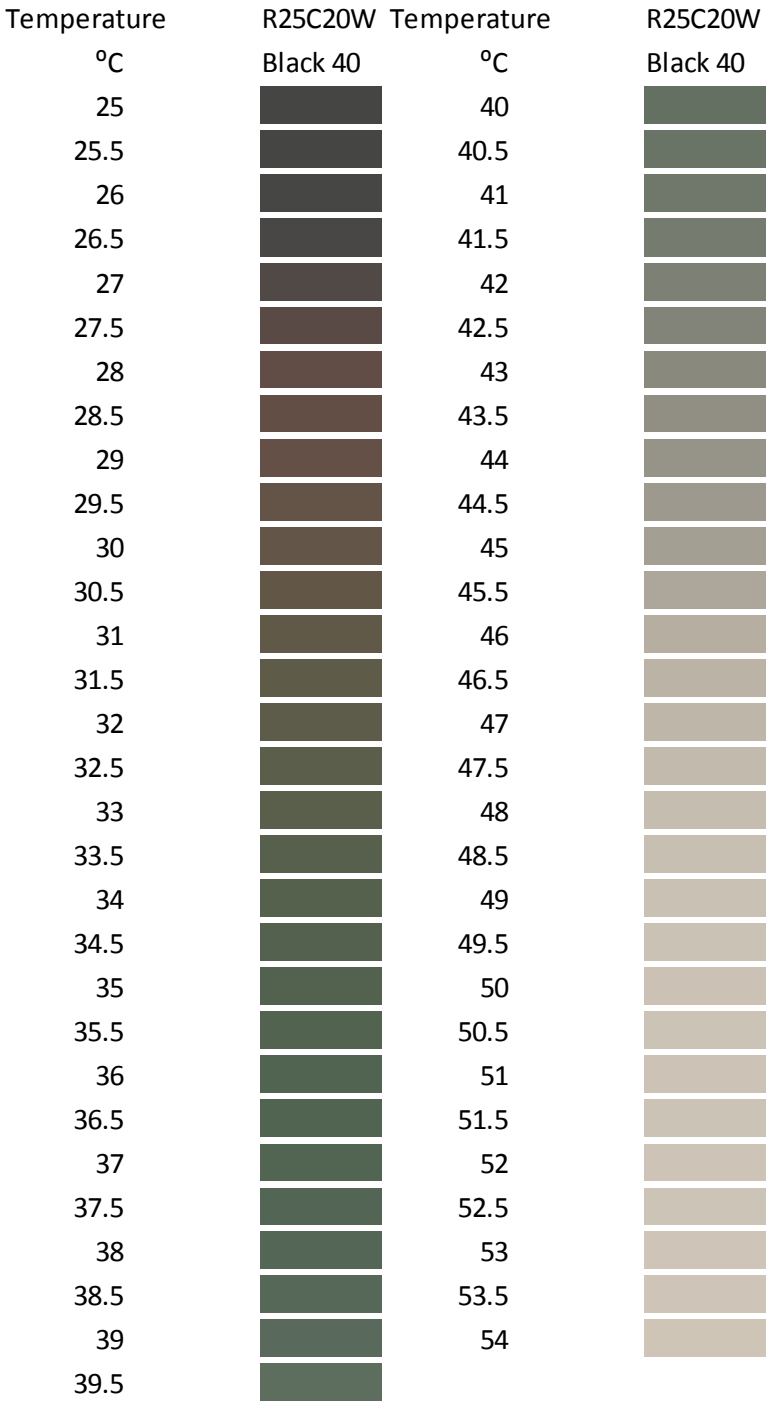

Figure 4.113 RGB colour display of R25C20W, coated on black leuco dye based thermochromic printed fabric

R25C20W was coated on the black leuco dye based thermochromic printed fabric and colour measurements were taken with temperature. Figure 4.112 shows the a^*b^* diagram, L^* values against temperature and reflectance curves. The colour saturation obtained from R25C20W in this case is much less as compared to the same liquid crystal coated directly on a black polyester sheet (section 4.4.1), indicated by the small scale used. The liquid crystal starts colour play at 25°C and the colour continues to develop in the first quadrant. The colour changes from red to yellowish green, through yellow. As the temperature increases, the black background also turns into grey. At

37°C, the a^*b^* curve diverts to the first quadrant. The colour play ends in the reddish yellow region, but close to the origin, at a point which indicates the background grey colour when the liquid crystal is in the isotropic phase. The gradual colour change towards the first quadrant near origin after diversion, rather than the third and fourth quadrants, indicate that the most wavelengths transmitted by the liquid crystals are reflected back by the light grey background. Therefore, the reflected colours of the liquid crystal are not apparent.

The lightness increases at the start of colour play of the liquid crystal. However, at around 40°C, it increases dramatically as black converts to grey in the background. The reflectance curves are broad with only small peaks as most of the incident light across the visible spectrum is reflected. As the temperature increases, the reflectance curves become broaden and with higher values. Figure 4.113 shows the colour display of the liquid crystal over leuco dye based thermochromics. The reflected colours are very dull and dark and mostly with greyish tone, due to low saturation consistent with the a^*b^* diagram. Brownish red colours are observed from 27°C to 29°C which then converts to yellowish brown, however, yellow colour is mostly dominated by grey. From 31°C, the colour changes gradually to dull green and eventually to grey around 41°C. The blue of the liquid crystal does not appear, because the background has become light grey and reflects most of the wavelengths transmitted by the liquid crystal.

4.5.3 R35C1W coated on Black Leuco Dye based Thermochromic Print

The a^*b^* diagram of R35C1W coated on the black leuco dye, Figure 4.114, also show low saturation. However, the liquid crystal proceeds through all four quadrants before the black background turns to light grey, due to the narrow temperature bandwidth of 1°C. It may also be due to the high reflection of this liquid crystal in fourth quadrant, as discussed and illustrated in section 4.4.2. The liquid crystal starts the colour play at 36°C and rapidly progresses from red to green, through yellow, until it achieves the maximum reddish blue. The blue colour is observed in this case as the background is still a reasonable black. After that point, the black background turns into grey and then light grey and the colour of liquid crystal progresses towards the reddish yellow region, where the light grey of the background lies.

The lightness curve shows a gradual increase up to 37°C, where it shows a peak which due to maximum lightness of the liquid crystal in the greenish yellow region.

Afterwards, the lightness curve shows a progressive increase until 47°C, where it achieves its maximum value. Some reflectance curves show small peaks at certain wavelengths which indicate the rapid change of colour through the whole spectrum. In Figure 4.115, the red and yellow colours of the liquid crystals are mostly dominated by grey due to low colour saturation. At 37.6°C, it reflects dull green which turns into blue at around 39°C. This blue turns into grey about 42°C and then gradually becomes light yellowish grey.

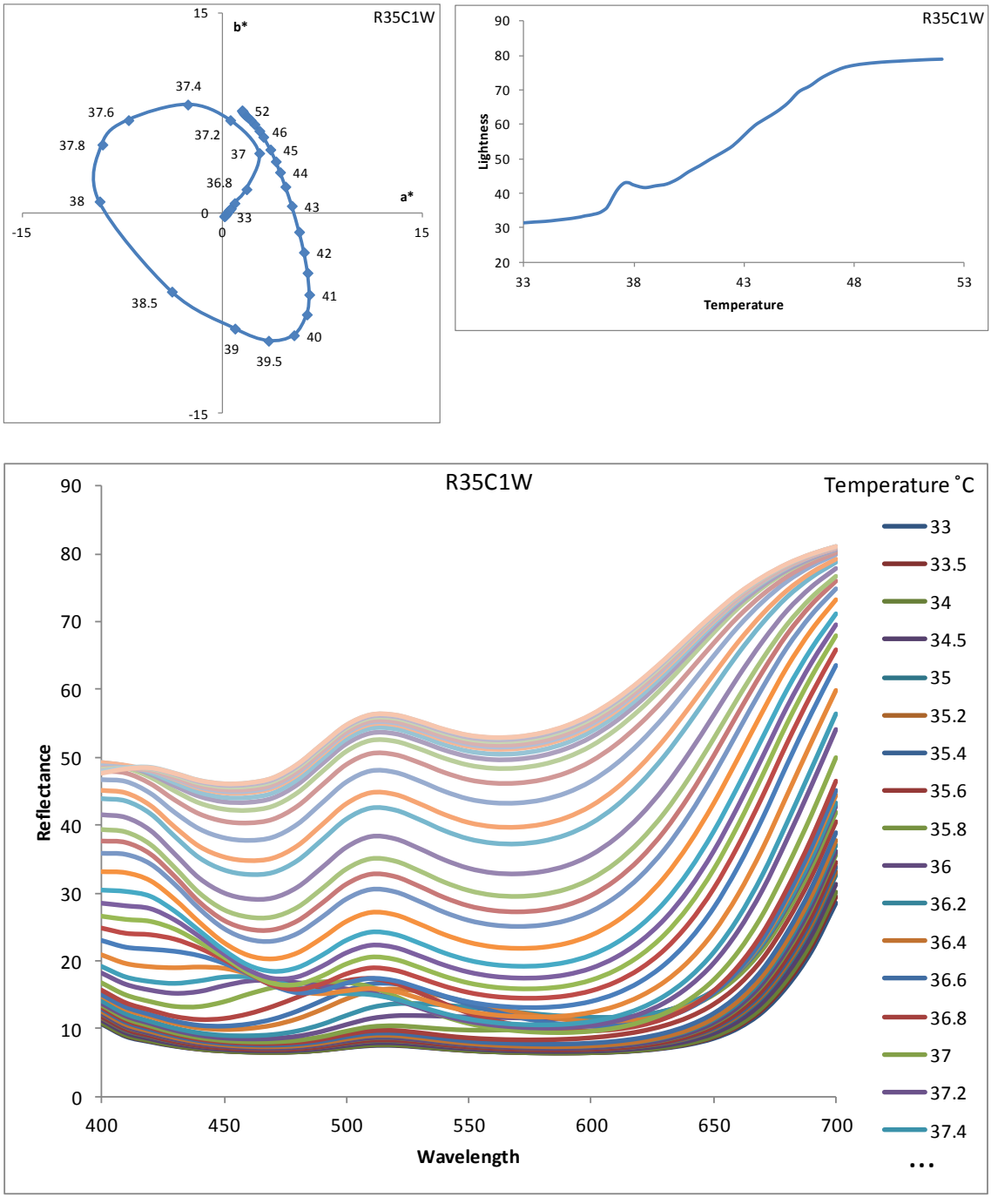

Figure 4.114 a*b* diagram, lightness and reflectance curves of R35C1W, coated on black leuco dye based thermochromic printed fabric

Temperature °C	R35C1W Black 40	Temperature °C	R35C1W Black 40
35		41.5	
35.2		42	
35.4		42.5	
35.6		43	
35.8		43.5	
36		44	
36.2		44.5	
36.4		45	
36.6		45.5	
36.8		46	
37		46.5	
37.2		47	
37.4		47.5	
37.6		48	
37.8		48.5	
38		49	
38.5		49.5	
39		50	
39.5		50.5	
40		51	
40.5		51.5	
41		52	

Figure 4.115 RGB colour display of R35C1W, coated on black leuco dye based thermochromic printed fabric

Some more liquid crystals coated on black leuco dye based thermochromic prints, having similar colour change phenomena as illustrated in sections 4.5.2-4.5.3, are given in appendix D.

Chapter 5. Conclusions and Future Work

5.1 Conclusions

Thermochromic pigments are well known in some areas of common usage such as thermometers, kettles, jewellery, cosmetics, umbrellas etc. However, the use of these pigments in textiles remains limited which may be due to limited scope of application methods, inadequate fastness properties, cost of these pigments etc. The primary aim of the research was to establish application methods for thermochromic pigments with improved fastness properties and to explain and widen the colour spectra provided by liquid crystals by layering them over each other and over leuco dye based thermochromic pigments. It was also an aim to assess the properties of these pigments in textile applications and to investigate the improvement of their performance if possible.

The leuco dye based and liquid crystal thermochromic pigments used in this study were provided by LCR Hallcrest. The slurry form of leuco dye based thermochromic pigments was available in magenta, orange, blue, green and black colours while blue and red colours were available in powder form. R25C20W, R30C20W, R35C1W, R35C5W and R40C5W liquid crystals were provided, especially made for the research purposes. The leuco dye based thermochromic pigments in slurry form were applied by screen printing. The properties of these pigments were assessed instrumentally by colour measurement. For consistent results, the optimum conditions for colour measurements were established as small aperture, specular included, UV light off, 3 flashes, 3 readings before acceptance and at a temperature of 22 ± 1°C. Colour measurement with temperature variation was carried out with the spectrophotometer used in conjunction with a digitally-controlled hot stage.

Leuco dye based thermochromic pigments are sensitive towards high temperatures where they lose colour strength in prints. It was found that the colour loss also depends on the exposure time, although with less impact. Therefore, it is proposed that the processing temperature of thermochromic prints should be kept as low as possible. However, temperatures of up to 110°C have little impact.

In the literature, the printing of fabric with thermochromic pigments is noted but the suitable binders and curing conditions are not described. Establishing a printing system becomes more important due to the sensitivity of these pigments to high temperatures

which narrows the choice of binders and curing conditions. The fastness properties, such as to washing, rubbing etc. which depend on binders and curing conditions, require improvement but not at the expense of colour strength. Therefore, commercially available binders recommended by providers, from different chemical classes, polyacrylate, silicon modified polyurethane, polyurethane and butadiene, were used. The butadiene-based binder gave good fastness properties along with good colour strength. The optimum curing conditions were established as 110°C for 10 minutes for the preferred binder in this study, with a small element of compromise.

The colour concentration normally used is determined by the required colour strength. However, above a certain concentration, a further increase does not affect colour strength, and would cause a wastage of pigment, raising the cost and adversely affecting fastness properties. Microencapsulated leuco dye based thermochromic systems contain a number of components which restricts the amount of colour-producing substance, thus limiting the colour strength. It was found that the maximum colour strength is normally achieved between 20% and 30% concentrations of pigment on the weight of the paste. Above this concentration causes a decrease in colour strength, probably due to opacity introduced by components other than colour former.

The lightfastness of leuco dye based thermochromic pigments is generally poor. Normally, additives to improve lightfastness are used in the formulations. In this study, research was carried out to improve lightfastness at the application stage. UV absorbers were found to be better lightfastness enhancers than antioxidants and HALS, probably due to the different mechanisms of protection. They absorb harmful UV radiation while the other additives protect by reacting with the chromophore or intermediate species produced during UV degradation. In the case of microencapsulated thermochromics, HALS and antioxidants cannot react with colour former due to inaccessibility, while UV absorbers may protect the colour former by absorbing UV radiation. Further investigation revealed that an increased amount of UV absorbers gave better performance. A non-phenolic UV absorber was more efficient than phenolic UV absorbers.

The powder form of leuco dye based thermochromic pigments were successfully incorporated into PP, LLDPE and EVA filaments by extrusion, over a range of temperatures from 130°C to 260°C. Ram extrusion was not suitable for thermochromic filaments due to lack of homogeneous mixing, although it provided a basis to assess

processing parameters of the polymers. Screw extrusion homogeneously mixed thermochromic powder into the polymers. The filaments were drawn on a drawing machine with a heating facility.

Thermochromic filaments were obtained which changed colour reversibly with temperature. In SEM images, PP and EVA filaments showed smooth surfaces while LLDPE was striated, which may be formed during drawing. SEM images showed thermochromic microcapsules as aggregates inside the filaments. The formation of aggregates probably occurs during manufacturing, as SEM images of powders also showed aggregates. There was no obvious sign of ruptured microcapsules from SEM images, which was anticipated as a possibility during extrusion. There is no indication of microcapsules on the surface of polymers, so that they appear to have become an integral part of filaments.

The colour strength might have been expected to be higher for the filaments processed at low temperature. However, the colour strength of filaments was found to be highest in LLDPE and lowest in EVA, with PP between these. The explanation may involve the role of optical properties of the polymers such as gloss, opacity, translucency and transparency or the level of dispersion of the pigment. Washing and rubbing tests of the filaments show no sign of pigment release. The lightfastness in PP and EVA is better than in LLDPE which may be due to better UV absorption properties or reflection due to the glossy surface. The lightfastness of the filaments was found to be better than the printed samples.

DSC scans of filaments show that the thermochromic pigments increase the onset and degradation peak temperatures, possibly due to the high degradation temperature of the polymer used in wall construction of microcapsules, which is mostly cross-linked melamine formaldehyde. It was found that the tensile strength of PP filaments was the highest and EVA lowest, with LLDPE in the middle. However, EVA is more stretchable than PP and LLDPE. The tensile properties such as maximum load, strength and tenacity are better in the case of unpigmented filaments than blue and red filaments, although the blue and red filaments are more stretchable. This indicates that the thermochromic microcapsules disrupt the filament structure and introduce weak points, while facilitating the polymer chains to slide over each other, before breakage.

Colour measurement of leuco dye based thermochromic prints with temperature variation showed that the change from coloured to colourless is gradual rather than sharp at the reported temperature. The colour change starts earlier than the reported activation temperature and a completely colourless state is normally not achieved even at high temperatures. The leuco dye based thermochromic pigments give colour by interaction of colour former and developer in the solid state of the solvent. The results indicate that the solvent melts over a temperature range and causes the disintegration of colour former and developer complex to occur gradually. The residual colour at high temperature probably indicates that complete disintegration of colour former and developer does not occur. Colour build up during cooling occurs at lower temperatures and is rapid, illustrating colour hysteresis, in which the re-integration on cooling occurs at lower temperatures as the solvent solidifies.

The liquid crystal thermochromics with different activation and bandwidth temperatures, when layered over each other, produce an unusual range of bright and intense colours, including orange, lilac, purple and pink. On the basis of extensive research carried out for over-layered combinations of liquid crystals, a system is proposed accounting for the nature of reflected colours:

- Individual liquid crystals change quickly through the red and yellow zone while in green and blue zone, they persist longer with varying temperature;

- The start and end of the colour play temperatures for a combination of over-layered liquid crystals depend on the liquid crystal with lower colour play start temperature and on the liquid crystal with higher end of colour play temperature respectively;

- The over-layered liquid crystals change colour initially according to the colour change of the liquid crystal with a lower activation temperature. The lightness increases rapidly as the colour play starts. The saturation of the over-layered form is lower than that of the liquid crystal with the lower activation temperature, when the other liquid crystal is in its smectic A phase because of its opacity;

- From the start of the colour play of the liquid crystal with the higher activation temperature, additive colour mixing is observed, i.e., the reflected wavelengths by the individual liquid crystals mix additively to give a new colour which is normally brighter and lighter;

- At any specific temperature, the saturation and brightness of colours of over-layered liquid crystals when both liquid crystals are in the cholesteric phase, depend on how different colours reflected by the individual liquid crystals are, and also opacity, thickness and sequence of layers of liquid crystals. Normally the effect is dominated by the upper layer;

- A destructive effect giving low saturation and brightness is observed in over-layered liquid crystals if the reflected colours by individual liquid crystals are in opposing positions in the a^*b^* diagram, and a broad reflection results;

- A higher saturation and brightness of over-layered liquid crystals is observed if the individual reflected colours are similar and thus interact constructively;

- A neutral effect, i.e., similar saturation and brightness in the over-layered form as that of individual liquid crystals is observed if the colours are close but not identical in the a^*b^* diagram;

- Normally, after achieving the maximum blue by both liquid crystals in over-layered form, the change towards the isotropic phase is rapid;

- The lightness curve is more difficult to interpret, probably due to complex optical effects in liquid crystals, especially when over-layered.

The combinations of over-layered liquid crystals may be prepared by coating one by one, on a black sheet or by layering over the liquid crystals, individually coated on transparent sheets and finally a black sheet to absorb the transmitted wavelengths. The colour change patterns are similar using the two methods. However, in the method using transparent sheets, the saturation and brightness of reflected colours reduce while the lightness increases possibly due to increased gloss effect of multiple sheets.

In over-layered combinations, the liquid crystals were coated on each other after drying of the first coated layer. In a comparative study of change in sequence of coated layers, it was found that the liquid crystal, present in upper layer, generally dominates the colour, especially in terms of the saturation and brightness of the over-layered form. Therefore, for brighter and saturated colours of over-layered form, it is suggested that the individual liquid crystal with brighter and more saturated colours should preferably be coated in the upper layer.

The over-layered liquid crystals show hysteresis in heating from smectic A phase to the isotropic phase and cooling from the isotropic phase to smectic A phase. The explanation is that during heating, the over-layered liquid crystals exhibit the plane or Grandjean texture which reflects selective colours according to the refractive indices and cholesteric pitch lengths of the liquid crystals. In contrast, during cooling, the liquid crystals enter into the cholesteric phase from the isotropic phase partially in the focal-conic texture which reflects similar selective colours as that of the plane texture but with lower saturation and brightness, although normally gives a milky effect. Therefore, for a specific colour to be achieved, it is necessary to know the history of the liquid crystals, whether the colour is achieved during heating or cooling.

The liquid crystals were also coated on a black leuco dye based thermochromic printed fabric. The black thermochromic print changes colour with temperature and causes a dynamic colour change of background from black to light yellowish grey. The liquid crystals coated on black thermochromic prints show an incomplete colour spectrum, mostly in the red, yellow and green zone, depending on their colour play start temperatures and temperature bandwidths. The complete spectrum can be observed with lower colour play start temperatures and shorter temperature bandwidths. The low colour saturation and brightness of the liquid crystals on thermochromic printed fabric, is due to the low intensity of black colour, and its dynamic colour change to give lighter backgrounds which reflect the transmitted wavelengths of light.

The study of over-layered liquid crystals has provided a scientific understanding of the additive colour mixing properties, which provides the basis to facilitate creative design applications, for which the RGB colour display approach provides a potentially useful tool.

5.2 Future Work

5.2.1 Ink Jet Printing

From the SEM results of blue and red thermochromic pigments, the sizes of microcapsules were in the range 1-5 micron. These microcapsules are found in aggregates. Provided that the sizes of microcapsules may be kept lower than 1 micron and aggregates disintegrate to individual microcapsules, these pigments have the potential to be used in ink formulation with a suitable dispersing agent and other ingredients for ink jet printing.

5.2.2 Lightfastness

Liquid crystals are normally used in the microencapsulated form. As the lightfastness of leuco dye based thermochromic pigments have been improved by using UV absorbers, an investigation of lightfastness improvement of liquid crystals might also be carried out using UV absorbers. As with the leuco dye type, HALS and antioxidant would not be expected to work because of the microencapsulation.

5.2.3 Incorporation of Liquid Crystals in Extrusion

Cholesteric liquid crystals reflect specific wavelengths depending on the refractive index and cholesteric pitch length and transmit the rest of wavelengths of white light. To see the reflected colour, normally a black background is used to absorb the transmitted wavelengths. Liquid crystal thermochromics might be incorporated in a suitable polymer and extruded with a device which can produce a black filament in the core. This will potentially open a wide area of applications for liquid crystals such as sensors, temperature-controlled displays, creative design applications etc.

5.2.4 Construction of Colour Prediction System for Over-layered Liquid Crystals

In over-layered liquid crystals, it is found that reflections may be constructive or destructive, depending on the additive mixing of similar or opposing colours respectively. It would be of interest to formulate an algorithm to predict the colour of over-layered liquid crystals in comparison with individual liquid crystals, at specific temperatures. The approach would be complex due to multiple transmission and reflection effects.

5.2.5 Microscopic Investigation of Over-layered Liquid Crystals

In over-layered form, individual liquid crystals may influence the saturation and brightness depending on the opacity in their smectic A phase, isotropic phase or near isotropic phase. A microscopic investigation would be interesting to observe the specific texture given by the individual liquid crystal at specific temperatures in over-layered form.

References

1. Bamfield P. Chromic Phenomena: Technological Applications of Colour Chemistry. London, The Royal Society of Chemistry; 2001, 1-41.

2. Periyasamy BS, Khanna G. Thermochromic colors in textiles. Available from: www.americosind.com. [cited on 29/02/2012]

3. Bouas-Laurent H, Durr H. Organic photochromism (IUPAC Technical Report). Pure and Applied Chemistry. 2001; 73 (4): 639–665.

4. Christie RM. Colour Chemistry. Royal Society of Chemistry; 2001. 186-188.

5. Samat A, Lokshin V. Organic Photochromic and Thermochromic Compounds Volum 2. Kluwer Academic/Plenum Publishers; 1999. 415-460.

6. Day JH. Thermochromism. Chemical Review. 1963; 63: 65–80.

7. Tajima M. Thermochromic Character of Dyes. Dyes and Pigments. 1987; 8: 119–127.

8. Burkinshaw SM, Griffiths J, Towns AD. Colour Science ’98. University of Leeds, Department of Colour Chemistry; 1999. 174-183.

9. Aitken D, Burkinshaw SM, Griffiths J, Towns AD. Textile applications of thermochromic systems. Review of Progress in Coloration. 1996; 26: 1–8.

10. Tilley RJD. Colour and Optical properties of Materials. 2nd edition. John Wiley & Sons Ltd.; 2011.

11. Yan J, Jiao M, Rao L, Wu S-T. Experimental demonstration of tunable phase in a thermochromic infrared-reflectarray metamaterial. Optics Express. 2010; 18 (2): 1330–1335.

12. Sen AK. Coated Textiles: Principles and Applications. 2nd edition. CRC Press; 2007. 187-188.

13. Kim S, Suh H, Cui J, Gal Y, Jin S, Koh K. Crystalline-state photochromism and thermochromism of new spiroxazine. Dyes and Pigments 2002; 53 (3): 251–256.

14. Hadjoudis E, Vittorakis M, Moustakali-Mavridis I. Photochromism and thermochromism of schiff bases in the solid state and in rigid glasses. Tetrahedron 1987; 43 (7): 1345–1360.

15. Hadjoudis E, Mavridis IM. Photochromism and thermochromism of Schiff bases in the solid state: structural aspects. Chemical Society Reviews 2004; 33 (9): 579–588.

16. Di Nunzio MR, Gentili PL, Romani A, Favaro G. Photochromism and Thermochromism of some Spirooxazines and Naphthopyrans in the Solid State and in Polymeric Film. The Journal of Physical Chemistry 2010; 114 (13): 6123–6131.

17. Bamfield P. Chromic Phenomena: Tecnological Applications of Colour Chemistry. Royal Society of Chemistry; 2001. 305-314.

18. Bamfield P. Chromic Phenomena: Technological Applications of Color Chemistry. Journal of the American Chemical Society 2002; 124 (46): 13960–13960.

19. Christie RM, Bryant ID. The application of instrumental colour measurement methods to thermochromic printing inks. Surface coatings international. 1995; 78: 332–336.

20. Christie RM, Bryant ID. An evaluation of thermochromic prints based on microencapsulated liquid crystals using variable temperature colour measurement. Coloration Technology. 2005 121 (4): 187–192.

21. Burkinshaw SM, Griffiths J, Towns AD. Reversibly thermochromic systems based on pH-sensitive functional dyes. Journal of Materials Chemistry. 1998; 8, 2677–2683.

22. Rihs G, Weish CD. Interaction of color formers and co-reactants. Part I. First crystal structures of the colorforming species composed of crystal violet lactone and metal. Dyes and Pigments. 1991; 15: 107-127.

23. Burkinshaw SM, Griffiths J, Towns AD. Reversibly thermochromic systems based on pH-sensitive. Journal of materials chemistry. 1998; 8: 2677–2683.

24. Naito K. Amorphous-crystal transition of organic dye assemblies: Application to rewritable color recording media. Applied Physics Letters, 1995, 67 (2), 211.

25. Bryant ID. Studies of thermochromic printing inks containing microencapsulated liquid crystalline materials, PhD thesis, Heriot Watt University. 1997.

26. Mendanha DV, Molina Ortiz SE, Favaro-Trindade CS, Mauri A, Monterrey-Quintero ES, Thomazini M. Microencapsulation of casein hydrolysate by complex coacervation with SPI/pectin. Food Research International. 2009; 42 (8): 1099–1104.

27. Saeki K. Microencapsulation of complex coacervation process using acid precurser gelatin. Applied Biochemistry and Biotechnology. 1984; 10: 251–254.

28. Nori MP, Favaro-Trindade CS, Matias De Alencar S, Thomazini M, De Camargo Balieiro JC, Contreras Castillo CJ. Microencapsulation of propolis extract by complex coacervation. LWT Food Science and Technology. 2011;44 (2): 429–35.

29. Siddiqui O, Taylor H. Physical factors affecting microencapsulation by simple coacervation of gelatin. The Journal of Pharmacy and Pharmacology. 1983; 35 (2): 70–73.

30. Mauguet MC, Legrand J, Brujes L, Carnelle G, Larre C, Popineau Y. Gliadin matrices for microencapsulation processes by simple coacervation method. Journal of Microencapsulation. 2002; 19 (3): 377–384.

31. Arshady R. Albumin microspheres and microcapsules: Manufacturing technique methodology. Journal of Controlled Release. 1990; 14: 111–131.

32. Arshady R. Preparation of microspheres and microcapsules by interfacial polycondensation techniques. Journal of Microencapsulation. 1989; 6 (1): 13–28.

33. Jabbari E. Morphology and structure of microcapsules prepared by interfacial polycondensation of methylene bis(phenyl isocyanate) with hexamethylene diamine. Journal of Microencapsulation. 2001; 18 (6): 801–809.

34. Kobašlija M, McQuade DT. Polyurea Microcapsules from Oil-in-Oil Emulsions via Interfacial Polymerization. Macromolecules 2006; 39 (19): 6371–6375.

35. Brown EN, Kessler MR, Sottos NR, White SR. In situ poly(urea-formaldehyde) microencapsulation of dicyclopentadiene. Journal of Microencapsulation 2003, 20 (6), 719-730.

36. Frere Y, Danicher L, Gramain P. Preparation of polyurethane microcapsules by interfacial polycondensation. European Polymer Journal 1998; 34 (2): 193–199.

37. Lu S, Xing J, Zhang Z, Jia G. Preparation and Characterization of Polyurea/Polyurethane Double-Shell Microcapsules Containing Butyl Stearate Through Interfacial Polymerization. Journal of Applied Polymer Science. 2011; 121: 3377–3383.

38. Pensé AM, Vauthier C, Benoit JP. Study of the interfacial polycondensation of isocyanate in the preparation of benzalkonium chloride loaded microcapsules. Colloid Polymer Science. 1994; 272 (2): 211–219.

39. Bouchemal K, Briançon S, Chaumont P, Fessi H, Zydowicz N. Microencapsulation of dehydroepiandrosterone (DHEA) with poly(ortho ester) polymers by interfacial polycondensation. Journal of microencapsulation. 2003 20 (5): 637–51.

40. Arshady R. Microspheres and microcapsules: A survey of manufacturing techniques. Part 1: Suspension cross-linking. Polymer Engineering and Science 1989; 29 (24): 1746–1758.

41. Arshady R. Microspheres and Microcapsules, a Survey of Manufacturing Techniques: Part III: Solvent Evaporation. Polymer Engineering and Science. 1990; 30 (15): 915–924.

42. Zhang P, Wu LB, Bu ZY, Li BG. Interfacial polycondensation of diphenolic acid and isophthaloyl chloride. Journal of Applied Polymer Science. 2008; 108 (6): 3586–3592.

43. Dawson TL. Changing colours: now you see them, now you don’t. Coloration Technology. 2010, 177–188.

44. US Patent 6,260,414: Liquid crystal, liquid level indicator. 2001.

45. Synnefa A., LCR Hallcrest TLC Literature Review, Thermal mapping and non-destructive testing, Energy. 1990;(C): 1–5.

46. Karlessi T, Santamouris M, Apostolakis K, Synnefa a., Livada I. Development and testing of thermochromic coatings for buildings and urban structures. Solar Energy. 2009; 83 (4): 538–551.

47. Hirota N, Hisamatsu N, Maeda S, Tsukahara H, Hyodo K. Thermochromism of poly(substituted thiophene) with urethane bond and its application to reversible thermal recording. Synthetic Metals. 1996; 80 (1): 67–72.

48. US Patent 6,685,094: Thermochromic bar code. 2004.

49. US Patent 4,666,949: Shimizu G. Thermochromic polyurethane foam. 1987.

50. US Patent 4,826,550: Shimizu G. Process for preparing molded product of thermochromic polyvinyl chloride. 1989.

51. US Patent 0138747 A1: Su HY. Hairbrush with thermochromic filaments and the method of manufacturing the same. 2005.

52. US Patent 016682 A1: Reversible thermochromic display article. 2006.

53. Liu L, Peng S, Wen W, Sheng P. Paper-like thermochromic display. Applied Physics Letters. 2007; 90 (21): 213,508.

54. US Patent 4,961,972: Shimizu G. Process for producing linear material. 1990.

55. US Patent 2,170,228: Shibhashi Y. Thermochromic textile material. 1986.

56. US Patent 0313325 A1: Ebejer C. Baby clothing comprising a thermochromic material.

57. US Patent 0074639 A1: Method of treating hair. 2005.

58. Carvalho A, Neves J, Heriberto J, Neves M. Contribution of thermochromic pigments for nanocoatings on jeanswear. Ljubljana, Slovenia: 41st International Symposium on Novelties in Textiles; 2010.

59. Rubacha M. Thermochromic cellulose fibers. Polymer advanced technology. 2007; 18: 323–328.

60. US Patent 0090510 A1: Ono Y, Ishimura N, Shibahashi Y. Thermochromic acrylic synthetic fibre, its processed article, and process for producing thermochromic acrylic synthetic fiber. 2002.

61. US Patent /0233379: O'Connor JG. Industrial fabric having a thermochromic sensor. 2008.

62. US Patent 0087566 A1: Carlyle T. Meltspun thermochromic fabrics. 2003.

63. US Patent 0237164 A1: Aperfine LM, Aperfine DB. Thermochromic water proof apparel. 2004.

64. US Patent 0143516 A1: Thermochromic elastic polymer substrate. 2009.

65. US Patent 0246292: Seeboth A, Kriwanek J, Lotzsch D. Thermochromic polymer layer and layer and method for production thereof. 2006.

66. US Patent 0121218: Senga K, Ito M. Thermochromic dry offset ink, and printed article produced using the same. 2002.

67. European Patent 0480162 A1: Masayasu K, Kusatsu-shi S. Dyeing method and dyed product. 1991.

68. Kulčar R, Gunde MK, Friškovec M. Thermochromic inks – dynamic colour possibilities. Dyes and Pigments. 2010; 86: 271–277.

69. Canal C, Villeger S, Cousty S, Roufet B, Sarrette J-P, Erra P, et al. Atom-sensitive textiles as visual indicators for plasma post-discharges. Applied Surface Science. 2008; 254 (18): 5959–66.

70. Robertson S. An Investigation of the Design Potential of Thermochromic Textiles used wih Electronic Heat-Profiling Circuitry, PhD thesis, Heriot Watt University. 2011.

71. Robertson S, Taylor S, Christie RM, Fletcher J, Rossini L. Designing with a responsive colour palette: The development of colour and pattern changing products. Advances in Science and Technology. 2008; 60: 26–31.

72. Christie RM, Robertson S, Taylor S. Design concepts for a temperature-sensitive environment using thermochromic colour change. Colour: Design & Creativity. 2007; 1: 1–11.

73. Gohl EPG, Vilenskly LD. Textile Science. 2nd edition. Longman Cheshire; 1983.

74. Little AF. An Investigation into Textile Applications of Photochromic Dyes. PhD thesis, Heriot Watt University 2008.

75. Oda H. New developments in the stabilization of leuco dyes: effect of UV absorbers containing an amphoteric counter-ion moiety on the light fastness of color formers. Dyes and Pigments 2005; 66 (2): 103–8.

76. Oda H. Photostabilization of organic thermochromic pigments: Action of benzotriazole type UV absorbers bearing an amphoteric counter-ion moiety on the light fastness of color formers. Dyes and Pigments. 2008; 76 (1): 270–276.

77. Oda H. Photostabilization of organic thermochromic pigments. Part 2: Effect of hydroxyarylbenzotriazoles containing an amphoteric counter-ion moiety on the light fastness of color formers. Dyes and Pigments. 2008; 76 (2): 400–405.

78. Ultraviolet Absorbers. http://www.specialchem4adhesives.com/ [cited on 15/01/2012].

79. Moura JCVP, Oliveira-Campos a. MF, Griffiths J. The effect of additives on the photostability of dyed polymers. Dyes and Pigments. 1997; 33 (3): 173–96.

80. Pospíšil J, Nešpurek S. Photostabilization of coatings. Mechanisms and performance. Progress in Polymer Science. 2000; 25 (9): 1261–335.

81. Cristea D, Vilarem G. Improving light fastness of natural dyes on cotton yarn. Dyes and Pigments. 2006; 70 (3): 238–45.

82. Yang Y, Naarani V. Improvement of the lightfastness of reactive inkjet printed cotton. Dyes and Pigments. 2007; 74 (1): 154–60.

83. Prefecture O. Effect of Ultraviolet Absorbing Agents on Photodegradation Behavior of a Disperse Dye Dyes and Pigments. 1998; 36 (3): 193–204.

84. Tsatsaroni EG, Kehayoglou a. H, Eleftheriadis IC, Kyriazis LE. Effectiveness of various UV-absorbers on the dyeing of polyester with disperse dyes. Part IV. Dyes and Pigments 1998; 38 (1-3): 65–75.

85. Lee JJ, Lee HH, Eom SI, Kim JP. UV absorber aftertreatment to improve lightfastness of natural dyes on protein fibres. Coloration Technology. 2001; 117.

86. Gijsman P, Hennekens J, Tummers D. The mechanism of action of hindered amine light stabilizers. Polymer Degradation and Stability. 1993; 39 (2): 225–33.

87. Carlsson DJ. Antioxidant Mechanism of Hindered Amine Light Stabilizers. Makromolekulare Chemie Macromolecular Chemistry and Physics. 1984; 8: 79–88.

88. Gijsman P. New synergists for hindered amine light stabilizers. Polymer Degradation and Stability. 2002; 43 (5): 1573–1579.

89. Gugumus F. Current trends in mode of action of Hindered Amine Light Stabilizers. Polymer Degradation and Stability. 1993; 40 (2): 167–215.

90. Sundaram K. Antioxidants - a research report, Technical Report NASA Ames Research Center, Moffett Field,CA.,USA (1982).

91. Chiu M. Light stabilizers and antioxidants Principles of Light stabilizers. Presentation of Double Bond Chemical, Bonding Partnership.

92. Khanra TK, Adhikari B, Maiti S. Multifunctional activities of benzazole derivatives in rubber vulcanization. Rubber Chemistry and Technology. 1993; 66: 30–37.

93. Yang R. A systematic statistical approach to polypropylene fibre process technology. 2000, PhD thesis, Heriot Watt University.

94. Cook JG. Handbook of textile fibres. 5th edition. Merrow Publishing Co. Ltd., England; 1984.

95. Brydson J. Plastic Materials. 7th edition. Oxford: Butterworth-Heinemann; 1999 Pages 120, 276-278.

96. Cowie JMG. Polymers: Chemistry & Physics of Modern Materials. 2nd edition. London: Blackie and Son Ltd., Chapman and Hall, USA; 1991.

97. Brydson J. Plastic Materials. 7th ed. Oxford: Butterworth-Heinemann; 1999 Pages 205-227.

98. Pappy D. Investigation into the relationship between processing parameters and stucture-property chraracteristics during extrusion of linear low density polyethylene tapes. 2004, PhD thesis, Heriot Watt University.

99. Liang JZ, Zhong L. Elongational properties of low density polyethylene using melt spinning technique. Polymer Testing. 2010; 29 (8): 972–976.

100. Brydson J. Plastic Materials. 7th ed. Oxford: Butterworth-Heinemann; 1999 Pages 386-388.

101. Albert J, Luft G. Runaway phenomena in the ethylene / vinylacetate copolymerization under high pressure 1. Chemical Engineering and Processing. 1998; 37: 55 – 59.

102. Ito S, Munakata K, Nakamura A, Nozaki K. Copolymerization of vinyl acetate with ethylene by palladium/alkylphosphine-sulfonate catalysts. Journal of the American Chemical Society 2009; 131 (41): 14606–14607.

103. Boone HW, Athey PS, Mullins MJ, Philipp D, Muller R, Goddard WA. Copolymerization studies of vinyl chloride and vinyl acetate with ethylene using a transition-metal catalyst. Journal of the American Chemical Society. 2002; 124 (30): 8790–8791.

104. Lee H-Y, Yang T-H, Chien I-L, Huang H-P. Grade transition using dynamic neural networks for an industrial high-pressure ethylene–vinyl acetate (EVA) copolymerization process. Computers & Chemical Engineering 2009; 33 (8): 1371–1378.

105. Chien I, Kan T, Chen B. Dynamic simulation and operation of a high pressure ethylene-vinyl acetate (EVA) copolymerization autoclave reactor. Computers & Chemical Engineering 2007; 31 (3): 233–245.

106. Fisher EG. Extrusion of Plastics. 3rd edition. Newnes-Butterworths; 1976.

107. Brydson J, Peacock D. Principles of Plastics Extrusion. 2nd edition, Applied Science Publishers; 1973

108. White JL, Potente H, editors. Screw Extrusion. Carl Hanser Verlag; 2003.

109. Rauwendaal C. Polymer Extrusion. 4th edition. Carl Hanser Verlag; 2001.

110. Crawford RJ. Plastic Engineering. 3rd edition. Butterworth-Heinemann; 1998.

111. Ziabicki A. Fundamentals of Fibre Formation: The Science of Fibre Spinning and Drawing. John Wiley & Sons Ltd.; 1976.

112. White JL, Dharod KC, Clark ES. Interaction of melt spinning and drawing variables on the crystalline morphology and mechanical properties of high-density and low-density polyethylene fiber. Journal of Applied Polymer Science. 1974; 18 (9): 2539–2568.

113. Sheehas WC, Cole TB. Production of Super-Tenacity Polypropylene Filaments. Polymer. 1964; 8: 2359–2388.

114. Krimm S, Tobolsky AV, Foun TT. Quantitative X-Ray Studies of Order in Amorphous and Crystalline Polymers - Quantitative X-Ray Determination of Crystallinity in Polyethylene. Journal of Polymer Science. 1951; 7 (1): 57–76.

115. Kolb R. Simultaneous measurements of small- and wide-angle X-ray scattering during low speed spinning of poly(propylene) using synchrotron radiation. Polymer 2000; 41 (4): 1497–1505.

116. Smith P, Lemstra PJ. Ultra-high-strength polyethylene filaments by solution spinning/drawing. Journal of Materials Science 1980; 15 (2): 505–514.

117. Chamberlin GJ, Chamberlin DG. Colour: Its Measurement, Computation and Application. London: Heyden & Son Ltd.; 1980.

118. McDonald R. Colour Physics for Industry. 2nd edition. Society of Dyers and Colourists; 1997.

119. Fairchild MD. Color Appearance Models. Harlow, England: Reading, Mssachusetts; 1997.

120. Overheim RD, Wagner DL. Light and Color. New York, USA: John Wiley & Sons, Inc.; 1982.

121. Hunter RS. The Measurement of Appearance. London: John Wiley & Sons, Inc.; 1975.

122. Derbyshire AN, Marshal WJ. Value analysis of dyes - a new method based on colour measurement. Society of dyers and colourists. 1980; 96: 166–176.

123. Garland CE. Shade and strength predictions and tolerances from spectral analysis of solutions. Textile Chemist and Colorist. 1973; 5: 227–231.

124. Dietrich H. XCmyk - CMYK to RGB calculator with source code. http://www.codeproject.com/KB/applications/xcmyk.aspx. 2003.

125. Abdullah N, Abu Talib AR, Mohd Saiah HR, Jaafar AA, Mohd Salleh MA. Film thickness effects on calibrations of a narrowband thermochromic liquid crystal. Experimental Thermal and Fluid Science. 2009; 33 (4): 561–578.

126. SDC multifibre DW fabric [cited on 29/01/2012]; http://www.sdcenterprises.co.uk/products/multifibre.asp.

127. Jones C. Field Emission SEM Training, Hitachi S-4300 FE SEM Heriot Watt University.

128. Oswald P, Pieranski P. Nematic and Cholesteric Liquid Crystals. Taylor & Francis Group; 2005.